

Facoltà di Farmacia e Scienze della Nutrizione e della Salute

Dipartimento di Scienze Farmaceutiche

---

“B. Telesio-Scuola di Dottorato di Scienza e Tecnica”

Materiali Organici di Interesse Farmaceutico

CHIM/09

XXIV ciclo

## Materiali Polimerici Funzionali per Applicazioni Farmaceutiche e Biomedicali

Direttore della Scuola: Prof. Roberto BARTOLINO

Supervisore: Dr. Sonia TROMBINO

Coordinatore del Curriculum: Prof. Bartolo GABRIELE

Candidata: Teresa FERRARELLI

e-mail dell'autore: [teresa.ferrarelli@yahoo.it](mailto:teresa.ferrarelli@yahoo.it)

Indirizzo dell'autore:  
Dipartimento di Scienze Farmaceutiche  
Università della Calabria  
Via Pietro Bucci, Ed. Polifunzionale 155  
87036 Arcavacata di Rende, Cosenza

Tel.: +39 0984 493296  
Tel.: +39 0961 964330  
Cell: +39 328 3227646

# Prefazione

## Introduzione Generale, Scopi e Organizzazione della tesi

### 1. Introduzione

La combinazione sinergica della scienza dei polimeri, dei concetti sul drug delivery e la tecnologia dei materiali offre preziose opportunità per l'ottenimento di nuovi materiali multifunzionali. In particolare, I sistemi polimerici giocano un ruolo fondamentale nel drug delivery modern grazie al fatto che sono in grado di controllare la velocità di rilascio di un farmaco, favorirne l'effettiva solubilizzazione nei mezzi, minimizzarne la degradazione, contribuire a ridurre la tossicità e facilitarne l'uptake intracellulare. Inoltre, questi sistemi contribuiscono in maniera significativa al miglioramento dell'efficacia terapeutica di un farmaco.

Il metodo attraverso il quale un farmaco viene rilasciato può giocare un ruolo determinante sulla sua efficacia. Alcune molecole farmacologicamente attive sono caratterizzate da una finestra terapeutica all'interno della quale si assiste alla massima efficacia terapeutica ma, al di sotto o al di sopra di questo range possono verificarsi rispettivamente fenomeni quali l'assenza dell'effetto e l'insorgenza di tossicità. D'altro canto, il progredire molto lento di nuove realtà terapeutiche per il trattamento di patologie croniche e invalidanti, favorisce sempre più l'ideazione e la messa a punto di nuovi approcci multidisciplinari per il rilascio di farmaci in prossimità degli organi bersaglio [1]. A partire da questi concetti, nuove idee sulla capacità di controllare la farmacocinetica, la farmacodinamica, la tossicità aspecifica, l'immunogenicità, la biorecognizione e l'efficacia dei farmaci sono state

generate. Queste nuove strategie, spesso chiamate drug delivery systems (DDS), si basano sull'interdisciplinarietà che combina la scienza dei polimeri, la biofarmaceutica, la coniugazione chimica e la biologia molecolare. Per minimizzare la degradazione dei farmaci e la conseguente perdita in principio attivo, per minimizzare l'insorgenza di effetti dannosi e per aumentare la biodisponibilità e la frazione di farmaco che si accumula in prossimità del sito d'azione, vari sistemi di rilascio sito-specifico sono in via di sviluppo: la caratteristica comune di molti sistemi a rilascio controllato risiede nel fatto che questi forniscono un rilascio continuo del principio attivo in un arco di tempo assai prolungato. Tra i carriers di farmaci, i più importanti sono i seguenti: idrogel, vescicole (liposomi e niosomi), polimeri e microparticelle costituite da polimeri naturali o sintetici insolubili o biodegradabili. Questi carriers possono diventare a lento rilascio, reattivi agli stimoli (es. sensibili al pH o alla temperatura) ed anche sito-specifici (es. attraverso coniugazione con anticorpi specifici o proteine specifiche per un determinato target) [2]. I polimeri trovano vaste applicazioni nel settore del drug delivery. Le ragioni includono la loro attività di superficie che li rende efficienti come stabilizzanti di sistemi colloidali e la loro capacità di gelificare; tutto ciò li rende utili in questo settore e nel campo dei sistemi auto-assemblanti composti da surfattanti a basso peso molecolare. Inoltre, i materiali polimerici esibiscono diverse proprietà desiderabili nel settore del drug targeting: biocompatibilità, biodegradabilità e capacità di funzionalizzazione. Attraverso la derivatizzazione e la manipolazione strutturale dei materiali polimerici, le molecole di un determinato farmaco possono essere incorporate all'interno del polimero. L'intrappolamento o l'incapsulazione all'interno di una matrice polimerica favorisce un maggiore controllo della sua farmacocinetica; ciò contribuisce a mantenere livelli di farmaco adeguati in corrispondenza del sito target. Le

tecniche utilizzate per legare un farmaco ad un polimero sono la coniugazione e la formazione di particelle. Tra le diverse classi di materiali polimerici utilizzate nel drug delivery, i copolimeri a blocchi, costituiti da blocchi di 2 o 3 differenti polimeri, i polisaccaridi e le proteine hanno trovato una vasta applicazione in campo farmaceutico. I materiali polimerici utilizzati in questo settore sono farmaci polimerici o in combinazione con piccole molecole o biomacromolecole [3]. Grazie alla possibilità di controllare la velocità di degradazione di un polimero è possibile ottenere un rilascio controllato in un vasto arco di tempo e la protezione di composti sensibili a particolari ambienti e distretti [4]. Il design di questi biomateriali richiede sostanziali requisiti affinché il sistema sia specifico e sensibile ad uno stimolo. Con questa tipologia di approccio possono essere ottenuti materiali multifunzionali ed intelligenti con cinetiche di rilascio specifiche per molecole individuali [5].

## **2. Scopo della tesi**

La presente tesi è stata realizzata presso il laboratorio di “Chimica Macromolecolare e Tecnologia Farmaceutica” del Dipartimento di Scienze Farmaceutiche (Università della Calabria). Il lavoro sperimentale di questo triennio è stato rivolto alla progettazione e alla preparazione di nuovi materiali polimerici naturali e sintetici da destinare ad applicazioni biomedicali e farmaceutiche. Inoltre, parte della suddetta tesi è stata svolta presso la School of Pharmacy (University College of London) e sotto la supervisione della Professoressa Ijeoma Uchegbu e del Dr Schatzlein; la ricerca durante questa esperienza estera è stata rivolta alla sintesi di un polimero a base di chitosano (palmitoil glicol chitosano), alla valutazione *in vitro* del suo comportamento a contatto con epitelii assorbenti e *in vivo* della sua biodistribuzione.

### **3. Organizzazione della tesi**

Grazie alla completezza dei differenti progetti di ricerca portati a termine durante questo corso di dottorato, è stato necessario suddividere la tesi in quattro sezioni indipendenti tra di loro.

La prima sezione riguarda la preparazione di un derivato antiossidante del cotone che è stato testato *in vivo* ed è risultato ampiamente applicabile nell'ambito della cura delle ferite infette e infiammate.

La seconda sezione contiene la derivatizzazione di carboidrati per l'ottenimento di sistemi micro- e nanoparticellari.

La terza sezione riguarda la modificazione di proteine quali la Gelatina ed il Collagene per l'ottenimento di biomateriali applicabili nel trattamento polmonare della tubercolosi e nel trattamento topico delle ferite rispettivamente.

La quarta ed ultima sezione riguarda la modificazione chimica di sostanze attive, quali la Curcumina, la Rifampicina e l'Acido Ellagico per la realizzazione di idrogel e sistemi microparticellari.

## **Bibliografia**

[1] SA Sreenivas, KV Pai. Thiolated Chitosans: Novel Polymers for Mucoadhesive Drug Delivery-A Review. *Tropical Journal of Pharmaceutical Research* **2008**, 7 (3): 1077-1088.

[2] Takeuchi H, Yamamoto H, Kawashima Y. Mucoadhesive nanoparticulate systems for peptide drug delivery. *Advanced Drug Delivery Review* **2001**; 47: 39-54.

[3] Hook AL, Anderson DG, Langer R, Williams P, Davies MC, Alexander MR. High throughput methods applied in biomaterial development and discovery. *Biomaterials* **2010**,31: 187–198.

[4] Couvreur, P., and Vauthier, C. Nanotechnology: Intelligent Design to Treat Complex Disease. *Pharmaceutical Research* **2006**, 23[7], 1417-1450.

[5] Kohane DS and Langer R. Polymeric biomaterials in tissue engineering. *Pediatr Res* **2008**, 63: 487–491.



Faculty of Pharmacy, Nutritional Sciences and Health Care

Department of Pharmaceutical Sciences

---

“B. Telesio-Doctoral School of Science and Technique”

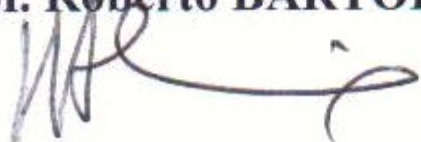
Organic Materials of Pharmacological Interest

CHIM/09

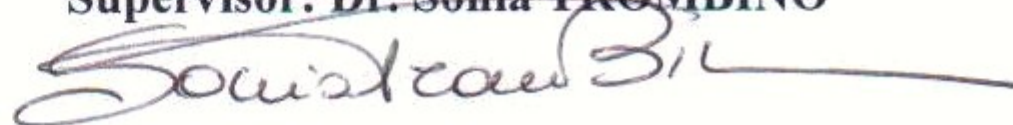
XXIV cycle, PhD thesis

# Functional Polymeric Materials for Pharmaceutical and Biomedical Applications

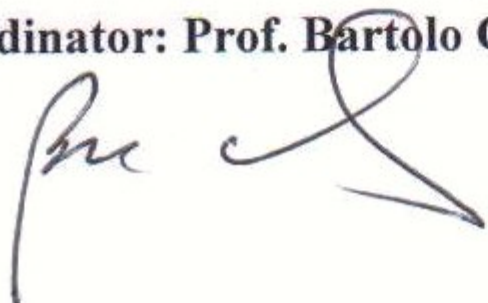
School Director: Prof. Roberto BARTOLINO



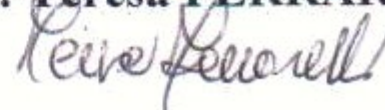
Supervisor: Dr. Sonia TROMBINO



Curriculum Coordinator: Prof. Bartolo GABRIELE



Candidate: Teresa FERRARELLI



Academic Year: 2010/2011



Author's e-mail: [teresa.ferrarelli@yahoo.it](mailto:teresa.ferrarelli@yahoo.it)

Author's address:  
Department of Pharmaceutical Sciences  
University of Calabria  
Via Pietro Bucci, Ed. Polifunzionale 155  
87036 Arcavacata di Rende, Cosenza

ph.: +39 0984 493296  
ph.: +39 0961 964330  
cell: +39 328 3227646

## PLEDGE AGAINST PLAGIARISM

I, Teresa Ferrarelli, hereby confirm that the work submitted in this report is my own and that I have not violated the University of Calabria's policy on plagiarism.

Date: 30/11/2011

  
\_\_\_\_\_  
(Teresa FERRARELLI)

**Table of Contents**

Preface: General Introduction, Aims and Organization of this Thesis..... 13

- 1. General Introduction ..... 13
- 2. Aims of this thesis ..... 16
- 3. Organization of this thesis..... 16

References ..... 19

SECTION 1: NATURAL FIBERS MODIFICATION FOR THE  
OBTAINMENT OF BIOMEDICAL MATERIALS..... 21

SYNTHESIS, CHARACTERIZATION, AND ANTI-INFLAMMATORY ACTIVITY  
OF DICLOFENAC-BOUND COTTON FIBERS ..... 22

Abstract ..... 22

- 1. Introduction ..... 23
  - 1.1 Wound dressings ..... 24
  - 1.2 Wound Healing..... 26
    - 1.2.1 Haemostasis and Inflammation..... 26
    - 1.2.2 Migration and Proliferation ..... 27
    - 1.2.3 Maturation..... 27
    - 1.2.4 Wound Exudate..... 27
  - 1.3 Effective Wound Management..... 28
    - 1.3.1 Debridement: removing the non viable tissue from a  
wound..... 28
  - 1.4 Classification of Dressings ..... 29
    - 1.4.1 Topical Pharmaceutical Formulations ..... 29
    - 1.4.2 Traditional Dressings ..... 30
    - 1.4.3 Modern Wound Dressings ..... 31
  - 1.5 Biological Dressings..... 31
  - 1.6 Medicated Dressings for Drug Delivery..... 33
    - 1.6.1 Antimicrobials ..... 33
    - 1.6.2 Growth Factors ..... 34

Table of contents

1.6.3 Supplements .....	34
1.7 Controlled Drug Delivery to the Wound .....	35
1.7.1 Advantages of Controlled Drug Delivery .....	35
1.7.2 Polymeric Drug Delivery Dressings .....	36
1.7.3 Mechanism of Controlled Delivery to Wounds .....	37
1.8 Diclofenac .....	38
1.9 Aim of the project .....	38
2. Materials and Methods .....	39
2.1 Chemicals .....	39
2.2 Cellulose Functionalization .....	39
2.3 Characterization and Determination of the Degree of Substitution of Functionalized Cotton Fibers .....	40
2.4 Thermal Behavior of Diclofenac-Linked Cellulose Fibers .....	42
2.5 In Vivo Evaluation of the Anti-Inflammatory Activity of Diclofenac-Linked Cotton Fibers .....	42
2.6 Immunohistochemistry .....	43
2.7 Statistical Analysis .....	44
3. Results .....	44
3.1 Synthesis and Characterization of Diclofenac- Bound Cotton Fibers .....	44
3.2 In Vivo Evaluation of the Anti-Inflammatory Activity of Diclofenac-Linked Cotton Fibers .....	46
3.3 Metabolic Effects of Diclofenac-Bound Cotton Fibers .....	49
4. Discussion .....	50
5. Conclusions .....	51
References .....	52

SECTION 2: CHEMICAL MODIFICATION OF CARBOHYDRATES  
FOR THE IMPLEMENTATION OF DRUG DELIVERY SYSTEMS ..59

PART A: MUCOADHESIVE MICROSPHERES DEXTRAN AND POLYETHYLENE GLYCOL-BASED FOR THE TREATMENT OF VAGINAL INFECTIONS.....	60
Abstract .....	60
1.1 Mucoadhesion in the vaginal environment.....	61
1.2 Bioadhesive polymers .....	65
1.3 Proposed mechanisms and promoters for bioadhesion .....	67
1.4 Polyethylene glycol as promoter of bioadhesion.....	69
1.5 Dextran-based hydrogels .....	70
1.6 Polymeric microspheres .....	70
2. Materials and Methods .....	72
2.1 Materials .....	72
2.2 Instruments .....	72
2.3 Synthesis of 6-carboxy dextran .....	73
2.4 Determination of carboxylic groups content in (1) by Methylene Blue Sorption.....	74
2.5 Protection of the primarily hydroxylic function of PEG 200 by tetrahydropyranylation.....	75
2.6 Acrylation of (2) .....	75
2.7 Deprotection of (3) .....	76
2.8 Esterification of 3 with 1: linkage of acryloyl-PEG to 6-carboxy dextran .....	76
2.9 Microspheres preparation based on (5) .....	76
2.10 Microspheres characterization.....	77
2.11 Swelling studies.....	78
2.12 Drug Incorporation into preformed microspheres by soaking procedure .....	79
2.13 In vitro release studies of ketoconazole from microparticles	79
3. Results and Discussion.....	80
3.1 Synthesis of 6-carboxy dextran .....	82

## Table of contents

3.2 Protection of the primarily hydroxylic function of PEG 200 by tetrahydropyranylation.....	82
3.3 Acrylation of PEG-THP .....	83
3.4 Deprotection of acryloyl-PEG-THP .....	84
3.5 Esterification of acryloyl-PEG with 6-carboxy dextran.....	85
3.6 Microspheres preparation by reverse phase emulsion polymerization.....	85
3.7 Microspheres characterization.....	89
3.8 Swelling studies on empty microspheres .....	90
3.9 Ketoconazole loading into preformed empty microspheres ....	90
3.10 In vitro ketoconazole release studies .....	91
4. Conclusions .....	93
References .....	95
<b>PART B: SYNTHESIS, CHARACTERIZATION, <i>IN VITRO</i> CELL UPTAKE AND <i>IN VIVO</i> BIODISTRIBUTION STUDIES OF A CATIONIC GLYCOL CHITOSAN POLYMER FOR ORAL ADMINISTRATION OF HYDROPHOBIC DRUGS.....</b>	
Abstract .....	99
1. Introduction .....	100
1.1 What is Nanotechnology?.....	100
1.2 Nanotechnology in Drug Delivery .....	102
1.3 Various nanocarrier systems.....	105
1.4 Biodegradable polymers and their impact.....	106
1.5 Importance of Surface Charge Density .....	109
1.6 Use of in vitro models to study cell uptake and mucoadhesion .....	111
1.7 Aim of the project.....	114
2. Materials and Methods .....	114
2.1 Materials .....	114
2.2 Degradation of Glycol Chitosan (GC48).....	115

2.3 Palmitoylation of degraded Glycol Chitosan (PGC) .....	115
2.4 Quaternization of PGC (GCPQ) .....	116
2.5 Structural analysis: NMR spectroscopy .....	117
2.6 Functional group determination: FT-IR .....	118
2.7 Self Assembly studies: .....	118
2.8 Photon Correlation Spectroscopy .....	119
2.9 Nanoparticles morphology: TEM .....	119
2.10 Molecular Weight Determination through Gel Permeation Chromatography .....	120
2.11 Fluorescent Labelling of GCPQ .....	120
2.12 Encapsulation studies .....	122
2.13 Synthesis of Radiolabelled GCPQ for in vivo biodistribution studies .....	123
2.14 Cell Studies .....	124
2.14.1 Caco-2 cells .....	124
2.14.2 HT29-MTX-E12 cells .....	124
2.14.3 Staining/detection of mucus: Mucus staining .....	125
2.14.4 Tight junction integrity determination: TEER .....	126
2.14.5 Idarubicin uptake studies: Confocal microscopy .....	126
2.15 Statistical Analysis .....	127
3. Results .....	127
3.1 Synthesis .....	127
3.2 Characterization .....	128
3.2.1 NMR .....	128
3.2.2 % Substitution degree .....	134
3.2.3 Molecular weight through NMR analyses .....	134
3.2.4 FT-IR .....	134
3.2.5 GPC-MALLS: Molecular Weight Determination .....	136
3.2.6 CAC .....	137

## Table of contents

3.2.7 PCS .....	139
3.2.8 TEM .....	140
3.2.9 Synthesis of Fluorescent Labelled GCPQ .....	141
3.2.10 Encapsulation Studies .....	144
3.3 In vivo biodistribution studies .....	144
3.4 Cell Studies.....	145
3.4.1 TEER .....	145
3.4.2 Mucus Layer Characterization: Mucus Staining.....	147
3.4.3 Confocal Images .....	147
3.5 Discussion.....	151
4. Conclusions and Future Works .....	159
References .....	160
SECTION 3: CHEMICAL MODIFICATION OF PROTEINS FOR THE IMPLEMENTATION OF DRUG DELIVERY SYSTEMS.....	167
PART A: SYNTHESIS AND <i>IN VITRO</i> ANTITUBERCULAR ACTIVITY OF ISONIAZID-GELATIN CONJUGATE.....	168
Abstract .....	168
1. Introduction .....	169
1.1 Gelatin for pharmaceutical applications: a matrix-molecule for nanoparticles preparation.....	169
1.2 The lungs as a delivery target for nanomaterials.....	173
1.3 Delivery of nanoparticles for the treatment of tuberculosis ..	179
1.4 Toxicity of inhaled ultrafine particles .....	181
1.5 Nanoparticles processing methods for pulmonary drug formulations.....	182
1.6 Aim of the project.....	184
2. Materials and methods .....	185
2.1 Materials .....	185
2.2 Measurements.....	186



2.3 Synthesis of the Antitubercular-Gelatin Conjugate.....	186
2.4 Calorimetric Analysis of the Antitubercular-Gelatin Conjugate .....	187
2.5 Oxidation Test .....	187
2.6 Antitubercular Activity.....	187
3. Results and discussion.....	188
3.1 Synthesis of INH-Gelatine conjugate .....	188
3.2 Characterization of INH-Gelatin Conjugate using <sup>1</sup> H-NMR	189
3.3 Characterization of INH-Gelatin Conjugate by Differential Scanning Calorimetry (DSC) .....	190
3.4 Oxidation Test .....	191
3.5 Antitubercular activity evaluation .....	192
4. Conclusions .....	193
References .....	195
PART B: COLLAGEN $\alpha$ -TOCOPHERULATE FOR TOPICAL APPLICATIONS: PREPARATION, CHARACTERIZATION AND ANTIOXIDANT ACTIVITY EVALUATION .....	
Abstract .....	201
1. Introduction .....	201
1.1 Adverse reactions to Collagen.....	206
1.2 Biodegradability and collagenases .....	207
1.3 Immunogenicity and biocompatibility.....	208
1.4 Collagen in wounds healing .....	208
1.5 Collagen-based drug delivery systems .....	209
1.6 Collagen sponges for wounds healing.....	210
1.7 Collagen as skin replacement .....	211
1.8 Collagen as bone substitute .....	211
1.9 Collagen as bioengineered tissues .....	211

Table of contents

1.10 Recent Advances in Collagen-Based Biomaterials: Dermal filler, wound dressing and delivery systems.....	212
1.11 Aim of the project.....	213
2. Materials and Methods.....	213
2.1 Materials.....	213
2.2 Instruments.....	214
2.3 Collagen derivatization.....	214
2.4 Antioxidant activity evaluation trough rat liver microsomal membranes.....	215
3. Results and discussion.....	216
3.1 Solid phase synthesis of collagen derivative.....	216
3.2 Antioxidant activity evaluation.....	219
4. Conclusions.....	220
References.....	222
<b>SECTION 4: HYDROGELS AND MICROSPHERES BASED ON ACTIVE MOLECULES.....</b>	<b>227</b>
<b>PART A: PREPARATION, CHARACTERIZATION AND <i>IN VITRO</i> ACTIVITIES EVALUATION OF CURCUMIN BASED MICROSPHERES FOR AZATHIOPRINE ORAL DELIVERY.....</b>	<b>228</b>
Abstract.....	228
1. Introduction.....	229
1.1 Curcumin and Azathioprine pharmacological activities.....	229
1.2 Microspheres as drug delivery systems for oral administration of drugs.....	231
1.3 Aim of the project.....	234
2. Materials and Methods.....	235
2.1 Chemicals.....	235
2.2 Measurements.....	236
2.3 Synthesis of Monoacrylated Curcumin (CA).....	236
2.4 Antiproliferative Activity Evaluation of CA.....	237

2.5 Antioxidant Activity Evaluation of CA .....	237
2.6 Microspheres Preparation .....	238
2.7 Swelling Studies .....	238
2.8 Azathioprine Loading by Soaking Procedure.....	239
2.9 Drug Release Studies.....	240
2.10 Statistical Analysis .....	240
3. Results and Discussion.....	240
4. Conclusions .....	246
References .....	248
<b>PART B: RESPIRABLE RIFAMPICIN-BASED MICROSPHERES CONTAINING ISONIAZID FOR TUBERCULOSIS TREATMENT .....</b>	<b>254</b>
Abstract .....	254
1. Introduction .....	255
1.1 Smart polymeric particles.....	256
1.2 Tuberculosis treatment .....	259
1.2.1 Particles for pulmonary targeted delivery.....	261
1.3 Antitubercular drugs .....	263
1.4 Aim of the project.....	265
2. Materials and Methods .....	267
2.1 Apparatus.....	267
2.2 Materials .....	267
2.3 Rifampicin Derivatization .....	268
2.4 Microspheres preparation .....	268
2.5 Size distribution analysis .....	269
2.6 Swelling studies.....	269
2.7 Drug Incorporation into preformed microspheres .....	270
2.8 In vitro drug release from microparticles .....	270
2.9 In vitro antitubercular activity evaluation .....	271

Table of contents

2.10 Statistical Analysis .....	272
3. Results and Discussion.....	272
4. Conclusions .....	278
References .....	280
<b>PART C: A NEW HYDROGEL ELLAGIC ACID AND GLYCINE-BASED CONTAINING FOLIC ACID AS SUBCUTANEOUS IMPLANT FOR BREAST CANCER TREATMENT: PREPARATION, CHARACTERIZATION AND ANTIOXIDANT ACTIVITY EVALUATION.....</b>	
Abstract .....	285
1. Introduction .....	286
1.1 Hydrogels as drug delivery systems .....	286
1.2 Folates in tumors targeting .....	292
1.3 Aims of the project .....	294
2. Materials and Methods .....	295
2.1 Reagents .....	295
2.2 Instruments .....	296
2.3 Synthesis of N-trytil glycine.....	296
2.4 Esterification of N-trytilglycine with Ellagic acid .....	297
2.5 Detritylation reaction (Removal of trityl group) .....	298
2.6 Acrylation .....	298
2.7 Hydrogel preparation.....	299
2.8 Antioxidant activity evaluation .....	299
2.9 Swelling studies.....	299
2.10 Incorporation of folic acid into preformed hydrogel .....	300
2.11 Drug release studies.....	301
3. Results and Discussion.....	301
3.1 Synthesis of N-trytil glycine.....	302
3.2 Esterification of N-trytilglycine with Ellagic acid .....	303
3.4 Detritylation reaction (Removal of trityl group) .....	304

Table of contents

3.5 Acrylation .....	305
3.6 Hydrogel preparation.....	307
3.7 Antioxidant activity evaluation .....	307
3.8 Swelling studies.....	308
3.9 Folic acid loading by soaking procedure.....	308
3.10 In vitro release studies .....	309
4. Conclusions .....	309
References .....	311



## **Preface**

### **General Introduction, Aims and Organization of this Thesis**

#### **1. General Introduction**

The synergic combination of polymeric science, drug delivery concepts and material technology offers challenging and precious opportunities for the achievement of new useful materials. In particular, polymeric systems play an important role in modern drug delivery, where they may allow control of the drug release rate, enhance effective drug solubility, minimize its degradation, contribute to reduce its toxicity and facilitate control of its uptake. Moreover, they contribute significantly to therapeutic efficiency.

The method by which a drug is delivered can have a significant effect on its efficacy. Some drugs have an optimum concentration range within which maximum benefit is derived, and concentrations above or below this range can be toxic or produce no therapeutic benefit at all. On the other hand, the very slow progress in the efficacy of the treatment of severe diseases, has suggested a growing need for a multidisciplinary approach to the delivery of therapeutics to target tissues [1]. Starting from this concept, new ideas on controlling the pharmacokinetics, pharmacodynamics, non-specific toxicity, immunogenicity, biorecognition, and efficacy of drugs were generated. These new strategies, often called drug delivery systems (DDS), are based on interdisciplinary approaches that combine polymer science, pharmaceutics, bioconjugate chemistry, and molecular biology. To minimize drug degradation and loss, to prevent harmful side-effects and to increase drug bioavailability and the fraction of the drug accumulated

## Preface

in the required zone, various drug delivery and drug targeting systems are currently under development: the common feature of many common controlled release devices is that they provide a continuous release over a prolonged period of time. Among drug carriers, the most important are the following ones: hydrogels, vesicles (liposomes and niosomes), polymers and microparticles made of insoluble or biodegradable natural and synthetic polymers. These carriers can be made slowly degradable, stimuli-reactive (e.g., pH or temperature-sensitive), and even targeted (e.g., by conjugating them with specific antibodies or proteins against certain characteristic components of the area of interest) [2]. Polymers find broad uses in drug delivery applications. Reasons include their surface activity, which makes them efficient stabilizers of colloidal drug delivery systems, their gel forming capacity, which allows many opportunities in drug delivery, and their formation of self-assembly structures analogous to those formed by low molecular weight surfactant. Moreover polymeric materials exhibit several desirable properties for drug carrier use including biocompatibility, biodegradability, and functionalization capability. Through functionalization and structural manipulation of polymeric materials, drug molecules can be incorporated within the polymer. Entrapping or encapsulating the drug within a polymer allows for greater control of its pharmacokinetic behaviour that maintains more appropriate steady levels of the drug at the site of delivery. Techniques that are used to couple the drug with the polymer include sequestering, conjugation, and particles formation. Besides the several classes of polymeric materials used in drug delivery, block copolymers, consisting of blocks of two or several polymers, polysaccharides and proteins have found widespread use in pharmaceutical field. Polymeric materials are being used as drug delivery



systems as a polymeric drug itself or in combination with small molecules or with biomacromolecules [3]. An aspect which has been highlighted in the relation to the use of polymers in drug delivery is their biodegradation. Due the possibility to control the degradation rate of polymers over wide ranges through, e.g., the polymer structure and composition, this process has been found to provide an interesting way to obtain a controlled drug release over a prolonged time, and to protect sensitive compound from harsh environment, e.g., in the stomach. If the polymer is non-degradable (e.g. polymethacrylates), the size needs to be below the renal threshold ensuring that it is not accumulated in the body. If the polymer is degradable (e.g. polyesters), the toxicity and/or immune response of the degradation products have to be considered as well. Besides their application in a passive fashion, synthetic polymers often adopt a more active role such as releasing a drug molecule, peptide or oligo/poly(nucleic acid) upon an external stimulus. In this case, we consider these polymers as stimuli responsive ones. Stimuli-responsive polymers mimic biological systems in a crude way where an external stimulus (e.g. change in pH or temperature) results in a change in properties [4]. This can be a change in conformation, change in solubility, alteration of the hydrophilic/hydrophobic balance or release of a bioactive molecule (e.g. drug molecule). This also includes a combination of several responses at the same time. In medicine, stimuli-responsive polymers and hydrogels have to show their response properties within the setting of biological conditions, hence there is a large variety of different approaches. Typical stimuli are temperature, pH, light and redox potential. The obvious change in pH along the GI tract from acidic in the stomach (pH=2) to basic in the intestine (pH=5-8) has to be considered for oral delivery of any kind of drug, but there are also more subtle

## Preface

changes within different tissue. Certain cancers as well as inflamed or wound tissue exhibit a pH different from 7.4 as it is in circulation.

Advances in bioactive biomaterials and drug delivery systems allow not only controlled release, but also protection of factors from degradation. Design of these advanced biomaterials requires substantial basic biological insight, since dose, timing and also the conditions for environmentally controlled release will be highly specific for each target tissue and disease. Materials can be designed to be multifunctional and smart, in order to provide sequential signals with different release kinetics for individual molecules [5].

### **2. Aims of this thesis**

The present thesis was realized in the Pharmaceutical Technology groups, Department of Pharmaceutical Sciences (University of Calabria) and deals about the development of polymeric materials for biomedical and pharmaceutical applications. In particular, many natural polymers, polyacrylic derivatives and proteins were modified in order to obtain materials useful for different applications. Moreover, part of the entire PhD was focused on the synthesis, characterization, *in vitro* cell uptake and *in vivo* biodistribution studies of a cationic glycol chitosan polymer for oral administration of hydrophobic drugs. This last project was carried out during an interesting and fruitful scientific visiting at the School of Pharmacy (University College of London) in the Department of Pharmaceutics under the supervision of Professor Ijeoma Uchegbu and Dr. Andreas Schatzlein.

### **3. Organization of this thesis**

Due to the multitude of independent projects, the present thesis is divided into four self-contained sections.

The first section, named “Natural Fibers Modification for the Obtainment of Biomedical Materials”, contains the preparation, characterization, and anti-inflammatory activity evaluation of a Diclofenac-bound cotton fiber. This innovative biomaterial was tested *in vivo* and revealed to possess an excellent activity; for this reason it could be successfully applied in the wounds dressings field.

The second section, named “Chemical Modification of Carbohydrates for the Implementation of Drug Delivery Systems”, is itself divided into two self-explained parts. The first part of this section concerns the preparation of mucoadhesives microspheres dextran-based for the treatment of vaginal infections. The second part of this second session, instead, contains all the experiments performed during my scientific visiting in the School of Pharmacy aimed at the development of a cationic palmitoylated glycol chitosan. This promising biopolymer was tested *in vitro* to assess its behaviour against absorptive epithelia and *in vivo* to investigate its biodistribution.

The third section, named “Chemical Modification of Proteins for the Implementation of Drug Delivery Systems”, is itself divided into two self-explained parts. Both are aimed to develop modified proteins based on gelatin and collagen for the preparation of new biomaterials. Particularly, gelatin was functionalized with isoniazid for the creation of nanoparticles employable in the field of tuberculosis treatment; collagen, instead, was covalently linked to  $\alpha$ -tocopherol for the realization of an antioxidant-conjugate for topical applications in the field of wound healing.

The fourth section, named “Hydrogels and Microspheres based on Active Molecules”, contains the preparation of hydrogels and microspheres carrying in their same polymeric structure some bioactive molecules

## Preface

covalently entrapped on the matrices. The active substances used for the development of these drug delivery systems were Rifampicin, Curcumin and Ellagic acid. The idea to incorporate, by a covalent bound, an active moiety into an acrylic-based polymeric device was applied in order to achieve a synergic action with the additional drug soaked into the prepared system.

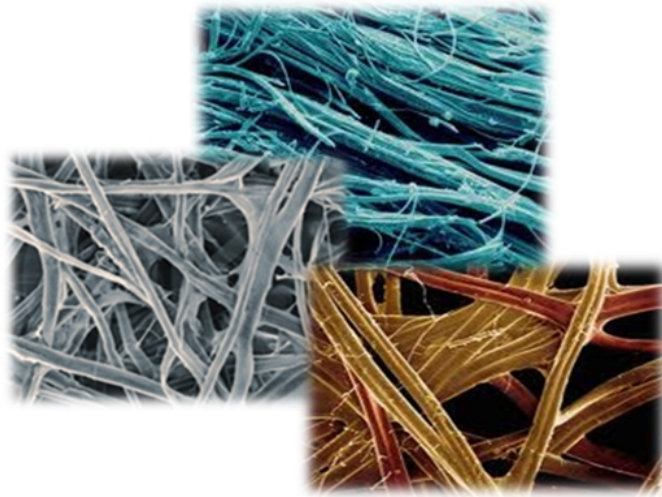
## References

- [1] SA Sreenivas, KV Pai. Thiolated Chitosans: Novel Polymers for Mucoadhesive Drug Delivery-A Review. *Tropical Journal of Pharmaceutical Research* **2008**, 7 (3): 1077-1088.
- [2] Takeuchi H, Yamamoto H, Kawashima Y. Mucoadhesive nanoparticulate systems for peptide drug delivery. *Advanced Drug Delivery Review* **2001**; 47: 39-54.
- [3] Hook AL, Anderson DG, Langer R, Williams P, Davies MC, Alexander MR. High throughput methods applied in biomaterial development and discovery. *Biomaterials* **2010**,31: 187–198.
- [4] Couvreur, P., and Vauthier, C. Nanotechnology: Intelligent Design to Treat Complex Disease. *Pharmaceutical Research* **2006**, 23[7], 1417-1450.
- [5] Kohane DS and Langer R. Polymeric biomaterials in tissue engineering. *Pediatr Res* **2008**, 63: 487–491.



## SECTION 1

### NATURAL FIBERS MODIFICATION FOR THE OBTAINMENT OF BIOMEDICAL MATERIALS



**SYNTHESIS, CHARACTERIZATION, AND ANTI-INFLAMMATORY  
ACTIVITY OF DICLOFENAC-BOUND COTTON FIBERS [1]**

**Abstract**

*Aim:* The present project deals about the synthesis of cellulose cotton fibers covalently linked to diclofenac moieties and the evaluation of the antinflammatory activity of this new biomaterial. In spite of recent progress in experimental and clinical medicine, the problem of chronic wounds treatment is still debated. In fact, conventional methods are based on the use of ointment-soaked bandages but several physical and biological factors contribute to make the efficacy of this method quite low. For this reason, we developed the idea to use modified cotton gauzes to prevent inflammation during wounds healing.

*Methods:* Diclofenac, a non steroidal antinflammatory drug, was covalently linked to the cellulose backbone of hydrophilic cotton fibers by a heterogeneous synthesis to produce a functionalized biopolymer with a satisfactory degree of substitution and antinflammatory activity. Diclofenac was directly linked to fibers microfibrils hydroxylic groups using THF with thionyl chloride.

*Results:* The obtained biopolymer was characterized by infrared spectroscopy (FT-IR) to confirm ester linkages. Finally, the antinflammatory activity was evaluated in a well-established in vivo model.

*Conclusions:* These biomaterials posses an excellent antinflammatory activity “in vivo” and so they can be efficiently employed in biomedical fields for chronic wounds management to ensure a valid protection against inflammation.



## **1. Introduction**

Before the 1960s, wounds dressing was merely considered as a passive therapy to avoid contamination and superinfection of the wound by environmental pathogens. Over the last few decades, pioneering research introduced the idea of an active role for dressing in establishing and maintaining an optimal environment for wound repair [2]. These new advances resulted in the development of functional active dressings which, by interacting with the wound they cover, create and maintain a moist and healing environment [3]. An ideal active dressing should protect wounds from inflammation, provide a safe environment, and be biocompatible [4]. Recently, bandages made from natural polymers such as starch, cellulose, chitin, chitosan, cotton, gelatin, alginate, and dextran were proposed as alternative materials for active wounds dressing [5-9]. These natural fibers were shown to favor wound occlusion, exudate transport, and drug dispensation with much reduced distress to the patient [10]. In particular, the controlled release of bioactive molecules to counteract the progression of infection and inflammation in chronic wounds management was considered a step forward in this research area. In this light, biomaterials in which the active molecules were simply absorbed on the polymer surface [11] were developed and medication-soaked gauzes were made available to patients [12,13]. However, the therapeutic use of soaked gauzes is limited by environmental and biological factors. A different approach consists in the preparation of modified natural polymers, for example, cellulose, covalently bound to bioactive molecules using primary hydroxylic groups. These new materials would be biocompatible, biodegradable, and nontoxic so they could be used to cover infected wounds.

## Section 1

### *1.1 Wound dressings*

Wound dressings and devices are an important segment of the medical and pharmaceutical wound care market worldwide. In the past, traditional dressings such as natural or synthetic bandages, cotton wool, lint and gauzes all with varying degrees of absorbency were used for the management of wounds. Their primary function was to keep the wound dry by allowing evaporation of wound exudates and preventing entry of harmful bacteria into the wound. It has now been shown however, that having a warm moist wound environment achieves more rapid and successful wound healing. The last two decades have witnessed the introduction of many dressings, with new ones becoming available each year. These modern dressings are based on the concept of creating an optimum environment to allow epithelial cells to move unimpeded, for the treatment of wounds. Such optimum conditions include a moist environment around the wound, effective oxygen circulation to aid regenerating cells and tissues and a low bacterial load. Effective wound management depends on understanding a number of different factors such as the type of wound being treated, the healing process, patient conditions in terms of health (e.g. diabetes), environment and social setting, and the physical chemical properties of the available dressings [14]. It is important therefore, that different dressings be evaluated and tested in terms of their physical properties and clinical performance for a given type of wound and the stage of wound healing, before being considered for routine use. A wound can be described as a defect or a break in the skin, resulting from physical or thermal damage or as a result of the presence of an underlying medical or physiological condition. According to the Wound Healing Society, a wound is the result of “disruption of

normal anatomic structure and function” [15]. Based on the nature of the repair process, wounds can be classified as acute or chronic wounds. Acute wounds are usually tissue injuries that heal completely, with minimal scarring, within the expected time frame, usually 8–12 weeks [16]. The primary causes of acute wounds include mechanical injuries due to external factors such as abrasions and tears which are caused by frictional contact between the skin and hard surfaces. Mechanical injuries also include penetrating wounds caused by knives and gun shots and surgical wounds caused by surgical incisions to for example remove tumours. Another category of acute wounds include burns and chemical injuries, which arise from a variety of sources such as radiation, electricity, corrosive chemicals and thermal sources [17]. Chronic wounds on the other hand arise from tissue injuries that heal slowly, that is have not healed beyond 12 weeks [18] and often reoccur. Such wounds fail to heal due to repeated tissue insults underlying physiological conditions [19] such as malignancies, persistent infections, poor primary treatment and other patient related factors. Chronic wounds include decubitus ulcers (bedsores or pressure sores) and leg ulcers (venous, ischaemic or of traumatic origin). Wounds are also classified based on the number of skin layers and area of skin affected [20]. Injury that affects the epidermal skin surface alone is referred to as a superficial wound, whilst injury involving both the epidermis and the deeper dermal layers, including the blood vessels, sweat glands and hair follicles is referred to as partial thickness wound. Full thickness wounds occur when the underlying subcutaneous fat or deeper tissues are damaged in addition to the epidermis and dermal layers. The properties of complex wounds can be summarised as: (a) extensive loss of the integument which comprises skin, hair, and

## Section 1

associated glands, (b) infection which may result in tissue loss, (c) tissue death or signs of circulation impairment and (d) presence of pathology.

### *1.2 Wound Healing*

Wound healing is a specific biological process related to the general phenomenon of growth and tissue regeneration. It progresses through a series of interdependent and overlapping stages in which a variety of cellular and matrix components act together to reestablish the integrity of damaged tissue and replacement of lost tissue [21]. It is composed by five overlapping stages that involve complex biochemical and cellular processes: haemostasis, inflammation, migration, proliferation and maturation phases.

#### *1.2.1 Haemostasis and Inflammation*

Bleeding usually occurs when the skin is injured and serves to flush out bacteria and/or antigens from the wound. In addition, bleeding activates haemostasis which is initiated by exudate components such as clotting factors. Fibrinogen in the exudate elicits the clotting mechanism resulting in coagulation of the exudates (blood without cells and platelets) and, together with the formation of a fibrin network, produces a clot in the wound causing bleeding to stop. The clot dries to form a scab and provides strength and support to the injured tissue. Haemostasis therefore, plays a protective role as well as contributing to successful wound healing. The inflammatory phase occurs almost simultaneously with haemostasis, sometimes from within a few minutes of injury to 24 h and lasts for about 3 days. It involves both cellular and vascular responses. The release of protein-rich exudate into the wound causes vasodilation through release of histamine and serotonin, allows phagocytes to enter the wound and engulf dead cells (necrotic tissue). Necrotic tissue which is

hard is liquefied by enzymatic action to produce a yellowish coloured mass described as sloughy. Platelets liberated from damaged blood vessels become activated as they come into contact with mature collagen and form aggregates as part of the clotting mechanism.

### *1.2.2 Migration and Proliferation*

The migration phase involves the movement of epithelial cells and fibroblasts to the injured area to replace damaged and lost tissue. These cells regenerate from the margins, rapidly growing over the wound under the dried scab (clot) accompanied by epithelial thickening. The proliferative phase occurs almost simultaneously or just after the migration phase and basal cell proliferation, which lasts for between 2 and 3 days. Granulation tissue is formed by the in-growth of capillaries and lymphatic vessels into the wound and collagen is synthesised by fibroblasts giving the skin strength and form. By the fifth day, maximum formation of blood vessels and granulation tissue has occurred. Further epithelial thickening takes place until collagen bridges the wound. The fibroblast proliferation and collagen synthesis continues for up to 2 weeks by which time blood vessels decrease and oedema recedes.

### *1.2.3 Maturation*

This phase (also called the 'remodelling phase') involves the formation of cellular connective tissue and strengthening of the new epithelium which determines the nature of the final scar. Cellular granular tissue is changed to an acellular mass from several months up to about 2 years [22].

### *1.2.4 Wound Exudate*

Wound exudate is a generic term given to liquid produced from chronic wounds, fistulae or other more acute injuries once haemostasis has been

## Section 1

achieved. It is essentially blood from which most of the red cells and platelets have been removed. Exudate is a key component in all the stages of wound healing, irrigating the wound continuously and keeping it moist [23]. The maintenance of a moist wound bed is widely accepted as the most ideal environment for effective wound healing. Exudate also supplies the wound with nutrients and provides favourable conditions for migration and mitosis of epithelial cells. In addition, exudate supplies the wound with leucocytes which helps to control bacteria and reduce the incidence of infection at the wound surface. In certain conditions such as chronic wounds, there is excessive amounts of exudates present which can lead to complications. Increased exudate levels may also be the result of liquefying hard and eschar-like necrotic tissue to produce a wet and sloughy mass by a process known as autolytic debridement.

### *1.3 Effective Wound Management*

Several factors apart from the choice of wound dressings need to be considered to ensure successful wound healing. In the case of chronic wounds, underlying factors such as disease, drug therapy and patient circumstance must all be reviewed and addressed before a particular wound dressing is applied.

#### *1.3.1 Debridement: removing the non viable tissue from a wound*

It is important to remove necrotic tissue or foreign material from areas around the wound to increase the chances of wound healing and this process is known as wound debridement. Debridement of the wound area is important because the open wound bed cannot be observed and assessed effectively with necrotic tissue. The presence of necrotic tissue or foreign material in a wound also increases the risk of infection and

sepsis and also prolongs the inflammatory phase, which inhibits wound healing. Several methods are employed for wound debridement including: surgical removal using scalpel and scissors, hydrotherapy or wound irrigation and autolytic removal by rehydration of necrotic tissue, for example using hydrogel dressings, enzymatic removal using bacterial derived collagenases or preparations such as streptokinase [24].

#### *1.4 Classification of Dressings*

Dressings are classified in a number of ways depending on their function in the wound (debridement, antibacterial, occlusive, absorbent, adherence), type of material employed to produce the dressing (e.g. hydrocolloid, alginate, collagen) and the physical form of the dressing (ointment, film, foam, gel) [25]. Dressings are further classified into primary, secondary and island dressings.

##### *1.4.1 Topical Pharmaceutical Formulations*

These were used commonly in the past and though now less widely used, they are still of some benefit in certain clinical settings for wound treatment. Traditional wound healing agents include topical liquid and semi-solid formulations as well as dry traditional dressings. Topical pharmaceutical formulations are prepared as liquid (solutions, suspensions and emulsions) and semi-solid (ointments and creams) and their use is widespread. Solutions such as povidone-iodine are most effective in the initial stages of wound healing for reducing bacterial load and as debriding and desloughing agents to prevent maceration of healthy tissue by the removal of necrotic tissue from the fresh wound. Antimicrobial agents such as silver, povidone-iodine and polyhexamethylene biguanide [26] are sometimes incorporated into dressings to control or prevent infection. Physiological saline solution is

## Section 1

used for wound cleansing to remove dead tissue and also washing away dissolved polymer dressings remaining in a wound [27]. Saline solution is also used to irrigate dry wounds during dressing change to aid removal with little or no pain. The major problem with liquid dosage forms, however, is short residence times on the wound site, especially where there is a measurable degree of suppuration (exuding) of wound fluid. Semi-solid preparations such as silver sulphadiazine cream and silver nitrate ointment used to treat bacterial infection remain on the surface of the wound for a longer period of time compared with solutions. For highly exuding wounds, semi-solid preparations are not very effective at remaining on the wound area as they rapidly absorb fluid, lose their rheological characteristics and become mobile.

### *1.4.2 Traditional Dressings*

Traditional dressings include cotton wool, natural or synthetic bandages and gauzes. Unlike the topical pharmaceutical formulations, these dressings are dry and do not provide a moist wound environment. They may be used as primary or secondary dressings, or form part of a composite of several dressings with each performing a specific function. Bandages are made from natural (cotton wool and cellulose) and synthetic (e.g. polyamide) materials which perform different functions. The use of soaked gauze for packing open surgical and cavity wounds has also been investigated in the light of their known shortcomings in comparison to the more recent dressings currently available for chronic wounds [28]. Sterile gauze pads are used for packing open wounds to absorb fluid and exudates with the fibres in the dressing acting as a filter to draw fluid away from the wound. Though gauze dressings can provide some bacterial protection, this is lost when the outer surface of the dressing



becomes moistened either by wound exudate or external fluids. In addition gauze dressings tend to become more adherent to wounds as fluid production diminishes and are painful to remove, thus causing patient discomfort. Gauze dressings also provide little occlusion and allow evaporation of moisture resulting in a dehydrated wound bed although gauze impregnated with soft paraffin is occlusive and easier to remove from the skin. It has been suggested that traditional dressings should be employed only for wounds that are clean and dry or used as secondary dressing to absorb exudates and protect the wound. Traditional wound healing agents have been largely replaced for chronic wounds and burns by the more recent and advanced dressings because topical liquid and semi-solid formulations do not remain on the wound surface long enough whilst dry traditional dressings do not provide a moist environment for wound healing.

#### *1.4.3 Modern Wound Dressings*

Modern dressings have been developed as an improvement upon the traditional wound healing agents described above. Their essential characteristic is to retain and create a moist environment around the wound to facilitate wound healing. The modern dressings are mainly classified according to the materials from which they are produced including hydrocolloids, alginates and hydrogels, and generally occur in the form of gels, thin films and foam sheets.

#### *1.5 Biological Dressings*

These dressings are made from biomaterials that play an active part in the wound healing process and sometimes referred to as 'bioactive dressings'. Bioactive wound healing dressings also include tissue engineered

## Section 1

products derived from natural tissues or artificial sources. These technologies usually combine polymers such as collagen, hyaluronic acid, chitosan, alginates and elastin [29]. Biomaterials have the advantage of forming part of the natural tissue matrix, are biodegradable and some play an active part in normal wound healing and new tissue formation. These characteristics make them attractive choices from a biocompatibility and toxicological point of view. In some cases they may be incorporated with active compounds such as antimicrobials and growth factors for delivery to the wound site. Collagen is a natural constituent of connective tissue and a major structural protein of any organ. Its structural, physical, chemical, biological and immunological properties have been discussed widely in the literature. Collagen is known to play a vital role in the natural wound healing process from the induction of clotting to the formation and appearance of the final scar. It stimulates formation of fibroblasts and accelerates the migration of endothelial cells upon contact with damaged tissue. The matrix can also be medicated, thus serving as a reservoir for drug delivery. The use of collagen matrices for delivery of different classes of antibiotic drugs have been discussed extensively [30]. Hyaluronic acid is a glycoaminoglycan component of extracellular matrix with unique physicochemical and biological functions such as lubrication of joints and inflammation processes. It is naturally biocompatible, biodegradable and lacks immunogenicity. Crosslinked hyaluronic acid hydrogel films have also been produced for use as polymeric drug delivery biomaterials [31]. Hyaluronic acid-modified liposomes as bioadhesive carriers for delivering growth factors to wound sites have been studied and reported. A recent open ended study of hyaluronic acid based dressing found them to be effective for managing acute wounds particularly in terms of its safety and efficacy [32]. Chitosan is known to

accelerate granulation during the proliferative stage of wound healing, and its wound healing application has been reviewed. Bioactive dressings are reported to be more superior to conventional and synthetic dressings such as gauze and hydrogel dressings respectively.

### *1.6 Medicated Dressings for Drug Delivery*

The active ingredients used in wound management have evolved alongside the pharmaceutical agents and dressings used to deliver them. The use of topical pharmaceutical agents in the form of solutions, creams and ointments to wound sites have already been described. For example solutions such as thymol and hydrogen peroxide used commonly for cleansing and debridement, also possess antiseptic and antibacterial actions. A new generation of medicated dressings incorporate new chemicals which have therapeutic value, and overcome some of the disadvantages associated with topical pharmaceutical agents. Traditional dressings commonly used to deliver drugs include plain gauze and paraffin impregnated gauze (tulle gras). The modern dressings used to deliver active agents to wounds include hydrocolloids, hydrogels, alginates, polyurethane foam/films and silicone gels. The incorporated drugs play an active role in the wound healing process either directly or indirectly as cleansing or debriding agents for removing necrotic tissue, antimicrobials which prevent or treat infection or growth agents (factors) to aid tissue regeneration. Some of the commonly used active compounds and the dressings (and novel polymer systems) used to deliver them to wound sites are described in the following paragraphs.

#### *1.6.1 Antimicrobials*

The purpose of applying antibiotics and other antibacterials is mainly to prevent or combat infections especially for diabetic foot ulcers, surgical

## Section 1

and accident wounds where the incidence of infections can be high due to reduced resistance resulting from extreme trauma. In some cases, the delivery of certain antibiotics from paraffin based ointments such as bismuth subgallate are known to take active part in the wound healing process [33]. Common antibiotics incorporated into available dressings for delivery to wounds include dialkyl carbamoyl chloride, povidone-iodine used with fabric dressing and silver used with most of the modern dressings. Other antibiotics delivered to wounds include gentamycin from collagen sponges, ofloxacin from silicone gel sheets and minocycline from chitosan film dressings. The delivery of antibiotics to local wound sites may be a preferred option to systemic administration for several reasons. Antibiotic doses needed to achieve sufficient systemic efficiency often results in toxic reactions such as the cumulative cell and organ toxicity of the aminoglycosides in the ears and kidneys [34].

### *1.6.2 Growth Factors*

Whilst antibacterial agents prevent or treat infections and can aid in wound healing, they do not necessarily take an active physiological part in the wound healing process. Growth factors are involved with cell division, migration, differentiation, proteins expression and enzyme production. The wound healing properties of growth factors are mediated through the stimulation of angiogenesis and cellular proliferation, which affects both the production and the degradation of the extracellular matrix and also plays a role in cell inflammation and fibroblast activity [35,36].

### *1.6.3 Supplements*

Another group of active compounds important to the wound healing process are vitamins and mineral supplements including vitamins A, C, E as well as zinc and copper. The dressings employed for the delivery of

vitamins and minerals include oil based liquid emulsions, creams, ointments, gauze and silicone gel sheets. Vitamin A is involved with epithelial cell differentiation, collagen synthesis and bone tissue development. It has also been shown to facilitate normal physiological wound healing as well as reversing the corticosteroid induced inhibition of cutaneous wound healing and post operative immune depression. Vitamin C is an essential compound for the synthesis of collagen and other organic components of the intracellular matrix of tissues such as bones, skin and other connective tissues. It is also involved with normal responses to physiological stressors such as in accident and surgical trauma and the need for ascorbic acid increases during times of injury. In addition, vitamin C aids in improving immune function particularly during infection. Vitamin E has been used in combination with silicone gel sheets for the treatment of hypertrophic and keloid scars [37].

### *1.7 Controlled Drug Delivery to the Wound*

Controlled release of drugs to a given target generally involves prolonging the action of the active drug over time by allowing continual release from a polymeric dosage form. There is however, little literature on the controlled delivery of drugs from polymeric wound dressings. The use of hydrophilic polymers as controlled release dressings has great promise because of the potential advantages they offer.

#### *1.7.1 Advantages of Controlled Drug Delivery*

Controlled delivery dressings can provide an excellent means of delivering drugs to wound sites in a consistent and sustained fashion over long periods of time without the need for frequent dressing change. Bioadhesive, synthetic, semisynthetic and naturally derived polymeric dressings are potentially useful in the treatment of local infections where

## Section 1

it may be beneficial to have increased local concentrations of antibiotics while avoiding high systemic doses [38] thus reducing patient exposure to an excess of drug beyond that required at the wound site. In addition, they are readily biodegradable and therefore can be easily washed off the wound surface, once they have exerted their desired effect. Improvement of patient compliance is another advantage especially in chronic wound management where patients usually undergo long treatments and frequent changing of dressings that can lead to noncompliance. A dressing that will deliver an active substance to a wound site in a controlled fashion for a sustained period of about a week could help solve or minimise this problem.

### *1.7.2 Polymeric Drug Delivery Dressings*

Most modern dressings are made from polymers which can serve as vehicles for the release and delivery of drugs to wound sites. The release of drugs from modern polymeric dressings to wounds has been sparsely reported in the literature with few clinical studies carried out to date. The polymeric dressings employed for controlled drug delivery to wounds include hydrogels such as poly(lactide-co-glycolide) [39] poly(vinylpyrrolidone), poly(vinylalcohol) and poly(hydroxyalkylmethacrylates) [40], polyurethane-foam [41], hydrocolloid and alginate dressings. Other polymeric dressings reported for drug delivery to wounds comprise novel formulations prepared from polymeric biomaterials such as hyaluronic acid, collagen and chitosan. Synthetic polymers employed as swellable dressings for controlled drug delivery include silicone gel sheets and lactic acid. Some of these novel polymeric dressings for drug delivery exist as patents [42]. Composite dressings comprising both synthetic and naturally occurring polymers

have also been reported for controlled drug delivery to wound sites. Sustained release tissue engineered polymeric scaffolds for controlled delivery of growth factors and genetic material to wound sites have also been reported. The modern dressings for drug delivery to wounds may be applied in the form of gels, films and foams whilst the novel polymeric dressings produced in the form of films and porous sponges such as freeze-dried wafers or discs or as tissue engineered polymeric scaffolds [43].

### *1.7.3 Mechanism of Controlled Delivery to Wounds*

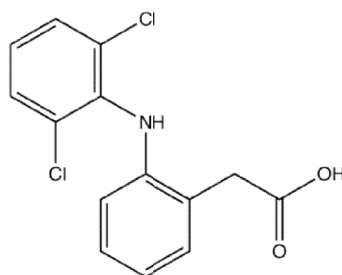
Drug release from polymeric formulations is controlled by one or more physical processes including (a) hydration of the polymer by fluids and (b) swelling to form a gel, (c) diffusion of drug through the swollen gel and (d) eventual erosion of the polymer gel [44]. Although there is little literature in this area for polymeric wound dressings such as hydrocolloids, alginate, hydrogels and polyurethane, it seems feasible that swelling, erosion and subsequent drug diffusion kinetics will play a part in controlled drug release from these dressings when they come into contact with wound exudate. Upon contact of a dry polymeric dressing with a moist wound surface, wound exudates penetrates into the polymer matrix. This causes hydration and subsequent swelling of the dressing to form a gel over the wound surface [45]. As with all polymers, the swelling observed is due to solvation of the polymer chains, which leads to an increase in the end-to-end distance of the individual polymer molecules. In certain wound dressings, the mechanism for drug release has been explained by the hydrolytic activity of enzymes present in the wound exudates [46] or from bacteria in the case of infected wounds. In an aqueous medium, the polymer also undergoes a relaxation process

## Section 1

resulting in slow, direct erosion (dissolution) of the hydrated polymer [47]. It is possible for both swelling and dissolution to operate simultaneously in wound dressings with each contributing to the overall release mechanism. Generally, however, the rate of release of drug is determined by the rate of diffusion of dissolution medium (exudates) into the polymer matrix [48].

### *1.8 Diclofenac*

Diclofenac is an efficient nonsteroidal anti-inflammatory drug used in different diseases such as arthritis, gout, sprains, fractures, back pain, and following minor and major surgery. It has also a very low aqueous solubility especially in gastric juice. This causes undesirable effects on the gastric mucosa when orally taken. For this reason we had the idea to covalently link it on cotton dressings such as a modified bandage to enhance the resolution of an inflammatory process developed in an infected wound (Figure 1).



**Figure 1:** *Molecular structure of Diclofenac*

### *1.9 Aim of the project*

In the present work, diclofenac moieties were covalently linked to cotton fibers to produce a functionalized biomaterial that displayed anti-inflammatory activity in an *in vivo* model of inflammation. In particular,



the ability of this cellulose-linked diclofenac to reduce local chronic inflammation was comparable to the anti-inflammatory effect of this nonsteroidal anti-inflammatory drug when administered intramuscularly.

## **2. Materials and Methods**

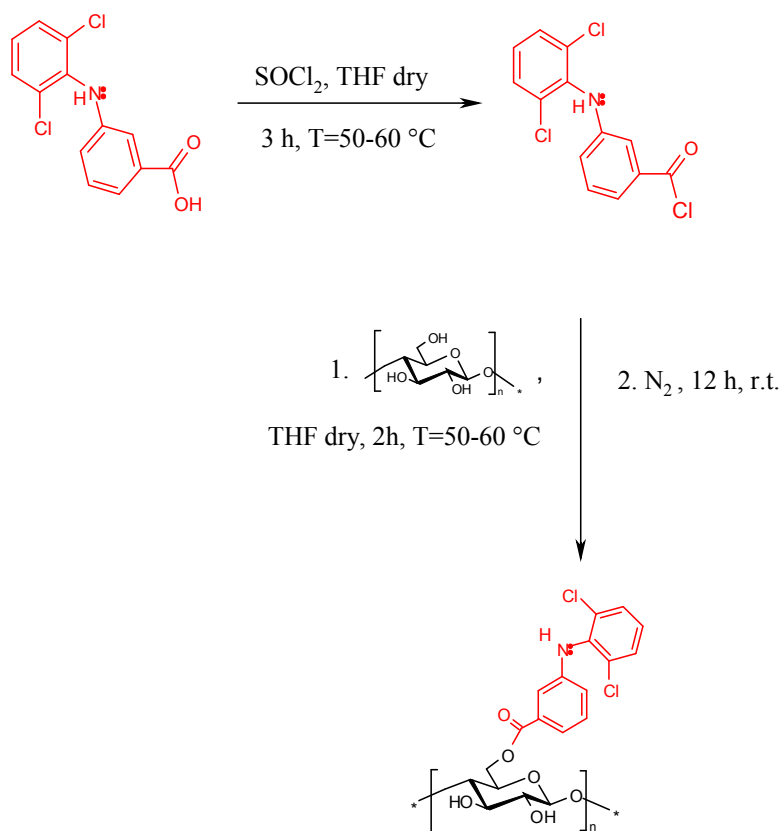
### *2.1 Chemicals*

Thionyl chloride, tetrahydrofuran (THF), acetonitrile, and diclofenac were purchased by Sigma-Aldrich (Sigma Chemical Co, St. Louis, MO), Fluka Chemika-Biochemika (Buchs, Svizzera), and Carlo Erba Reagenti (Milano, Italia). Cotton fibers were hydrophilic commercially available cotton fibers.

### *2.2 Cellulose Functionalization*

A functionalized biopolymer was obtained by heterogeneous synthesis [49], as described in Scheme 1. Briefly, diclofenac (6.6 mmol, 1.956 g) was dissolved in 150 mL of dry THF, thionyl chloride (20 mmol, 1.3 mL) was then added in little excess, and the reaction mixture was allowed to react for 2 h at 50-60 °C with magnetic stirring and under a N<sub>2</sub> reflux. This step allows the formation of the more reactive species diclofenac acyclic chloride that easily binds to the free primary hydroxylic groups of glucose units forming an ester bond. After that, a sample of cellulosic cotton fiber (0.121 g) was added and the reaction was conducted for 3 h under the same conditions. The reaction was maintained overnight at room temperature under magnetic stirring. The product obtained through this two-step procedure was washed with an aqueous saturated solution of sodium bicarbonate to achieve neutrality and then with acetonitrile. Finally, functionalized cotton was dried under vacuum [50] and the calculated yield was 47.4% (0.142 g of the pure product with DS 0.86).

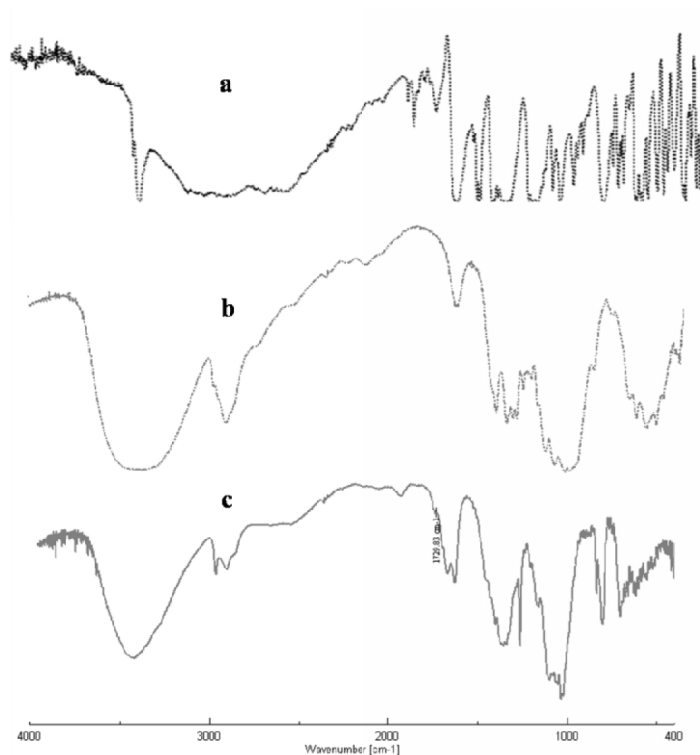
## Section 1



**Scheme 1:** One-pot synthesis to diclofenac-bound cotton

### 2.3 Characterization and Determination of the Degree of Substitution of Functionalized Cotton Fibers

The diclofenac-linked cotton underwent FT-IR spectroscopy to obtain qualitative information about the cotton fibers after derivatization. FT-IR spectra were performed by using a Jasco 4200 spectrometer and KBr lamins. The FT-IR spectra of unreacted cotton fibers (Figure 2a), diclofenac-linked cotton fibers (Figure 2b), and diclofenac (Figure 2c) were recorded. The spectrum in Figure 2b shows the characteristic peak of the carboxylic group of ester at  $1729\text{ cm}^{-1}$ .



**Figure 2:** *FT-IR spectra of diclofenac (a), cotton (b) and diclofenac-linked cotton fibers (c). All infrared spectra were recorded with a FT-IR-spectrometer in the spectral region from 4000 to 400  $\text{cm}^{-1}$  at an instrument resolution of 2  $\text{cm}^{-1}$ . For each spectrum, 25 scans were recorded.*

The degree of substitution was determined by volumetric analysis, dispersing a sample of 50 mg of ester derivative in 5 mL of 0.25 M methanolic sodium hydroxide solution under reflux for 17 h. The dosing, in return for the excess of sodium hydroxide, was realized by titration with 0.1 N HCl (first equivalent point) [51]. The moles of chloride acid used between the first and second equivalence correspond to the moles of free esters. The degree of substitution (DS) was determined by the equation:

## Section 1

$$DS = \frac{MM_{\text{glucose unit}}}{\left(\frac{g_{\text{sample}}}{n_{\text{free ester}}}\right) - MM_{\text{free ester}} - MM_{\text{H}_2\text{O}}}$$

In this equation,  $MM_{\text{glucose unit}}$  is the molecular mass of a glucose unit;  $g_{\text{sample}}$  is the weight of the sample;  $n_{\text{free ester}}$  is the number of moles of free ester;  $MM_{\text{free ester}}$  is the molecular mass of free ester; and  $MM_{\text{H}_2\text{O}}$  is the molecular mass of water. The possibility that diclofenac-linked cotton fibers could spontaneously release diclofenac under pro-inflammatory conditions was also addressed. Briefly, 50 mg of diclofenac-linked cotton fibers were incubated at 37 °C in phosphate-buffered saline (PBS), pH 5.5, under shaking and dark for 5, 14, 21, and 28 days. At each time point, 1 mL of PBS, pH 5.5, was analyzed with a spectrophotometer at a wavelength of 275 nm and an extinction coefficient of 9900 M<sup>-1</sup> cm<sup>-1</sup>. The amount of diclofenac in PBS was evaluated against a calibration curve of pure diclofenac (\*\*\*) in PBS pH 5.5.

### *2.4 Thermal Behavior of Diclofenac-Linked Cellulose Fibers*

Differential scanning calorimetry (DSC) was performed with a DSCNETZSCH 200 by heating 4-5 mg of sample, placed in sealed and pierced 40 μL aluminum pans, at 5 °C min<sup>-1</sup>. Scans of each component were carried out under a flux of nitrogen. Each sample was analyzed at least in triplicate. All data are expressed as mean value.

### *2.5 In Vivo Evaluation of the Anti-Inflammatory Activity of Diclofenac-Linked Cotton Fibers*

All studies were conducted in accordance with the Guidelines of the Italian Ministry of Health for animal care (D.M. 116/1992). Wistar rats were anaesthetized by using chloral hydrate, 400 mg/kg, given by the

intraperitoneal route (i.p.), and 25 mg of either sterile cotton or diclofenac-bound cotton pellets were implanted subcutaneously on the dorsal region under sterile conditions. After 5, 14, 21, and 28 days, rats were euthanized by using an overdose of chloral hydrate (1 g/kg i.p.). The cotton pellets were carefully removed with the attendant shell of granulation tissue and weighed [52,53]. The degree of inflammation was first evaluated by measuring the whole granuloma weight with respect to the initial dry weight of cotton pellets; in fact, the granuloma weight is proportional to the amount of granulation tissue deposited on the cotton pellet. To be more accurate about the degree of inflammation, foreign body granulomas were analyzed by hematoxylin/eosin staining for identifying inflammatory cells and by immunohistochemistry (IHC) using an antimacrophage antibody (anti-CD68 or anti-ED1, Abcam, Cambridge, U.K.). Finally, IHC by using an anticyclooxygenase (COX)-2 antibody was performed on both unreacted and diclofenac-linked cotton fibers. In selected experiments, rats were implanted with sterile cotton pellets as above and treated for 5 days with diclofenac 4-20 mg/kg intramuscularly (i.m.), whereas control rats were treated with saline by the same route (vehicle group). On the fifth day, rats were sacrificed as described above and the granuloma weights were evaluated. At this time point, the rat body weight and food and water intakes were measured and compared with those in the diclofenac-bound cotton fiber group.

### *2.6 Immunohistochemistry*

Foreign body granulomas were routinely fixed overnight in 4% buffered formalin and embedded in paraffin. Sections of tissue samples (4  $\mu\text{m}$ ) were subjected to a immunoperoxidase biotin-avidin reaction in the labeled streptavidinbiotin method (LSAB) for COX-2 and CD68. In

## Section 1

detail, the section for immunohistochemistry was cut and mounted on 3-aminopropyltriethoxysilane-coated slides (Sigma Chemicals; Milan, Italy), allowed to dry overnight at 37 °C to ensure optimal adhesion, dewaxed, rehydrated, and treated with 0.3% H<sub>2</sub>O<sub>2</sub> in methanol for 10 min to block endogenous peroxidase. For antigen retrieval, the section was microwave treated in 10 mM citrate buffer at pH 6 for 10 min and allowed to cool for 20 min (for COX-2), and an enzymatic treatment with Pronase (5 min) was done for CD68. Endogenous biotin was saturated using a biotin blocking kit (Vector Laboratories; Burlingame, CA). The section was incubated at room temperature for 30 min with the COX-2 polyclonal anti-COX-2 antibody (dilution 1:200 Cayman Chemical; Ann Arbor, U.S.A.) and with mouse monoclonal anti CD68 antibody (dilution 1:100). Binding was visualized using biotinylated secondary antibody and the streptavidin-biotin peroxidase complex developed with diaminobenzidine. Finally, slides were counterstained with hematoxylin.

### *2.7 Statistical Analysis*

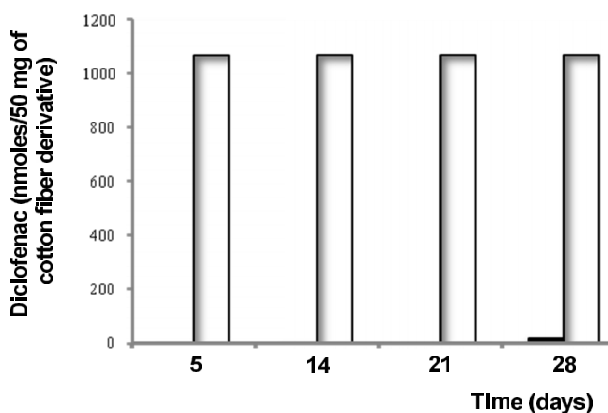
Data are expressed as mean (standard error of the mean (SEM) of *N* replicates per group. Statistical analysis was performed using ANOVA combined two-tailed student's *t* tests for comparison within two groups. Differences were considered significant at  $P < 0.05$ .

## **3. Results**

### *3.1 Synthesis and Characterization of Diclofenac- Bound Cotton Fibers*

As shown in Figure 2c, the product of the reaction between diclofenac and cotton fibers exhibited a FT-IR spectrum characterized by the distinctive peak of the ester carboxylic group at 1729 cm<sup>-1</sup>. Interestingly, neither unreacted cotton (Figure 2b) nor diclofenac (Figure 2a) showed

this characteristic peak. The FT-IR spectrum of the blend composed by cotton fibers and diclofenac compared to those of starting materials and diclofenac-bound cotton fibers resulted in the overlapping of diclofenac and cotton fibers typical peaks (data not shown). The calculated degree of substitution for functionalized cotton was 0.86, a very significant value considering the difficulties due to the proper nature of cotton fiber and to the heterogeneous strategy of synthesis. Thermal characterization of prepared conjugate was also performed by recording DSC thermograms: diclofenac-linked cotton fibers showed the absence of the typical endotherm of diclofenac itself (167.4 °C) and the presence of a broad endothermic peak analogous to that observed in the unreacted cotton (113.5 °C). On the other hand, thermograms of the blend composed by cotton fibers and diclofenac revealed the presence of peaks belonging to starting materials. In addition, diclofenac-bound cotton fibers release only negligible amounts (less than 2%) of diclofenac even at pH 5.5 and 37 °C up to 28 days of incubation (Figure 3).

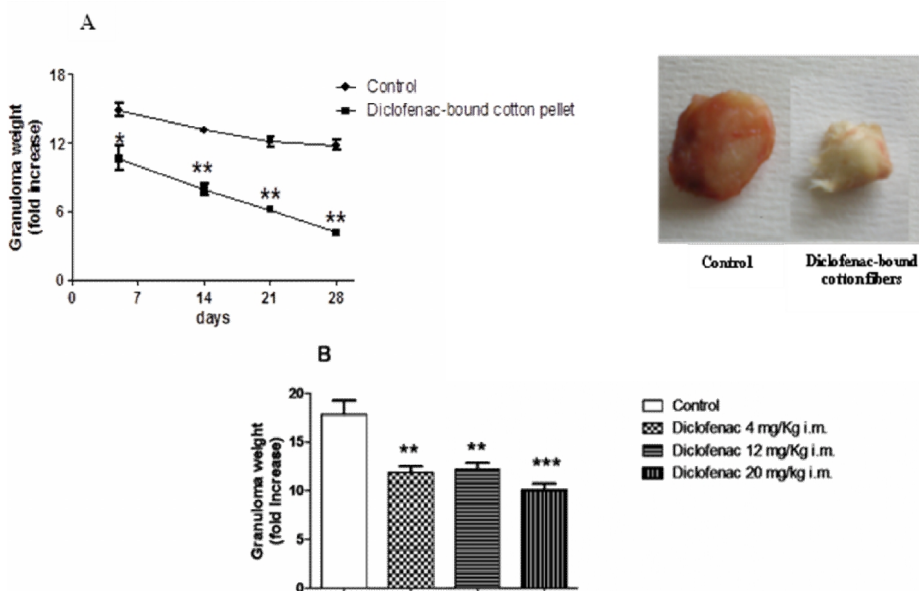


**Figure 3:** Time course of diclofenac release from cotton fiber derivative. White bars, diclofenac bound to cotton fibers; black bar, diclofenac released.

## Section 1

### 3.2 In Vivo Evaluation of the Anti-Inflammatory Activity of Diclofenac-Linked Cotton Fibers

As shown in Figure 4A, diclofenac-linked cotton pellets significantly inhibited the formation of foreign body granulomas over 28 days. The inhibition of granuloma formation was also substantiated by the different external nature of the granulomas (Figure 4A, right).

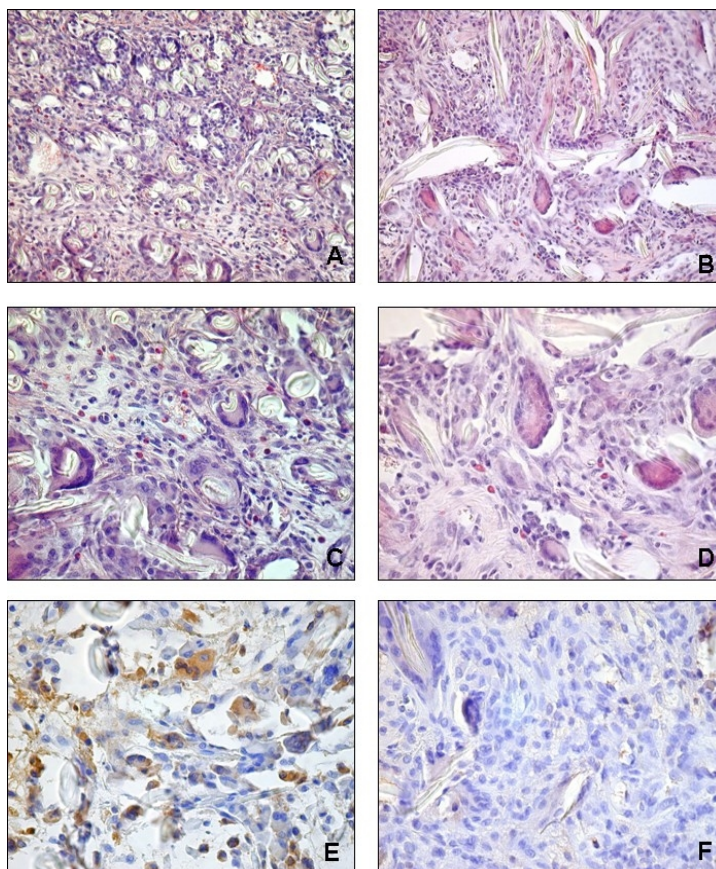


**Figure 4:** Antinflammatory effect of diclofenac-linked cotton fibers. Data are expressed as fold increase in granuloma weight versus dry weight of the cotton pellets, mean  $\pm$  SEM of 8 replicates per group. \* $P < 0.05$  and \*\* $P < 0.01$  versus control (sterile cotton fibers).

The hematoxylin/eosin staining of control granulomas after 5 days revealed the presence of amorphous fibers surrounded by a severe inflammatory infiltrate characterized by both granulocyte and lymphocyte cell population (Figure 5A,C). Furthermore, at the periphery of the lesion, many foreign-body giant cells were found (Figure 5A,C). On the contrary, only a mild inflammatory lymphocytic infiltrate with scattered giant cells

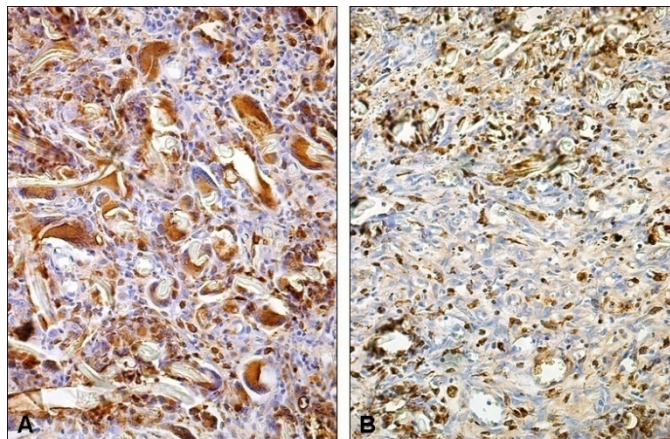


was found in the granulomas formed by the diclofenac-bound cotton fibers 5 days after the implant (Figure 5B,D).



**Figure 5:** *Morphological evaluation of the granulation tissue components in foreign body granulomas.*

The anti-inflammatory activity of diclofenac-bound cotton fibers was finally demonstrated by the evidence that the macrophage infiltrate was markedly lower in the granulomas formed by the diclofenac-bound cotton pellets than control granulomas 5 days after the implant (Figure 6).



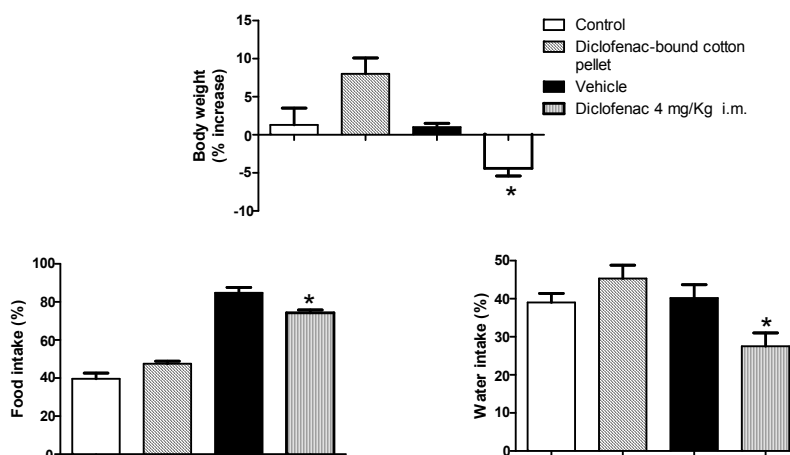
**Figure 6:** *Morphological evaluation of CD-68-positive cells in foreign body granulomas. A) Control (original magnification x200); B) Diclofenac-bound cotton fibers (original magnification x200).*

To better characterize the mechanistic role of diclofenac in this different pattern of inflammation, granulomas underwent immunohistochemistry by using a specific anti-COX-2 antibody. In fact, diclofenac exerts its main anti-inflammatory properties by inhibiting COX activity, thus, avoiding the tissue accumulation of pro-inflammatory compounds such as prostaglandins. In particular, diclofenac modulated COX-2 expression in numerous experimental models of chronic inflammation [54,55]. As shown in Figure 5E,F, positive COX-2 immunostaining was detected in the inflammatory infiltrate in control granulomas, whereas no immunostaining for COX-2 was observed in the granulation tissue formed by the diclofenac-bound cotton fibers 5 days after the implant. To further appreciate the *in vivo* anti-inflammatory activity of the diclofenac-bound cotton fibers, specific experiments were carried out by treating rats with parenteral diclofenac and then evaluating the formation of foreign body granulomas. As shown in Figure 4B, diclofenac 4-20 mg/kg *i.m.* significantly reduced the weight of granulation tissue in respect to vehicle after as little as 5 days of treatment. When cotton-linked diclofenac was

compared with parenteral diclofenac, it appeared that the former has an anti-inflammatory activity comparable to that of 4 mg/kg i.m.

### 3.3 Metabolic Effects of Diclofenac-Bound Cotton Fibers

Five days after surgery, rats implanted with diclofenac bound cotton fibers were evaluated for body weight and food and water intakes. As a comparison, rats implanted with sterile cotton fibers and receiving 4 mg/kg diclofenac i.m. for 5 days were selected. As shown in Figure 7, rats treated with diclofenac, 4 mg/kg i.m., for 5 days underwent a significant reduction in body weight as well as food and water intakes, with these metabolic changes being usually considered hallmarks of systemic toxicity. On the contrary, rats implanted with diclofenac-bound cotton pellets did not exhibit any significant change in the above-mentioned metabolic signs. Similar results have been obtained also at longer time points (data not shown).



**Figure 7:** Body weight, food and water intakes in rats implanted with diclofenac-bound cotton fibers. \* $P < 0.05$  versus vehicle group.

#### **4. Discussion**

In this paper the preparation of a new biomaterial, namely, a diclofenac-bound cotton fiber, was described (Figure 2). The reason why such a new biomaterial would improve the current therapeutic approach to wound healing is quite straightforward. In fact, the use of gauzes, even deriving from natural polymers, soaked with anti-inflammatory or anti-infective drugs posed some limitations. The main concern related to soaked gauzes was the evaporation and the uncontrolled absorption of the active principles they carry depending on physicochemical and biological parameters. Among the physical factors, worthy of mentioning is environmental temperature, whereas the abundance of blood vessels in the subcutaneous and dermal tissues could be responsible for an undesired systemic absorption and drug toxicity. In particular, anti-inflammatory drugs such as diclofenac, although very useful to counteract local inflammation if absorbed through blood vessels, could originate severe side effects on both the gastrointestinal tract and kidney. For this reason, this drug and congeners should not be used for active wound dressing through soaked gauzes. Conversely, the covalent binding to cotton fibers allows diclofenac to be indifferent to environmental factors and elicit a “topical” anti-inflammatory activity without significant toxic effects due to systemic absorption. This hypothesis was corroborated by the experimental results shown in this study. In fact, 5 days after surgery, the chronic inflammatory response in rats implanted with sterile cotton fibers was maximum, as shown both by granuloma weight and pro-inflammatory cell infiltrate, and gradually decreased, reaching over 28 days (Figures 4-6 and data not shown). On the contrary, the anti-inflammatory activity of diclofenac-bound cotton fibers increased over time, reaching a maximum 28 days after implantation (Figure 4). This last

finding supported the hypothesis of the biocompatible nature of this new biomaterial. The covalent binding of diclofenac to cotton fibers through an ester bond did not allow us to exclude a possible release of the active principle mediated by the esterases within the inflamed tissue. However, our experiments performed by incubating diclofenac-bound cotton pellets at 37 °C and under acidic conditions, as during inflammation, demonstrated that the amount of free diclofenac released from cotton fibers over 28 days was negligible (Figure 3). Consistent with these data are also our *in vivo* results, which demonstrated that rats implanted with a diclofenac-bound cotton pellet did not exhibit signs of systemic drug toxicity, such as weight loss or reduced food and water intakes over 28 days, whereas rats treated with parenteral diclofenac at the lower dose of 4 mg/kg displayed these hallmarks of systemic toxicity as early as 5 days (Figure 7 and data not shown). Therefore, even if through indirect evidence, the possibility of a systemic toxic effect of free diclofenac released from cotton fibers could be excluded.

## **5. Conclusions**

In the present study, anti-inflammatory cotton fibers were successfully prepared by binding diclofenac moieties onto a cellulose backbone. The results suggested that these biomaterials have an excellent local anti-inflammatory activity, and so this synthetic strategy can be used to obtain versatile biopolymers that could be efficiently employed in biomedical fields for the treatment of chronic wound management and to ensure a valid protection against inflammation.

**References**

- [1] R. Cassano, S. Trombino, T. Ferrarelli, E. Barone, V. Arena, C. Mancuso, N. Picci. Synthesis, Characterization, and Anti-Inflammatory Activity of Diclofenac-Bound Cotton Fibers. *Biomacromolecules* 2010, *11*, 1716–1720.
- [2] Degim, Z. *J. Drug Targeting* **2008**, *16*, 437-448.
- [3] Huang, M. H.; Yang, M. C. *Int. J. Pharm.* **2008**, *346*, 38-46.
- [4] Lou, C. W. *Fibers Polym.* **2008**, *9*, 286-292.
- [5] Muzzarelli, R. A. A.; Guerrieri, M.; Poteri, G.; Muzzarelli, C.; Armeni, T.; Ghiselli, R.; Cornelissen, M. *Biomaterials* **2005**, *26*, 44-54.
- [6] Mi, F. L.; Shyu, S. S.; Wu, Y. B.; Lee, S. T.; Shyong, J. Y.; Huang, R. N. *Biomaterials* **2001**, *22*, 165-73.
- [7] Kim, I. Y.; Yoo, M. K.; Seo, J. H.; Park, S. S.; Na, H. S.; Lee, H. C.; Kim, S. K.; Cho, C. S. *Int. J. Pharm.* **2007**, *341*, 35-43.
- [8] Edwards, J. V.; Howley, P.; Cohen, I. K. *Int. J. Pharm.* **2004**, *284*, 1-12.
- [9] Lin, F. H.; Tsai, J. C.; Chen, T. M.; Chen, K. S.; Yang, J. M.; Kang, P. L.; Wu, T. H. *Mater. Chem. Phys.* **2007**, *102*, 152–8.
- [10] Miraftaba, M.; Qiaoa, Q.; Kennedy, J. F.; Ananda, S. C.; Groocockc, M. R. *Carbohydr. Polym.* **2003**, *53*, 225-231.
- [11] Adamopoulos, L.; Montegna, J.; Hampikian, G.; Argyropoulos, D. S.; Heitmann, J.; Lucia, L. A. *Carbohydr. Polym.* **2007**, *69*, 805-810.
- [12] Zilberman, M.; Elsner, J. J. *J. Controlled Release* **2008**, *130*, 202-215.
- [13] Denkbaz, B.; Ozturk, E.; Ozdem, N.; Kecec, K.; Agalar, C. *J. Biomater. Appl.* **2004**, *18*, 291-303.

- [14] Morgan DA. Wounds-What should a dressing formulary include? *Hosp Pharmacist* **2002**, 9:261-266.
- [15] Lazarus GS, Cooper DM, Knighton DR, Margolis DJ, Percoraro ER, Rodeheaver G, Robson MC. Definitions and guidelines for assessment of wounds and evaluation of healing. *Arch Dermatol* **1994**, 130:489-493.
- [16] Percival JN. Classification of wounds and their management. *Surgery* **2002**, 20:114-117.
- [17] Naradzay FX, Alson R. Burns, thermal. **2005** *Web MD*.
- [18] Harding KG, Morris HL, Patel GK. Science, medicine and the future: Healing chronic wounds. *Br Med J* **2002**, 324:160-163.
- [19] Moore K, McCallion R, Searle RJ, Stacey MC, Harding KG. Prediction and monitoring the therapeutic response of chronic dermal wounds. *Int Wound J* **2006**, 3:89-96.
- [20] Krasner D, Kennedy KL, Rolstad BS, Roma AW. The ABCs of wound care dressings. *Wound Manag* **1993**, 66:68-69.
- [21] Shakespeare P. Burn wound healing and skin substitutes. *Burns* **2001**, 27:517-522.
- [22] Eccleston GM. Wound dressings. In: Aulton ME, editor. *Pharmaceutics: The science of dosage form design. 3rd edition*. UK: Churchill Livingstone. **2007** pp 264-271.
- [23] Gray D, White RJ. The wound exudate continuum: An aid to wound assessment. *Wounds UK: Applied wound management Suppl.* **2004**, pp 19-21.
- [24] Schultz GS, Sibbald RG, Falanga V, Ayello EA, Dowsett C, Harding K, Romanelli M, Stacey MC, Teot L, Vanscheidt W. Wound bed preparation: A systematic approach to wound management. *Wound Repair Regen* **2003**, 11: S1-S28.

Section 1

- [25] Falabella AF. Debridement and wound bed preparation. *Dermatol Ther* **2006**, 19:317-325.
- [26] Motta GJ, Milne CT, Corbett LQ. Impact of antimicrobial gauze on bacterial colonies in wounds that require packing. *Ostomy Wound Manag* **2004**, 50:48-62.
- [27] Fukunaga A, Naritaka H, Fukaya R, Tabuse M, Nakamura T. Our method of povidone-iodine and gauze dressings reduced catheter-related infection in serious cases. *Dermatology* **2006**, 212: 47-52.
- [28] Dinah F, Adhikari A. Gauze packing of open surgical wounds: Empirical or evidence-based practice? *Ann R Coll Surg Engl* **2006**, 88:33-36.
- [29] Ishihara M, Nakanishi K, Ono K, Sato M, Kikuchi M, Saito Y, Yura H, Matsui T, Hattori H, Uenoyama M, Kurita A. Photocrosslinkable chitosan as a dressing for wound occlusion and accelerator in healing process. *Biomaterials* **2002**, 23: 833-840.
- [30] Ruszczak Z, Friess W. Collagen as a carrier for on-site antibacterial drugs. *Adv Drug Deliv Rev* **2003**, 55:1679-1698.
- [31] Luo Y, Kirke KR, Prestwich GD. Crosslinked hyaluronic acid hydrogel films: New biomaterials for drug delivery. *J Control Release* **2000**, 69:169-184.
- [32] Voinchet V, Vasseur P, Kern J. Efficacy and safety of hyaluronic acid in the management of acute wounds. *Am J Dermatol* **2006**, 7:353-357.
- [33] Nelson EA, O'Meara S, Craig D, Iglesias C, Golder S, Dalton J, Claxton K, Bell-Syer SE, Jude E, Dowson C, Gadsby R, O'Hare P, Powell J. A series of systematic reviews to inform a decision analysis for sampling treating infected diabetic foot ulcers. *Health Technol Assess* **2006**, 10:1-221.



- [34] Chu HQ, Xiong H, Zhou XQ, Han F, Wu ZG, Zhang P, Huang XW, Cui YH. Aminoglycoside ototoxicity in three murine strains and effects on NKCC1 of stria vascularis. *Chin Med J* **2006**, 119: 980-985.
- [35] Komarcevic A. The modern approach to wound treatment. *Med Pregl* **2000**, 53:363-368.
- [36] Defail AJ, Edington HD, Matthews S, Lee WC, Marra KG. Controlled release of bioactive doxorubicin from microspheres embedded within gelatin scaffolds. *J Biomed Mater Res* **2006**, 79:954-962.
- [37] Porto da Rocha R, Lucio DP, Souza Tde L, Pereira ST, Fernandes GJ. Effects of a vitamin pool (vitamins A, E, and C) on the tissue necrosis process: Experimental study on rats. *Aesthetic Plast Surg* **2002**, 26:197-202.
- [38] Lee JW, Park RJH. Bioadhesive-based dosage forms: The next generation. *J Pharm Sci* **2000**, 89:850-866.
- [39] Katti DS, Robinson KW, Ko FK, Laurencin CT. Bioresorbable nanofiber-based systems for wound healing and drug delivery: Optimisation of fabrication parameters. *J Biomed Mater Res B Appl Biomater* **2004**, 70:286-296.
- [40] Thorn RM, Greenman J, Austin A. An in vitro study of antimicrobial activity and efficacy of iodine-generating hydrogel dressings. *J Wound Care* **2006**, 15:305-310.
- [41] Rayman G, Rayman A, Baker NR, Jurgevicene N, Dargis V, Sulcaite R, Pantelejeva O, Harding KG, Price P, Lohmann M, Thomsen JK, Gad P, Gottrup F. Sustained silver-releasing dressing in the treatment of diabetic foot ulcers. *Br J Nurs* **2005**, 9:109-114.

Section 1

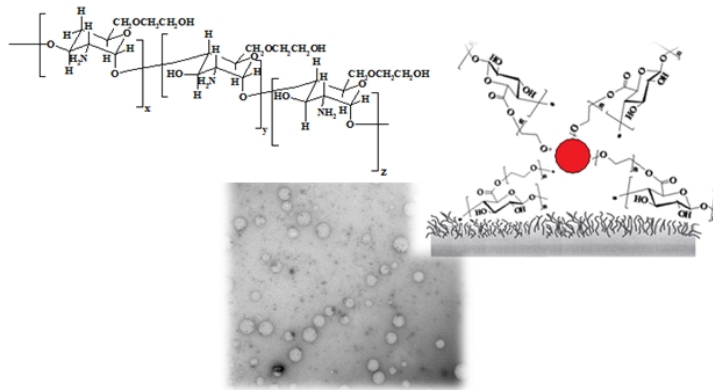
- [42] Qin Y, Keith D, Nephente W **1997**. Dehydrated hydrogels. World patent WO 9739781.
- [43] Sakchai W, Churrerat P, Srisagul S. Development and in vitro evaluation of chitosan-eudragit RS 30D composite wound dressings. *AAPS Pharm SciTech* **2006**, 7:E1-E6.
- [44] Gimeno MJ, Garcia-Esteo F, Garcia-Honduvilla N, San Roman J, Bellon JM, Bujan J. A novel controlled drug-delivery system for growth hormone applied to healing skin wounds in diabetic rats. *J Biomater Sci Polym Ed* **2003**, 14:821-835.
- [45] Aoyagi S, Onishi H, Machida Y. Novel chitosan wound dressing loaded with minocycline for the treatment of severe burn wounds. *Int J Pharm* **2007**, 330:138-145.
- [46] Dubose JW, Cutshall C, Metters AT. Controlled release of tethered molecules via engineered hydrogel degradation: Model development and validation. *J Biomed Mater Res A* **2005**, 74A:104-116.
- [47] Siepmann J, Peppas NA. Hydrophilic matrices for controlled drug delivery: An improved mathematical model to predict the resulting drug release kinetics (the “Sequential Layer” model). *Pharm Res* **2000**, 17:1290-1298.
- [48] Joshua S. Boateng, Kerr H. Matthews, Howard N.E. Stevens, Gillian M. Eccleston. Wound Healing Dressings and Drug Delivery Systems: A Review *Journal of Pharmaceutical Sciences* **2008**, 97(8).
- [49] Klemm, D.; Philipp, B.; Heinze, T.; Heinze, U.; Wagenknecht, W. In *Comprehensive Cellulose Chemistry*; Klemm, D., Philipp, B., Heinze, T., Heinze, U., Wagenknecht, W., Eds.; Wiley-WCH Verlag GmbH: Weinheim, Germany, **1998**; Vol. 2, pp 197-308.
- [50] Cassano, R.; Trombino, S.; Bloise, E.; Muzzalupo, R.; Iemma, F.; Chidichimo, G.; Picci, N. *J. Agric. Food Chem.* **2007**, 55, 9489-9495.

- [51] Trombino, S.; Cassano, R.; Bloise, E.; Muzzalupo, R.; Leta, S.; Puoci, F.; Picci, N. *Macromol. Biosci.* **2008**, *8*, 86-95.
- [52] Meier, R.; Schuler, W.; Desaulles, P. *Experientia* **1950**, *6*, 469–471.
- [53] Meier, R. K.; Stucki, J. C.; Aulesbrook, K. A. *Proc. Soc. Exp. Biol. Med.* **1953**, *84*, 624-628.
- [54] Alvarez-Soria, M. A.; Herrero-Beaumont, G.; Moreno-Rubio, J.; Calvo, E.; Santillana, J.; Egido, J.; Largo, R. *Osteoarthritis Cartilage* **2008**, *16*, 1484-1493.
- [55] Alvarez-Soria, M. A.; Largo, R.; Santillana, J.; Sanchez-Pernaute, O.; Calvo, E.; Hernández, M.; Egido, J.; Herrero-Beaumont, G. *Ann. Rheum. Dis.* **2006**, *65*, 998-1005.



## SECTION 2

# CHEMICAL MODIFICATION OF CARBOHYDRATES FOR THE IMPLEMENTATION OF DRUG DELIVERY SYSTEMS



- **Part A:** Mucoadhesive microspheres dextran and polyethylene glycol-based for the treatment of vaginal infections;
- **Part B:** Synthesis, characterization, *in vitro* cell uptake and *in vivo* biodistribution studies of a cationic glycol chitosan polymer for oral administration of hydrophobic drugs.

## PART A

### MUCOADHESIVE MICROSPHERES DEXTRAN AND POLYETHYLENE GLYCOL-BASED FOR THE TREATMENT OF VAGINAL INFECTIONS

#### **Abstract**

*Aim:* Synthesis and preparation of polymeric systems based on dextran, a polysaccharide of bacterial origin, and polyethylene glycol, non-toxic and biocompatible material, for the controlled release of an antifungal drug, such as ketoconazole, in the vaginal environment.

*Methods:* Polyethylene glycol monosubstituted with an acrylic moiety was linked to 6-carboxy dextran and then this final product was subjected to radical polymerization with a comonomer in order to obtain a three-dimensional structure as microspheres for the controlled release of ketoconazole. The obtained materials were submitted to studies on their ability to absorb and retain water, as well as on their therapeutic potential as a carriers of drug molecules.

*Results:* Microspheres have higher affinity towards the aqueous media at pH 8. These latters, loaded with ketoconazole, were also subjected to preliminary release studies conducted in the pH conditions described above showing that ketoconazole is significantly released within 24 hours at pH=8 and, in particular, the release is greater in the first 4 hours. This is probably due to interactions of drug with the hydroxyl groups of dextran glucosidic rings. In fact, the high content of heteroatoms in ketoconazole enhances the formation of hydrogen bonds with these groups, resulting in an increased entrapment of the drug on microspheres surface rather than in their inner.

*Conclusions:* Obtained data suggest the possibility of using dextran-based microspheres as mucoadhesive systems for the controlled and site-specific release of active molecules useful in the treatment of vaginal mycosis.

## **1. Introduction**

Mucoadhesive drug delivery systems (MDS) have become hugely interesting in the last 10-15 years. Their ability to stick to mucous membranes (mucosa, from Lat. *mucus*) attracted attention as a pathway for resolving the problem of low bioavailability of traditional delivery systems (DS) used in the oral cavity and on the surface of the eye or other organs where movement of tissues or production of various secretions prevents prolonged retention of the medicinal agent (MA) [1]. The MDS concept evolved from the original idea of increasing the effectiveness of local therapy of infectious diseases of the mucosa to effective use of the intranasal and buccal pathways of administration for systemic action of drugs [2]. Many drug delivery systems are based on so called “mucoadhesive polymers”.

### *1.1 Mucoadhesion in the vaginal environment*

Mucoadhesion is another version of the bioadhesion because the target is still the underlying tissue. The polymers used in this field are able to swell rapidly when placed in aqueous environment and therefore exhibiting a controlled drug release. Since the first presentation of the concept of mucoadhesion, many attempts have been undertaken to improve the adhesive properties of such polymer systems [3]. Consequently, the therapeutic efficacy of locally acting drugs can be improved by their increased availability at the target membrane. Rational

design of future formulations need to include attention to vehicle properties that optimize vaginal coating and retention. Apart from local effective drugs, the vagina provides also a promising site for systemic drug delivery, because of its large surface area and rich blood supply [4]. This route of administration offers advantages compared to other routes. Considerable progress has been made in this research area over the past few years and, at present, the anatomy and physiology, microflora and secretions of the vagina are well understood. In contrast, the scientific knowledge regarding the possibilities of drug delivery via the vagina is limited. To date, there are only a limited number of vaginal dosage forms available, although various possibilities are presently being explored. The currently available vaginal delivery systems have limitations, such as leakage, messiness and low residence time, which contribute to poor subject or patient compliance. Attempts are being made to develop novel vaginal drug delivery systems that can meet the clinical as well as the requirements of the patients. However, despite all the advantages of a vaginal application, changes of the membrane during the menstrual cycle and postmenopausal must be taken into account. In postmenopausal women the reduced epithelial thickness may change the original absorption rates of drugs significantly. It should be taken into account that formulations interact with the vaginal fluids and cause changes in viscosity. The interactions depend upon the specific macromolecules which are the thickening agents for gels or important auxiliary agents in tablets. Therefore, these macromolecules, such as poly(acrylates), cellulose-derivatives, dextran, chitosan and many others, are very important excipients for future formulations. The vagina plays a major role in reproduction and it is an important organ of the reproductive tract. It is a strong canal of muscle and approx. 7.5 cm long that extends from



the uterus to the vestibule of the external genitalia. The vagina is positioned between rectum, bladder and urethra. The function and construction is significantly different to the intestinal wall. In contrast to the intestine, there is no peristaltic motion but it is also not rigid. The vaginal wall consists of three layers: the epithelial layer, the muscular coat and tunica adventitia. A cell turnover of about 10–15 layers is estimated to be in the order of 7 days. The epithelium is a noncornified, stratified squamous epithelium. The thickness is dependent on age. With hormonal activity the vaginal epithelium increases in thickness and is highest in the proliferative stage and reaches the highest glycogen content during ovulation. The epithelium thickness is also dependent on the different life stages like newborn, child, adult and menopause. The main blood supply to the vagina is through the vaginal branch of the uterine artery. The vagina has unique features in terms of microflora, pH and cyclic changes, and these factors must be considered during the development and evaluation of vaginal delivery systems. The ecology of the vagina is influenced by factors such as the glycogen content of epithelial cells, glucose, pH, hormonal levels, trauma during sexual intercourse, birth-control method, age, antimicrobial treatment and delivery. The vaginal flora is a dynamic system mainly consisting of Lactobacillus (Doderlein's bacilli) which is the most prevalent organism in the vaginal environment together with many other facultative and obligate aerobes and anaerobes. Normal microflora, predominantly lactobacilli, produce sufficient lactic acid to acidify vaginal secretions to pH 3.5–4.5. This value is maintained by the lactobacilli which convert glycogen from exfoliated epithelial cells into lactic acid [5]. The pH changes with age, stages of menstrual cycle, infections and sexual arousal. In most of the women, a pH gradient exists in the vagina.

Menstrual, cervical and uterine secretions and semen act as alkalising agents and increase the pH. The pH plays also a role in amount of drug absorption and is important for drug delivery systems. The conception of such a drug delivery system should correlate to the amount of the vaginal fluid in order to exclude a loosening of the epithelium barrier. The anatomical position, the rich blood supply and the large surface area of the vagina predestines it as an application site for systemic drug delivery. In numerous studies a good permeability to a wide range of compounds including peptides and proteins has been shown [6]. The vaginal route offers a favorable alternative to the parenteral route for some drugs such as bromocriptine [7], propranolol, oxytocin [8] calcitonin, LHRH agonists, human growth hormone and steroids used in hormone replacement therapy or for contraception [9]. Compared to the oral cavity, the vagina might serve as a route for the delivery of hormonal contraceptives owing to the lack of drug interactions observed in the gastrointestinal tract. However, despite all these advantages, the vagina has not been extensively explored for systemic delivery because of gender specificity and cyclic variations. The vaginal route also has potential for the uterine targeting of active agents such as progesterone and danazol [10]. The plasma concentrations of vaginally administered progesterone were found to be higher in the uterine artery than in the radial artery, indicating a preferential distribution of progesterone to the uterus. This confirmed the existence of direct local transport from the vagina to the uterus, termed the “first uterine pass effect”. Despite the fact that vaginal delivery is only available for females there are a number of advantages for the vaginal route of administration like: the avoidance of hepatic first-pass metabolism; this has been reflected e.g. by the greater bioavailability of propranolol after vaginal administration compared with oral delivery. It

overcomes the inconvenience caused by pain, tissue damage and probable infection by parenteral routes. Another advantage is the possible self-insertion and removal of the dosage form. In addition to being gender specific, the vaginal route is less preferable in terms of convenience depending on the dosage form. Another disadvantage is the influence of the estrogen concentration on the permeability of the vaginal membrane, which can influence the pharmacokinetics of drugs designed for systemic action.

### *1.2 Bioadhesive polymers*

Several bioadhesive polymers have been reported for different mucosal sites such as the buccal cavity, stomach and intestine. An increasing interest has been shown for vaginal bioadhesive tablets. With respect to their facilitated and shorter registration, the polymers which were already in use as pharmaceutical excipients were tested for their mucoadhesive properties. Smart et al. [11] published a list of mucoadhesive polymers together with a rank order of their mucoadhesive force. Their in-vitro test system consisted of a homogenized mucus which was obtained by scraping guinea-pig intestines. The force required to detach a glass plate coated with the test polymer from this mucus gel was measured. In general the polymers had a high molecular weight and hydrophilic functional groups. Several groups of polymers have been tested as vaginal delivery systems:

*Poly(acrylates)*: in most of the vaginal preparations poly (acrylic acid) derivatives have been used as bioadhesive polymers. Since the 1980s local contraceptives are used and have been investigated for their absorption [12].

## Section 2 – PART A

*Chitosan:* in contrast to the poly(acrylates), chitosan is a natural polycationic copolymer consisting of glucosamine and N acetylglucosamine units. Chitosan also shows mucoadhesive properties and antimicrobial activity. The use of natural polymers is valuable based on proven biocompatibility and safety. Chitosan possesses favorable properties and hence has applications in the pharmaceutical and biomedical fields. It is a promising bioadhesive material at physiological pHs. This polymer possesses OH and NH<sub>2</sub> groups that can give rise to hydrogen bonding. These properties are considered essential for mucoadhesion. Moreover, chitosan is suited for repeated adhesion, since it did not become inactivated after the first contact and no drop in mucoadhesion resulted. Formation of interpolymer complexes of chitosan with alginate and sodium carboxymethylcellulose (CMC) was investigated [13]. One study accounts for the possible use of chitosan in mixtures of different ratios with anionic polymers for the preparation of mucoadhesive tablets to be used as a vaginal delivery system for metronidazole [14]. Furthermore chitosan-4-thio-butyl amidin-conjugates (chitosan-TBA) could be of advantage for mucoadhesive vaginal drug delivery systems [15].

*Cellulose-derivatives:* within the listed polymers displaying mucoadhesive properties especially sodium carboxy methylcellulose had excellent mucoadhesive properties. Gynol II, a contraceptive Jelly<sup>®</sup>, contains sodium carboxymethylcellulose as a mucoadhesive polymer and is used as a spermicidal contraceptive in conjunction with barrier methods of contraception.

*Hyaluronic acid and derivatives:* hyaluronic acid microspheres as vaginal drug delivery systems are suggested for the systemic delivery of

calcitonin by the vaginal route. A further development of such microspheres were based on hyaluronan esters.

*Starch*: insulin was administered vaginally to sheep as an aqueous solution and as a lyophilized powder within bioadhesive starch microspheres.

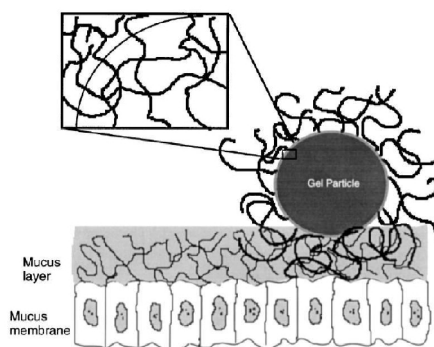
*Poly(ethylene glycol)*: the use of poly(ethylene glycol) offers a number of possibilities for controlled drug release in dependence of physical properties such as molecular weight (3000-8000), specific hydrates and changing diffusion coefficient of crystalline/rubbery hydrogels which affect the diffusion of drugs through the water swollen matrix and across the polymer boundary. The advantage of starting with a dry, drug impregnated polymer is to obtain the desirable zero order release rate [16]. Although the quantitative bio(muco)adhesiveness of polyethylene glycol was quoted as poor, Graham et al. reported a hydrogel prepared from polyethylene glycol 600 providing constant release rates for prostaglandin E<sub>2</sub> (PGE<sub>2</sub>). The polymer was almost colorless, opaque, tough and could be swollen by solvents. Polymer vaginal pessaries containing 10 mg PGE<sub>2</sub> released the 90% of PGE<sub>2</sub> during 24 h [17].

To date most of the existing dosage forms are based on the synthetic poly(acrylates) but in the near future natural compounds such as chitosan, dextran or carrageenan and new derivatives will gain more significance [18].

### *1.3 Proposed mechanisms and promoters for bioadhesion*

The adhesion of a polymer to a tissue involves the contribution of three main regions: the surface of the bioadhesive material, the first layer of natural tissue and the region of interface between the two layers. The development of a device depends on understanding precisely how these

three components interact with each other, so it is possible to edit the properties and improving their adhesion. The adhesion between a polymer and the tissue is mainly due to three types of interaction: physical or mechanical bonds, chemical bonds, secondary or primary chemical bonds, ionic or covalent ones. The functional groups that can give hydrogen bonds are: hydroxyl, carboxyl, sulfate groups and amino groups, both on the bioadhesive material that on the mucus glycoproteins. The primary bonds are formed by chemical reaction between polymer and substrate. This type of bond is desirable only when the connection between the substrate and the adhesive must be permanent, such as in orthopedic or dental applications. For this reason, most of bioadhesive bonds [19] is achieved through physical bonds, hydrogen bonds, or other secondary bonds. The hydrogen bond is the most important type of secondary bond in bioadhesion and, consequently, polymers containing hydroxyl and carboxyl groups, such as polyethylene glycol, poly(vinylalcohol), poly(acrylic acid), poly(hydroxy alchilmethacrylate) and their respective copolymers are ideal candidates thanks to the high density of their associated chains that can provide a number of anchor points able to sustain the attractive forces. The adhesion of the drug delivery system can be enhanced by two types of promoters: the free polymer chains in the interface and the polymer chains placed on the surface of the system. Promoters are polymeric chains, different from the chains that take part in the basic structure of the system, useful for the sustenance of attractive forces (Figure 1).



**Figure 1:** *Polymeric chains of promoters sustaining adhesive forces*

An additional advantage of promoters, covalently linked to the basic structure of the drug delivery system, is the ability to promote a site-specific release. In fact, the matrix may have units designed specifically to adhere with a particular surface. It is well known that certain amino acid sequences are complementary to some sequences on the cell and mucosal surfaces. For example, the amino acid sequences Arg-Gly-Asp and other, if attached to the matrix, may promote adhesion by binding with specific cell surface glycoproteins. Even more useful would be the ability to stick selectively to diseased tissues.

#### *1.4 Polyethylene glycol as promoter of bioadhesion*

Polyethylene glycol (PEG), characterized by two terminal primary hydroxyl groups, is the most common commercial polymer, widely used as an inert polymeric support in organic synthesis and as a conjugating agent for biologically active molecules due to its unique characteristics of solubility and stability. In particular, the formation of a stable bond with PEG allows the stabilization and solubilization "*in vivo*" of pharmacologically active molecules, reducing their toxicity and antigenicity, as well as enhancing cell penetration. In addition, the

solubility of the PEG can solve the problems related to the transport and distribution of these drugs in tissues.

### *1.5 Dextran-based hydrogels*

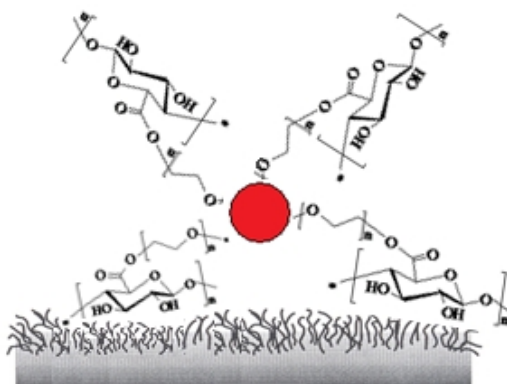
Dextran hydrogels have received an increased attention due to their variety of biotechnological and biomedical applications. Owing to their low tissue toxicity and high enzymatic degradability at desired sites, dextran hydrogels have been frequently considered as a potential matrix system for controlled release of bioactive agents. Several approaches to prepare dextran hydrogels have been adopted. Dextran hydrogels have been studied extensively in various areas, such as drug carriers. Due to their good tissue biocompatibility and the possibility of to transport specific drugs, they appear to be a viable alternative to the existing drug carriers [20].

### *1.6 Polymeric microspheres*

Polymeric microspheres are the most modern and widely used system for the modified release of drugs; they can encapsulate small molecules, like proteins or nucleic acids; generally produced with biocompatible materials, they can sustain the release of active molecules for long periods of time. Dextran microspheres are generally obtained by radical polymerization reaction in reverse phase emulsion. With this innovative and versatile technique is very easy to obtain materials with adaptable properties. In the systems obtained with this method, dextran chains are highly cross-linked through covalent bonds and this gives them more stability and mechanical strength compared to systems where the same chains are connected by weak interactions and/or easily hydrolysable bonds. The radical polymerization has a chain growth mechanism that



begins with the formation of primary radicals produced by cleavage of a suitable initiator. In order to propagate the reaction on the polysaccharide chains [21], allowing cross-linking, on these chains functional groups capable of interacting with the radical species and to be converted into active centers of propagation, must be present. These functional groups are not present on dextran molecules, they have to be introduced with appropriate derivatisation using a chemical containing a feature likely to radical polymerization or double bonds able of undergoing free radical polymerization, such as acrylic and methacrylic compounds (Figure 2).



**Figure 2:** *Mucoadhesive polymeric microspheres dextran-based*

Characteristics of obtained microspheres depend on the degree of crosslinking, which is in turn influenced by the degree of substitution of dextran (DS) and the amount of monomer and reticulant agent used in the polymerization reaction. This work is devoted to the design, synthesis and evaluation of polymeric systems based on dextran, a polysaccharide of bacterial origin, and polyethylene glycol, non-toxic and biocompatible material, for the controlled release of antifungal drugs in the vaginal environment. Polyethylene glycol monosubstituted with an acrylic moiety was linked to 6-carboxy dextran and then this final product was subjected

to radical polymerization with a comonomer in order to obtain a three-dimensional structure as microspheres for the controlled release of ketoconazole. The obtained materials were submitted to studies on their ability to absorb and retain water, as well as on their therapeutic potential as a carriers of drug molecules.

## **2. Materials and Methods**

### *2.1 Materials*

All solvents of analytical grade, were purchased from Carlo Erba Reagents (Milan, Italy): acetone, chloroform, dichloromethane, ethanol, ethyl ether, isopropanol, methanol, N, N-dimethylformamide (DMF), n-hexane, hydrochloric acid (37%), formic acid and tetrahydrofuran (THF). N-hexane, chloroform, N,N-dimethylformamide (DMF) and tetrahydrofuran were purified by standard procedures. Dextran from *Leuconostoc* spp. (Mr 15000-20000), Poly(ethylene) glycol 200, 3,4-dihydro-2H-pyran, aluminum chloride hexahydrate, sodium nitrite, acryloyl chloride, triethylamine, methylene blue, boric acid, sodium hydroxide, sorbitan trioleate (Span 85), polyoxyethylene sorbitan trioleate (Tween 85) N,N,N',N'-Tetramethylethylenediamine (TMEDA), methylene bisacrylamide (MBA), ammonium persulfate (APS), dicyclohexylcarbodiimide (DCC), dimethylaminopyridine (DMAP) and thionyl chloride (SOCl<sub>2</sub>) were purchased from Sigma-Aldrich (Sigma Chemical Co, St. Louis, MO, USA).

### *2.2 Instruments*

The infrared spectra were performed on KBr pellets using a FT-IR spectrometer Perkin-Elmer 1720, in the range 4000-400 cm<sup>-1</sup> (16 scans). The <sup>1</sup>H-MNR were performed by a spectrometer Burker VM30; the

chemical shifts are expressed in  $\delta$  and are related to the solvent. The structures of synthesized compounds was confirmed by GC-MS Hewlett Packard 5972. The UV-VIS spectra were carried out using JASCO-530 UV spectrophotometer. Samples were freeze-dried using a freeze-drying "Micro Modulyo Edwards apparatus". Dimensional analyses of microparticles were realized trough a Dinamic Laser Light Scattering Brookhaven 90 plus particle size analyzer.

### *2.3 Synthesis of 6-carboxy dextran (1)*

Reaction was carried out in agreement with the procedure reported in literature [22]. In a three-neck flask fitted with a reflux condenser, funnel dripper, magnetic stirring, thoroughly flamed and maintained under nitrogen bubbling, dextran (0,5 g, 0,0333 mmol) was dissolved in H<sub>3</sub>PO<sub>4</sub> 85% w/w (20 mL) and magnetically stirred for 2 hours until complete dissolution. Afterthat, the first aliquot of sodium nitrite (0.5 gr, 7.2 mmol) was added maintaining a vigorous agitation for 15 minutes. Stirring was stopped for 5 hours during which a stable foam was produced; this latter was destroyed by stirring and adding a second aliquot of sodium nitrite. The same procedure was repeated 3 hours later. After a total reaction time of 10 hours, 5 mL of formic acid 85% w/w were added in order to destroy the excess of sodium nitrite. Finally, the polymer was washed and precipitated with cold acetone and diethyl ether (esotermic reaction). The product was washed with distilled water until neutrality was achieved, with an aqueous solution of ethanol 50% v/v and then with absolute ethanol. The oxidized polymer was dried under vacuum and at high temperature by using a vacuum pump and an oil bath. Oxidation was confirmed trough FT-IR spectrometry.

Section 2 – PART A

*2.4 Determination of carboxylic groups content in (I) by Methylene Blue Sorption.*

A weighted sample of (1) was suspended in 25 mL of aqueous methylene blue chloride solution (300 mg/L) and 25 mL of borate buffer pH 8.5 for 1 h at 20 °C in a 100 mL flask and then filtered. Ten milliliters of the filtrate were transferred to a 100 mL calibrated flask. Then 10 mL of 0.1 N HCl and subsequently water, up to 100 mL, were added. Then the methylene blue content of the liquid was determined photometrically, employing a calibration plot ( $\epsilon = 86126 \text{ ml/mg} \times \text{cm}^{-1}$ ), and from the result the total amount of free, nonsorbed, methylene blue is calculated. The carboxyl group content of the sample is obtained according to the following equation:

$$\text{mmol of COOH/g of oven-dry sample} = [(7.5 - A) \times 0.00313] / E$$

where  $A$  is the total amount of free methylene blue (mg) and  $E$  is the weight of oven-dry sample (g) [23]. Table 1 shows the amounts of reagents and solvents used, and the content of carboxylic groups COOH expressed in mmol/g.

<i>6-carboxy dextran</i>	<i>Reagents</i>			<i>Solvent</i>	<i>COOH content</i>
(g)	Borate buffer pH 8.5 (ml)	HCl 0.1N (ml)	BM (ml)	H <sub>2</sub> O (ml)	mmol COOH/g
0.05	25.0	10.0	25.0	100.0	0.80

**Table 1**

*2.5 Protection of the primarily hydroxylic function of PEG 200 by tetrahydropyranylation (2)*

In a two-neck flask fitted with a reflux condenser, funnel dripper, magnetic stirring, thoroughly flamed and maintained under nitrogen bubbling, PEG200 (22.54 ml, 100 mmol) was allowed to react in the presence of 3,4-dihydro-2H-pyran (8.53 ml, 110 mmol) and aluminum chloride hexahydrate (0.24 gr, 1 mmol). The mixture was maintained under reflux and magnetic stirring for 1 hour at 30 °C [24]. Reaction was monitored through TLC on aluminium oxide plates (eluent mixture chloroform/methanol 1:1). After that, reaction mixture was hydrolyzed and extracted with chloroform to remove any trace of unprotected PEG200. The obtained product, in the form of liquid, was characterized through FT-IR and <sup>1</sup>H-NMR spectroscopies.

*2.6 Acrylation of (2)*

In a three-neck flask fitted with a reflux condenser, funnel dripper, magnetic stirring, thoroughly flamed and maintained under nitrogen bubbling, a small amount of (2) (10 mL, 39 mmol) and triethylamine (6.56 ml, 47 mmol) were dispersed in 10 mL of dry THF. After that, acryloyl chloride (3.82 ml, 47 mmol) dissolved in 5 mL of dry THF was added dropwise. This mixture was left under reflux and magnetic stirring at 25 °C for 24 hours [25]. Reaction was monitored through TLC on silica gel plates (eluent mixture: chloroform); the product (3) was purified through a chromatographic column on silica gel, dried under vacuum and characterized through FT-IR and <sup>1</sup>H-NMR spectroscopies.

### *2.7 Deprotection of (3)*

In a three-neck flask fitted with a reflux condenser and magnetic stirring, thoroughly flamed and maintained under nitrogen bubbling, product **3** (1 gr, 2.94 mmol) and aluminum chloride hexahydrate (0.004gr, 2999.85 mmol) were dissolved in 30 mL of dry chloroform; dry methanol (1mL, 24,65 mmol) was also added. Mixture was left under reflux and magnetic stirring for 24 hours at 25 °C [24]. Product **4** was dried under vacuum and characterized trough FT-IR and <sup>1</sup>H-NMR spectroscopies.

### *2.8 Esterification of 3 with 1: linkage of acryloyl-PEG to 6-carboxy dextran (5)*

In a three-neck flask fitted with a reflux condenser and magnetic stirring, thoroughly flamed and maintained under nitrogen bubbling, 6-carboxy dextran (0.63 gr, 0.8 mmol ×g<sup>-1</sup> of dry sample) was dissolved in 5 mL of dry DMF. Reaction was left under reflux and magnetic stirring at 35°C for 30 minutes [26]. Afterthat, DCC (0.066 gr, 0.32 mmol) and DMAP (6,1×10<sup>-3</sup> g, 0.05 mmol) were added and the system was stirred for 30 minutes. Reaction was, finally, carried out at room temperature and then **4** (acryloyl-PEG) was added (0.0462 gr, 0.32 mmol). Mixture was kept under magnetic stirring for 72 hours and monitored trough TLC on silica gel (eluent mixture chloroform:methanol 4:1). In the end, reaction mixture was hydrolyzed and extracted with chloroform. Product **5** was dried under vacuum and characterized trough FT-IR and <sup>1</sup>H-NMR spectroscopies.

### *2.9 Microspheres preparation based on (5)*

Microspheres based on **5** were produced by radical copolymerization technique. Briefly, a cylindrical glass reactor of 100-150 ml equipped

with mechanical stirrer and dripping funnel, screw cap with puncture-proof rubber septum was flamed in a nitrogen flow and after cooling was immersed in a bath thermostatically controlled at 40° C. Then, required amount of *n*-hexane (20 ml) and chloroform (18 ml), constituting the dispersant phase, were introduced into the reactor. After 30 min of N<sub>2</sub> bubbling, this mixture was treated with distilled water containing **5** (0.5 gr), MBA (0.009gr, 5.8 x 10<sup>-2</sup> mmoli) and ammonium persulfate such as radical initiator (0.8gr, 3.5 mmol). Under stirring at 1000 rpm, the mixture was treated with Span85 and Tween85, then after 10 min with TMEDA and stirring was continued for another 60 min [21]. The amounts of all reagents used in these experiments are reported in Table 2. The microspheres so obtained were filtered, washed with 50 ml portions of 2-propanol, ethanol, acetone and diethyl ether and dried overnight under vacuum at 40 °C. Their characterization was effected by light scattering, FT-IR spectrometry, optical microscopy and SEM.

<b>Aqueous dispersed phase</b> <i>Reagents (mg)</i>	<b>Organic continuous phase</b> <i>CHCl<sub>3</sub>/<i>n</i>-hexane (ml/ml)</i>	<b>Microspheres</b> <i>mg (conv. %)</i>
<b>5</b> (5·10 <sup>3</sup> mg) MBA (9 mg)	18/20	1·10 <sup>3</sup> mg (83%)

For polymerisation, the amount of aqueous phase is 3 ml; initiator system is (NH<sub>4</sub>)<sub>2</sub>S<sub>2</sub>O<sub>8</sub>/TMEDA (150 mg/150 µl); surfactants are Span 85/Tween 85 (100 µl /50 µl).

**Table 2:** Copolymerization of **5** with MBA

### 2.10 Microspheres characterization

Obtained samples were characterized in terms of swelling behaviour at different pH values, drug loading efficiency, drug release trends, dimensions and morphology (through Dinamic Light Scattering and

Optical Microscopy). Moreover microspheres were characterized by FT-IR spectrometry in order to confirm that polymerization occurred by considering the disappearance of characteristic bands of acrylic double bonds.

### *2.11 Swelling studies (determination of the percentage of water regain)*

The swelling behaviour was investigated in order to check the hydrophilic affinity of spherical microparticles. Typically, aliquots (50 mg) of dried materials were placed in a tared 5 ml sintered glass filter (Ø 10 mm; porosity G3), weighed, and left to swell by immersing the filter in a beaker containing the swelling media. The experiment was carried out at 37 °C and the pH values were selected to simulate the physiologic vaginal pH (4.5) and the vaginal pH during infections (8). Three replicates were used for each pH value. At predetermined times (1, 4 and 24 h), the excess of water was removed by percolation and then the filter was centrifuged at 3500 rpm for 15 min and weighed. The filter tare was determined after centrifugation with only water. The weights recorded at different times were averaged and used to give the equilibrium swelling degree [ $\alpha\%$ ] by the following equation:

$$\alpha = \frac{(W_s - W_d)}{W_d} \times 100$$

where  $W_s$  and  $W_d$  are the weights of swollen and dried microspheres, respectively [21]. Each experiment was carried out in triplicate and the results were in agreement within  $\pm 4\%$  standard error.



### *2.12 Drug Incorporation into preformed microspheres by soaking procedure*

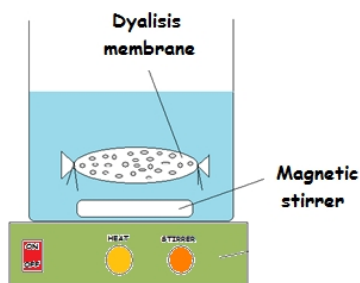
Preformed matrix (10 mg) was allowed to swell in a concentrated solution of ketoconazole obtained dissolving 10 mg of the drug in 4 mL of a water/ethanol solution (volume ratio 3:2) [27]. This soaking procedure was conducted for 72 hours under slow mechanical stirring at room temperature, to avoid any chemical degradation of the entrapped drug. Afterthat, microspheres were filtered and dried at reduced pressure in presence of P<sub>2</sub>O<sub>5</sub> until a constant weight was reached. Finally, the loading efficiency percentage (LE %) was determined by UV-Vis spectroscopy analysis ( $\epsilon=50 \text{ ml/mg}\cdot\text{cm}^{-1}$ ,  $\lambda=220 \text{ nm}$ ) of filtered solvent according to the following equation:

$$LE\% = \frac{M_i - M_0}{M_i} \times 100$$

where  $M_i$  is the mass of drug in the solution prior to loading,  $M_0$  is the mass of drug in solution after loading, monitored by measuring absorbance at a wavelength of 220 nm.

### *2.13 In vitro release studies of ketoconazole from microparticles*

The release profile of the entrapped drug was performed in dialysis membranes (Spectra/Por<sup>®</sup>, cut-off 12 000 Da) by suspending 10 mg of loaded microspheres in 10 mL of a phosphate buffer solution pH=8. The membrane was then placed in a beaker containing 100 mL of the same buffer, as described above, at pH=8 used as a medium simulating the vaginal environment during infections. Moreover, this study was conducted at 37 °C in a shaking thermostated bath. The experiment was carried out in triplicate and for 24 hours (Figure 3).



**Figure 3:** *In vitro* release studies

At each interval, a fixed volume of the outer solution was taken out, analyzed spectrophotometrically employing a calibration plot ( $\epsilon=50$  ml/mg $\times$ cm $^{-1}$ ,  $\lambda=220$  nm), and replaced with a fresh volume of the same buffer in order to maintain sink conditions throughout the whole experiment. The percentage of released drug was expressed in relation to the absorbance of the corresponding volume taken out at each interval [28].

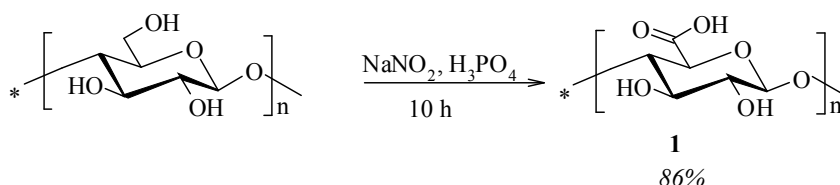
### 3. Results and Discussion

Recent literature data show the growing interest towards polymeric biocompatible materials for the controlled and site-specific release of drugs. For this reason, in this work the major part of the efforts were employed in the realization of mucoadhesive microspheres carrying antimicrobial drug such as ketoconazole for the treatment of vaginal infections [29]. Bioadhesive systems have the main function of being attached to a biological surface thus enhancing drug absorption and its time of permanence in the human body. In this context, many polymers such as polyethylene glycol have been employed in order to confer mucoadhesive properties to drug delivery systems based on themselves.

Mucoadhesive microspheres offer a unique carrier system for many pharmaceuticals and can be tailored to adhere to any mucosal tissue, including those found in eyes, oral cavity and throughout the respiratory, urinary, vaginal and gastrointestinal tracts. The mucoadhesive microspheres can be used not only for controlled release but also for targeted delivery of the drugs to specific sites in the body. Recent advances in medicine have envisaged the development of polymeric drug delivery systems for protein/peptide drugs and gene therapy. These challenges put forward by the medical advances can be successfully met by using increasingly accepted polymers e.g. polyacrylates, chitosans, polyethylene glycols etc [30]. Thanks to all these advantages, for the realization of mucoadhesive microspheres, polyethylene glycol was used as spacer group having regards to its biocompatibility. In particular it is a polyol commercially available in a wide variety of molecular weights; its hydroxyl groups are able to be derivatized and thus this allows its use in the design of pharmaceutical carriers. The particular attention paid to PEG [31] also arises from its unique chemical properties: it is soluble in water, as in many other solvents, it can be obtained with various types and degrees of chemical modifications, particularly its acryloyl derivative can be easily polymerized and it is able to link biomolecules of larger or smaller size allowing a good degree of cell adhesion. The best technique that allows the formation of microparticulate systems has been the reverse suspension polymerization. Using this methodology, it was possible to create a matrix based on polyethylene glycol, derivatized with an acrylic moiety on one of its hydroxyl groups, and dextran, whose effectiveness as a carrier of drugs was evaluated by loading it with ketoconazole [32], a specific antifungal drug for the treatment of vaginal infections.

### 3.1 Synthesis of 6-carboxy dextran (**1**)

The first objective was to carry out a selective oxidation of the hydroxyl function in position 6 (Scheme1) of dextran in order to obtain a carboxyl group susceptible to subsequent esterification reaction [22].

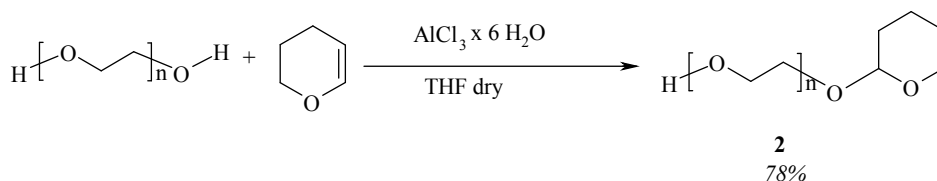


**Scheme 1:** Oxidation of dextran

The reaction was conducted in the presence of phosphoric acid and sodium nitrite; the obtained product (**1**) was characterized by FT- IR spectroscopy. . FT-IR (KBr)  $\nu$  (cm<sup>-1</sup>): 3443 (-OH), 1741 (-COOH). Yield: 86%.

### 3.2 Protection of the primarily hydroxylic function of PEG 200 by tetrahydropyranylation (2)

Reaction was carried out in the presence of 3,4-dihydro-2H-pyran useful in the protection of one of the terminal primarily hydroxyl group of PEG in a temporary way, in order to have just one free hydroxyl group that will be employed for the next step of acrylation (Scheme 2).

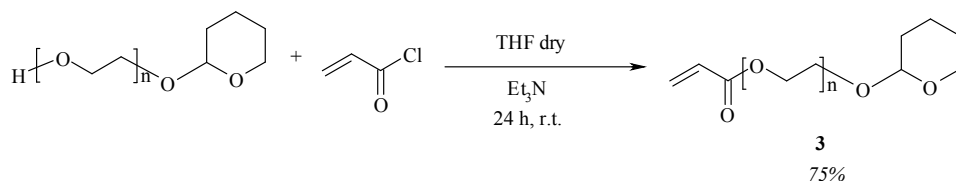


**Scheme 2:** Protection of PEG

For the obtainment of the monoprotection of PEG200, aluminum chloride hexahydrate was used to catalyze the binding of the protective group quite hindering but easily removable. The reaction mechanism involves an initial attack of the hydroxyl group of PEG with release of one molecule of hydrochloric acid [25]. While most of the existing protocols require distillates and/or dry reagents, this method tolerates the presence of moisture and is suitable for the preparation of THP-ether derivatives even at higher water content. An important feature of this method is the obtainment of a monoprotected derivative, difficult to be achieved in the presence of n-diols (such as PEG) through conventional methods [24]. Significant advantages of this methodology are the high reaction rate, the absence of volatile solvents and ease of obtaining protection and deprotection using the same catalyst. The final product (**2**) was characterized through FT-IR, GC/MS and  $^1\text{H-NMR}$  spectroscopies. FT-IR (KBr)  $\nu$  ( $\text{cm}^{-1}$ ): 3429 (-OH). M/Z: 85 (100%), 239 (4%).  $^1\text{H-NMR}$  ( $\text{CD}_3\text{CN}$ )  $\delta$  (ppm): 4,510 (1H, m), 3,710 (2H, m), 3,526 (2H, m), 3,446-3,351 (4nH, m), 1,593-1,987 (6H, m). Yield: 78%.

### 3.3 Acrylation of PEG-THP (**3**)

The mechanism of this reaction consists in the nucleophilic attack of the free hydroxyl group of PEG-THP towards the electrophilic carbon of carbonyl group of acryloyl chloride; this step involves the formation of hydrochloric acid that is neutralized by triethyl amine (Scheme 3).

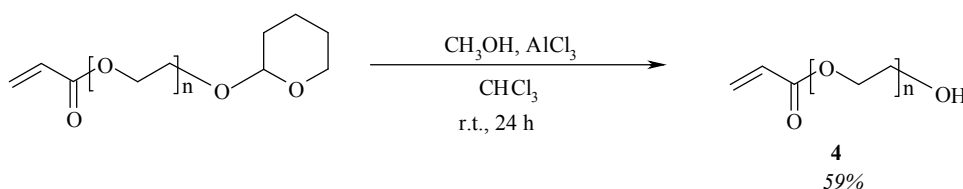


**Scheme 3:** Acrylation of monoprotected PEG

The degree of functionalization doesn't depend on the reaction time is closely related to the amount of acryloyl chloride used. The obtained compound (**3**) was characterized through the common spectroscopic techniques. FT-IR (KBr)  $\nu$  ( $\text{cm}^{-1}$ ): 1724 ( $-\text{COOR}$ ), 947, 915 ( $-\text{CH}=\text{CH}_2$ ).  $^1\text{H-NMR}$  ( $\text{CDCl}_3$ )  $\delta$  (ppm): 6,28 (1H, dd), 6,09 (1H, dd), 5,64 (1H, dd), 4,55 (1H, m), 4,343-4,325 (2H, m), 3,742-3,467 (4nH, m), 3,59 (2H, m), 1,51-2,10 (6H, m). Yield: 75%.

### 3.4 Deprotection of acryloyl-PEG-THP

The third step involves the removal of the protecting groups from the primary hydroxyl group of PEG200, so that it can be available for the next reaction of esterification (Scheme 4).

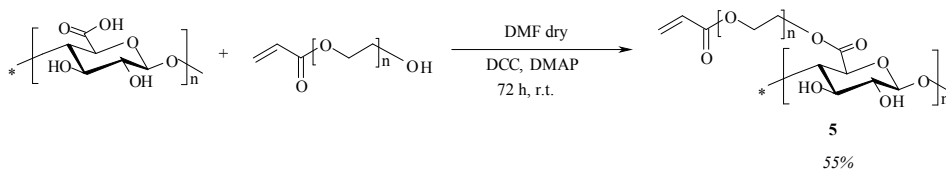


**Scheme 4:** *Deprotection of the monoacrylic derivative*

The protecting group used has the advantage of being easily removed by using a solution of methanol/aluminum trichloride, the reaction of deprotection [24] provides the corresponding free hydroxyl function. The final product (**4**) was characterized through FT-IR and  $^1\text{H-NMR}$  spectroscopies. FT-IR (KBr)  $\nu$  ( $\text{cm}^{-1}$ ): 3443 ( $-\text{OH}$ ), 1726 ( $-\text{COOR}$ ), 950, 912 ( $-\text{CH}=\text{CH}_2$ ).  $^1\text{H-NMR}$  ( $\text{CDCl}_3$ )  $\delta$  (ppm): 6,25 (1H, dd), 6,13 (1H, dd), 5,90 (1H, dd), 4,324 (2H, m), 3,55 (2H, m), 3,450-3,344 (4nH, m). Yield: 59%.

### 3.5 Esterification of acryloyl-PEG with 6-carboxy dextran (**5**)

The last step involves the esterification [22] of the carboxyl group of dextran with the hydroxyl group of PEG using a condensing agent such as dicyclohexyl carbodiimide (DCC), which binds oxygen (-OH) of the carboxylic group of dextran, increasing its electrophilicity and susceptibility towards the attack by the hydroxyl group of PEG. For this reaction also dimethyl aminopyridine (DMAP), a base and a nucleophilic catalyst, was used in order to counteract any decrease in pH due to acid formation in the reaction and enhance the production of the more nucleophilic and more reactive ionized form of alcohol (-O<sup>-</sup> instead of -OH) (Scheme 5).



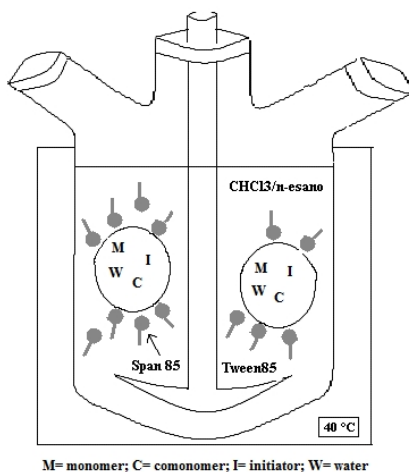
**Scheme 5:** Esterification step

The obtained product (**5**) was purified through extraction, dried under vacuum and characterized through FT-IR. FT-IR (KBr)  $\nu$  (cm<sup>-1</sup>): 3436 (-OH), 1769 (-COOR), 1724 (-COOH), 942, 917 (-CH=CH<sub>2</sub>). Yield: 55%.

### 3.6 Microspheres preparation (**6**) by reverse phase emulsion polymerization

The preparation of microspheres based on **5** was performed using the technique of reverse phase emulsion polymerization. This technique consists of adding an aqueous solution of a monomer (dispersed phase) in an excess of organic solvent immiscible with water (dispersing phase).

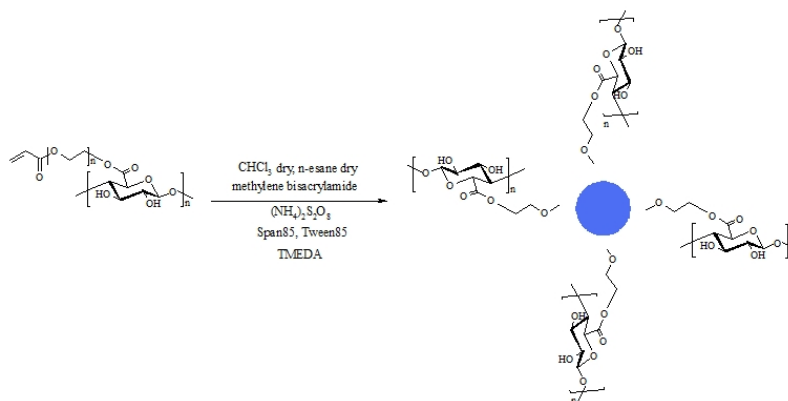
Under stirring, small droplets of dispersed phase appear and in order to decrease their interfacial free energy assume a spherical shape. The radical polymerization [21] provides a chain growth mechanism that begins with the generation of primary radicals after cleavage of a suitable initiator. These radicals react with the acrylic function present on PEG200 (previously derivatized) determining the progressive cross-linking. In this case we used a mixture of organic solvents consisting of dry chloroform (18 ml) and n-hexane (20 ml), while the dispersed phase consists of an aqueous solution (4 ml) containing **5** (42 mg,  $1,14 \times 10^{-4}$  mol) (Figure 4).



**Figure 4:** Instrumentation for radical polymerization

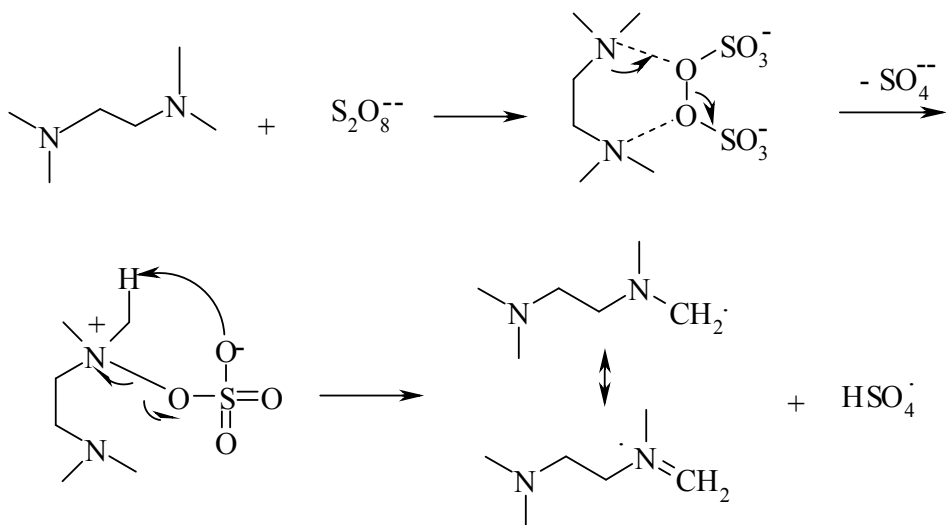
The density of the organic phase was adjusted by adding one of the two solvents until the obtainment of an aqueous phase in neutral equilibrium with the organic phase (Scheme 6).





**Scheme 6:** *Microspheres preparation*

The tendency of droplets to aggregate can be countered by decreasing their collisions with vigorous shaking (900-1000 rpm / minute). These drops are more stable in the organic phase by the addition of a mixture of surfactants: Tween 85 and Span 85. The polymerization is initiated by the addition under stirring of a radical initiator, ammonium persulfate ((NH<sub>4</sub>)<sub>2</sub>S<sub>2</sub>O<sub>8</sub>), which decomposes to form primary radicals at a temperature of 35-40 ° C. Then, after about 10 minutes of stirring, TMEDA was added acting as an accelerator for the decomposition of ammonium persulfate (Scheme 7).



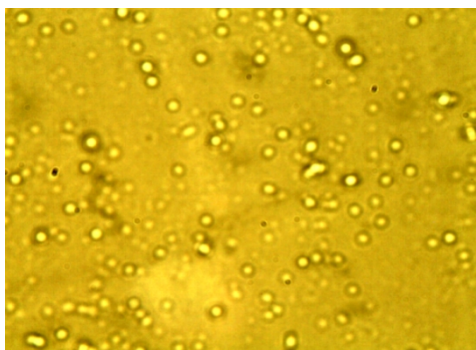
**Scheme 7:** *Decomposition of ammonium persulfate*

The main advantage of free radical polymerization [33] in reverse phase suspension is that microparticles obtained with this process have firmly crosslinked by covalent bonds between carbon atoms PEG200 chains, and this gives them greater stability compared to systems where the same chains are linked by weak interactions and/or easily hydrolysable bonds. The average diameter of particles, generally obtained with this technique, is included in the wide range of 1 mm-10  $\mu\text{m}$  even though the range 30-300  $\mu\text{m}$  is more common. The particle size is determined by many parameters, related to the nature and ratio between reagents as well as the characteristics of the reactor, where this term summarizes the speed and type of agitation, and also the shape and size of this latter. Some generalizations have been made and we can say that the average diameter of particles is directly proportional to the interfacial tension between the two liquid phases and the volume fraction of dispersed phase, while it is inversely proportional to the speed of agitation, to the density of the droplets of monomer and to the size of the blades of agitation [34]. At the

end of the reaction product (6) was washed with isopropanol, ethanol and acetone and observed with an optical microscope and analyzed using dynamic light scattering.

### *3.7 Microspheres characterization*

Microspheres were characterized in terms of size and polydispersity: dynamic light scattering analyses revealed the presence of microparticulate systems with a good polydispersity index and a mean particle diameter of  $2 \mu\text{m} \pm 0.8$ . Moreover optical microscopy revealed the presence of particles in the same dimensional range and with a spherical shape (Figure 5).



**Figure 5:** *Optical micrography of microparticles*

Due to the high specific surface area, these materials are able to easily and effectively adsorb drugs from aqueous solutions. The spherical shape and porous surface are suitably characteristics that the matrix polymer must possess in order to obtain an interesting ratio volume/surface. Greater porosity results in a higher surface exposure towards the entrapped substance, thus increasing the possibility of interaction between drug and matrix. FT-IR analyses revealed that polymeric matrix doesn't possess

## Section 2 – PART A

anymore bands awardable to the acrylic double bonds; this means that all the double bonds have been employed in the cross-linking reaction with the comonomer methylene bisacrylamide.

### *3.8 Swelling studies on empty microspheres*

The affinity of microparticles towards aqueous media was determined by studying their swelling degree ( $\alpha\%$ ) at two different pH (8 and 4.5) and at different time intervals (1h, 4h and 24h ). Table 3 shows the different values of  $\alpha\%$  at two different pH and at different time intervals. Each experiment was carried out in triplicate and the results were in agreement within  $\pm 4\%$  standard error.

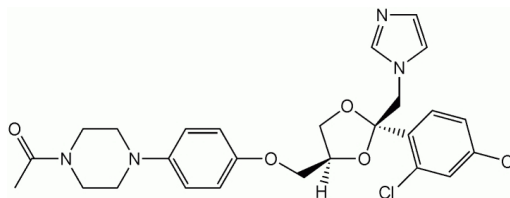
pH	Time (h)		
	1	4	24
8.0	496%	654%	654%
4.5	79.8%	76.5%	77%

**Table 3:** *Swelling behaviour of microspheres at different pH values*

### *3.9 Ketoconazole loading into preformed empty microspheres*

The excellent results obtained by the swelling studies allowed to use these microparticulate systems for the vaginal delivery of antifungal drug such as ketoconazole. Ketoconazole is a synthetic antifungal drug used to prevent and treat fungal skin and mucosal infections, especially in immunocompromised patients such as those with AIDS or those on

chemotherapy. Ketoconazole is very lipophilic, which leads to accumulation in fatty tissues (Figure 6).



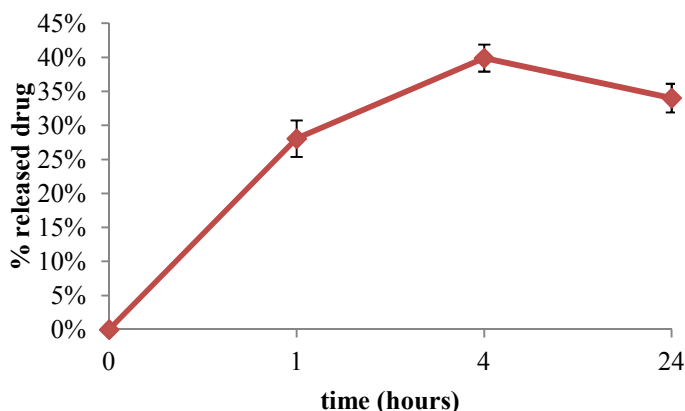
**Figure 6:** Ketoconazole chemical structure

Its mechanism of action is quite complicated and involves ergosterol, the bioregulator of membrane fluidity and asymmetry and consequently of membrane integrity in fungal cells [35]. Drug loading was carried out by using the soaking procedure: the drug in contact with the outer surface of the microspheres establishes weak interactions with the matrix mainly on the surface. However, the chemical nature of the drug and the matrix and the loading time allow to a portion of the active molecules to interact with the core of the microspheres. During the soaking, the synthesized polymer increases in volume but retains its three-dimensional structure without breaking up as it is insoluble in water. Results revealed that the loading efficiency percentage (LE%), determined by UV-VIS spectroscopy analyses, is equal to  $55\% \pm 1.8$  ( $n=3$ ).

### 3.10 *In vitro* ketoconazole release studies

Release studies were conducted on aliquots of microspheres at pH = 8 and at different time intervals (1h, 4h and 24h) by using a shaking thermostated water bath that maintains temperature at 37 ° C. This pH value was chosen because under these experimental conditions microspheres show the best swelling behavior and because this value is

typical of vaginal infections. The experiment was repeated in triplicate and the values expressed as percentage of effectively loaded drug are reported in the graph (Figure 7).



**Figure 7:** *Ketoconazole release profile*

The obtained results have been particularly interesting. The amount of drug released from microspheres and the trend followed by the release are not easily predictable. In fact, this phenomenon is a function of several factors, such as the speed of water penetration into the system, which allows the polymer matrices to go from a dehydrated state to a swelling state; interactions between drug and matrix; chemical and physical properties of the loaded drug, the temperature of the experiment and the crosslinking degree of microparticles. The latter factor, in addition to influencing the diffusion rate of the drug in the fluid surrounding the microparticle [36], also affects the speed with which the transition from the collapsed state of matrix to the swollen state occurs and so it determines the mechanism of release. The prevalence of one of these factors on the others may determine the outcome but, more likely, the result comes from the particular combination of these parameters that is

established for each individual case. A factor that could affect the release trend and that must be considered is the loading of the drug on microspheres: when molecules can easily penetrate the mesh of the carrier, stronger and more stable interactions could occur and, therefore, the drug will be released in smaller amounts.

Ultimately, this work led to the development of mucoadhesive crosslinked macromolecular systems that show different affinity for the aqueous medium in which they are immersed, depending on the pH value of the latter. The release properties of polymeric matrices were determined and the results suggested their possible use as systems for the vehiculation and the controlled release of ketoconazole in the vaginal cavity during inflammatory conditions.

#### **4. Conclusions**

The objective of this work was the incorporation of ketoconazole, a drug with antifungal and anti-inflammatory activity, used for systemic and deep infections, in microspheres based on polyethylene glycol and dextran. The swelling degree of microspheres not containing ketoconazole was studied by swelling studies conducted at two different pH and at defined time intervals. In particular, phosphate buffers were used at pH 8, to mimic the typical conditions of the vaginal environment during infections, and pH 4.5, to simulate the physiological environment. The obtained results revealed that the microspheres have higher affinity towards the aqueous media at pH 8. These latter, loaded with ketoconazole, were also subjected to preliminary studies conducted in the pH conditions described above. These studies showed that ketoconazole is significantly released within 24 hours at pH=8 and, in particular, the release is greater in the first 4 hours. This is probably due to interactions

## Section 2 – PART A

of drug with the hydroxyl groups of dextran glucosidic rings. In fact, the high content of heteroatoms in ketoconazole enhances the formation of hydrogen bonds with these groups, resulting in an increased entrapment of the drug on microspheres surface rather than in their inner. Obtained data suggest the possibility of using dextran-based microspheres as mucoadhesive systems for the controlled and site-specific release of active molecules useful in the treatment of vaginal mycosis.

Actually, there are studies still in progress on the evaluation *in vitro* of mucoadhesive properties and pharmacological activity of the new carrier.



## References

- [1] M.I. Ugwoke, R.U. Agu, N. Verbeke, and R. Kinget. *Adv. Drug. Delivery Rev.* **2005**, 57(11): 1640-1665.
- [2] J. K. Vasir, K. Tambwekar, S. Garg. *Int. J. Pharm.* **2003**, 255:13-32.
- [3] C. Valenta, C. Kast, I. Harich, A. Bernkop-Schnurch. Development and in vitro evaluation of a mucoadhesive vaginal delivery system for progesterone. *J. Control. Release* **2001**, 77: 323-332.
- [4] K. Vermani, S. Garg. The scope and potential of vaginal drug delivery. *PSTT* **2000**, 3: 359-364.
- [5] E.R. Boskey, R.A. Cone, K.J. Whaley, D.R. Moench. Origins of vaginal acidity: high D/L lactate ratio is consistent with bacteria being the primary source. *Hum. Reprod.* **2001**, 16: 1809-1813.
- [6] D.P. Benzinger, J. Edelson, Absorption from the vagina. *Drug Metab. Rev.* **1983**, 14: 137-168.
- [7] V.M. Jasonni, R. Raffelli, A. de March, G. Frank, C. Flamigni. Vaginal bromocriptine in hyperprolactinemic patients and puerperal women. *Acta Obstet. Gynecol. Scand.* **1991**, 493-495.
- [8] N. Agarwal, A. Gupta, A. Kriplani, N.P. Bhatla, Six hourly vaginal misoprostol versus intracervical dinoprostone for cervical ripening and labor induction. *J. Obstet. Gynaecol. Res.* **2003**, 29: 147-151.
- [9] R.K. Malcolm, The intravaginal ring. *Drugs Pharm. Sci.* **2003**, 126: 775-790.
- [10] N. Einer-Jensen, E. Cicinelli, P. Galantino, V. Pinto, B.H.R. Barba. Uterine first pass effect in postmenopausal women. *Hum. Reprod.* **2002**, 17 (12): 3060-30.
- [11] J.D. Smart, I.W. Kellaway, H.E.C. Worthington. An in vitro investigation of mucosa-adhesive materials for use in controlled drug delivery. *J. Pharm. Pharmacol.* **1984**, 36: 295-299.

- [12] M. Chvapil, C.D. Eskelson, V. Stiffel, J.A. Owen, W. Droegemueller. Studies on nonoxynol-9: II. Intravaginal absorption, distribution, metabolism and excretion in rats and rabbits. *Contraception* **1980**, 22: 325-339.
- [13] A. El-Kamel, M. Sokar, V. Naggar, S. Al Gamal, Chitosan and sodium alginate-based bioadhesive vaginal tablets. *AAPS PharmSci* **2002**, 44.
- [14] A. Bernkop Schnurch, M. Hornof, D. Guggi, Thiolated chitosans. *Eur. J. Pharm. Biopharm.* **2004**, 57:9-17.
- [15] A. Bernkop-Schnurch, M. Hornof, T. Zoidl. Thiolated polymers-Thiomers: Modification of chitosan with 2-iminothiolane. *Int. J. Pharm.* **2003**, 260: 229-237.
- [16] N.B. Graham, M.E. McNeill. Hydrogels for controlled drug delivery. *Biomaterials* **1984**, 5: 27-36.
- [17] M.E. McNeill, N.B. Graham, Vaginal pessaries from crystalline/rubbery hydrogels for the delivery of prostaglandin E2, *J. Control. Release* **1984**, 1: 99-117.
- [18] C. Valenta . The use of mucoadhesive polymers in vaginal delivery. *Advanced Drug Delivery Reviews* **2005**, 57: 1692-1712.
- [19] Singla AK, Chawla M. and Singh A. Potential applications of carbomer in oral mucoadhesive controlled drug delivery system. *Drug Dev. Ind. Pharm.* **2000**, 26: 913-924.
- [20] W.N.E. van Dijk-Wolthuis, J.A.M. Hoogeboom, M.J. van Steenberghe, S.K.Y. Tsang and W.E. Hennink, Degradation and release behavior of dextran-based hydrogels. *Macromolecules* **1997**, 30: 4639-4645.
- [21] Iemma, F., Spizzirri, G., Puoci, F., Muzzalupo, R., Trombino, S., Cassano, R., Leta, S., Picci, N. pH-Sensitive hydrogels based on bovine

serum albumin for oral drug delivery. *Internal Journal of Pharmaceutics* **2006**, 312: 151-157.

[22] Cassano, R., Trombino, S., Bloise, E., Muzzalupo, R., Iemma, F., Chidichimo, G., Picci, N. New Broom Fiber Derivates: Preparation and Characterization. *Journal of Agricultural and Food Chemistry* **2007**, 55: 9489-9495.

[23] Klemm, D.; Philipp, B.; Heinze, T.; Heinze, U.; Wagenknecht, W. Experimental protocols for the analysis of cellulose—appendix to Volume 1. In *Comprehensive Cellulose Chemistry*; Klemm, D., Philipp, B., Heinze, T., Heinze, U., Wagenknecht, W., Eds.; Wiley-VCH Verlag GmbH: Weinheim, Germany **1998**, 1: 236.

[24] Vasudevan, V., Namboodiri and Rajender, S. Solvent-Free Tetrahydropyranlation of Alcohols and Phenols and Their Regeneration by Catalytic Aluminum Chloride Hexahydrate **2002**, 43: 1143-1146.

[25] Zalipsky, S., Halmiton, C. Functionalized Poly(ethylene glycol) for Preparation of Biologically Relevant Conjugates. *Bioconjugate Chem* **1995**, 6: 150-165.

[26] Trombino, S., Cassano, R., Bloise, E., Leta, S., Puoci, F., Picci, N. Design and Synthesis of Cellulose Derivates With Antioxidant Activity. *Macromolecular Bioscience* **2007**, 85-96.

[27] James, D., Hoeschele, L., Anidyak, K., Vincent, L., Peggy, L. In Vitro Analysis of the Interaction between Sucralfate and Ketoconazole. *Antimicrobial Agents and Chemotherapy* **1994**, 38: 19-325.

[28] Wolthuis, V., D., Franssen, O., Talsma, H., Kettens-van den Bosch, J., J., *Macromolecules* **1995**, 28: 6317-6322.

[29] De Ascentiis, A., Colombo, P. and Peppas, N. A. Screening of potentially mucoadhesive polymer microparticles in contact with rat intestinal mucos. *Eur. J. Pharm. Biopharm* **1995**, 41: 229-234.

- [30] Rajput G, Majmudar F, Patel J, Thakor R, Rajgor NB. Stomach-specific Mucoadhesive Microspheres as a Controlled Drug Delivery System. *Sys Rev Pharm* **2010**, 8:7-20.
- [31] Whitaker, Mj., Quirk, R., Howdle, S. Growth Factor Release from tissue engineering Scaffolds. *Pharm Pharmacol* **2001**, 53: 1427-1437.
- [32] James, D., Hoeschele, L., Anidyak, K., Vincent, L., Peggy, L. In Vitro Analysis of the Interaction between Sucralfate and Ketoconazole. *Antimicrobial Agents and Chemotherapy* **1994**, 38: 319-325.
- [33] Harris, J.M. Polyethylene Glycol Chemistry: Biotechnical and Biomedical Applications *Plenum Press, NY*, (1992).
- [34] Scully D.B. *J. Appl. Pol. Sci.* 20, 7299 (1976).
- [35] Hitchcock, C., K. Dickinson, S. B. Brown, E. G. Evans, and D. J. Adams. Interaction of azole antifungal antibiotics with cytochrome P450-dependent 14  $\alpha$ -sterol demethylase purified from *Candida albicans*. *J. Biochem* **1990**, 266:475-480.
- [36] Sannino, A., Netti, PA., Madaghiele, M., Coccoli, V., Luciani, A., Maffezzoli, A., Nicolais, L. Synthesis and characterization of macroporous poly(ethylene glycol)-based Hydrogels for tissue engineering application. *Biomedical Mater* **2006**, 2: 229-236.

## PART B

### **SYNTHESIS, CHARACTERIZATION, *IN VITRO* CELL UPTAKE AND *IN VIVO* BIODISTRIBUTION STUDIES OF A CATIONIC GLYCOL CHITOSAN POLYMER FOR ORAL ADMINISTRATION OF HYDROPHOBIC DRUGS**

#### **Abstract**

*Purpose:* The aim of the present project was to synthesize and characterize a quaternized palmitoyl glycol chitosan polymer for the realization of nanoparticulate systems. The *in vivo* polymer biodistribution by radiolabelling and its *in vitro* behaviour against an absorptive epithelia were evaluated.

*Method:* Quaternary ammonium palmitoyl glycol chitosan (GCPQ) was synthesized and characterized via NMR, FT-IR, PCS, UV-spectroscopy (methyl orange probe), ITC and TEM. A fluorescent hydrophobic dye (Idarubicin) was encapsulated into the positively charged polymeric NPs made of fluorescently labeled GCPQ. Prepared NPs were used after purification in cell uptake studies in a mucus free and mucus producing cell lines, Caco-2 and HT29-MTX-E12 respectively. Confocal microscopy was used qualitatively to assess Idarubicin internalization capacity over time. Moreover the same polymer was subjected to *in vivo* biodistribution studies by covalently linking it to the Bolton-hunter reagent.

*Results:* <sup>1</sup>H-NMR illustrated attachment of substitution groups to the carbohydrate backbone and determined their MW whereas FT-IR confirmed attachment of functional groups. PCS analysis confirmed cationic charge on GCPQ NPs. CAC studies showed that GCPQ is more

favourable for hydrophobic domains and form stable aggregates. MTT assay calculated the cytotoxicity of the formulation against two different cell lines, Caco-2 and HT29-MTX-E12. Moreover, the polymer did not open tight junctions of cells. Mucus monolayer was characterized and confocal images showed that GCPQ is not absorbed the cells. Biodistribution studies displayed a very interesting behaviour of the polymer such as a useful excipient for oral administration of hydrophobic drugs.

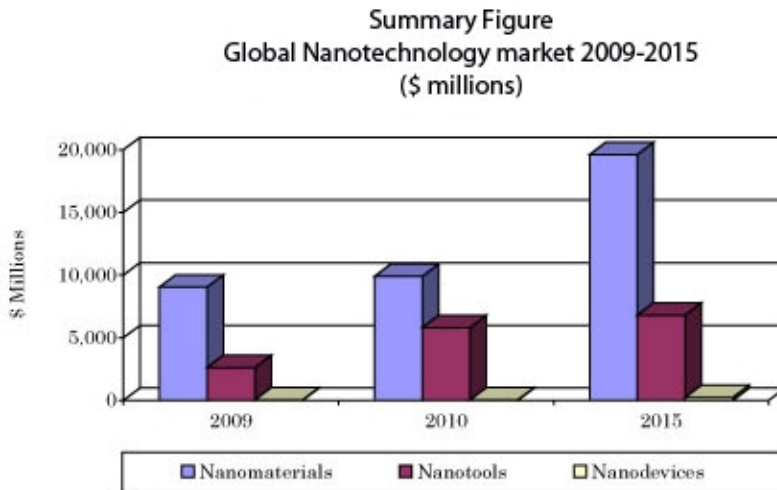
*Conclusions:* Cationic charge is important for bioadhesion and uptake of drugs and could be possible mechanism for increased bioavailability of drugs using GCPQ; Idarubicin internalization was faster especially in HT29-MTX-E12 cells indicating the importance of cationic charge for interaction with mucus barriers. Surface charge density can influence NP uptake and this physiochemical property is important to be studied for efficient in drug delivery. Particularly, GCPQ is a good and promising candidate for the preparation of modified formulations to be administered orally. These data are confirmed by the detection of the radioactivity levels in the excised organs of adult mice dosed orally with the radiolabelled polymer.

## **1. Introduction**

### *1.1 What is Nanotechnology?*

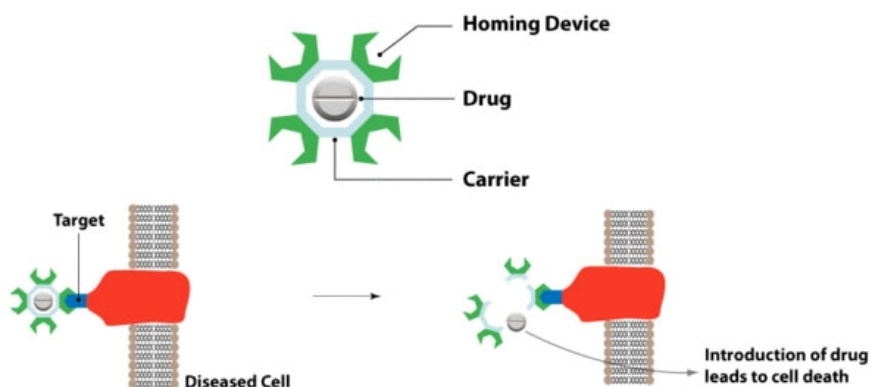
The design, characterization and application of various nanosized (size range 1-1000 nm) structures, devices and systems are cumulatively known as Nanotechnology. Around 2005, the global investment for nanotechnologies lied at € 5 billion, where € 2 billion came from private sectors and was said to increase over € 1 trillion by 2011-2015 having a fourfold increase in the number of patents from 1995 (531 patents) to

2001 (1976 patents) showing an explosive development in the Pharmaceutical field [1]. Another report claimed worldwide sale revenues for nanomaterials will increase from \$ 9,027.2 million in 2009 to approximately \$ 19,621.7 million in 2015 as demonstrated in Figure 1 [2].



**Figure 1:** *The global market for nanotechnology (2009-2015)*

Paul Ehrlich claimed that a toxin for the organism in question can be targeted with the agent of selectivity if an agent is able to target the organism in the first place leading to the creation of a “magic bullet” to eradicate the disease-causing organism [3]. Therefore, targeted drug delivery (especially for anticancer treatment) can be achieved by creating various chemical compounds that have an affinity to the organism just like the effect of antitoxins to toxins effectively destroying tumour cells and micro-organisms as a consequence as demonstrated in Figure 2 [4].



**Figure 2:** A schematic representation of “magic bullet” by Paul Ehrlich (Bioimaging, 2008)

### 1.2 Nanotechnology in Drug Delivery

In drug delivery, the biggest challenge faced is the delivery of drug to the correct site of action in order to achieve good efficacy and prevent side effects [5]. NPs have proven to be successful and efficacious achievement of targeted drug delivery as it possesses satisfactory size properties, longer shelf life capacity and high entrapment ability [6]. They have proven to lead to efficacious delivery of drugs across various biological barriers and some examples are as follows:

- Intravenous delivery

This route of administration has been extensively employed for the delivery of drugs to the brain. The brain, tightly protected and segregated from the blood circulation, has posed a challenge for drug delivery for a number of years. Drugs are not able to pass the blood brain barrier (BBB) in adequate amounts leading to poor brain concentrations. Various factors contribute to this problem like large sized molecules and quick metabolism by enzymes prohibiting the drug to reach the target site. NPs have proven an efficient system for the drug targeting directly to this



organ; a study showed by Ringe et al used Dalargin (enkephalin-type peptide); an analgesic, bound to the various combinations of NPs (polysorbate 80 and poly(butylcyanoacrylate)) and injected it intravenously in mice. The results showed that coating the drug to NPs of polysorbate 80 and poly (butylcyanoacrylate) resulted in antinociceptive effect by avoiding clearance by the reticuloendothelial system (RES) and was able to protect the drug from the RES consisting of phagocytotic cells concluding the delivery to the BBB [7]. Their small size lead to more selective delivery and reduced drug toxicity.

- Intranasal delivery

Intranasal administration has provided a rapid route from the nose to the brain for the delivery of where NPs can easily enter the olfactory neurons. The efficacy of intranasal delivery of NPs was demonstrated by a study using Thyrotropin-releasing hormone (TRH) and other neuropeptides that attenuated seizures by olfactory nerve, paracellular and microvascular uptake [8]. Specific uptake can also be increased by conjugation with bioactive ligands to the surface of PEG and PLA NPs.

- Pulmonary delivery

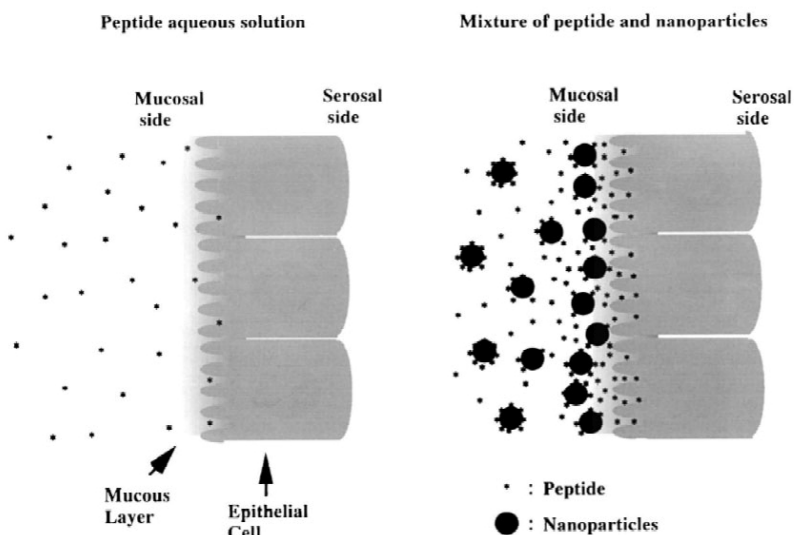
Delivery of drugs to the lungs provides direct application of the drug to the organ itself leading to a targeted treatment and this has been found to be highly useful for critical diseases like pulmonary arterial hypertension (PAH). NPs via the pulmonary route has been found to have a higher specificity to the organ leading to better distribution of the drug in the body and prolonged drug release. A study aerosolized 5(6)-carboxyfluorescein (CF) (hydrophilic drug) in order to entrap it into the NPs made up of biodegradable and biocompatible polyester DEAPA (poly[vinyl 3-(diethylamino)propylcarbamate-co-vinyl acetate-co-vinyl alcohol]-*graft*-poly(d,l-lactide-co-glycolide)) whose efficacy was tested

using isolated, perfused and ventilated rabbit lung model. High encapsulation levels were achieved with these NPs and the *in vitro* model study showed that CF-DEAPA NPs was effectively delivered as a result of a burst effect that was dependent on the diffusion, swelling and biodegradation effects of the NPs resulting in a stable concentration plateau in the perfusate [9]. Therefore NPs for pulmonary delivery can help in the improvement of drug bioavailability and reduce the dosing frequency and provide flexible incorporation of hydrophilic and hydrophobic drugs [10].

- Oral delivery

NPs can be taken via the oral route as a result of transcytosis via M cells, uptake via Peyer's patches and intracellular uptake via intestinal mucosa's epithelial cells. One study showed the efficacy of NPs via the oral route for the treatment of Tuberculosis by using three anti-tuberculosis drugs: Rifampin, Isoniazid and Pyrazinamide encapsulated by poly(lactide-co-glycolide) (PLGA) NPs. *In vivo* studied showed the drug encapsulated NPs where detected after 4 days (Rifampin) and 9 days (Isoniazid and Pyrazinamide) as a result of adhesion of the NPs to the mucosa increasing the concentration between the luminal and serosal sides enhancing the absorption and consequently the bioavailability. NP systems are also becoming a wide interest in the pharmaceutical field for the delivery of macromolecule like peptide and protein drugs. The challenges faced are that these molecules are hydrophilic and display inadequate partitioning in cell membranes leading to poor absorption [11] and have suffered from low permeability, poor solubility and instability in the gut [12] resulting in poor bioavailability, reduced pharmacological effects and inter & intrasubject variability. NPs help in the shielding of the drug from gastrointestinal degradation by enhancing absorption and drug contact

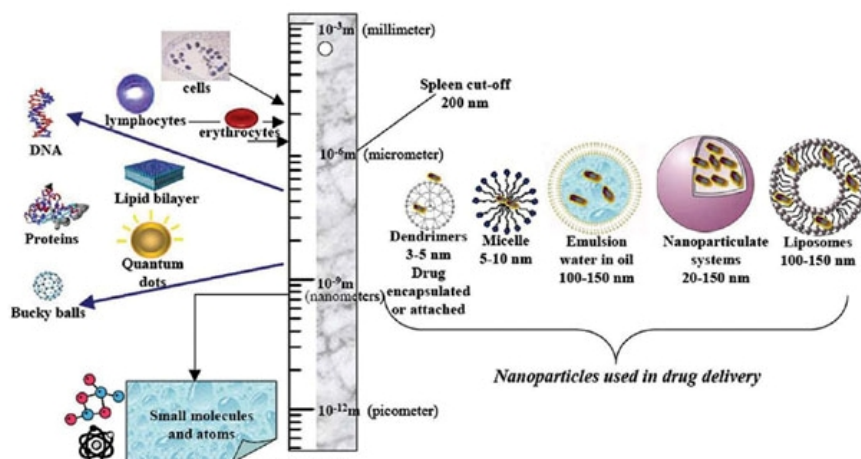
[13]. A study showed NPs containing novel graft polymer with both hydrophobic and hydrophilic backbone was able to enhance the absorption of salmon calcitonin in rats by the mechanism of mucoadhesion that increased the stability and provided protection in the gastrointestinal tract as demonstrated in Figure 3.



**Figure 3:** *Mucoadhesion properties of NPs consisting of novel graft polymers for the delivery of peptides via the oral route*

### *1.3 Various nanocarrier systems*

The first approved nanoparticulate formulation was an immunosuppressant drug used for rejection seen during organ transplant approved in 2000 in China by the name of Rapamune (Wyeth Pharmaceuticals) [14]. Nanocarriers come in various forms as demonstrated in Figure 4 [3].



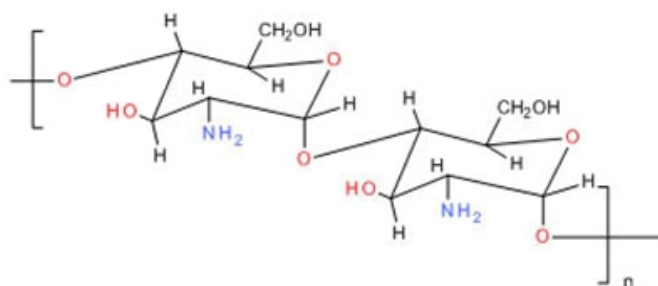
**Figure 4:** *Various nanocarrier systems employed in Nanotechnology*

#### 1.4 Biodegradable polymers and their impact

There are a number of absorption enhancers available however their major setbacks are the toxicity they display (EDTA chelators) or disruption of actin filaments (surfactants). Bile salts and fatty acids are found to result in irreversible damage when administered intranasally resulting in the damage of nasal mucosa [15]. Biodegradable polymers have become extensively useful in drug delivery. They have been found extremely useful for overcoming various transmucosal barriers, example: in oral delivery, they protect those drugs with poor permeability and stability in the gastric and intestinal fluids enhancing the bioavailability by overcoming the degradation faced by the harsh environment of the stomach and intestinal motility; reducing toxicity and helps in efficient targeting of therapeutic agents. Even for brain delivery and gene delivery, they behave as a non-viral vector allowing efficient cellular internalization, endosomal escape including nucleus uptake. Coating with a polymer can reduce the toxicity, protecting them from chemical/enzymatic degradation [16]. The main key factor to overcome

this is the use of bioadhesive interactions to mucosal barriers is to increase their absorption by having closer contact with the absorptive membrane creating a concentration gradient between the loaded drug with the nanoparticle and the circulation. The polymer can adhere for a longer time due to strong intermolecular hydrogen bonds and allows penetration into the mucosal layer [17].

One of the commonly used biodegradable polymers is chitosan. Chitosan is a deacetylated form of chitin mainly found in the shells of crustaceans and is recognized for its biocompatibility and biodegradability [18], its chemical structure seen in Figure 5.

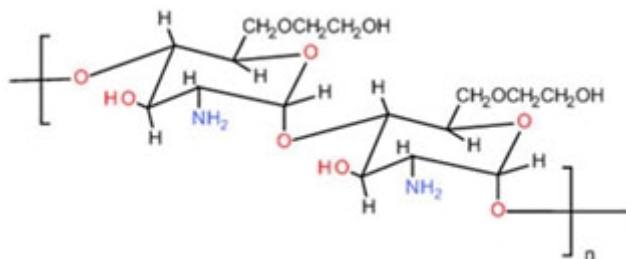


**Figure 5:** *Structure of Chitosan*

β-(1-4)-linked glucosamine repeating units have a large number of amino and hydroxyl groups providing derivitization options and immobilization of biologically active species [19]. Enhanced gastrointestinal absorption by chitosan has gained considerable attention over the years [20]. Especially for the absorption of peptides orally example: uptake of polypeptides like calcitonin and insulin via paracellular pathway and sustained oral delivery due to prolonging the retention time in the stomach. Presence of mucus in the gastrointestinal tract will enhance the properties of chitosan (via mucoadhesion) by promoting the residence time of the mucoadhesive particles [21] as there is an increased contact

between the drug and the absorption site therefore better transport via epithelial barrier is seen. It has also helped in the delivery of vaccines intranasally and chitosan glutamate (salt form of chitosan) showed a reduction in blood glucose concentration when tested intranasally in sheep and rats. It has also been used as a non-viral vector in gene delivery [22] its unique cell transfectant properties due to the primary amine groups present in the repeating monomer units (which has also been useful for the grafting of different moieties). It has been reported to protect the DNA content from degradation by lysosomal enzymes [23]. The use of such polymers can even help improve and enhance transmucosal delivery of drugs (oral, intranasal, pulmonary). The success of chitosan has also been bolstered due to its rapid wound healing by platelet adhesion and activation, thrombus formation and blood coagulation leading to efficient healing acceleration because of interaction between positively charged chitosan and negatively charged plasma protein under acidic conditions. Its wide range of properties makes this polysaccharide highly advantageous as a drug delivery system including lack of systemic toxicity. However, the main drawback of chitosan is its poor solubility in pH above 6. This polycation (apparent  $pK_a$  5.5) loses its charge leading to precipitation in neutral and basic environment making it unreliable for absorption enhancement. Various surface modifications have been made to the -OH and -NH<sub>2</sub> groups present (which allows hydrogen bonding) [24] and literature have demonstrated such modifications ranging from thiolated chitosans to phosphorylated chitosans, N-alkyl and acylated chitosan [25]. One type of modification of particular interest is Glycol chitosan, GC (Figure 6) which has ethylene branches that increases the solubility and steric stabilization as a result of the pendant glycol branches present [26]. Its functional amino group

widens the interest of this polysaccharide in drug delivery for many modifications can be done to improve physicochemical and drug delivery properties. They form stable self-aggregated NP structure in physiological pH and research has reported them as successful carrier for the delivery of hydrophobic drugs and genes.



**Figure 6:** Structure of Glycol chitosan

Other modifications including graft copolymerized chitosans have also been reported, mainly by the addition of poly (acryl amide), Poly (vinyl) alcohol but one of the most commonly used and popular graft polymer is Poly (ethylene) glycol (PEG). It is reported to have good immunogenicity, biocompatibility and is non-toxic. It also possesses qualities like flexibility due to its hydrophilic nature, lack of antigenicity and steric repulsion and has enhanced adhesive properties [27].

### 1.5 Importance of Surface Charge Density

For the successful biological application of NPs, it is important to target both the lesion and cell interior site correctly, therefore, there should be a good understanding of its uptake profile and subcellular localization of NPs. The study of surface charge density and its interaction with mucosal membranes helps to explain it [28]. Surface modification offers better drug targeting, (cellular binding, uptake and intracellular transport) thus,

over the years various surface charge densities have been introduced to expand the applications of polymer carriers in the biomedical fields and a number of literatures have proved compared, contrasted and shown the benefit of positive, negative and neutral charges:

- Positive Charge

Uchegbu et al synthesized a polysoap called Quarternary ammonium palmitoyl glycol chitosan (GCPQ) by introducing a palmitoyl group and positive surface charge by quaternization using methyl iodide [29]. Quaternization has posed various advantages ranging from higher solubility in physiological pH (therefore overcoming the disadvantage of solubility seen with chitosan alone), better permeation profile and amphiphilic nature and ability to interact with the negative mucin glycoproteins and epithelium. The cationic nature of chitosan has also seen to enhance antimicrobial activity due to the binding sialic acids to phospholipids. A recent study demonstrated high encapsulation efficiency of insulin with quaternized chitosan which exposed their positive charge towards the aqueous environment to interact with the negatively charged surface enhancing insulin uptake when administered via the colonic route. Sustained drug release for 5 hours was noted due to the enhanced solubility of the polymer in neutral and alkaline media, hence proving the efficiency of positive charge [30]. Cationic dendrimers can interact better with negatively charged DNA and proteins via electrostatic interactions facilitating adhesion and lysosomal escape by endocytosis. This influences its intracellular trafficking and consequently their cell uptake. Positive charge of chitosan based NPs can increase the influx of chloride ions causing a ‘proton sponge effect’ by osmotic swelling and lysosome rupture which can help in the treatment of diseases involving metabolic, signalling and pathogenic processes.



- Negative charge

Juliano et al reported anionic liposomes clear faster than neutral and cationic liposomes as proteins and calcium present in the blood plasma have a tendency to coalesce with the anionic liposomes [31]. The half life of dextran in blood circulation was seen to be prolonged in the presence of a negative charge. Another study indicated negative charge causes more rapid clearance of NPs in blood circulation as compared to the neutral and positive charges. Negatively charged liposomes were reported to target the scavenger receptors on the macrophage surface and have been found to cause lesser toxicity than the positively charged liposomes [32].

- Neutral charge

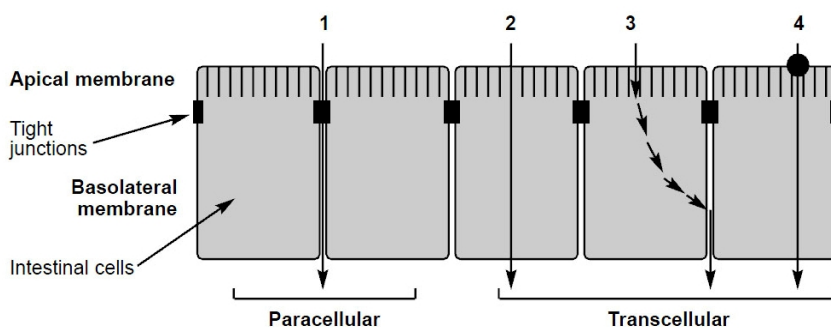
Yamamoto et al showed the importance of a neutral surface charge density from electrostatic repulsion between anionic micelles and cell surface that lead to reduced non-specific uptake by liver and spleen as compared to the neutral ones.

This highlights that surface charge can greatly influence the ability of a polymer to interact with the cell membranes and epithelium affecting the cellular uptake and bioadhesion which can alter the pharmacokinetic and pharmacodynamic profiles. By controlling the surface charge density, various therapeutic efficacies can be achieved, thus, it is crucial to understand and report the importance of surface charge densities and their influence and impact on the drug delivery.

### *1.6 Use of in vitro models to study cell uptake and mucoadhesion*

The efficacy and cellular mechanism including *in vivo* fate of NPs can be studied using *in vitro* models like colonic tumour cell lines like Caco-2 and HT29-MTX-E12 cells to study drug absorption, permeation and

transepithelial transport of drugs [33]. When Caco-2 cells are cultured on permeable inserts; they instantly differentiate into monolayers resembling that of enterocytes. Each transport route depends on various factors and properties of a drug ranging from lipophilicity, size and ability to hydrogen bond. Transcellular transport via the enterocytes is the most important route for hydrophobic drugs strongly depending on its lipophilicity. Another route is the paracellular transport via the tight junctions usually predominant in hydrophilic drugs; less prominent but also important route noted is carrier mediated transport collectively demonstrated in Figure 7.

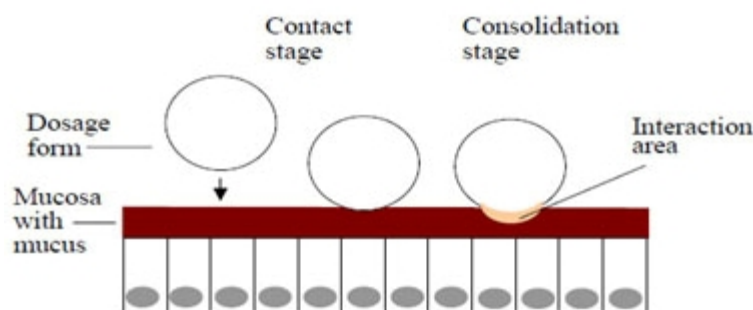


**Figure 7:** Mechanism of transport across intestinal epithelium: 1) Paracellular; 2) Transcellular passive diffusion; 3) Transcytosis; 4) carrier mediated up-take at apical domain with passive diffusion in basolateral domain

Caco-2 cells are useful as a screening model for drugs which consists of various CYP isoenzymes and phase II enzymes (glutathione S-transferase and sulphanotranferase). They restrict paracellular transport of drugs (rate-limiting barrier) due to tight junctions therefore by using polymers, we can deduce whether they will be able to open the tight junctions or not by measuring their epithelial integrity on basis of its transepithelial electrical resistance (TEER) [33]. Though Caco-2 cells are considered a

good representative for enterocytes in the small intestine, they lack a mucus layer [34]. Intestinal mucus comprises of high MW glycoproteins whose thickness varies in various sections of the GIT and is found to be a barrier for the delivery of drugs [35]. By using a mucus secreting line like HT29-MTX-E12 cells, a better representation of the intestinal cell is demonstrated (subclone of human adenocarcinoma intestinal cell line, HT29 which are less differentiated than Caco-2 but in presence of methotrexate medium, mucus monolayer is formed) and mucoadhesive properties can be thoroughly studied to understand the effect of mucus which is seen to influence the permeability of both lipophilic and hydrophilic drugs its paracellular permeability being 50 folds higher than Caco-2 [33]. It is important to understand the various mechanisms underlying the transport of a polymer when in contact with mucus (a rate limiting step for lipophilic drugs). It can be described as follows:

1. Contact stage: contact between the mucus layer and the polymer
2. Consolidation stage: spontaneous diffusion leading to formation of various bonds (hydrogen bonding, Van der Waals forces including electrostatic and hydrophobic interactions) resulting to interpenetration [36] (Figure 8).



**Figure 8:** *Stages of mucoadhesion*

Mucoadhesion acts via certain bonds: ionic (oppositely charged ions), covalent (electron sharing), hydrogen (hydrogen atom covalently links to electronegative atoms), Van der Waals forces (dipole-dipole and dipole-induced) and hydrophobic bonds (indirect: usually in non-polar groups). The negative charge present on the terminal sialyl and ester sulphate moieties (mucin glycans) leads to the interaction between the polymer and the cell membrane [37].

### *1.7 Aim of the project*

The aim of the present project was to synthesize and characterize a quaternized palmitoyl glycol chitosan polymer for the realization of nanoparticulate systems. The *in vivo* polymer biodistribution by radiolabelling and its *in vitro* behaviour against absorptive epithelia were evaluated.

## **2. Materials and Methods**

### *2.1 Materials*

GC (77%, titration), deuterated solvents, PNS ( $\geq 99.5\%$  TLC), N-methyl-2-pyrrolidone ( $\geq 99.0\%$ ), sodium bicarbonate (99.7-100.3%), methyl iodide (99%), diethyl ether ( $\geq 99.5\%$ ), Sephadex G-25, Idarubicin Hydrochloride, Hematoxylin Mayer's Solution and 4',6-Diamidino-2-phenylindole (DAPI) were supplied from Sigma-Aldrich Co., UK. Hydrochloric acid (32%) and Sodium hydroxide (98.9%) were supplied from Fisher Scientific (UK). Sodium iodide ( $\geq 99.5\%$ ), Amberlite® IRA-93 Cl<sup>-1</sup> free base, Hydroxylamine Hydrochloride, Alcian blue 8GS, Absolute ethanol (99.7%), Paraformaldehyde EM grade, Methyl orange and Sodium tetraborate decahydrate (99.5%) were supplied from Fluka Chemika (UK). Visking dialysis membranes, MW cut off 3.5, 7 & 12 kDa

were purchased from Medicell International Ltd (UK). Bolton-Hunter reagent was supplied by Perkin Helmer (USA). HT29-MTX-E12 cells Passage 41 were a generous gift of Professor David Brayden, University College Dublin, Ireland; Caco-2 cells Passage 8 were purchased by ATCC (American Tissue Culture Collection, USA).

### *2.2 Degradation of Glycol Chitosan (GC48)*

Un-degraded GC (5g) was dissolved in hydrochloric acid (4M, 380ml) and stirred for 20 minutes prior to being stirred in a preheated water bath (50°C, 125 rpm) for 48 hours. It was cooled and underwent exhaustive dialysis against distilled water (5L) with 6 changes using Visking cellulose tubing (MW cut off 3.5 kDa) for 24 hours before freeze drying to give a white, crystalline cotton-like mass of GC48.

### *2.3 Palmitoylation of degraded Glycol Chitosan (PGC)*

GC48 and sodium bicarbonate were mixed in a mixture of absolute ethanol (24 ml) and distilled water (76 ml) where Palmitic acid N-hydroxysuccinimide ester (PNS) previously dissolved in absolute ethanol (150 ml) was added drop-wise to the mixture of degraded GC48 and left stirring for 72 hours covered in foil to avoid photolytic degradation. Ethanol was evaporated under reduced pressure using Heidolph rotavapor pump (51°C) and was extracted with diethyl ether (3x150 ml). Exhaustive dialysis was carried out against distilled water (5L) with 6 changes using Visking cellulose tubing (MW cut off 12 kDa) for 24 hours before freeze drying to give a dense white mass of PGC. All amounts are reported in the table below (Table 1).

Reagent	Mass (mg)	Moles	Molar ratio
GC48	500	2.4 mM	1
PNS	781	2.2 mM	0.92
Sodium bicarbonate	376	4.48 mM	2

**Table 1:** *Palmitoylation step*

#### 2.4 Quaternization of PGC (GCPQ)

PGC (300 mg) and N-methyl-2-pyrrolidone (25 ml) were stirred for 3 hour at room temperature (25°C). Sodium hydroxide was dissolved in the minimum amount of ethanol and was added along with methyl iodide and sodium iodide to the reaction mixture (36°C) in an oil bath where nitrogen gas was passed for 3 hours. Precipitation was carried out by adding diethyl ether (300 ml) and leaving it overnight to obtain a brown precipitate (Table 2). It was washed with diethyl ether (3x200 ml) and dissolved in distilled water (100 ml) to obtain a clear solution. Exhaustive dialysis was carried out against distilled water (5L) with 6 changes using Visking cellulose tubing (MW cut off 7 kDa) for 24 hours. Amberlite IRA-93 Cl<sup>-1</sup> was packed in a column with hydrochloric acid (1M, 150ml) and washed with distilled water (10L) and the dialysate was passed through where the filtered elute from the column was collected and sent for freeze drying to obtain GCPQ as a white fibrous solid.

Reagent	Mass (mg)	Moles	Molar ratio
Sodium hydroxide	40	1 mM	1
Sodium iodide	45	3 mM	1
Methyl iodide	1000	7 mM	25

**Table 2:** *Quaternization of Palmitoyl Glicol Chitosan*

### 2.5 Structural analysis: NMR spectroscopy

Polymer samples (2.0-3.0 mg) were dissolved in D<sub>2</sub>O (0.6 ml) and vortexed until solubilised and transferred to a tube (WILDMAD NMR tube, Sigma Aldrich, UK) and analysed with Bruker AMX 400 MHz spectrometer. Presence of a palmitoyl group reduces polymer solubility in D<sub>2</sub>O alone therefore the polymer (2.0-3.0 mg) was dissolved in MeOD (0.6 ml) and a few drops of D<sub>2</sub>O and vortexed until completely solubilised. A drop of CH<sub>3</sub>COOD was added if any turbidity was present. Substitution degree (SD) is calculated as follows:

$$\begin{aligned} \% \text{Acetylation} &= \frac{(\text{chemical shift of acetyl protons}/\text{number of acetyl protons})}{(\text{chemical shift of sugar protons}/\text{number of sugar protons})} \times 100 \\ &= \frac{\% \text{Palmitoylation}}{(\text{chemical shift of sugar protons} / \text{number of sugar protons})} \times 100 \\ \% \text{Quaternization} &= \frac{(\text{chemical shift of quaternary ammonium protons}/\text{number of quaternary protons})}{(\text{chemical shift of sugar protons} / \text{number of sugar protons})} \times 100 \end{aligned}$$

NMR can give the molecular weight of the polymers:

a. GC48

$$N = \frac{\text{sugar area}}{\text{number of sugar protons} \times \text{anomeric area}}$$

$$\text{Molecular weight (MW)} = \text{theoretical value} \times N$$

where N is the number of repeating monomers

b. GCPQ

$$\begin{aligned} &(\% \text{ palmitoylation} \times \text{its theoretical value} \times N) + (\% \text{quaternization} \times \text{its theoretical value} \times N) \\ &+ (\text{MW of GC48}) \end{aligned}$$

*2.6 Functional group determination: FT-IR*

A few mg of polymer was placed on a zinc selenide crystal and scanned 32 times using Perkin Elmer Spectrum-100 FTIR spectrometer with Spectrum FTIR software (Perkin Elmer Instruments, Cambridge, UK) equipped with Universal Attenuated Total Reflectance accessory.

*2.7 Self Assembly studies:*

i. Methyl orange probe UV-spectroscopy

A solution of methyl orange (25  $\mu\text{m}$ ) was prepared in borate buffer (0.02M) and used to make serial dilutions of the polymers from 10 mg/ml to 0.0001 mg/ml followed by probe sonication (75% output, 10 minutes) in icy water and incubated for 1 hour at room temperature (25°C) before there were analyzed by UV-Vis spectrophotometer (UV-1650 PC, UV Vis Spectrophotometer, Shimadzu, UK) with a UV range of 300-500 nm using UVProbe 2.21 software. The borate buffer was the control in this experiment.

ii. ITC

Enthalpy of change ( $\Delta H$ ) on demicellization was measured by taking a polymer solution in water (2mg/ml) and probe sonicated (75% output, 20 minutes) in icy water, degassed and then analyzed by VP-ITC MicroCalorimeter (MicroCal, LLC, Northampton, MA). A syringe with degassed water and polymeric solution were taken and kept in the sample hole avoiding air bubbles. A total of 30 injections were given (injection volume: 10 $\mu\text{l}$ , injection interval: 360s, temperature 25°C) and data was processed by MicroCaL Origin® version 7.0 Software. Standard Gibbs free energy of micellization ( $\Delta G_{\text{demic}}$ ) can be calculated from:

$$\Delta G_{\text{demic}} = -RT \ln K$$



where  $R$  is the universal gas constant (8.3144 J/mol/K),  $T$  is the absolute temperature (in Kelvin) and  $K$  is cmc in mole fraction. The enthalpy change of demicellization ( $\Delta H_{\text{demic}}$ ) calculated from the experiment can help in the calculation of  $\Delta S_{\text{demic}}$  [38]:

$$\Delta G_{\text{demic}} = \Delta H_{\text{demic}} - T\Delta S_{\text{demic}}$$

$$\Delta G_{\text{demic}} = -\Delta G_{\text{mic}}$$

Similarly,  $\Delta S_{\text{mic}}$  can be calculated as follows:

$$\Delta G_{\text{mic}} = \Delta H_{\text{mic}} - T\Delta S_{\text{mic}}$$

### *2.8 Photon Correlation Spectroscopy*

Particle size and zeta potential were read by Malvern Zetasizer 3000HS<sub>A</sub>, Malvern Instruments Ltd, UK with the following parameters: light angle: 90°, temperature: 25°C, viscosity: 0.89mPa.s, refractive index: 1.331.

#### *i. Zeta potential*

It was determined by probe sonicating (75% output, 10 minutes) a polymer solution in water (1mg/ml) in icy water and filtering it (0.22  $\mu\text{m}$  Millipore filter) after diluting it to 1:5 with PBS (pH 7.4) and was analyzed by Malvern Zetasizer for its mobility, KCps and zeta potential.

#### *ii. Particle size*

A polymer solution in water (1 mg/ml) was probe sonicated (75% output, 10 minutes) in icy water and filtered (0.22  $\mu\text{m}$  Millipore filter) and was kept in a cuvette and analyzed for its Zaverage, KCps and polydispersity. The particle size for both filtered and unfiltered polymeric solutions was determined.

### *2.9 Nanoparticles morphology: TEM*

A fresh polymer stock in water (1mg/ml) was probe sonicated (75% output, 10 minutes) in icy water, filtered (0.22  $\mu\text{m}$  Millipore filter) and a

## Section 2 – PART B

drop was kept on a film and negative stained with 1% uranyl acetate aqueous solution and analyzed by Philips/FEI CM120 Bio Twin Transmission Electron Microscope.

### *2.10 Molecular Weight Determination through Gel Permeation Chromatography*

The molecular weight of GCPQ48 was measured using GPC-MALLS: a 7600 Series Solvent D-Gasser, Jasco PU-2080 Plus Intelligent HPLC Pump (Jasco, UK), Waters 717plus Autosampler (Millipore, UK), DAWN EOS multi-angle laser light scattering detector (Wyatt Technology Corporation, USA), Optilab DSP Interferometric Refractometer (Wyatt Technology Corporation, USA) and quasi elastic light scattering, QELS (Wyatt Technology Corporation, USA). Toluene and BSA were used for calibration and normalisation of the DAWN EOS multi-angle laser light scattering ( $\lambda = 690$  nm) detector respectively. The data were computed using ASTRA for Windows version 4.90.08 software. The mobile phase was acetate buffer (0.3M CH<sub>3</sub>COONa / 0.2M CH<sub>3</sub>COOH, pH 5), methanol (35: 65). Samples (5 - 10mg ml<sup>-1</sup>) were filtered (0.2 $\mu$ m, 200 $\mu$ l) and injected on to a POLYSEP<sup>TM</sup>-GFC-P 4000 column (300 x 7.8mm, exclusion limit for PEG = 20,000 Da, Phenomenex, U.K.) fitted with a POLYSEP<sup>TM</sup>-GFC-P guard column (35 x 7.8mm, Phenomenex, U.K.) using a flow rate of 0.8 ml min<sup>-1</sup>.

### *2.11 Fluorescent Labelling of GCPQ*

A green fluorescent dye named 5-Carboxyfluorescein N-Succinimidyl ester was attached to a quaternary ammonium palmitoyl glycol chitosan (GCPQ). The GCPQ used for this reaction was synthesized performing a 48 hours degradation reaction of starting glycol chitosan; the level of

palmitoylation was  $19.4 \pm 2.0\%$  and the level of quaternisation was  $7.48 \pm 2.75\%$  ( $n=4$ ). The protocol followed to perform this reaction was adapted from Amersham (GE Healthcare)'s protocol for labelling with N-hydroxysuccinimide (NHS) esters and Adeline Siew's PhD thesis at the School of Pharmacy (Uchegbu group). These dyes couple to the GCPQ at the amine group using the same mechanism as palmitoylation with the palmitic acid N-hydroxysuccinimide. Most dyes are available as an NHS ester, and this should be applicable to them.

Briefly, GCPQ48 (100 mg) was dissolved in sodium bicarbonate buffer (0.1 M, 10 mL). 5-Carboxyfluorescein N-Succidinimidyl ester (5 g) was dissolved in DMSO (0.5 mL) and an aliquot (100  $\mu$ L) added to the GCPQ48 solution. The reaction was incubated for 1 hour at room temperature with continuous stirring and protected from light. The reaction was stopped by adding freshly prepared hydroxylamine (1.5 M, 0.1 mL). The fresh hydroxylamine was prepared by dissolving hydroxylamine hydrochloride (210 mg mL<sup>-1</sup>) in distilled water and adjusting the pH to 8.5 with a solution of sodium hydroxide (5 M). The resulting hydroxylamine solution was diluted with an equal volume of distilled water and mixed well. The hydroxylamine containing reaction was incubated for one hour at room temperature and the conjugate isolated by dialysis (MWCO 12-14 kDa) and purified through a Sephadex G25 column (100 mL). The reaction was protected from light during the whole process. The obtained derivative was characterized by gel permeation chromatography (GPC-MALLS), FT-IR and NMR as previously described in Adeline Siew's PhD thesis at the School of Pharmacy (Uchegbu group).

### 2.12 Encapsulation studies

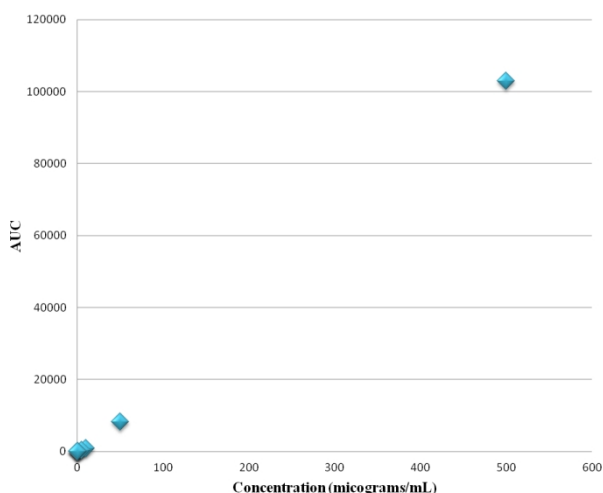
i. Nanoparticle preparation: *Solvent evaporation technique*

The hydrophobic dye used was Idarubicin. The fluorescent polymer (15mg) was dissolved in dextrose (1.5ml) and the wetted polymer (10 mg/ml) was pipetted into a solution (0.5 ml) of ethanol/Idarubicin (3 mg/ml). The mixture was left stirring overnight to evaporate the ethanol and probe sonicated (75% output, 20 minutes) in icy water. Centrifugation (5 minutes, 2000 rpm) removed the unencapsulated dye. Both phases i.e. the pellet in the tube and the supernatant were collected in a clean eppendorf.

ii. Idarubicin quantification: *HPLC*

The drug loading efficiency was evaluated by using HPLC. Idarubicin hydrochloride was loaded into nanoparticles in a ratio 1:5 with GCPQ by dissolving both of them in dextrose 5% w/v and probe sonicating on ice for 10 minutes. The amount of formulation to seed in each insert was calculated on the basis of the  $IC_{50}$  value of the drug for the two different cell lines. In fact Idarubicin  $IC_{50}$  value was found to be around 0.02  $\mu\text{g/ml}$  [5]. GCPQ was dissolved in 5 w/v% dextrose by vortexing and probe sonication on ice at 75% power output for 10 min. GCPQ solution was then added to the idarubicin ethanolic solution and the formulation was sonicated on ice for 10 min and left stirring overnight. The formulation was filtered through a 0.45  $\mu\text{m}$  filter prior to analysis. The filtrate from the formulation was diluted with the mobile phase (water: acetic acid: methanol 54: 1: 45 v/v) and chromatographed (50  $\mu\text{l}$ ) over an Onyx Monolith C18 column (100 x, Agilent Technologies Instruments), at a mobile phase flow rate of 1.5  $\text{mL min}^{-1}$  and with the wavelength set at 254 nm. The limit of detection was 0.05  $\mu\text{g ml}^{-1}$ , and the linear peak area–

concentration over the range 0.05–500  $\mu\text{g mL}^{-1}$  had a correlation coefficient of 0.9996 (Figure 9).



**Figure 9:** Calibration plot of Idarubicin hydrochloride

### 2.13 Synthesis of Radiolabelled GCPQ for *in vivo* biodistribution studies

GCPQ was radiolabelled using a modification of the method previously reported [39]. Briefly, GCPQ ( $10 \text{ mg mL}^{-1}$ ) was dissolved in borate buffer (0.1 M, pH 6.6). To this solution was added (97.5  $\mu\text{l}$  of trimethylamine per 5 mg of GCPQ48). The GCPQ48 solution ( $10 \text{ mg mL}^{-1}$ , 300  $\mu\text{l}$ ) was added to the dry Bolton-Hunter reagent (10  $\mu\text{Ci}$ , 4  $\mu\text{l}$ ) and the reaction stirred for 20 min. The reaction mixture was then purified dialysis. The quantity of bound and free [ $^{125}\text{I}$ ] iodide in the preparation before and after purification was assessed by TLC (alumina) using toluene, ethyl acetate (20: 80) as the mobile phase.  $^{125}\text{I}$ -labelled GCPQ was spotted at the base of the plate and allowed to ascend the TLC plate along with a control sample of free  $^{125}\text{I}$ -Bolton Hunter Reagent. The radiolabelled polymer contained no more than 5%w/w of free label [39].

## Section 2 – PART B

### *2.13.1 In vivo biodistribution of Radiolabelled GCPQ*

$5 \times 10^6$  counts  $\text{min}^{-1}$  (cpm) of radiolabelled polymer was diluted to 2 mL with NaCl (0.9%w/v). From this stock the labelled polymer (200 $\mu\text{L}$ ,  $5 \times 10^5$  cpm) was administered orally to adult mice (20-25 g). Animals were killed at various time intervals and blood and the major organs harvested. Samples were then assayed for radioactivity using a WIZARD 2470 gamma counter (PerkinElmer, UK). Results were expressed as % of the administered dose.

### *2.14 Cell Studies*

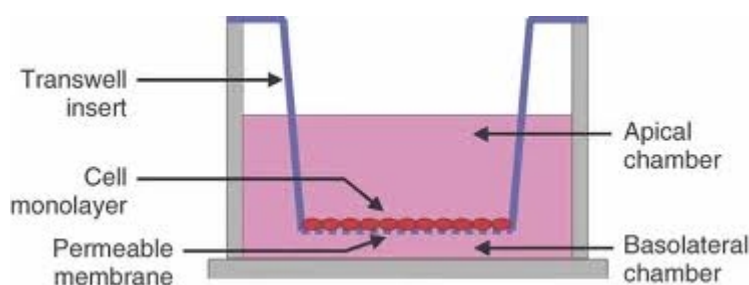
#### *2.14.1 Caco-2 cells*

Caco-2 cells (passage 8-15) were seeded on Transwell<sup>®</sup> 12 well plate having a polycarbonate membrane (area 1  $\text{cm}^2$ , pore diameter 0.4  $\mu\text{m}$ ) at a seeding density of  $1.44 \times 10^5$  cells/ml (equivalent to  $7.2 \times 10^4$  cells/insert or to  $6.4 \times 10^4$  cells/  $\text{cm}^2$ ). The medium used was MEM supplemented with FBS (10% w/v), sodium pyruvate (1 mM), non-essential amino acid (1% w/v), L-glutamine (1% w/v), penicillin (100  $\mu\text{g}/\text{ml}$ ) and streptomycin (100  $\mu\text{g}/\text{ml}$ ). Cell suspension was added to the apical compartment (0.5ml) and medium added to the basolateral compartment (1.5ml) and incubated (37°C, 5% humidity, 95%  $\text{CO}_2$ ). The medium in both the apical and basolateral sides were changed every other day. A diagrammatic representation of the transwell studies is shown in Figure 10.

#### *2.14.2 HT29-MTX-E12 cells*

HT29-MTX-E12 cells (passage numbers 40-50) were seeded on Transwell<sup>®</sup> 12 well plate having a polycarbonate membrane (area 1  $\text{cm}^2$ , pore diameter 0.4  $\mu\text{m}$ ) at a seeding density of  $1.34 \times 10^5$  cells/ml (equivalent to  $6.72 \times 10^4$  cells/insert or to  $6 \times 10^4$  cells/  $\text{cm}^2$ ). The medium

used was DMEM supplemented with FBS (10% w/v), L-glutamine (1% w/v), penicillin (100 µg/ml) and streptomycin (100 µg/ml). Cell suspension was added to the apical compartment (0.5ml) and medium added to the basolateral compartment (1.5ml) and incubated (37°C, 5% humidity, 95% CO<sub>2</sub>). The medium in both the apical and basolateral sides were changed every other day. For both cell lines, at least 21 days were given to allow the cells to mature and form a monolayer after which both the TEER and cell-uptake studies were done.



**Figure 10:** *Transwell<sup>®</sup> 12-well plates with polycarbonate permeable cell culture insert*

#### 2.14.3 Staining/detection of mucus: Mucus staining

Cells at passage 41 with a seeding density of  $3.48 \times 10^5$  cells/well were seeded on a 24 well plate (round sterilized coverslip present at the bottom). Attachment of cells under the coverslip was avoided by initially adding cell suspension (0.5ml) in each well and left for 2 hours before adding the rest of it (1.5ml) The medium was changed every 2 days. Coverslips were fixed in 3% paraformaldehyde in PBS (pH 7.4) for 30 minutes (25°C). Staining (pH 2.5) was done by adding 10 drops of alcian blue (1%) in acetic acid (3%) mixture and incubating it (37°C, 5% humidity, 95% CO<sub>2</sub>) for 15 minutes. It was washed with PBS (pH 7.4) and 12 drops per well of hematoxylin was added in each well and

## Section 2 – PART B

incubated (37°C, 5% humidity, 95% CO<sub>2</sub>) for 15 minutes. It was finally washed with PBS and mounted on a slide with aqueous mounting medium and observed under optical microscope (Nikon Microphot FXA).

### *2.14.4 Tight junction integrity determination: TEER*

Polymer dispersions (5 mg/ml) were prepared in HBSS containing Ca<sup>2+</sup> and Mg<sup>2+</sup> supplemented with penicillin (100 U/ml) and streptomycin (100 U/ml). The culture medium was first aspirated from the Transwells<sup>®</sup> and HBSS was added into both the apical (0.5ml) and basolateral (1.5ml) compartments and the cells incubated for an hour (37°C, 95% of humidity and 10% CO<sub>2</sub>). The TEER of the monolayer in HBSS was then measured prior to the addition of the polymer solutions (0.5 ml) in the apical chambers. TEER measurements were carried out at 40 minutes intervals. After 160 minutes, polymer solutions were removed and replaced with fresh HBSS and the TEER was measured again after one hour to determine if the effect of the polymer on the monolayers was reversible. The values coming from the measurements in HBSS alone (empty inserts that is without monolayers) were taken as negative control and PEI was taken as the positive control. The TEER of the monolayers were measured using a Millicell<sup>®</sup>-ERS meter (Millipore, Bedford, MA, USA) connected to a pair of electrodes which were separately placed in the apical and basolateral compartments.

### *2.14.5 Idarubicin uptake studies: Confocal microscopy*

The TEER value taken for Caco-2 cells was around 500-600 Ω·cm<sup>2</sup> and for HT29-MTX-E12 300-400 Ω·cm<sup>2</sup>. The IC<sub>50</sub> value determined the concentration of the polymer solution in each well. Idarubicin encapsulated polymers was kept in the apical compartment and incubated



(37°C, 95% humidity, 5% CO<sub>2</sub>) at various time points (0.5, 1, 2 and 4 hour). At each time interval, the insert was washed twice with DPBS and fixed with Paraformaldehyde (2%) in PBS (pH 7.2) for 10 minutes. The insert was washed with PBS (pH 7.2) and Triton X-100 solution (0.2%) in PBS (pH 7.2) to permeabilize the cells. Nuclei staining was done with DAPI (4',6-diamidino-2-phenylindole) starting with a stock solution (2.5 mg/ml) diluted to make a final concentration of 100 ng/ml (300 nM) in PBS. The polycarbonate membrane was fixed to the insert was properly detached and mounted with Superglue to fix the coverslip. A control experiment without the polymer was done; one with the cell monolayers with DAPI alone and the other with DAPI and Nile red. The images were obtained by Confocal microscopy Zeiss LSM 710 with a 30 mW 405 nm diode laser including 25 mW argon ion laser using the software of Zen 2009.


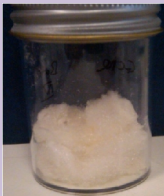
### *2.15 Statistical Analysis*

Experiments were done in triplicates where results and graphs are presented as average  $\pm$  stdev. Significance differences were calculated by student t-test (two populations) on Origin 6.0 software. Probability values of  $p < 0.05$  were considered statistically significant.

## **3. Results**

### *3.1 Synthesis*

Synthetic results of GC48 and GCPQ (all hygroscopic in nature) are presented in Table 3:

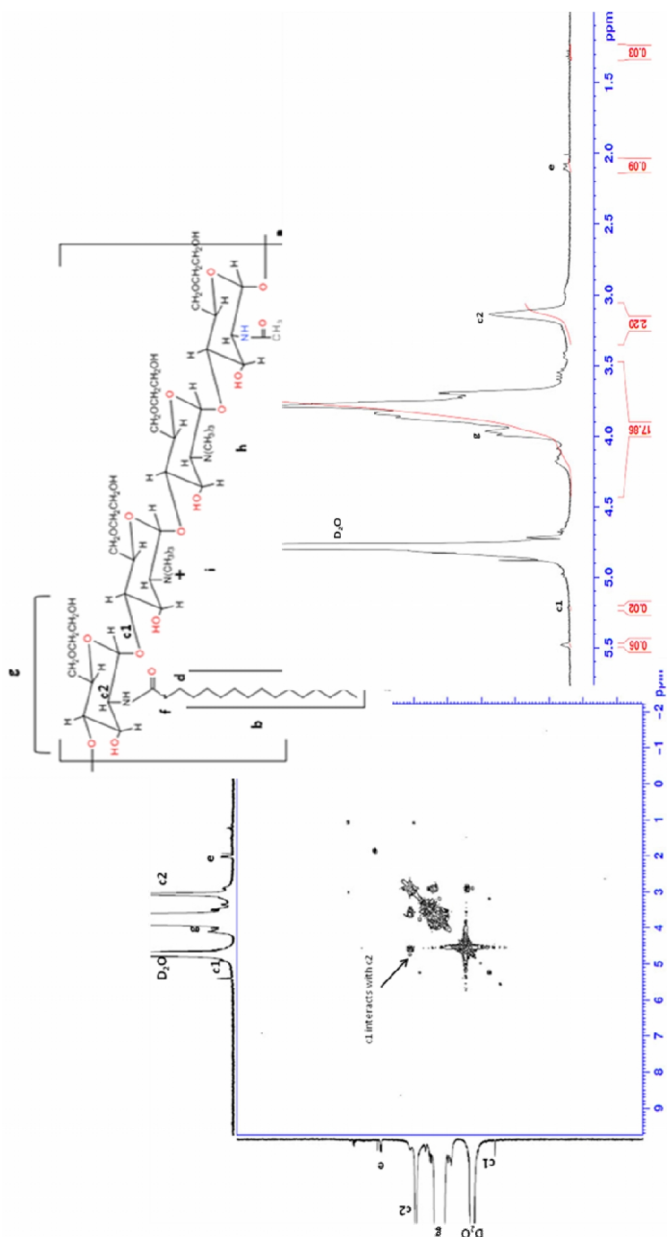
Polymer:	<b>GC48</b>	<b>GCPQ</b>
Practical yield	90 %	56%
Organoleptic properties	White, crystalline fluffy mass	White, fluffy mass
		

**Table 3:** *Synthetic results*

### 3.2 Characterization

#### 3.2.1 NMR

The spectrum for GC48 is seen in Figure 11. The proton assignments are as follows:  $\delta$ 2.0 for CH<sub>3</sub> (Acetyl-GC),  $\delta$ 3.0-3.3 for CH (sugar proton),  $\delta$ 3.4-4.4 for sugar proton,  $\delta$ 4.4 for the D<sub>2</sub>O (solvent peak) and  $\delta$ 5.2 for CH (sugar proton). The presence of c1 is determined at  $\delta$ 5.2 is confirmed when a cross peak is made which shows an interaction between c1 and c2.



**Figure 11:**  $^1\text{H-NMR}$  and  $^1\text{H-COSY}$  of Glycol Chitosan 48 (GC48) done in few drops of  $\text{D}_2\text{O}$

The  $^1\text{H-NMR}$  of PGC (Figure 12) shows the introduction of the palmitoyl group to GC48. The proton assignments for PGC are:  $\delta 0.85$  for  $\text{CH}_3$  (palmitoyl),  $\delta 1.15-1.40$  for  $\text{CH}_2$  (palmitoyl),  $\delta 1.55-1.70$  for  $\text{CH}_2$  (palmitoyl deshielded by carbonyl),  $\delta 1.95$  for acetyl-GC,  $\delta 2.20$  for  $\text{CH}_2$

Section 2 – PART B

(adjacent to carbonyl protons),  $\delta$ 2.95-3.15 for CH (sugar),  $\delta$ 3.30 for Methanol (solvent),  $\delta$ 3.40-4.40 for sugar protons,  $\delta$ 4.55 for D<sub>2</sub>O and  $\delta$ 4.70-5.15 for CH (sugar). As compared to the GC48, the CH's peak (c2) at  $\delta$ 2.95-3.15 moved only slightly upfield but seems more suppressed than before. This point is where modifications (like palmitoyl group) in this case attaches it to and as a result shows that the palmitoyl group has attached to GC48. Point off attachment of palmitoyl group is further confirmed by COSY which shows various interactions once cross peaks are made. c1 and c2 are confirmed by their cross peak with one another whereas 3 distinct interactions show the presence of the palmitoyl group: CH<sub>3</sub> and CH<sub>2</sub> from the palmitoyl chain labelled as a and b respectively, CH<sub>2</sub> from the palmitoyl and CH<sub>2</sub> deshielded by the carbonyl protons labelled as b and d respectively and lastly CH<sub>2</sub> adjacent to the carbonyl protons and CH<sub>2</sub> from the palmitoyl chain labelled as f and d respectively are seen to interact with each other.

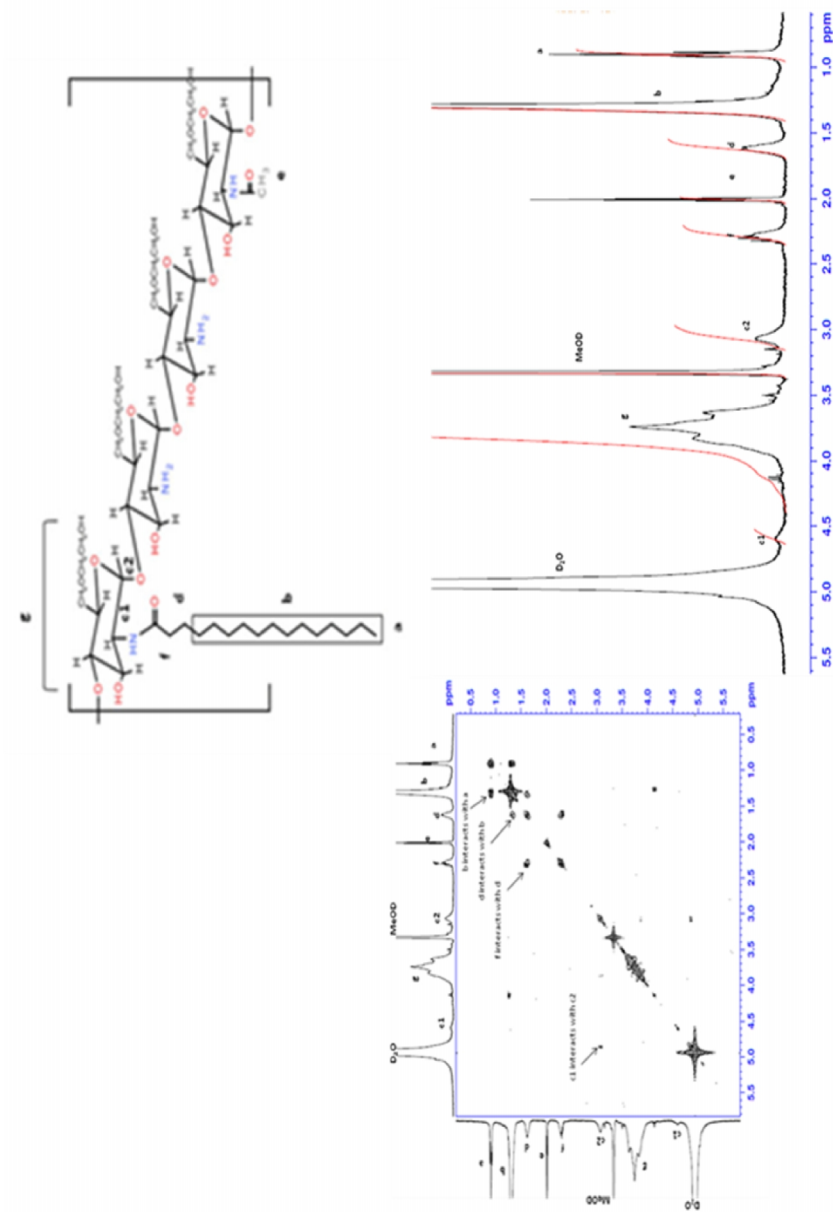
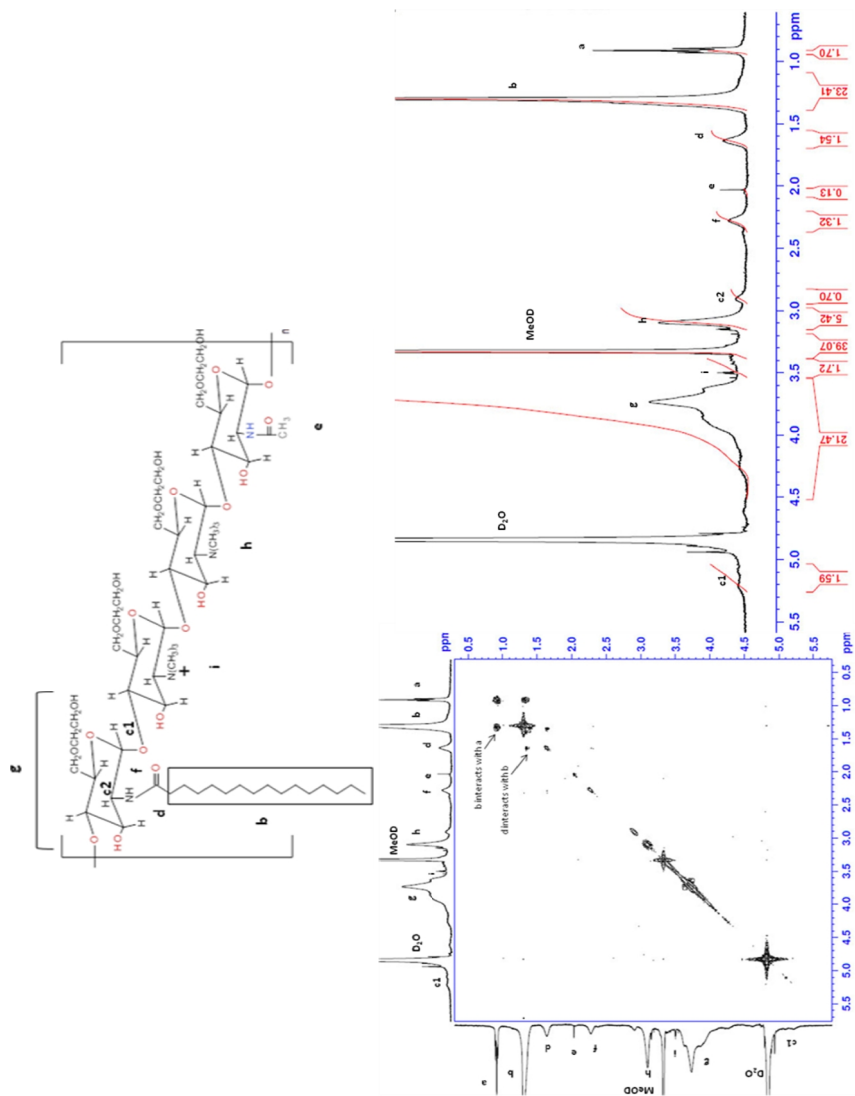


Figure 12: <sup>1</sup>H-NMR and <sup>1</sup>H-COSY of Palmitoyl Glycol Chitosan (FGC) done in CD<sub>3</sub>OD and few drops of D<sub>2</sub>O

The NMR result of GCPQ is seen in Figure 13. The proton assignments for GCPQ are as follows:  $\delta$ 0.85 for CH<sub>3</sub> (palmitoyl),  $\delta$ 1.10 for CH<sub>2</sub> (palmitoyl),  $\delta$ 1.55 for CH<sub>2</sub> (palmitoyl deshielded by carbonyl),  $\delta$ 2.05 for acetyl-GC,  $\delta$ 2.20 for CH<sub>2</sub> (adjacent to carbonyl protons),  $\delta$ 2.85 for CH (sugar),  $\delta$ 3.0-3.20 for CH<sub>3</sub> (dimethyl amino GC),  $\delta$ 3.30 for MeOD

Section 2 – PART B

(solvent),  $\delta$ 3.45 for CH<sub>3</sub> (trimethyl amino GC),  $\delta$ 3.55-4.50 for sugar protons,  $\delta$ 4.50-5.0 for D<sub>2</sub>O (solvent) and  $\delta$ 5.0 for CH (sugar). Addition of a palmitoyl and quaternized group suppressed c2 peak (the peak is not as sharp as seen originally from GC48's spectrum) and has shifted slightly upfield ( $\delta$  2.90 when originally it was  $\delta$ 3.0-3.3). From the COSY two prominent cross peaks are seen; one indicating the interaction between the CH<sub>2</sub> of palmitoyl and CH<sub>3</sub> of the palmitoyl chain and the other one showing the interaction between CH<sub>2</sub> of palmitoyl that is deshielded by the carbonyl protons and the CH<sub>2</sub> of palmitoyl that is adjacent to the carbonyl protons. However, no cross peak was seen to show the interaction of c1 and c2 which can be due to the number of scans that was done during analysis.



**Figure 13:** <sup>1</sup>H-NMR and <sup>1</sup>H-COSY of Quaternary Palmitoyl Glycol Chitosan (GCPO) in CD<sub>3</sub>OD, few drops of D<sub>2</sub>O and a drop of CD<sub>3</sub>COOD

## Section 2 – PART B

### 3.2.2 % Substitution degree

Using the equations previously reported, % acetylation was calculated for GC48 and % SD was calculated for GCPQ as shown below in Table 4.

<b>GC48</b>	%Acetylation:	1.51%
<b>GCPQ</b>	%Palmitoylation:	9.024 ± 1.272*
	%Quaternization:	14.499 ± 4.108*

**Table 4:** %Acetylation and %SD for GC48 and GCPQ(\*n=5)

### 3.2.3 Molecular weight through NMR analyses

Using equation previously reported, the number of monomers (N) was calculated to be 33. With this value, molecular weights of the polymers were calculated as shown in Table 5.

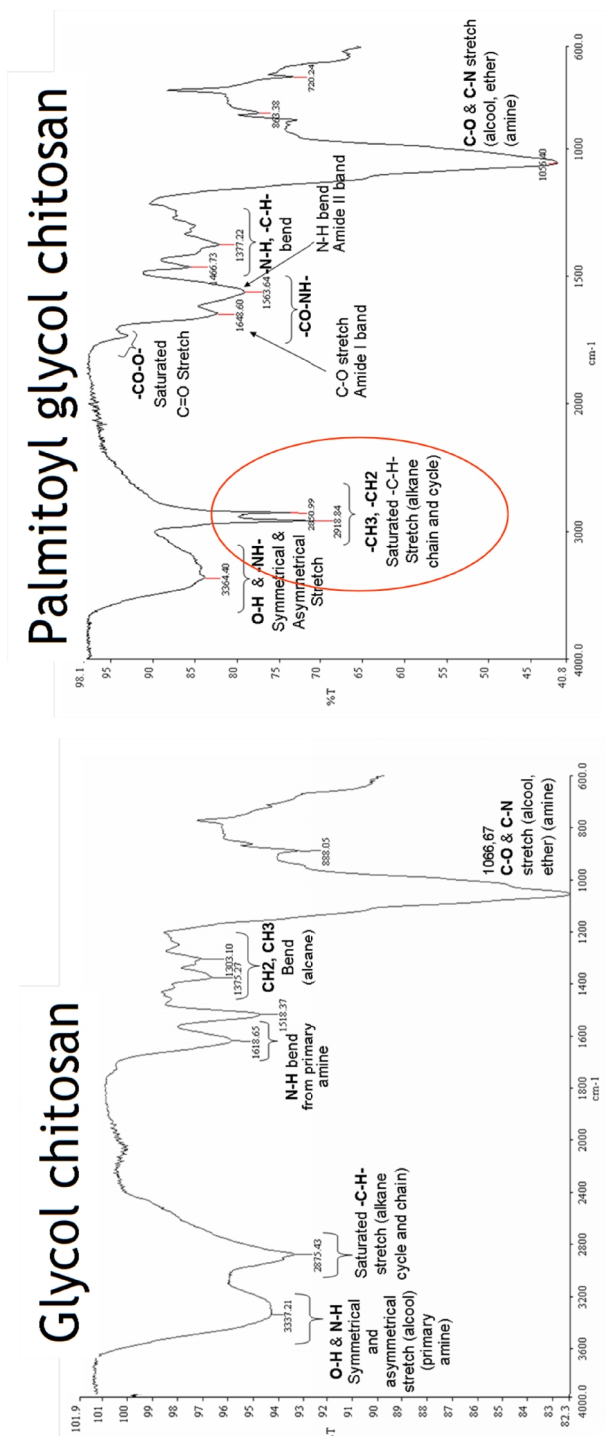
Polymer	<b>GC48</b>	<b>GCPQ</b>
Molecular weight (g/mol)	6,765	8,798

**Table 5:** Molecular weights of the polymers using NMR spectroscopy

### 3.2.4 FT-IR

The FT-IR results for GC48 and GCPQ are shown in Figure 14 in which all the main differences due to the presence of new functional groups are evidenced.





**Figure 14:** FT-IR spectra of GC and PGC showing the characteristic twin bands in the PGC spectrum at 2800–2900  $cm^{-1}$

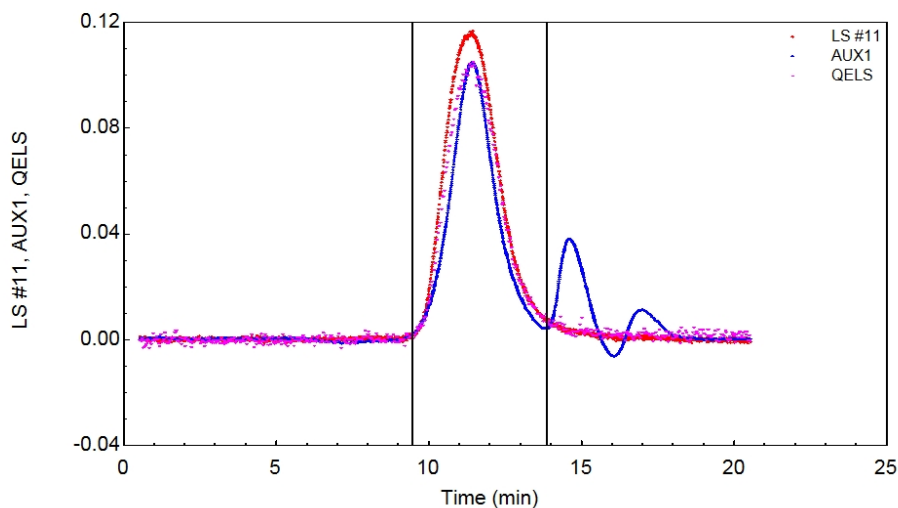
3.2.5 GPC-MALLS: Molecular Weight Determination

The molecular weights for the polymers GC48 and GCPQ48 are given in Table 6. Results achieved with this technique are quite in agreement with the calculations performed using  $^1\text{H-NMR}$  spectra.

Polymer	Mw (Da)	Mn (Da)	Mw/Mn
GCPQ	9795	9499	1.03
GC48	8015	6128	1.175

**Table 6:** Molecular weight calculated through GPC-MALLS.

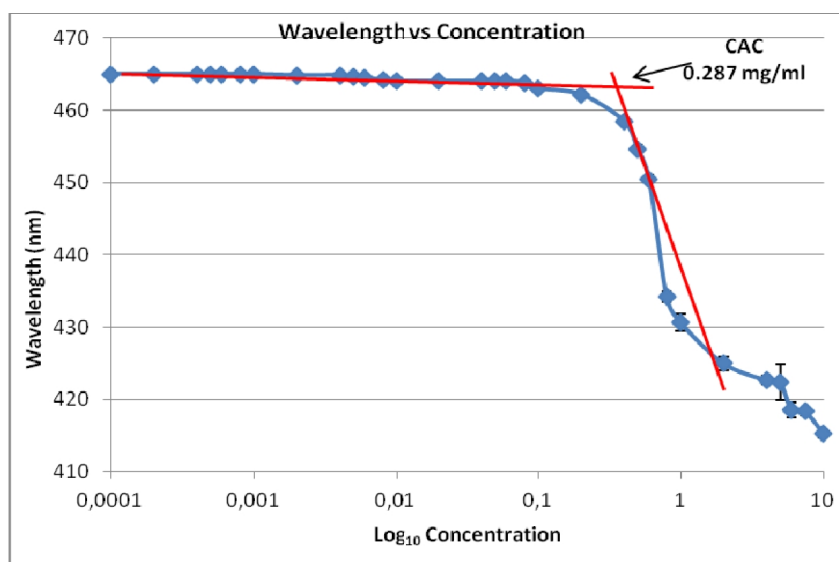
A sample chromatogram appears in Figure 15.



**Figure 15:** Gel permeation chromatogram (light scattering-LS, refractive index-AUX1, quasielastic light scattering (QELS) of GCPQ48. Chromatography conditions are as detailed in the text above.

## 3.2.6 CAC

A  $\lambda_{\max}$  of 465 nm of methyl orange (25  $\mu\text{m}$ ) was recorded in borate buffer (0.02M) at 25°C where various dilutions with varying concentrations were made to observe a shift of methyl orange and a graph of wavelength vs concentration was plotted to observe this and record the CAC value. The CAC value can be measured by the intersection of the lines from the plot between wavelength and concentration as shown in Figure 16. A hypsochromic shift from 465 to 434 nm was observed in GCPQ confirming the presence of hydrophobic domain. The data points were performed in triplicates showing average  $\pm$  std dev to show from intersection that GCPQ has a CAC value of 0.287 mg/ml ( $p < 0.01$ ).



**Figure 16:** CAC results of GCPQ (A). Data points represent means  $\pm$  stdev when  $n=3$ . They are significantly different ( $p < 0.01$ )

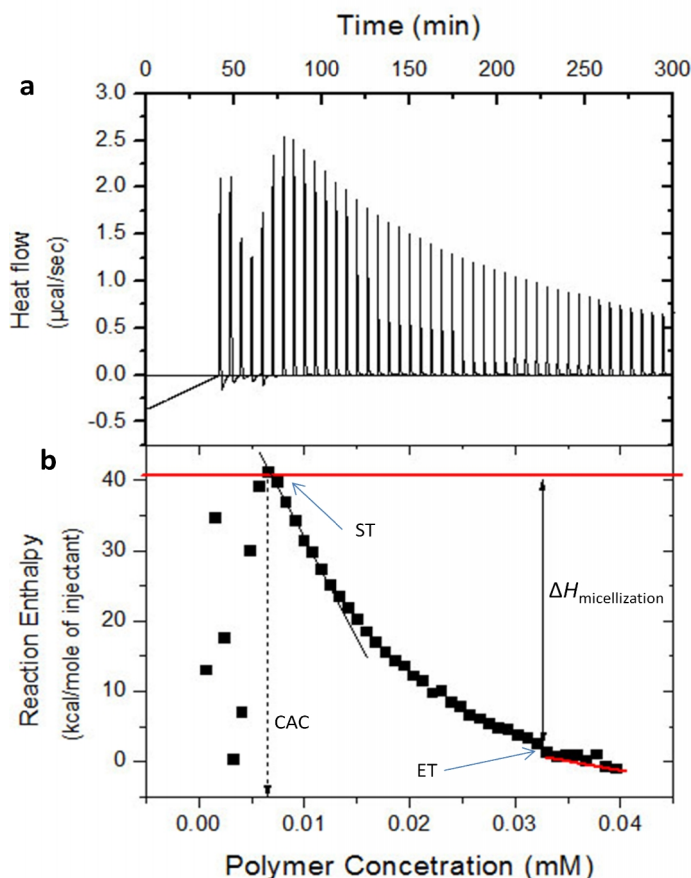
Using ITC, a concentration of 2mg/ml was taken at 25°C (298 K) to help measure both CAC and  $\Delta H_{\text{demic}}$  as seen in Figure 17. An enthalpy change was observed due to dilution of micelles, demicellization of micelles and dilution of micelles. A change in the slope (start of transition, ST) is the

concentration of micelles at which it further addition of micelles do not demicellize. This reduces the enthalpy change and a point comes where further demicellization is terminated (end of transition, ET) resulting in a plateau [38]. The difference in enthalpy between the 1<sup>st</sup> and 3<sup>rd</sup> concentration gives  $\Delta H_{mic}$ . Positive values of  $\Delta S_{mic}$  at 298 K in both cases is a result of micelles formation as there is an increase in entropy (entropy driven) and loss of enthalpy that destroy the water molecules that surround the hydrocarbon chain. The result from methyl orange probe UV-spectroscopy and ITC are shown in Table 7:

Methyl orange probe UV	ITC				
	CAC (mg/ml)	$\Delta H_{mic}$ (kJ/mol)	Polymer concentration (mM)	CAC ( $\mu$ M)	$\Delta G_{mic}$ (kJ/mol)
0.287	30.3 $\pm$ 4.5	0.00619 $\pm$ 0.0005	57.19	10.03	68

**Table 7:** CAC results using methyl orange probe UV-spectroscopy and ITC

Each data was performed in triplicates for both methyl orange probe UV and ITC and a comparison of the values recorded for the polymers demonstrated they are significantly different from each other,  $p < 0.01$ .



**Figure 17:** Dilution/demicellization of enthalpogram for GCPQ: *a.* Demonstrating the heat flow of the polymer at 298 K, *b.* Process enthalpy vs polymeric concentration in the cell, heat of micellization shown by the arrow, CAC is the point at which a drop in the curve is observed.

### 3.2.7 PCS

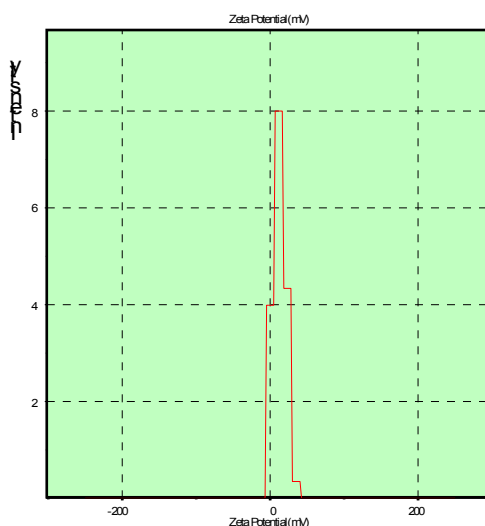
Zeta potential results confirms introduction of the positive charge due to the successful attachment of the modified groups. Intensity vs Zeta potential (mV) shows the distribution of the surface charge of the polymer in Figure 18. Unfiltered particle sizes had a wide range of particle sizes resulting in multiple peaks and a wider distribution. Filtration reduced particle size. Table 8 summarizes collective PCS data; each analysis was

Section 2 – PART B

performed in triplicates, each results are significantly different from each other ( $p < 0.01$ ).

Zeta Potential			Particle Size					
KCps	Mobility	Zeta Potent (mV)	Unfiltered			Filtered		
			KCps	ZAve (nm)	PD	KCps	ZAve (nm)	PD
287 ±2.81	1.35 ±0.02	17.0 ±0.31	423 ±13.6	533 ±31.0	0.44 ±0.06	84 ±3.4	93 ±3.5	0.53 ±0.06

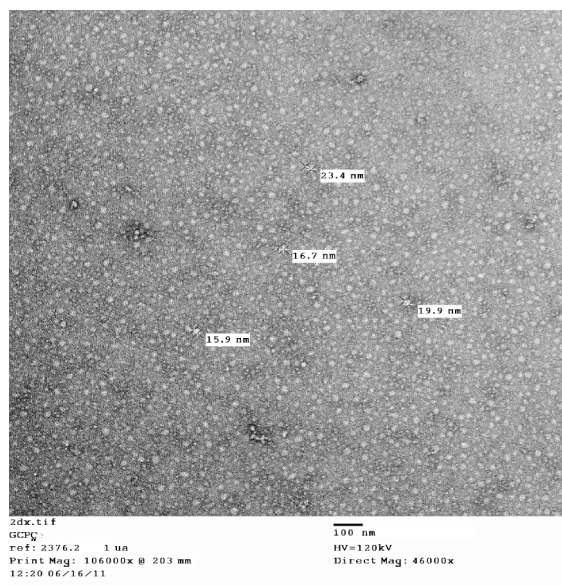
**Table 8:** PCS results showing Zeta Potential and Particle Size (unfiltered and filtered) of GCPQ



**Figure 18:** A plot of Intensity vs zeta potential (mV) of GCPQ.

### 3.2.8 TEM

After the polymer was probe sonicated and filtered, its images were recorded and are presented in Figure 19. The GCPQ particles appear to be round and spherical in shape forming micelles in water, therefore this confirms the particle size results that were performed earlier.

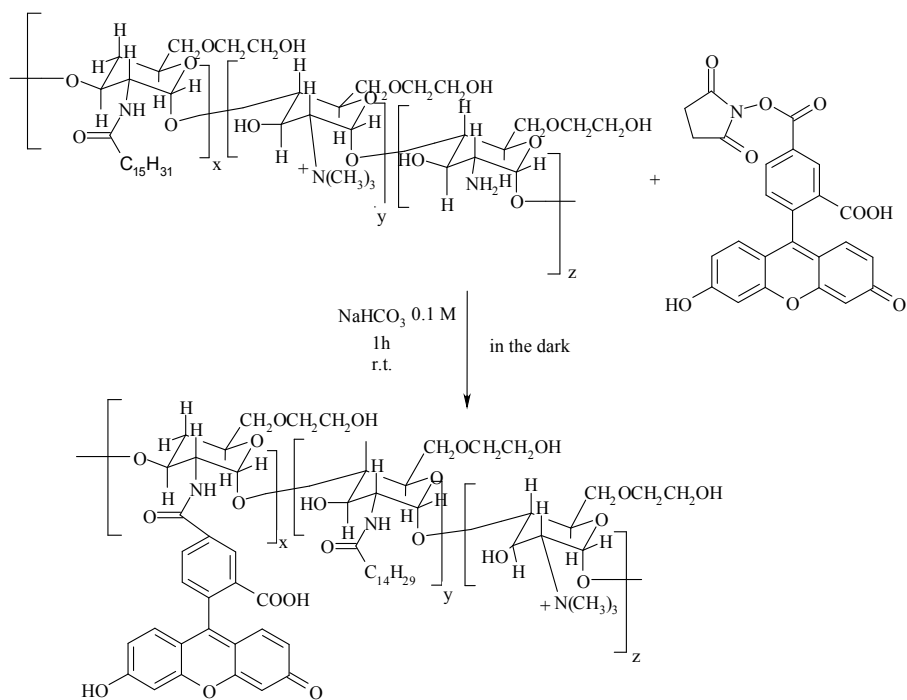


**Figure 19:** TEM results of GCPQ to show the formation of micelles.

### 3.2.9 Synthesis of Fluorescent Labelled GCPQ

This reaction was conducted according to the synthetic strategy reported in Figure 20.

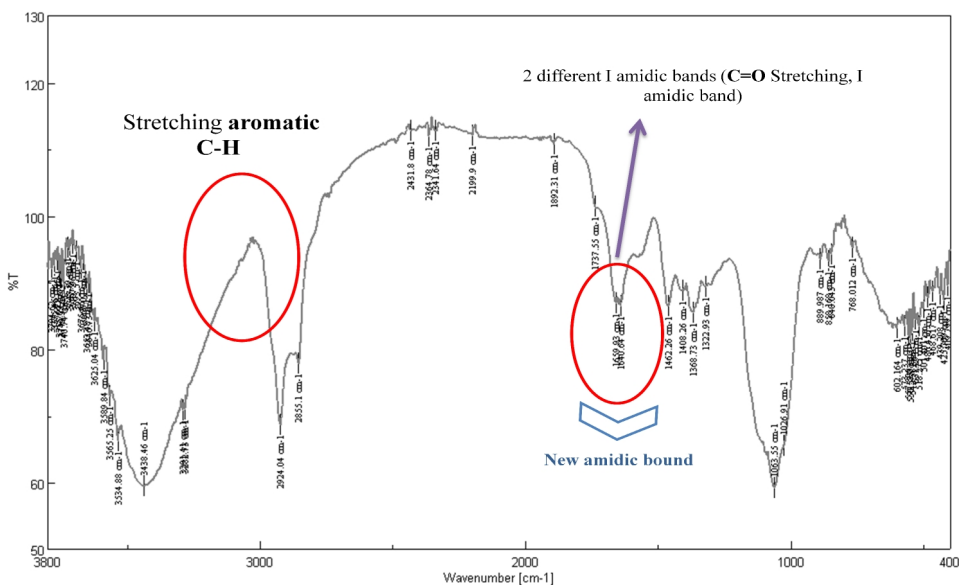
Section 2 – PART B



**Figure 20:** *Synthesis of Fluorescent Labelled GCPQ (FL-GCPQ).*

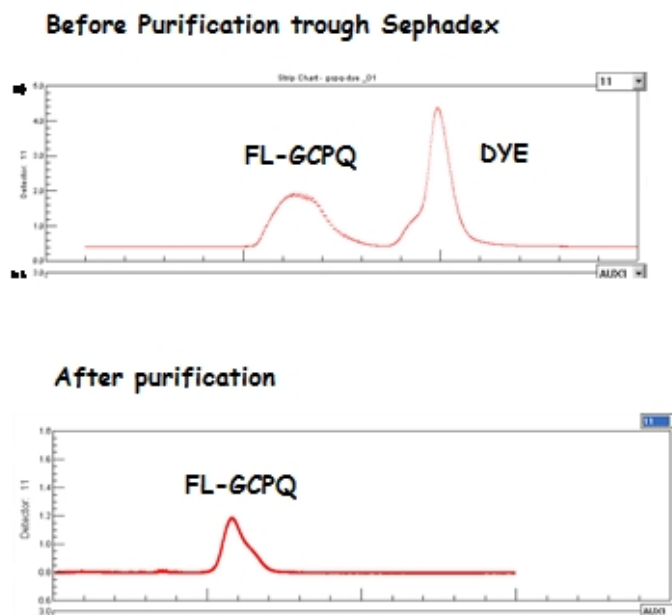
The obtained product was characterized through FT-IR (Figure 21) and GPC-MALLS (Figure 22).





**Figure 21:** FT-IR spectrum of FL-FCPQ.

GPC-MALLS is an analytical technique able to detect differences in the molecular weight of the polymers. In this case it was performed to assess that no free dye was present in the sample after purification through Sephadex (Figure 22). The eluent mixture used was the following one: acetate buffer (0.3 M  $\text{CH}_3\text{COONa}$ /0.2 M  $\text{CH}_3\text{COOH}$ , pH=5) and methanol (ratio 35:65). The column used was a Polysep<sup>TM</sup>-GFC-P 4000 (300 x 7.8 mm, Phenomenex, U.K.).



**Figure 22:** GPC chromatograms showing the production of GCPQ48 labelled with 5-Carboxyfluorescein.

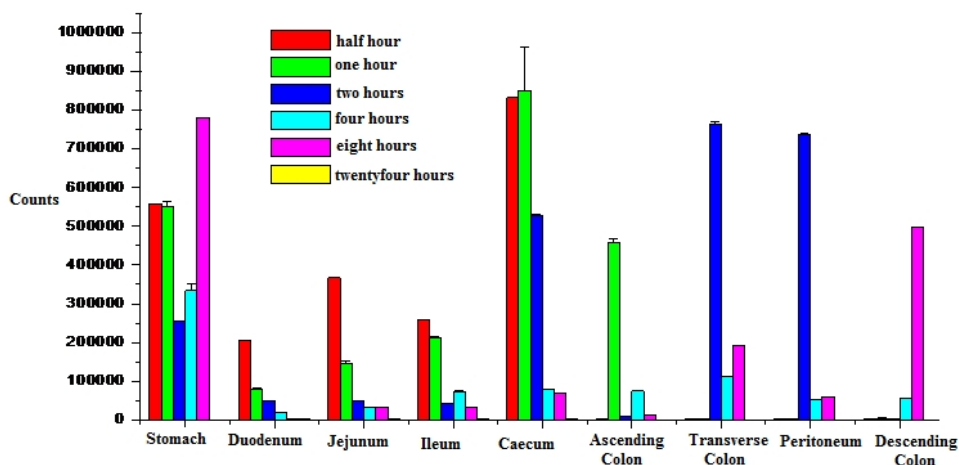
### 3.2.10 Encapsulation Studies

Terminal filtration of the formulation with 0.45  $\mu\text{m}$  filters was not adequate to remove drug nanocrystals in the sense that no difference was found between the percentage of entrapped drug calculated before filtration and after. Therefore, the formulation was spun at 1000 rpm x 10 min and then filtered. Even the additional spinning step has eliminated the presence of free drug in the formulation so it was assumed that all the drug has been entrapped in the nanoparticles.

### 3.3 In vivo biodistribution studies

Samples were assayed for radioactivity using the gamma counter. Results were expressed as % of the administered dose. As it can be seen in Figure

23, the polymer is not absorbed from the gut; in this graph, in fact, only the levels in the gastro-intestinal tract were reported because the radioactivity levels in the other organs were no quantitatively appreciable at all.



**Figure 23:** Graph showing GCPQ levels in the gut

Finally, results show clearly that only a minor and unappreciable amount of polymer is absorbed and this is probably awardable to the absorption of low molecular weight polymer chains still residues in the administered samples. The travel from the stomach to the colon is clear and the complete elimination after 24 hours makes the polymer a really good oral absorption excipient.

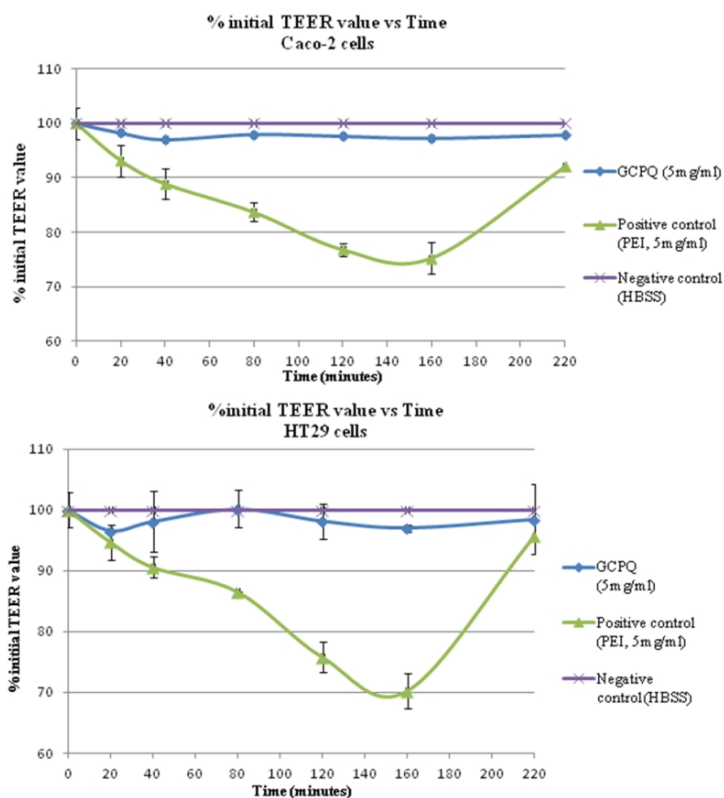
### 3.4 Cell Studies

#### 3.4.1 TEER

TEER measurements for GCPQ performed on both Caco-2 and HT29-MTX-E12 cells using HBSS alone as the negative control and PEI (known for opening the tight junctions) as the positive control were performed. A graph between % initial TEER value and time (interval to

Section 2 – PART B

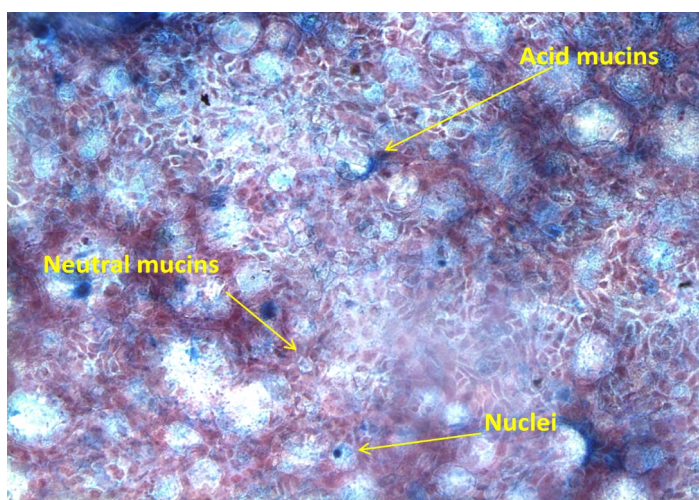
220 minutes) was plotted for the polymer in Caco-2 and HT29-MTX-E12 cells separately as seen in Figure 24. The TEER of the Caco-2 monolayers after 21 days was around  $572 \Omega \text{ cm}^2$ ; instead the TEER of the HT-29 monolayers was around  $348 \Omega \text{ cm}^2$ . The TEER is a reflection of the paracellular permeability as well as an indication of monolayer integrity. GCPQ didn't cause any reductions in the TEER values of the two different cell lines: Caco-2 anyway shows a stronger TEER compared to HT29 being a tighter cell line [40].



**Figure 24:** TEER results of Caco-2 (A) and HT29-MTX-E12 cells (B). Data points represent averages  $\pm$  stdev when  $n=3$  and when GCPQ was compared to both the negative and positive control, they were significantly different from each other ( $p < 0.01$ ).

### *3.4.2 Mucus Layer Characterization: Mucus Staining*

To check if HT29-MTX-E12 cells produced mucus, their monolayer was characterized by staining it with alcian blue and observed under a light microscope (Figure 25). The image shows various round shaped cells that grew on top of each other leading to an increase in thickness of the monolayer. Alcian blue staining proved the presence of a mucus layer where an even distribution of staining was observed. Acid mucins were stained blue, nuclei stained pale blue and neutral mucins magenta in colour.



**Figure 25:** *Mucus monolayer of HT29-MTX-E12 cells after alcian blue staining demonstrating a distribution of mucus components.*

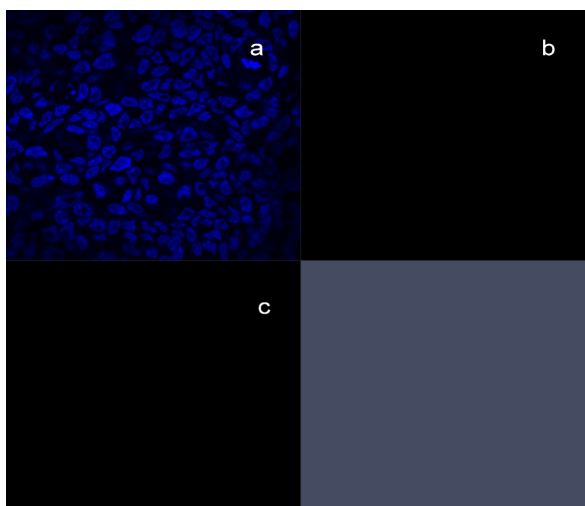
### *3.4.3 Confocal Images*

In order to investigate the fate of the polymer and the drug once in contact with Caco-2 or HT29-MTX-E12 monolayers, a Zeiss LSM 710 Laser Scanning Confocal Microscopy Imaging system was used to qualitatively detect fluorescence. The lasers were adjusted in the red fluorescence to yield an excitation wavelength of 543 nm and in the green fluorescence to yield an excitation wavelength of 488 nm. Images revealed nuclei blue

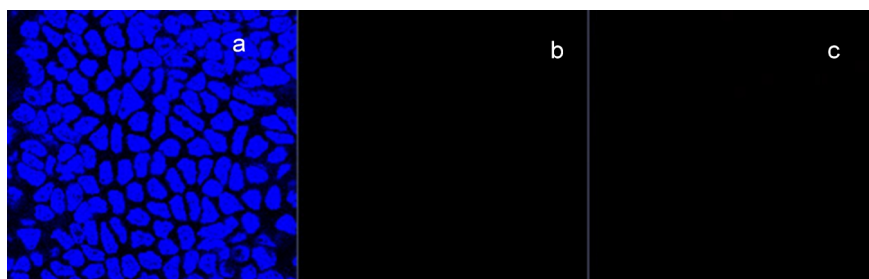
stained and the green particles corresponding to the polymer; zeta-stacks (zeta optical sections) confirmed also the presence of the red fluorescent drug idarubicin in the cells [41]. Interpretation of confocal images was very difficult due to the autofluorescence of biological samples and to a photobleaching process during which the molecular structure of a dye is altered as a result of the absorption of the excitation light leading to a gradual reduction of fluorescence intensity. Anyway, the following images show that probably GCPQ adheres to the cell surface especially in presence of mucus and is not taken up in the cells. 5-Carboxyfluorescein is a green fluorescent probe with an excitation wavelength of 492 nm and an emission wavelength of 517 nm. Idarubicin is a red fluorescent drug with an excitation wavelength of 470 nm and an emission wavelength of 580 nm. DAPI is a blue fluorescent dye probe with an excitation wavelength of 358 nm and an emission wavelength of 461 nm. When DAPI forms the complex DAPI-DNA the emission is usually fixed at 460 nm, instead when it forms the complex DAPI-RNA the emission is usually fixed at 500 nm.

In order to understand results, it could be useful to analyze every single time-point comparing their zeta sections and also the different images coming from the two different monolayers.

For both cell line the control was investigated by using a monolayer stained only with DAPI (Figure 26 and 27) in which no green and red fluorescences were detected:

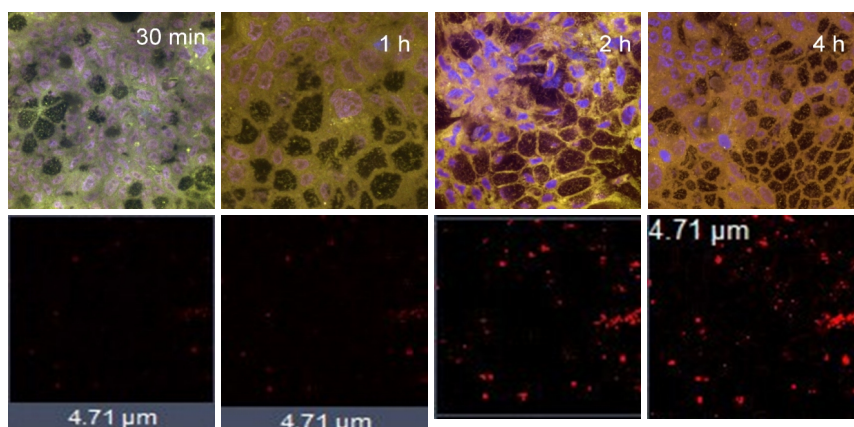


**Figure 26:** *DAPI control on HT29-MTX-E12 monolayers; a)blue channel, b)green channel, C)red channel*

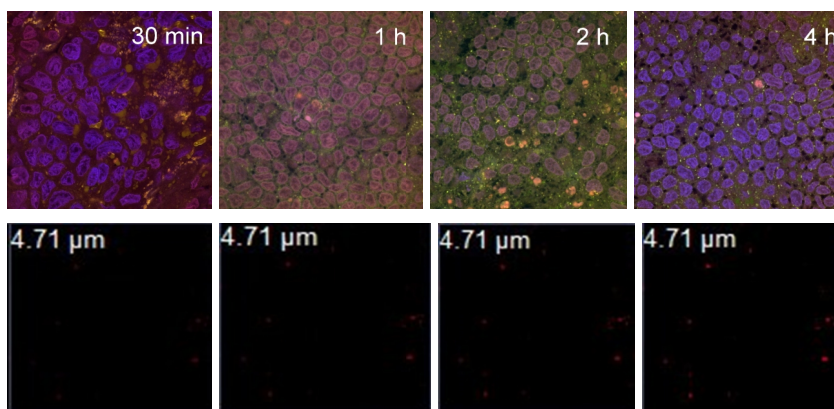


**Figure 27:** *DAPI control on Caco-2 monolayers; a)blue channel, b)green channel, c)red channel*

Confocal optical zeta sections in 0.40  $\mu\text{m}$  intervals taken through the midplane of cells are shown. The upper panels of Figure 28 and 29 show fluorescence overlays, respectively of HT29-MTX-E12 and Caco-2, and the lower panels show the fluorescence in the same median optical section (4.71  $\mu\text{m}$ ). In the optical section, showing only the green and red channels, only red fluorescence can be detected due to drug absorption.



**Figure 28:** *HT29-MTX-E12 monolayers confocal images at different time-points showing the fluorescence overlays (upper panels) and an optical sections (lower panels)*

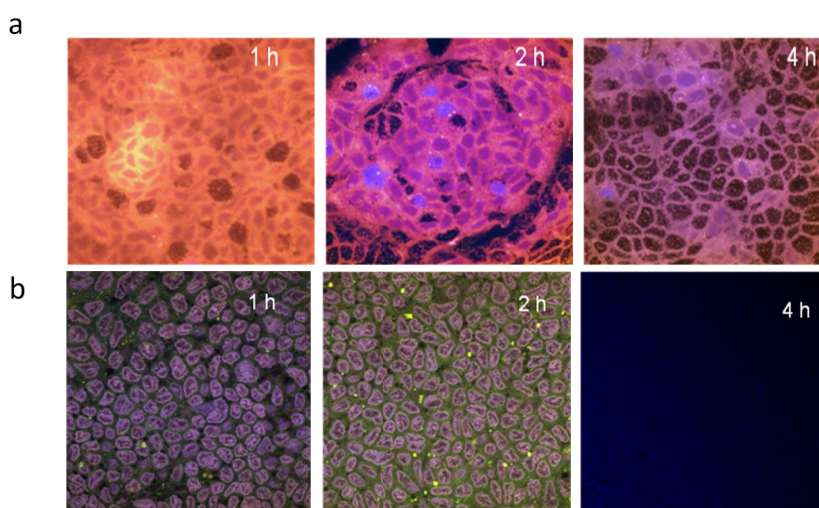


**Figure 29:** *Caco-2 monolayers confocal images at different time-points showing the fluorescence overlays (upper panels) and an optical sections (lower panels)*

Results revealed first of all that the polymer is not absorbed in the cells; this evidence is true for both cell lines and is supported by the total absence of green fluorescence in the confocal optical zeta sections taken through the midplane of the cells. Moreover a substantial difference can be underlined between the two cell lines: the drug absorption, measured on the basis of the visual intensity in the red channel observing optical sections, seems to be more consistent for HT29-MTX-E12 in which the presence of the mucus together with the bioadhesive properties of the



chitosan derivative enhance drug internalization into cells. Moreover, idarubicin alone (used as control) in the same amount, especially after 4 hours of incubation, kills the majority of the cells in the monolayer. This doesn't happen with the formulation, meaning that in some ways the formulation plays a delayed release of the drug. Figure 30a (referred to HT29-MTX-E12) and Figure 30b (referred to Caco-2) explain the latter concept: the free drug, especially after 4 hours, explains its anticancer activity killing the major part of the cells; in particular after 4 hours Caco-2 monolayers are completely destroyed.



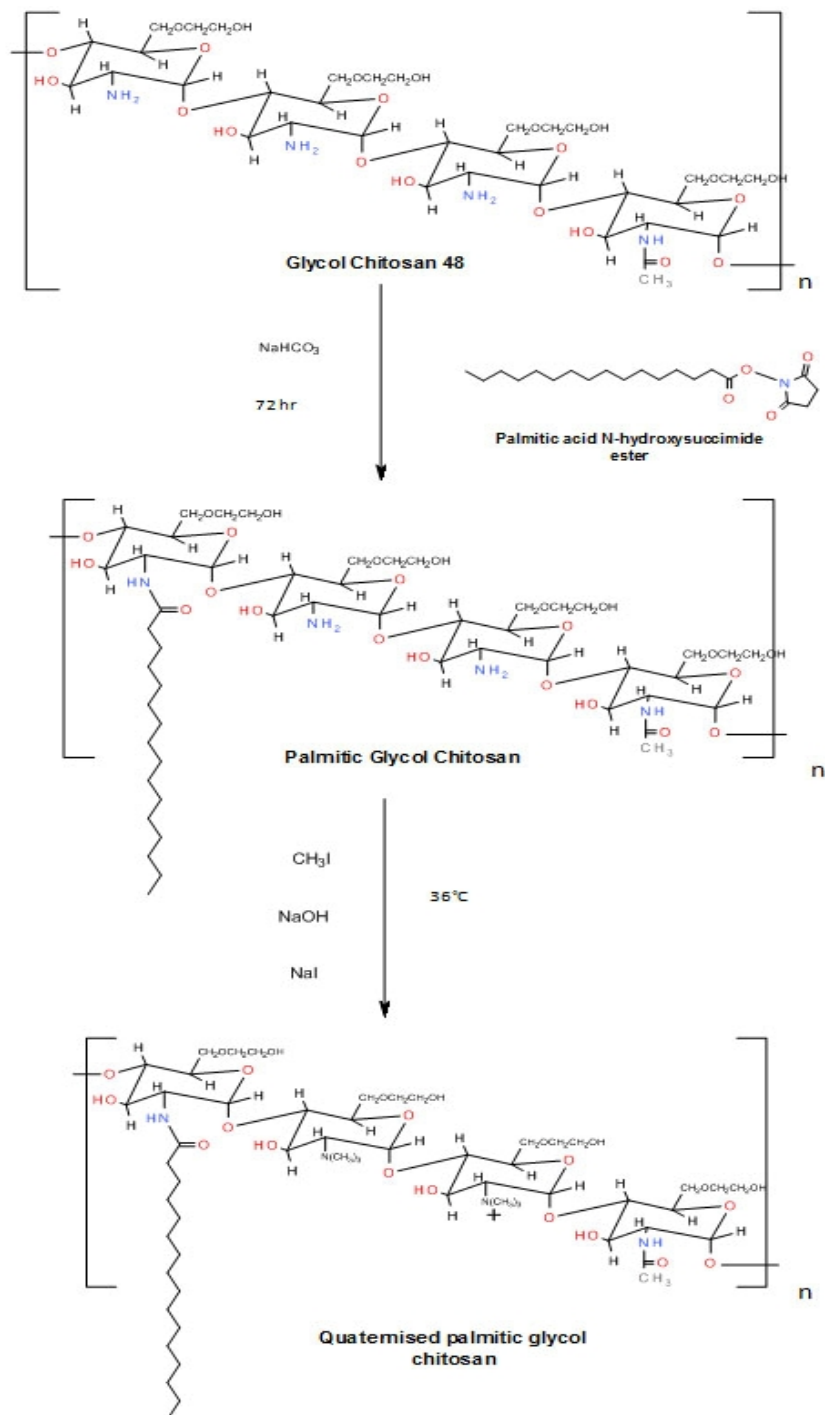
**Figure 30:** Confocal images of free Idarubicin hydrochloride in HT29-MTX-E12 (a) and Caco-2 (b)

### 3.5 Discussion

The schematic route for the synthesis of GCPQ is shown in Figure 31. Addition of a hydrophobic chain and a quaternary ammonium group was achieved by N-alkylation of the free amino groups present. For GCPQ, the positive surface charge was introduced by N-alkylation by using an inorganic base, NaOH which was used to decrease the degradation of

Section 2 – PART B

chitosan and maintain the global  $pK_a$  of the polysaccharide. Quaternization is seen to be temperature dependent, i.e. higher the temperature, higher will be the level of quaternization. To obtain a % quaternization in the range of 8-15%, the temperature was set at 36°C. The charge density was seen to increase as a result of electrostatic hindrance of the molecule [42]. Introduction of a hydrophobic backbone allowed the formation of micelles and the quaternary group increased the solubility of GCPQ in various solvents.



**Figure 31:** Schematic representation of GCPQ synthesis.

GC after 48 hour of degradation (GC48) (for a molecular weight range of 12-14 kDa) was used to synthesize GCPQ via PGC and these polymers were confirmed using  $^1\text{H-NMR}$  and COSY. Point of attachment was confirmed by the shift of c2 and % SD calculated. FTIR is a useful technique for detecting changes in the functional groups [43]. Various functional groups in GC48 and GCPQ were noted with a change in their wavelength. Presence of palmitoyl group was confirmed between  $2900\text{-}2800\text{ cm}^{-1}$  and  $1710\text{-}1700\text{ cm}^{-1}$ . The presence of the positive charge i.e. area of quaternization was confirmed at  $1464\text{ cm}^{-1}$  for GCPQ.

CAC describes the micellization of a polymer which can be studied by a solvatochromic dye like methyl orange [44]. This dye undergoes a hypsochromic shift as a result of polar to non-polar transition [45] a change in absorption demonstrating the aggregation phenomenon. It is the initial appearance of the micelles in solution: further addition of a surfactant results it in being constant in its monomeric form whereas micelles are formed above this concentration. Intramolecular micellization is the aggregation formation caused by the contraction in the molecular dimensions in the side chains of the hydrophobic domains solubilising water-insoluble organic molecules. Various factors influence the CAC of a polymer like the sequence, length of the block chains and temperature (to keep temperature constant, all measurements were done after 1 hour incubation at room temperature,  $25^\circ\text{C}$ ). Hydrophobic modification has also found to play an important role leading to spontaneous aggregation [29]. Methyl orange has a  $\lambda_{\text{max}}$  of 465 nm in sodium borate buffer (0.02M); when polymeric solutions of GCPQ are added, the wavelength of methyl orange is seen to shift towards the blue region, a shift from  $\pi$  to  $\pi^*$  known as the H-aggregation and the aggregation behaviour is seen to follow Beer Lamberts law. A shift from

465 nm to a shorter wavelength in GCPQ is due to the reduction in concentration with the subsequent serial dilutions. The results show that GCPQ (0.287 mg/ml) has a low CAC which is thermodynamically favourable for the hydrophobic domain. There is a reduction in the size of the head group due to an increase in the electrostatic interaction between volume of the apolar and ionic groups [46]. This property of GCPQ can be extremely useful in surfactant and emulsion formulations.

ITC is a useful technique to study drug-surfactant interactions where a measure of enthalpy of interaction can be noted as a result of various processes like surfactant and drug dilution, drug dissolution and solubilisation and surfactant absorption [47]. At room temperature (25°C/298 K),  $\Delta S_{mic}$  was positive for GCPQ and  $\Delta H_{mic}$  is endothermic in both cases. The micellization phenomenon of these polymers is entropy driven (positive  $\Delta S_{mic}$  and negative  $\Delta G_{mic}$ ) since the hydrophobic domain increases hydrogen bonds once it interacts with water causing electrostatic repulsion and resulting in amphiphile aggregation.

PCS data showed the successful introduction of surface charge density; polymeric micelles with controlled surface charge have posed a challenge for a long time mainly during the size control processes and incorrect correlation between physiochemical processes and biological processes of the polymers. Surface charge density of NPs can play a more predominant role than hydrophobicity and surface chemistry when it comes down to explaining the mechanisms of cell uptake mainly phagocytosis [48]. Results show that GCPQ attained a cationic charge ( $17.0 \pm 0.3$  mV). Information about particle size is important to understand cellular transport; larger particle size will be not be transported by transcellular pathway in contrary to smaller particle size:

## Section 2 – PART B

1. Paracellular pathway: usually limited to particles having a size of less than 50 nm
2. Endocytic pathway via endocytosis having a size range of 100-200 nm
3. Lymphatic uptake: by particles less than 5 micrometer resulting in adsorption by M cells present in the Peyer's patches

It can determine the fate of NPs; larger particles get phagocytised in a shorter time as compared to the smaller particles due to coalesces within the cell surface. Adhesion and interaction with biological cells are affected. MW and hydrophobicity can strongly influence the particle size (hydrophilic group increases vesicle curvature due to increase in relative head group area shielding hydrophobic regions to attain minimal energy state. There is an increase in vesicle curvature due to increased ratio of headgroup area to hydrocarbon volume/chain length for low molecular weight polymers as compared to high molecular weight polymers however a decrease in flexibility of the molecule will be noted. MW and surface area are directly proportional to one another where the surface area of the sphere is given by  $\pi d^2$  where d is the diameter of the sphere [49].

Idarubicin, being hydrophobic in nature, was seen to be well encapsulated with GCPQ due to the hydrophobicity level of GCPQ which is seen to have favourable encapsulation for hydrophobic drugs.

Cell uptake studies in the 2 cell lines were done when they formed a monolayer after 21 days and were important to characterize it. HT29-MTX-E12 cells secrete mucus which was confirmed by alcian staining that stained acid mucins, nuclei and neutral mucins blue, light blue and magenta respectively. Mucins are glycosylated proteins that are secreted by the goblet cells in the intestinal epithelium [12]. Cytotoxicity studies

were carried out to calculate the IC<sub>50</sub> value (50% inhibition of cell growth) [15]. The principle being cleavage of MTT's tetrazolium ring with the mitochondrial dehydrogenation enzyme of the viable cells, colour intensity being directly proportional to the amount of formazon formed. Factors that influence cytotoxicity are MW and positive charge density [50]. It is usually reported that a cationic charge will be more cytotoxic than the anionic charge due to an interaction between the cationic charge and anionic glycoproteins in the cell compartment causing a steric effect with the methyl pendent groups resulting in lower cell viability due to failure of dimethylamino's methyl pendent groups to shield the positive charges. The ability of the polymer to open the tight junctions was tested in both cell lines by measuring their TEER values using HBSS alone as the negative control and PEI as the positive control. Opening the cell junctions indicates paracellular transport but since there was no TEER reduction, a different cell transport system could have been possible.

Images of permeability and cell uptake/bioadhesion studies were visualized by CLSM that offered a 3D reconstruction of the sample analysed displaying an outside and inside view of various structures. This quantitative and non-destructive technique helps in the visualization of structures along (x,y,z) spatial dimensions [51]. Triple staining with DAPI (blue) , Carboxyfluorescein (green) and Idarubicin (red) was useful to distinguish between the different cellular components where DAPI has a tendency of cleaving with the DNA and nucleus of the cell staining them blue in return. CLSM images in both cell lines showed GCPQ had more internalization of drug in HT29-MTX-E12 due to a strong association of cationic charge with the mucins on the cells surface [34]. Cationic charge resulted in higher bioadhesion and cell uptake (other

factors influencing cell uptake are time, temperature and concentration). Internalization can be concluded from the disruption of the cellular membrane by adsorptive endocytosis and electrostatic forces of attraction which can explain the lag phase between 30 minutes of incubation till about 120 minutes when clear drug cellular internalization is seen for GCPQ [37].

In HT29-MTX-E12 cells, more mucoadhesion and drug internalization is seen. Though mucus is a barrier, the cationic charge of GCPQ could have potentiated the consolidation stage of mucoadhesion by increasing the polymer-mucus interaction causing higher interpenetration into the mucus. Stronger electrostatic interaction is caused between GCPQ and the negative charges on the cell membrane due to sialic and phospholipid head groups present in the mucus layer resulting in a higher residence time for absorption [31]. However, a high quaternization level might not be that advantageous, its flexibility can decrease leading to a decrease in mucoadhesion as a consequence therefore it is important to control the surface charge density. This study and literature has concluded the importance of quaternization to the absorption enhancement of such biodegradable polymers. The hydrophobic nature of Idarubicin contributes to the type of interaction that could have taken place with the mucus layer; due to its hydrophobicity, the probability of hydrophobic interactions may be higher.

Results obtained through confocal imaging are completely in agreement with the levels of radioactive polymers found in the excised organs after oral administration to adult mice of radiolabelled GCPQ. The obtained polymer is an excellent candidate such as excipient for oral administration of hydrophobic drugs.



#### **4. Conclusions and Future Works**

This research concluded the successful synthesis of a cationic (GCPQ) low MW amphiphilic polymer that was characterized and helped in the encapsulation of a hydrophobic dye (Idarubicin) whose cell uptake and bioadhesion were studied *in vitro* in two cell lines (with and without mucus) to study the effect of surface charge density. The results showed that a positive charge density is essential for successful drug uptake into cells and bioadhesion. To further assess the cell bioadhesion and uptake efficiency, quantitative methods to characterize them should be done like fluorescence microscopy and flow cytometry. Other *in vitro* models and quantitative techniques can be incorporated to understand the mechanism of cell transport and bioadhesion better. Moreover, *in vivo* studies of biodistribution were successfully in agreement with data coming from bioadhesion and cell up-take studies.

## References

- [1] Sahoo, S.K., Parveen, S. and Panda, J.J. The present and future of nanotechnology in human health care *Nanomedicine: Nanotechnology, Biology, and Medicine* **2007**, 3: 20-31.
- [2] BCC Research (2010). Nanotechnology: A realistic market assessment Accessed from <http://www.bccresearch.com/report/NAN031D.html>.
- [3] Arruebo, M., Fernández-Pacheco, R., Ibarra, M.R. and Santamaria, J. Magnetic nanoparticles for drug delivery. *Nanotoday* 2007, 2: 22-32.
- [4] Gensini, G.F., Conti, A.A. and Lippi, D. The contributions of Paul Ehrlich to infectious disease *Journal of Infeccion* **2007**, 54:221-224.
- [5] De Jong, W.H. and Borm, P.J.A. Drug Delivery and nanoparticles: applications and hazards *International Journal of Nanomedicine* **2008**, 3: 133-149.
- [6] Wu, Y., Yang, W., Wang, C., Hu, J. and Fu, S. Chitosan nanoparticles as a novel delivery system for ammonium glycyrrhizinate *International journal of Pharmaceutics* **2005**, 295:235-245.
- [7] Ringe, K., Walz, C.M. and Sabel, B.A. Nanoparticle Drug Delivery to the Brain *Encyclopedia of Nanoscience and Nanotechnology* **2004**, 7: 91-104.
- [8] Kubek, M.J., Domb, A.J. and Veronesi, M.C. Attenuation of kindled seizures by intranasal delivery of neuropeptide-loaded nanoparticles *Neurotherapeutics: The Journal of the American Society for Experimental NeuroTherapeutics* **2009**, 6:359-371.
- [9] Beck-Broichsitter, M., Gauss, J., Packhaeuser, C.B., Lahnstein, K., Schmehl, T., Seeger, W., Kissel, T. and Gessler, T. Pulmonary drug delivery with aerosolizable nanoparticles in an *ex vivo* lung model. *International Journal of Pharmaceutics* **2009**, 367: 169-178.

- [10] Gelperina, S., Kisich, K., Iseman, M.D. and Heifets, L. The potential advantages of nanoparticle drug delivery systems in chemotherapy of tuberculosis *American Journal of Respiratory and Critical Care Medicine* **2005**, 172: 1487-1490.
- [11] Kotzé, A.F., Lueßen, H.L., de Boer, A.G., Verhoef, J.C. and Junginger, H.E. Chitosan for enhanced intestinal permeability: prospects for derivatives soluble in neutral and basic environments *European Journal of Pharmaceutical sciences* **1998**, 7:145-151.
- [12] Agüeros M., Areses, P., Campanero, M.A., Salman H., Quincoces G., Peñuelas, I. and Irache, J.M. Bioadhesive properties and biodistribution of cyclodextrin-poly(anhydride) nanoparticles *European Journal of Pharmaceutical Sciences* **2009**, 37:231-240.
- [13] Yin, L., Ding, J., He, C., Cui, L., Tang, C. and Yin, C. Drug permeability and mucoadhesion properties of thiolated trimethyl chitosan nanoparticles in oral insulin delivery *Biomaterials* **2009**, 30:5691-5700.
- [14] Bawa, R. Nanoparticle-based therapeutics in humans: a survey *Nanotechnology Law and Business* **2008**, 5: 135-155.
- [15] Mao, S., Germershaus, O., Fischer, D., Linn, T., Schnepf, R. and Kissel, T. Uptake and Transport of PEG-Graft-Trimethyl-Chitosan Copolymer-Insulin Nanocomplexes by Epithelial Cells *Pharmaceutical Research* **2005**, 22:2058-2068.
- [16] Jallouli, Y., Paillard, A., Chang, J., Sevin, E. and Betbeder, D. Influence of surface charge and inner composition of porous nanoparticles to cross blood-brain barrier *in vitro International Journal of Pharmaceutics* **2007**, 344: 103-109.
- [17] Roy, S., Pal, K., Anis, A., Pramanik, K. and Prabhakar, B. Polymers in mucoadhesive drug delivery systems: a brief note *Designed monomers and polymers* **2009**, 12: 483-495.

- [18] Nam, H.Y., Kwon, S.M., Chung, H., Lee, S.Y., Kwon, S.H., Jeon, H., Kim, Y., Park, J.H., Kim, J., Her, S., Oh, Y.K., Kwon, I.C., Kim, K. and Jeong, S.Y. Cellular uptake mechanism and intracellular fate of hydrophobically modified glycol chitosan nanoparticles *Journal of Controlled Release* **2009**, 135:259-267.
- [19] Hoven, V.P., Tangpasuthadol, V., Angkitpaiboon, Y., Vallapa, N. and Kiatkamjornwong, S. Surface-charged chitosan: Preparation and protein adsorption *Carbohydrate Polymers* **2007**, 68: 44-53.
- [20] Kowapradit, J., Opanasopit, P., Ngawhiranpat, T., Apirakaramwong, A., Rojanarata, T., Ruktanonchai, U. and Sajomsang, W. *In vitro* permeability enhancement of in intestinal epithelial cells (caco-2) monolayer of water soluble quaternary ammonium chitosan derivatives *AAPS PharmSciTech* **2010**, 11: 497-508.
- [21] Plapied, L., Vandermeulen, G., Vroman, B., Pr eat, V. and des Rieux, A. Bioadhesive nanoparticles of fungal chitosan for oral DNA *delivery International Journal of Pharmaceutics* **2010**, 398: 210-218.
- [22] Yuan, Y., Tan, J., Wang, Y., Qian, C. and Zhang, M. Chitosan nanoparticles as non-viral gene delivery vehicles based on atomic force microscopy study *Acta Biochim Biophys Sin* **2009**, 41:515-526.
- [23] Gan, Q., Wang, T., Cochrane, C. and McCarron, P. Modulation of surface charge, particle size and morphological properties of chitosan-TPP nanoparticles intended for gene delivery *Colloids and Surfaces B: Biointerfaces* **2005**, 44: 65-73.
- [24] Cui, F., Qian, F. and Yin, C. Preparation and characterization of mucoadhesive polymer-coated nanoparticles *International Journal of Pharmaceutics* **2006**, 316: 154-161.

- [25] Prabakaran, M. Chitosan derivatives as promising materials for controlled drug delivery *Journal of Biomaterials Applications* **2008**, 23: 5-36.
- [26] Trapani, A., Sitterberg, J., Bakowsky, U. and Kissel, T. The potential of glycol chitosan nanoparticles as carrier for low water soluble drugs *International Journal of Pharmaceutics* **2009**, 375: 97-106.
- [27] Deng, L., Qi, H., Yao, C., Feng, M. and Dong, A. Investigation on the properties of methoxy poly (ethylene glycol)/chitosan graft copolymers *J. Biomater. Sci. Polymer Edn* **2007**, 18: 1575-1589.
- [28] Yue, Z.G., Wei, W., Lv, P.P., Yue, H., Wang, L.Y., Su, Z.G. and Ma, G.H. Surface charge affects cellular uptake and intracellular trafficking of chitosan-based nanoparticles *Biomacromolecules* **2011**, 7: 2440-2446.
- [29] Uchegbu, I.F., Sadiq, L., Arastoo, M., Gray, A.I., Wang, W., Waigh, R.D. and Schätzleina, A.G. Quaternary ammonium palmitoyl glycol chitosan- a new polysoap for drug delivery *International Journal of Pharmaceutics* **2001**, 224: 185-199.
- [30] Bayat, A., Dorkhoosh, F.A., Dehpour, A.R., Moezi, L., Larijani, B., Junginger, H.E. and Rafiee-Tehrani, M. Nanoparticles of quaternized chitosan derivatives as a carrier for colon delivery of insulin: ex vivo and in vivo studies *International Journal of Pharmaceutics* **2008**, 356: 259-266.
- [31] Xiao, K., Li, Y., Luo, J., Lee, J.S., Xiao, W., Gonik, A.M., Agarwal, R.G. and Lam, K.S. The effect of surface charge on in vivo biodistribution of PEG-oligocholic acid based micellar nanoparticles *Biomaterials* **2011**, 32: 3435-3446.

- [32] Kelly, C., Jefferies, C. and Cryan, S.A. Targeted liposomal drug delivery to monocytes and macrophages *Journal of Drug Delivery* **2011**, 2011: 1-11.
- [33] Artursson, P., Palm, K. and Luthman, K. Caco-2 monolayers in experimental and theoretical predictions of drug transport *Advanced Drug Delivery Reviews* **2001**, 46: 27-43.
- [34] Behrens, I., Pena, A.I.V., Alonso, M.J. and Kissel, T. Comparative uptake studies of bioadhesive and non-bioadhesive nanoparticles in human intestinal cell lines and rats: the effect of mucus on particle adsorption and transport *Pharmaceutical Research* **2002**, 19: 1185-1193.
- [35] Bravo-Osuna, I., Vauthier, C., Farabollini, A., Palmieri, G.F. and Ponchel, G. Mucoadhesion mechanism of chitosan and thiolated chitosan-poly (isobutyl cyanoacrylate) core-shell nanoparticles *Biomaterials* **2007**, 28: 2233-2243.
- [36] Jintapattanakit, A., Junyaprasert, V.B. and Kissel, T. The role of mucoadhesion of trimethyl chitosan and PEGylated trimethyl chitosan nanocomplexes in insulin uptake *Journal of Pharmaceutical Sciences* **2009**, 12: 4818-4830.
- [37] Keely, S., Rullay, A., Wilson, C., Carmichael, A., Carrington, S., Corfield, A., Haddleton, D.M. and Brayden, D.J. *In vitro* and *ex vivo* intestinal tissue models to measure mucoadhesion of poly (methacrylate) and *N*-trimethylated chitosan polymers *Pharmaceutical Research* **2005**, 22: 38-49.
- [38] Chooi, K.W., Gray, A.I., Tetley, L., Fan, Y. and Uchegbu, I.F. The Molecular Shape of Poly (propylenimine) dendrimer amphiphiles has a profound effect on their self assembly *Langmuir* **2010**, 26: 2301-2316.
- [39] Richardson SCW, Kolbe HJV, Duncan R, *International Journal of Pharmaceutics* **1999**, 178: 231-243.

- [40] Meaney C, O'Driscoll C. Mucus as a barrier to the permeability of hydrophilic and lipophilic compounds in the absence and presence of sodium taurocholate micellar systems using cell culture models. *European Journal of Pharmaceutical Sciences* **1999**, 8(3):167-75.
- [41] Ayush Verma, Oktay Uzun, Yuhua Hu, Ying Hu, Hee-Sun Han, Nicki Watson, Suelin Chen, Darrell J. Irvine, Francesco Stellacci. Surface-structure-regulated cell-membrane penetration by monolayer-protected nanoparticles. *Nature Materials* **2008**, 7, 588-595.
- [42] Domard, A., Rinaudo, M. And Terrassin, C. New method for the quaternization of chitosan *International Journal of Biological Macromolecules* **1986**, 8: 105-107.
- [43] Wang, J.W. and Hon, M.H. Preparation of Poly(ethylene glycol)/chitosan membranes by a glucose-mediating process and *in vitro* drug release *Journal of Applied Polymer Science* **2005**, 96:1083-1094.
- [44] Li, G., Liu, J., Pang, Y., Wang, R., Mao, L., Yan, D., Zhu, X. and Sun, J. Polymeric Micelles with water-insoluble drug as hydrophobic moiety for drug delivery *Biomacromolecules* **2011**, 12: 2016-2026.
- [45] Qu, X., Khutoryanskiy, V.V., Stewart, A., Rahman, S., Papahadjopoulos-Sternberg, B., Dufes, C., McCarthy, D., Wilson, C.G., Lyons, R., Carter, K.C., Schätzlein, A. and Uchegbu, I.F. Carbohydrate-based micelle clusters which enhance hydrophobic drug bioavailability by up to 1 order of magnitude *Biomacromolecules* **2006**, 7: 3452-3459.
- [46] Buwalda, R.T. and Engberts, J.B.F.N. Aggregation of dicationic surfactants with methyl orange in aqueous solution *Langmuir* **2001**, 17:1054-1059.
- [47] Patel, R., Buckton, G. and Gaisford, S. The use of isothermal calorimetry to assess the solubility enhancement of simvastatin by a range of surfactant *Thermochimica Acta* **2007**, 456: 106-113.

[48] He, C., Hu, Y., Yin, L., Tang, C. and Yin, C. Effects of particle size and surface charge on cellular uptake and biodistribution of polymeric nanoparticles *Biomaterials* **2011**, 31: 3657-3666.

[49] Wang, W., McConaghy, A.M., Tetley, L. and Uchegbu, I.F. Controls on polymer molecular weight may be used to control the size of palmitoyl glycol chitosan polymeric vesicles *Langmuir* **2001**, 17 : 631-636.

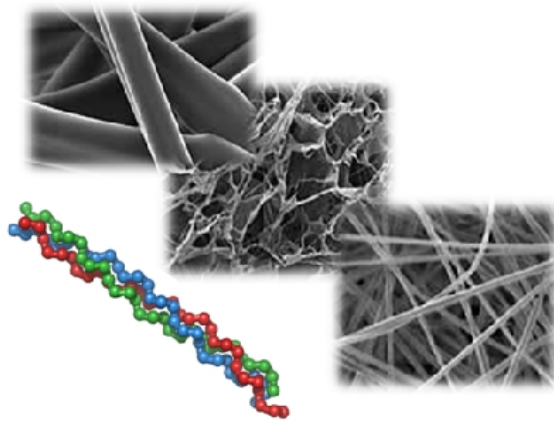
[50] Fischer, D., Li, Y., Ahlemeyer, B., Krieglstein, J. and Kissel, T. *In vitro* cytotoxicity testing of polycations: influence of polymer structure on cell viability and hemolysis *Biomaterials* **2003**, 24: 1121-1131.

[51] Lamprecht, A., Schäfer, U.F. and Lehr, C.-M. Characterization of microcapsules by confocal laser scanning microscopy: structure, capsule wall composition and encapsulation rate *European Journal of Pharmaceutics and Biopharmaceutics* **2000**, 49: 1-9.



## SECTION 3

### CHEMICAL MODIFICATION OF PROTEINS FOR THE IMPLEMENTATION OF DRUG DELIVERY SYSTEMS



- **Part A:** Synthesis and *in vitro* antitubercular activity of isoniazid-gelatin conjugate;
- **Part B:** Collagen  $\alpha$ -tocopherulate for topical applications: preparation, characterization and antioxidant activity evaluation.

## PART A

### SYNTHESIS AND *IN VITRO* ANTITUBERCULAR ACTIVITY OF ISONIAZID- GELATIN CONJUGATE [1]

#### **Abstract**

*Aim:* Covalently linkage of a drug with antitubercular activity, as isoniazid (INH), to a biomacromolecule, as gelatin widely used in the pharmaceutical, cosmetic and food industry.

*Methods:* A novel and simple method to synthesize antitubercular-protein conjugate by solid phase synthesis was developed employing a carboxy polystyrene resin. In this way a gelatin conjugate bearing INH, covalently linked to a protein, was synthesized.

*Results:* Calorimetric and  $^1\text{H-NMR}$  analyses were performed to verify the bond formation between the antitubercular drug and gelatin. Since INH after absorption delivers toxic metabolites, was performed an oxidation test with *tert*-butyl hydroperoxide, to assess the amount of toxic metabolites released from the prodrug (gelatine linked to isoniazid), compared to the isoniazid itself. Spectrophotometric analysis revealed that protein derivative is an excellent isoniazid prodrug since there was a 40% reduction in release of toxic metabolites (isonicotinic acid) by the prodrug. The results clearly showed that antitubercular moieties, covalently linked to a natural polymer, allow to introduce in the macromolecule peculiar features for specific pharmaceutical applications. In addition, anti-tubercular activity of the new polymer was determined by Middlebrook 7H11 medium against *Mycobacterium Tuberculosis Complex*.

*Conclusions:* The new isoniazid-gelatin conjugate has shown significant anti-tubercular activity and for this reason should be useful as an efficacious tool in tuberculosis (TB) treatment for the preparation of nanoparticulate systems.

## **1. Introduction**

### *1.1 Gelatin for pharmaceutical applications: a matrix-molecule for nanoparticles preparation*

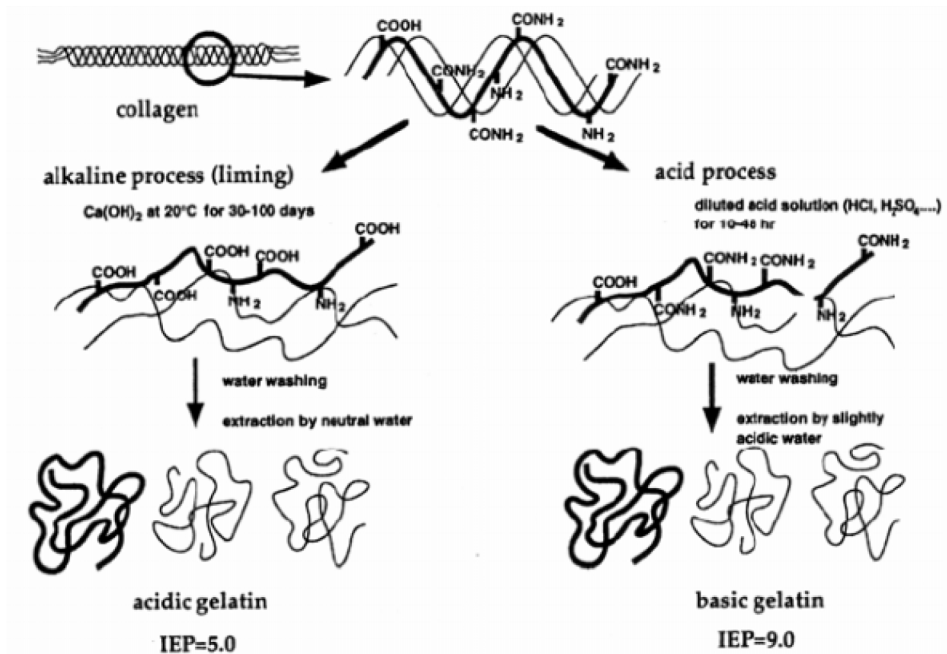
Gelatin is the thermally and hydrolytically denatured product of collagen [2], the most abundant protein in animals and it has also been used extensively for industrial, pharmaceutical, and medical applications. Moreover, gelatin is one of the most used materials of natural origin for the stabilization of labile substances such as vitamins, pharmaceuticals, or enzymes and it is widely employed in industry due to its biocompatibility, biodegradation, nontoxicity and nonimmunogenicity. Thanks to the various potential uses of gelatin, it is useful to investigate its modification to develop new materials with improved properties [3]. Concerning nanodevices suitable for drug delivery, there has already been tremendous progress within the last 30 years, from the first liposomal approach to various present colloidal systems that enable temporal and spatial site-specific delivery. Typical properties of these novel nanocarriers are:

- a) Protection of the drugs from degradation;
- b) Enhancement of the drug absorption by facilitating the diffusion through the epithelium;
- c) Modification of the pharmacokinetics and the drug tissue distribution profile;
- d) Improvement of the intracellular penetration and distribution.

One very popular subtype of these colloidal delivery systems are nanoparticles. They are by definition solid, submicron-sized particles that possess a matrix structure typically based on polymers or macromolecular substances. Drugs or tracers to be delivered with these particles can either be adsorbed onto the surface, entrapped in the particle matrix or dissolved in the particle core. When searching for potential matrix-molecules, good particle preparation properties are just one aspect. Aside from this, potential candidates should ideally be highly biocompatible and biodegradable, feature various accessible sites to e.g. attach targeting ligands, and finally, be easy to obtain and cheap in production. Due to this, approaches based on natural macromolecules and proteins that originally go back to the early days of colloidal carrier system development have performed a certain renaissance within the last years. Back in time, these approaches failed due to limited reproducibility as well as instabilities and inhomogeneities of the produced nanoparticles. Nowadays, technological and scientific progress offers new and highly precise tools that facilitate the development of new preparation procedures for high quality nanoparticles based on the originally old approaches. In the development process of a nanoparticulate drug delivery system for *in vivo* application, biodegradability without toxic by-products is one of the major claims, a potential matrix molecule has to fulfill. Within the past decades, a multitude of protocols described in literature used synthetic or natural base products for the preparation of biodegradable nanoparticles. With regards to nanoparticles based on synthetic polymers, polylactide (PLA), polyglycolide (PLG), and poly(D,L-lactide-co-glycolide) (PLGA) nanoparticles represent the most extensively investigated ones. Further polymers discussed as promising approaches are poly(cyanoacrylate) (PCA), poly(alkylcyanoacrylate)

(PACA), poly( $\epsilon$ -caprolactone) (PCL) and poly(ester-anhydride) (PEA). In addition to these polymers, natural biopolymers and macromolecules such as chitosan, sodium alginate, albumin, collagen and gelatin represent a second fundamental class of base materials for nanoparticles. Among these, nanoparticles of proteinaceous origin, e.g. albumin, collagen and gelatin have raised specific interest. Due to their intrinsic protein structure with the high number of different accessible functional groups, they bear multiple modification opportunities for coupling of e.g. targeting-ligands, crosslinkers, and shielding substances. In the present project, gelatin nanoparticles have been chosen as a promising drug delivery system candidate. Typically, this natural biopolymer is present in other fields of our daily life. It gives gummi bears consistency and without gelatin containing icing, ingredients such as fruits would not stick to a cake. Consequently, the foodstuff industry is the major purchaser of the tonnages of gelatin that are produced every year. However, the amount of gelatin being applied in pharmaceutical industry is not negligible, as far as capsules and ointments are concerned [4]. But also for current research in fields of delivery vehicles for the controlled release of biomolecules such as proteins and nucleotides, gelatin has generated increased interest [5]. While gelatin and the delivery systems based on this polymer are biocompatible and biodegradable without toxic degradation products, they are furthermore known for high physiological tolerance and low immunogenicity since decades. But the basically beneficial properties of gelatin contributed to its proven record of safety which is also documented by the classification as “Generally Recognized as Safe” (GRAS) excipient by the US Food and Drug Administration (FDA). The natural source of gelatin are animals. It is obtained by mainly acidic or alkaline, but also thermal or enzymatic degradation of the structural

protein collagen. Collagen represents 30% of all vertebrate body protein. More than 90% of the extracellular protein in the tendon and bone and more than 50% protein in the skin consists of collagen. The characteristic molecular feature of collagen being responsible for its high stability is the unique triple-helix structure consisting of three polypeptide  $\alpha$ -chains. Among the 27 collagen types that have been isolated so far, only collagen type I (skin, tendon, bone), type II (hyaline vessels) and type III are used for the production of gelatin. According to origin and pretreatment of collagen, two major types of gelatin are commercially produced (Figure 1). Gelatin type A (acid) is obtained from porcine skin with acidic pretreatment prior to the extraction process. The second prevalent gelatin species, type B (basic), is extracted from ossein and cut hide split from bovine origin. Thereby, an alkaline process, also known as “liming” is applied. During this extraction also the amide groups of asparagine and glutamine are targeted and hydrolyzed into carboxyl groups, thus converting many of the residues to aspartate and glutamate. Consequently, the electrostatic nature is affected, in contrast to collagen and gelatin type A having an isoelectric point (IEP) of pH 9.0, the higher number of carboxyl groups per molecule reduces the IEP to pH 5.0.



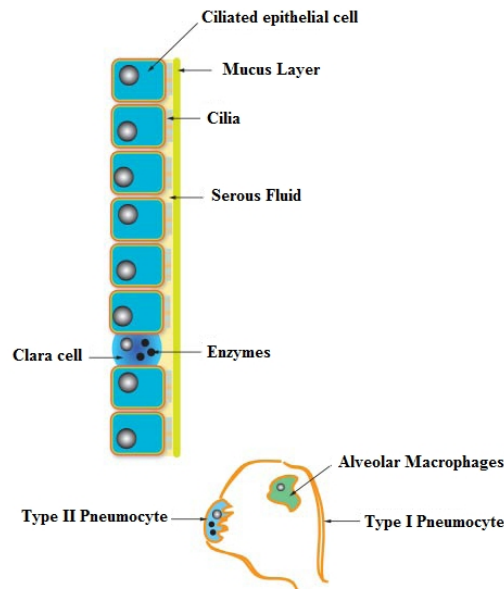
**Figure 1:** Preparative process for acidic and basic gelatins from collagen  
 1.2 The lungs as a delivery target for nanomaterials

Over the last decades, colloidal drug delivery systems and especially nanoparticles have received great attention. Nanoparticles can be administered via different routes of administration such as parenteral, oral, intraocular, transdermal or pulmonary inhalation. Aerosol therapy using particulate drug carrier systems is becoming a popular method to deliver therapeutic or diagnostic compounds either locally or systemically [6]. This is due to the large alveolar surface area suitable for drug absorption, the low thickness of the epithelial barrier, extensive vascularization and relatively low proteolytic activity in the alveolar space compared to other routes of administration and the absence of the first-pass metabolism [7]. In general, nanoparticle delivery to the lungs is an attractive concept because it can cause retention of the particles in the lungs accompanied with a prolonged drug release if large porous

nanoparticle matrices are used [8]. On the other hand studies have shown that nanoparticles uptake by alveolar macrophages can be reduced if the particles are smaller than 260 nm. Both effects combined might improve local pulmonary drug therapy. However, the particle size of medically used nanoparticles is too small to be suitable for direct lung delivery. A prerequisite for deep lung delivery is the design of proper carrier systems. Successful delivery of inhaled particles depends mostly on particle size and particle density, and hence, the mass median aerodynamic diameter. The respirable fraction of an inhalable powder is generally the fraction of particles with an aerodynamic diameter ranging between 1 and 5  $\mu\text{m}$ . This size range guarantees a maximum deposition in the deep lung [9]. The primary functions of the lungs are to enable gas exchange between the blood and the external environment, and to maintain homeostatic systemic pH. The respiratory system is composed of the trachea, which bifurcates into the bronchi. The bronchi continue to branch into smaller bronchioles, and ultimately the terminal bronchi, which end with the alveolar sac. The conducting airways are lined with ciliated columnar epithelium, which transition to a cuboidal shape approaching the distal airways. The lumen of the bronchial airways is lined with a thin layer of serous fluid, upon which floats a layer of mucus, which helps to entrap aerosolized particles. The coordinated, rhythmic beating of the cilia constantly moves this mucous layer toward the proximal airways, where it is either swallowed or expectorated (mucociliary clearance). Particles settling in the peripheral lung have been reported to have a residence time of approximately 24 hours in a healthy adult patient. The alveolar surface is primarily composed of type I pneumocytes, which share a basement membrane with the pulmonary capillaries. The alveoli also contain type II pneumocytes, which secrete lung surfactant to prevent alveolar collapse,



and macrophages, which are responsible for clearing large particles. There are approximately 300 million alveoli in the lungs, with a combined surface area that is greater than 100 m<sup>2</sup>, and with an alveolar epithelium as thin as 0.1 mm. This large surface area, combined with an extremely thin barrier between the pulmonary lumen and the capillaries, creates conditions that are well suited for efficient mass transfer. Once deposited, drugs encounter a variety of physicochemical and biological barriers. These include mucus barriers and catabolic enzymes in the tracheobronchial region, and macrophages in the alveolar region (Figure 2). Pulmonary delivery may well represent a possible route to deliver peptides and small protein therapeutics [10].



**Figure 2:** *Various biological barriers to drug delivery via the lung.*

The fate of inhaled nanomaterials depends on regional distribution in the lung, because disposition within the lung is a complex function of the kinetics of absorption and non-absorptive clearance mechanisms [11].

Once nanomaterials are deposited onto the lining of the respiratory tract, they first contact the mucous layer within the airways or the surfactant-lining fluid layer within the alveolar region. Airway mucus is a complex aqueous secretion of airways, comprising electrolytes, proteins, glycoproteins (e.g., mucins) and debris of cells. The components vary much depending on environmental and disease states. The surfactant lining layer (10–20 nm in thickness) that covers the alveolar surface is composed of 90% in weight of phospholipids and 10% in weight of specific proteins. Both airway and alveolar surface liquids are coated with at least a monolayer of highly surface active lung surfactant, which are primarily water insoluble long-chain phospholipids. They form liquid crystals but not micelles in aqueous media to maintain the functions of the lungs: facilitation of gas exchange and prevention of alveoli collapse by reducing the lung air interface surface tension. It was found that regardless of the nature of the nanomaterials surfaces, they will be submersed into the lining fluids after their deposition. Study of interactions between different nanoparticles and lung surfactant film indicated that the smaller the size of nanoparticle, the more can be incorporated into the surfactant film. However, the surface pressure of the surfactant film does not change significantly with the incorporation of nanoparticles, i.e. the size dependent incorporation of nanoparticles does not destabilize the lung surfactant film. Once deposited within the lung lining fluid, there are separate biokinetics for lung absorption and non-absorptive clearances. The kinetics of dissolution of inhaled particulates determines whether the inhaled nanomaterials will dissolve in the epithelial lining fluid for lung absorption or whether such nanomaterials will undergo non-absorptive clearances. Inhaled nanomaterials that are either lipid soluble, or soluble in intracellular or extracellular fluids

undergo chemical dissolution in situ. Low molecular weight hydrophobic molecules are thought to be rapidly absorbed (within seconds) by passive diffusion through the lung epithelial membrane. The kinetics of diffusion in the alveoli is much faster than that in the small airways, mainly because lung absorption mostly occurs from the air-side surface of the alveoli to the pulmonary capillaries. The alveoli have a thin monolayer (0.1–0.4  $\mu\text{m}$ ) composed of extremely broad and thin Type I cells and small compact Type II cells, and a large surface area (more than 100  $\text{m}^2$ ). Only a small portion of inhaled nanoparticles is absorbed from the tracheobronchial airways which have a much thicker layer of column-shaped epithelial cells (10–60  $\mu\text{m}$ ) and lower surface area (1–2  $\text{m}^2$ ). This is supported by Fick's law. Low molecular weight hydrophilic molecules can be absorbed by active transport via specific transporters, or by passing through the tight junctions. The kinetics of active absorption should depend upon the lung-regional expression and functionality of receptors or transporters. It was recently reported that the absorption of large molecule immunoglobulins of the IgG class (150 kDa) might occur in the upper airways by receptor-mediated transcytosis of IgG. Solutes and soluble components may be eventually cleared into blood and lymphatic circulation. Inhaled nanomaterials that are insoluble in mucus and lining fluid, are not able to be rapidly absorbed, and may undergo physical translocation. This is different depending on lung region in which the nanoparticles have been deposited. The uptake of deposited particles by alveolar macrophages depends on the particle size and composition of coating material. Particles of 1–3  $\mu\text{m}$  in diameter are far better taken up than those of 6  $\mu\text{m}$  by macrophages, which have cell diameters about 15–22  $\mu\text{m}$ . Particles of less than 0.26  $\mu\text{m}$  can escape from phagocytosis by macrophages [12]. Due to the small size, the chance of

nanoparticles undergoing phagocytosis in the alveoli is much lower than micron-sized particles. Thus, depending on size and surface reactivity, nanoparticles may be transported across cellular and sub-cellular membranes by different mechanisms. As a result, most nanoparticles will be no longer retained as free particles on the epithelium as inhaled and deposited [13]. Recently, it was reported that inhaled nanomaterials may also influence organs other than the lungs. Inhaled ultrafine technetium ( $^{99m}\text{Tc}$ ) labelled carbon particles, which are very similar to the ultrafine fraction of actual pollutant particles, diffused into the systemic circulation of hamsters within 5 minutes. Nemmar et al. [14] concluded that phagocytosis by macrophages and/or endocytosis by epithelial and endothelial cells may be responsible for particle translocation to the blood, along with other mechanisms. There are recent reports that inhaled nanoparticulates have been found in the brain, probably traveling from the nasal nerves [15]. This suggests that nanoparticles may travel to sites away from the site of deposition in the lungs. However, no definite conclusion about the systemic translocation of inhaled nanoparticles can be drawn to date, based on the conflicting results of human and animal studies. It was reported that rapid translocation to the liver (more than 50%) of  $^{13}\text{C}$ -labelled nanoparticles with a diameter of 26 nm occurred within 24 hours following inhalation in a rat model [16]. In another rat study, only less than 1% iridium nanoparticles (15–20 nm in diameter) were found in secondary organs of rats, but the nanoparticles were distributed widely throughout the body to such organs as liver, spleen, kidneys, brain and heart [17]. Kato et al. [18] have provided morphological data showing that inhaled polystyrene particles are transported into the pulmonary capillary space, presumably by

transcytosis; nevertheless, other research groups did not find any detectable particulates in the body other than the lungs [19].

### *1.3 Delivery of nanoparticles for the treatment of tuberculosis*

Nanoparticulate drug delivery systems have considerable potential for the treatment of tuberculosis. *Mycobacterium tuberculosis* invades and begins its replication within alveolar macrophages before the bacterium spreads out. Therefore, tuberculosis can be seen as a disease involving macrophages which makes nanoparticles an ideal drug carrier. Macrophage targeting was introduced by Löbenberg and Kreuter [20] to deliver anti-viral drugs directly to macrophages which represent an important HIV pool within the body. Approximately one-third of the world population is infected with *Mycobacterium tuberculosis*, resulting in more than eight million new cases and two million deaths annually. Although potentially curative treatments have been available for almost half a century, tuberculosis (TB) remains, today, the leading cause of preventable deaths in the world [21,22]. Recent implementation of the World Health Organization's strategy (directly observed therapy, short-course) has been problematic, and TB represents a major burden in many developing countries. One of the main problems is noncompliance to prescribed regimens, primarily because TB treatment involves continuous, frequent multiple drug dosing [23]. Adherence to treatment and the outcome of therapy could be improved with the introduction of long-duration drug formulations releasing the antimicrobial agents in a slow and sustained manner, which would allow reduction in frequency and dosing numbers [24]. One way to solve this problem is the development of drug delivery systems such as colloidal carriers. Liposomes, microspheres and nanoparticles are a well-known example of

this strategy.<sup>[7-10]</sup> Today, versatility of particulate technologies enables tailoring of the nanoparticle based drug delivery systems with consideration of the target, desired pharmacokinetic profile, and route of administration.

The potential advantages of direct delivery of the TB drug to the lungs include the possibility of reduced systemic toxicity, as well as capability to achieve higher drug concentration at the main site of infection. Moreover, in contrast to the oral administration, inhaled drugs are not subjected to first-pass metabolism. Although identifying novel anti-TB agents remains a priority, the development of the nanoparticle-based delivery systems for currently used agents may represent a cost-effective and promising alternative capable of improving their therapeutic efficacy. Over the past few decades, there has been considerable interest in developing biodegradable nanoparticles (NPs) as effective drug delivery devices. Various polymers have been used in drug delivery research as they can effectively deliver the drug to a target site thus increasing their therapeutic benefit, while minimizing side effects [25]. Controlled release of pharmacological active agents to the specific site of action, at therapeutically optimal rate and dose regimen, has been a major goal in designing drug delivery systems. Nanoparticles generally vary in size from 10 to 1000 nm. The drug is dissolved, entrapped, encapsulated or linked to a NP polymer matrix and, depending on the preparation method, nanoparticles can be obtained as nanospheres or nanocapsules. In particular nanocapsules are colloidal carrier systems in which the drug is confined into a core surrounded by a thin polymer membrane, while nanospheres are matrix systems in which the drug is physically and uniformly dispersed in the polymer. In recent years, biodegradable polymeric NPs have attracted considerable attention as potential drug

delivery system especially for their ability to target particular organs/tissues [26]. In particular, nanoparticle-based drug delivery systems have a considerable potential for treatment of tuberculosis (TB).

#### *1.4 Toxicity of inhaled ultrafine particles*

It has been shown that nanoparticles can translocate from the respiratory tract, via different pathways to other organs/tissues and induce direct adverse responses in remote organs [27]. A major concern with nanoparticle therapeutics is the unforeseen negative health impact that nanoparticles may have. In addition to the possible inherent toxic effects of nanoparticles, some materials used to formulate nanoparticles may have toxic effects and therefore may not be viable for developing therapeutic products. For example, the toxicity of polycyanoacrylates has been demonstrated by Brzoska et al. The authors prepared poly(butyl)cyanoacrylate and poly(hexyl)cyanoacrylate nanoparticles in a method similar to that described by Zhang et al. [28], using either Dextran 70 stabilizer or poloxamer-188 [29]. They determined that both types of nanoparticles caused an increase in lactate dehydrogenase (LDH) activity in human pulmonary epithelial cells. The degree of toxicity was greater for the poly(butyl)cyanoacrylate and independent of the stabilizer used, which stands to reason because shorter chain polycyanoacrylates have been associated with higher cytotoxicity. The degree of toxicity also increased with increasing nanoparticle concentration, most likely due to the subsequent increase in polycyanoacrylate concentration. Despite this, Dailey et al. [30] have shown that PLGA nanoparticles induce less inflammation than polystyrene particles of similar size when delivered to the lungs. Based on this observation, nanoparticle toxicity in the lungs may be more dependent on material choice than particle size. Therefore,

there may be alternative polymers that can be investigated for use in pulmonary nanoparticle drug formulations that could mitigate toxicity.

### *1.5 Nanoparticles processing methods for pulmonary drug formulations*

The principal methods for the production of nanoparticles may be classified into three main categories: wet processes, dry processes, and other processes (Table 1).

<b>General process</b>	<b>Specific methodology</b>
<b>Wet processes</b>	<ul style="list-style-type: none"><li>• Wet massing</li><li>• Fluid bed processors</li><li>• Spray drying</li><li>• Pan granulation</li><li>• Extrusion</li></ul>
<b>Dry processes</b>	<ul style="list-style-type: none"><li>• Roller compaction</li><li>• Slugging</li></ul>
<b>Other processes</b>	<ul style="list-style-type: none"><li>• Humidification</li><li>• Prilling</li><li>• Melt pelletization</li></ul>

**Table 1:** *Nanoparticles processing methods*

Although some or all these methods are used in the pharmaceutical industry, wet processes have been, and continue to be the most widely used agglomeration process.

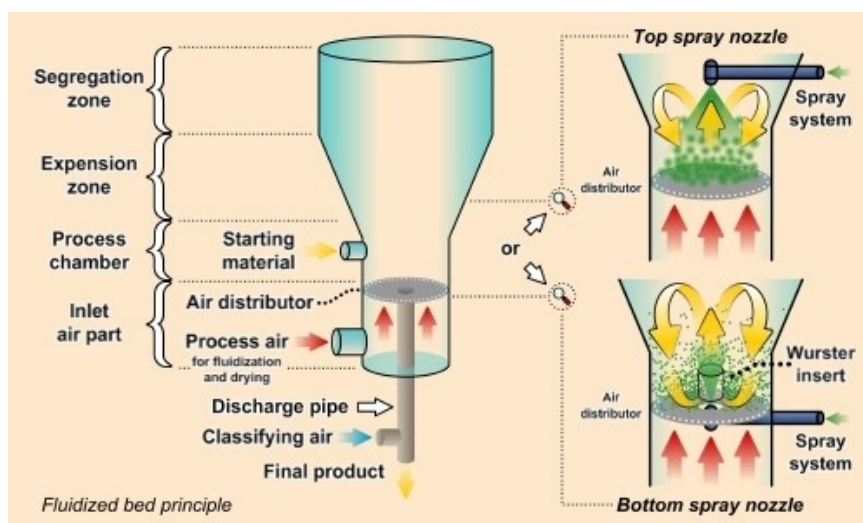
Many chemical processing technologies have been used to produce nanostructured materials suitable for pulmonary delivery. Spray drying is



a well-established method commonly used in the pharmaceutical industry for producing a dry powder from a liquid phase. In recent years, it has been identified as a suitable method for the preparation of proteins intended for pulmonary, nasal and controlled oral delivery [31]. It offers the advantage of drying and particle formation in a single-step continuous and scalable process with particle engineering possibilities. Furthermore, various particle properties such as particle size, bulk density and flow properties can easily be tuned via simple manipulation of the process parameters or spray dryer configuration. Therefore, spray drying is potentially a versatile and commercially viable technique for formulating protein and peptide drugs. The field of spray drying is constantly evolving. Since the first development of spray drying technology in the early 1870s [32], there have been numerous efforts undertaken to refine the equipment and technology to ensure relevance and attractiveness to the food and pharmaceutical industry. In drug delivery, nanoparticles are favored over microparticles due to their small size and higher specific surface area which favorably results in much improved dissolution rates and bioavailabilities [33, 34].

Fluidized bed technique has been used in pharmaceutical industry for drying, coating, and recently granulating. Wurster [35] first described granulation in the fluid bed. Among many types of fluidized bed processors, the Wurster process, a spouted bed process assisted by a draft tube and a bottom spray, has been characterized by fine particle coating which is made possible by relatively fast particle motion in the draft tube. Even in the Wurster process, fine particles tend to agglomerate easily and adhere to the chamber wall, leading to the unfavorably enlarged particle size and size-dependent drug content and release of produced microcapsules. Therefore, among various microencapsulation methods,

the Wurster process has been characterized as a method to produce relatively large microcapsules, micro and nanospheres (Figure 3). However, the Wurster process has an advantage for the construction of multi-layered and composite particles, mostly free from the physico-chemical properties of drugs and additives [36].



**Figure 3:** Schematic representation of Wurster process

### 1.6 Aim of the project

The aim of this work was to obtain a novel antitubercular-protein conjugate for the development of nanoparticle carriers for pulmonary delivery of isoniazid and other loaded drugs like rifampicin as an efficacious tool in TB treatment. For this purpose INH was covalently linked to the biodegradable polymer gelatin. The synthetic strategy proposed in the present paper appears to be very useful because it allows to obtain a matrix made of a protein covalently linked to an antitubercular drug useful for the realization of nanoparticulate systems, for example by the spray-drying technique, carrying both in their surface and in their

interior two drugs with synergic actions. The purpose of realizing a gelatin derivative, covalently coupled with an antitubercular drug, was attained by using a carboxy-polystyrene resin in N-methyl pyrrolidone as reaction solvent. Carboxylic groups of this resin were transformed in acyclic chloride ones. Subsequently gelatin –NH<sub>2</sub> groups were covalently coupled to the resin obtaining an amidic bound. At the end isoniazid with its idrazinic groups formed another amidic-like bound with carboxylic groups of gelatin. The gelatin conjugate was obtained by hydrolysis under mild acidic conditions and characterized by <sup>1</sup>H-NMR spectroscopy. Its antibacterial activity, against *Mycobacterium Tuberculosis Complex*, was also evaluated. The possibility to covalently link antitubercular moieties in a proteic structure, by solid phase synthesis, represents an interesting innovation that significantly improves the performance of the biomacromolecules, opening new applications in the biomedical and pharmaceutical fields.

## **2. Materials and methods**

### *2.1 Materials*

All solvents of analytical grade, were purchased from Carlo Erba Reagents (Milan, Italy). Dichloromethane, diethylether, N-methyl-pirrolidone, thionyl chloride, gelatin, isoniazid and trifluoroacetic acid were purchased from Sigma-Aldrich (Sigma Chemical Co, St. Louis, MO, USA). Resin (carboxypolystyrene HL, 100-200 MESH, 1% DVB) was purchased from Merck AG. Middlebrook 7H11 medium was purchased from (Becton Dickinson, USA).

## 2.2 Measurements

<sup>1</sup>H-NMR spectra were processed using a spectrometer Burkert VM30; chemical shifts are expressed in  $\delta$  and referred to the solvent. UV-VIS spectra were realized through a UV-530 JASCO spectrophotometer. The samples were lyophilized utilizing a "Freezing-drying" Micro moduly apparatus, Edwards. The calorimetric analyses (DSC) were performed using a Netzsch DSC200 PC.

Antitubercular activity was evaluated with the Becton Dickinson Detection Instrument (Becton Dickinson, USA).

## 2.3 Synthesis of the Antitubercular-Gelatin Conjugate

The reaction was carried out according to the procedure reported in literature [37, 38]. In a Disa vial equipped with magnetic stirrer, carefully flamed and maintained in an inert atmosphere, we added 0.4 g of carboxypolystyrene resin suspended in 20 mL of N-methylpyrrolidone. After that we added 0.0435 mL of thionyl chloride ( $6.45 \cdot 10^{-4}$  mol) and 0.32 mL of pyridine ( $3.96 \cdot 10^{-3}$ ). The reaction mixture was kept in continuous magnetic stirring at 25° C. After three hours, we added 0.017 g of gelatin. The reaction mixture was left under reflux at 100° C and maintained in continuous magnetic stirring. After one hour, we added 0.082 g of isoniazid ( $6.45 \cdot 10^{-3}$  mol), 0.32 mL of pyridine ( $3.96 \cdot 10^{-3}$  mol). The reaction was left under reflux for about 72 hours at 25°C. At the end of the reaction, the mixture was added of 20 ml of 5% trifluoroacetic acid in dichloromethane in order to promote the cleavage of the resin which was then recovered by filtration. The solution was added of diethyl ether to allow the precipitation of gelatin derivative. The precipitate was filtered, dissolved in distilled water, frozen and finally

lyophilized to remove the aqueous solvent. The reaction product was analyzed by  $^1\text{H-NMR}$  ( $\text{D}_2\text{O}$ ).

#### *2.4 Calorimetric Analysis of the Antitubercular-Gelatin Conjugate*

Calorimetric analyses of the samples were carried out using a DSC. In a standard procedure about 6.0 mg of dried sample were placed inside a hermetic aluminum pan and, then, sealed tightly by a hermetic aluminum lid. The thermal analyses were performed from 25 to 300° C under a dry nitrogen atmosphere with a flow rate of 25 mL min<sup>-1</sup> and heating rate of 5 °C min<sup>-1</sup>.

#### *2.5 Oxidation Test*

The gelatin derivative and the commercially available isoniazid were, separately, solubilized in a solution consisting of 6 mL of phosphate buffer (PBS) pH=7.4 and 500 μL of tert-butyl hydroperoxide (*tert*-BOOH,  $0.25 \cdot 10^{-3}$  mol). The obtained solutions were left in the dark for two hours at 37 °C in a shaking bath [39]. Subsequently, the formation of one of the major toxic metabolites, isonicotinic acid, was monitored by measuring the absorbance at a wavelength of 261.5 nm ( $\epsilon = 3520 \text{ L} \cdot \text{mmol}^{-1} \cdot \text{cm}^{-1}$ ).

#### *2.6 Antitubercular Activity*

The antitubercular activity of the isoniazid-gelatin conjugate was tested in Middlebrook 7H11 medium using double dilution technique [40]. Briefly, the polymer was diluted in order to obtain a solution 2 μg/mL and then was submitted to a doubling dilution. 100 μl of each of these concentrations was inoculated in Mycobacteria Growth Indicator Tube (MGIT) that was incubated in MGIT 960 Becton Dickinson Detection

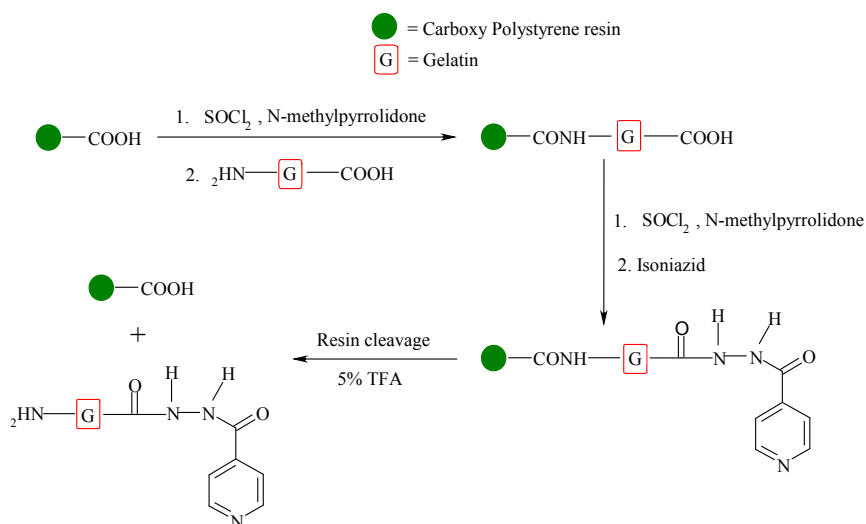
Instrument (Becton Dickinson, USA) for the antimicrobial activity measurement.

### **3. Results and discussion**

#### *3.1 Synthesis of INH-Gelatine conjugate*

Gelatin a natural and non-toxic polymer commonly used for pharmaceutical and biomedical applications, because of its biodegradability and biocompatibility in physiological environments, it was chosen as polymer backbone to be functionalized with INH to obtain a biomacromolecule with raised antitubercular properties. Gelatin is obtained by controlled hydrolysis of an insoluble protein, collagen, which is found abundantly in the connective tissues. The specific release in the lungs of drugs could be affected through the action of two enzymes: the esterases and the amidases. Derivatization of the gelatin with isoniazid was obtained by a heterogeneous reaction of amidation. This biopolymer could be used to obtain nanocapsules useful also to entrap other antitubercular drugs (rifampicin, pirazinamide etc.) to be administered by inhalation. The purpose of this reaction, in heterogeneous phase, was the derivatization of gelatin with isoniazid (INH). The reaction occurred in N-methylpyrrolidone and was initially promoted the chlorination of C-terminal groups of the resin by using thionyl chloride (SOCl<sub>2</sub>) in excess. Then pyridine (Py) (nucleophilic catalyst) and gelatin were added in order to form an amide bond with the resin. The Py buffers the acid environment. Thionyl chloride then reacted with the gelatin C-terminal group. So adding isoniazid, we allowed the formation of an amide bond between the terminal acyl chloride group of gelatin and isoniazid hydrazinium group. To achieve the cleavage of the resin 5% trifluoroacetic acid in dichloromethane (Scheme 1) was used. The

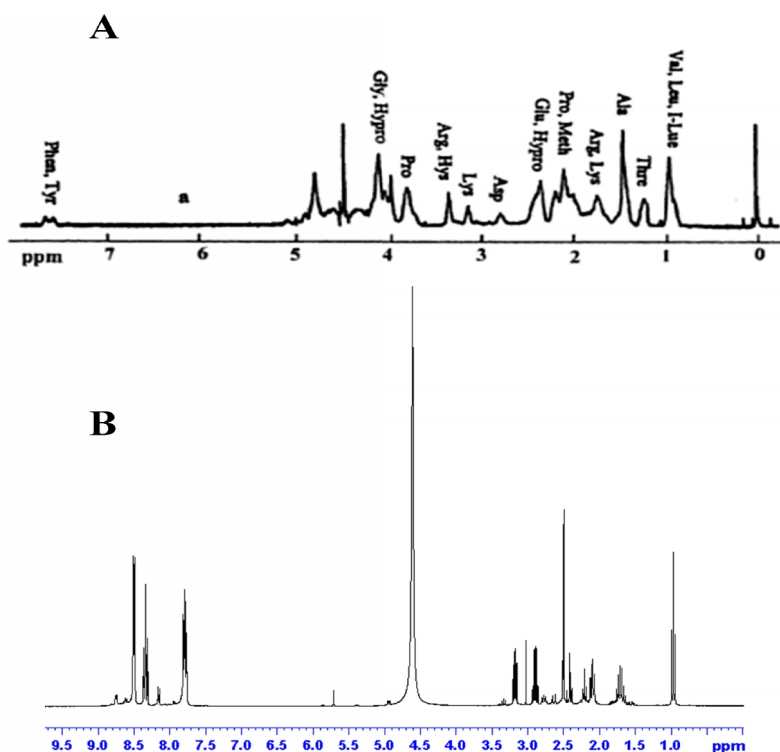
solution was filtered and the resin was recovered and dried under vacuum. The solution was then mixed with diethyl ether to promote the precipitation of gelatin derivative. The biopolymer was then collected by filtration, dissolved it in distilled water and frozen. Afterthat product was collected by lyophilization.



**Scheme 1:** Synthetic route to INH-Gelatin conjugate

### 3.2 Characterization of INH-Gelatin Conjugate using <sup>1</sup>H-NMR

The spectrum of gelatin shows the presence of numerous peaks, characteristic of aminoacids forming the peptide. The spectrum of the gelatin derivative, displays the presence of isoniazid benzene rings in the range of aromatic groups (7.5-9 ppm), confirming thus the existence of the covalent bond between gelatin and isoniazid (Figure 4).



**Figure 4:**  $^1\text{H-NMR}$  spectra of commercially available gelatin (A) and of INH-Gelatin Conjugate (B).

### 3.3 Characterization of INH-Gelatin Conjugate by Differential Scanning Calorimetry (DSC)

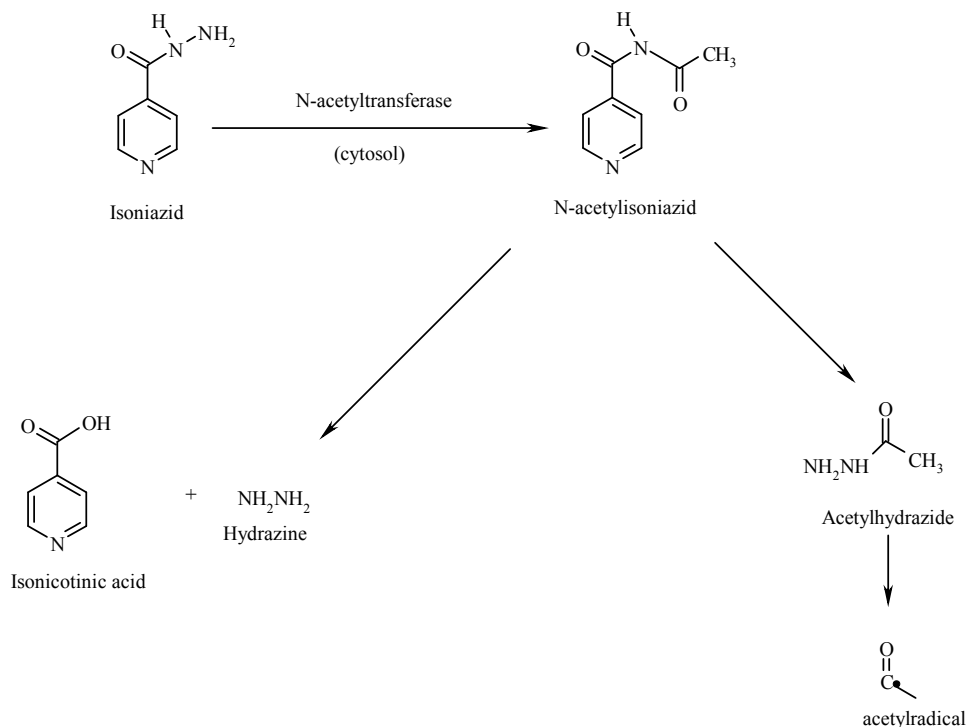
The calorimetric analysis reveals the presence of commercial gelatin broad endothermic peak centered at 85 °C. On the other hand, as confirmation of derivatization, the DSC spectrum of gelatin derivative reveals the absence of the pure isoniazid transition peak (170 °C). Thermal characterization of the prepared conjugates was also performed by recording DSC thermograms of dried antitubercular-gelatin, blank gelatin, and pure INH. As far as DSC of gelatin is concerned, a broad endothermic peak, located around 60-180 °C, has been assigned to the



glass transition of  $\alpha$ -amino acid blocks in the peptide chains;  $\Delta H_t$  associated to this transition was -242.1 J per grams of protein derivative.

### *3.4 Oxidation Test*

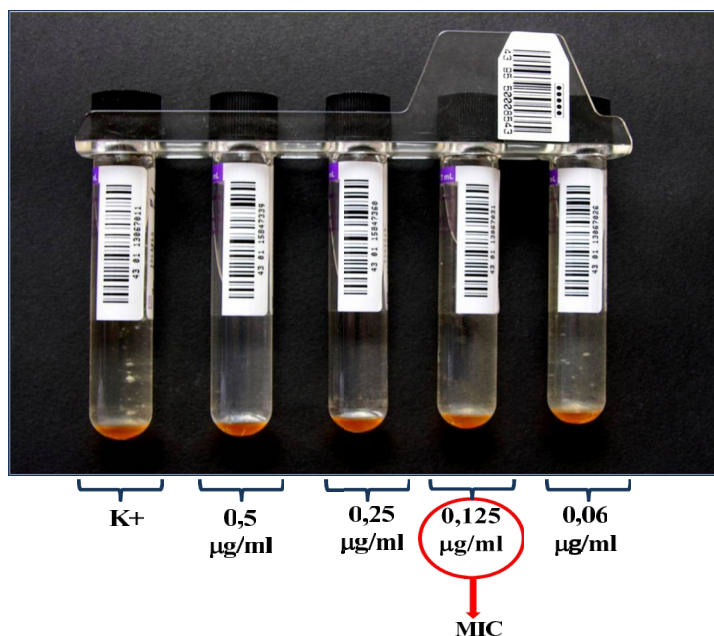
The oxidation test was performed to assess the amount of toxic metabolites released from the prodrug (gelatine linked to isoniazid), compared to the isoniazid. Initially a solution, consisting of a phosphate buffer (PBS) and a pro-oxidant agent (*tert*-BOOH), was prepared and then the prodrug and the drug were introduced separately in it. Spectrophotometric analysis allows us to assess the amount of metabolites released by drug and prodrug, respectively, after insulting them with *tert*-BOOH,. Since there is a 40% reduction in metabolites release, such as isonicotinic acid, from the prodrug compared to the drug, the test reveals that our derivative is an excellent prodrug that can reduce the isoniazid intrinsic toxicity (Scheme 2).



**Scheme 2:** Conversion of Isoniazid in its toxic metabolites.

### 3.5 Antitubercular activity evaluation

The isoniazid-gelatin conjugate was tested for its antimycobacterial activity in vitro, against *Mycobacterium Tuberculosis Complex* in Middlebrook 7H11 medium by double dilution technique. The polymer has shown significant anti-microbial activity expressed as minimum inhibitory concentration (MIC). MIC is the minimum concentration of compound required to give 90% inhibition of bacterial growth. As shown in Figure 5, the obtained conjugate exhibited excellent antimycobacterial activity equal to 0,125 µg/mL and analogous to that of isoniazide in vitro (0.1 µg/mL).



**Figure 5:** Minimum inhibitory concentration (MIC) value of isoniazid-gelatin conjugate against *Mycobacterium Tuberculosis Complex*.  $K^+$  is the positive growth control.

#### 4. Conclusions

Gelatine was suitably derivatized with isoniazid in order to prepare a new biopolymer to be used as isoniazid prodrug and as material to encapsulate rifampicin or other drugs for the TB treatment of. The synthesis on solid phase, allowed to initially form an amide bond between the N-terminal group of gelatin and the C-terminal groups of the resin. C-terminal group of gelatin was then activated with thionyl chloride. The obtained derivative, treated with isoniazid, led to the desired product. The presence of this derivatization was then confirmed by  $^1\text{H-NMR}$  and DSC analyses. An “in vitro” test was used to assess the antibacterial activity of conjugate. This test shows a positive behavior of polymer in inhibition of bacteria proliferation. The results suggested that the biomaterial possesses an excellent antitubercular activity comparable to that isoniazid in vitro.

Then, binding the antitubercular drug to a highly biocompatible and economic polymer such as gelatin, the obtained derivative could be used for the preparation of drug delivery systems to be administered by inhalation. Oxidation studies showed that the drug, covalently linked to gelatine, releases a smaller amount of toxic metabolites, compared to the free drug. Using special techniques such as spray drying [41] or the Wurster process, in fact, antitubercular gelatin could be used to encapsulate other drugs like rifampicin or pyrazinamide [42]. The amidases present both in lungs and in plasma could split the link so they can deliver isoniazid first and then, gradually, the other anti-tubercular encapsulated drug [43]. The nanocapsules resulting from this process would thus have an important synergistic effect on tuberculosis [44].

## References

- [1] Roberta Cassano, Sonia Trombino, Teresa Ferrarelli, Paolina Cavalcanti, Cristina Giraldi, Francesco Lai, Giuseppe Loy and Nevio Picci. Synthesis and *in vitro* antitubercular activity of isoniazid-gelatin conjugate. *Journal of Pharmacy and Pharmacology*. SUBMITTED.
- [2] Liu S *et al.* Nanosized gold-loaded gelatin/silica nanocapsules. *Adv Mater* 2005; 17: 1862-1866.
- [3] Saraogi GK *et al.* Gelatin nanocarriers as potential vectors for effective management of tuberculosis. *Int J Pharm* 2010; 385: 143-149.
- [4] Djagny, K. B., Wang, Z., and Xu, S.; () Gelatin: A valuable protein for food and pharmaceutical industries: Review. *Critical Reviews In Food Science And Nutrition* 2001, 41[6], 481-492.
- [5] Young, S., Wong, M., Tabata, Y., and Mikos, A. G. Gelatin as a delivery vehicle for the controlled release of bioactive molecules. *Journal of Controlled Release* 2005, 109[1-3], 256-274.
- [6] L. Ely, W. Roa, W.H. Finlay, R. Löbenberg, Effervescent dry powder for respiratory drug delivery, *Eur. J. Pharm. Biopharm.* 2007, 65(3): 346-353.
- [7] S. Gill, R. Löbenberg, T. Ku, S. Azarmi, W. Roa, E.J. Prenner, Nanoparticles: characteristics, mechanisms of action and toxicity in pulmonary drug delivery-a review, *J. Biomed. Nanotechnol.* 2007, 3: 107-119.
- [8] N. Tsapis, D. Bennett, B. Jackson, D.A. Weitz, D.A. Edwards, Trojan particles: large porous carriers of nanoparticles for drug delivery, *Proc. Natl. Acad. Sci.* 2002, 99: 12001–12005.

- [9] C. Bosquillon, C. Lombry, V. Preat, R. Vanbever, Influence of formulation excipients and physical characteristics of inhalation dry powders on their aerosolization performance, *J. Control. Release* 2001, 70: 329-339.
- [10] Mark M. Bailey, Cory J. Berkland. Nanoparticle Formulations in Pulmonary Drug Delivery. *Medicinal Research Reviews* 2009, 29 (1): 196-212.
- [11] Sakagami, M. In vivo, in vitro and ex vivo models to assess pulmonary absorption and disposition of inhaled therapeutics for systemic delivery. *Adv. Drug Deliv. Rev* 2006, 58: 1030-1060.
- [12] Chono, S., Tanino, T., Seki, T., Morimoto, K. Influence of particle size on drug delivery to rat alveolar macrophages following pulmonary administration of ciprofloxacin incorporated into liposomes. *J. Drug Target.* 2006: 14, 557-566.
- [13] Nel, A., Xia, T., Madler, L., Li, N. Toxic potential of materials at the nanolevel. *Science* 2006, 311: 622-627.
- [14] Nemmar, A., Vanbilloen, H., Hoylaerts, M.F., Hoet, P.H., Verbruggen, A., Nemery, B. Passage of intratracheally instilled ultrafine particles from the lung into the systemic circulation in hamster. *Am. J. Respir. Crit. Care Med.* 2001, 164: 1665-1668.
- [15] Donaldson, K., Stone, V., Tran, C.L., Kreyling, W., Borm, P.J. *Nanotoxicology. Occup. Environ. Med.* 2004, 61: 727-728.
- [16] Oberdorster, G., Sharp, Z., Atudorei, V., Elder, A., Gelein, R., Lunts, A., Kreyling, W., Cox, C. Extrapulmonary translocation of ultrafine carbon particles following whole-body inhalation exposure of rats. *J. Toxicol. Environ. Health A* 2002, 65: 1531-1543.
- [17] Kreyling, W.G., Semmler, M., Erbe, F., Mayer, P., Takenaka, S., Schulz, H., Oberdorster, G., Ziesenis, A. Translocation of ultrafine

- insoluble iridium particles from lung epithelium to extrapulmonary organs is size dependent but very low. *J. Toxicol. Environ. Health A* 2002, 65: 1513-1530.
- [18] Kato, T., Yashiro, T., Murata, Y., Herbert, D.C., Oshikawa, K., Bando, M., Ohno, S., Sugiyama, Y. Evidence that exogenous substances can be phagocytized by alveolar epithelial cells and transported into blood capillaries. *Cell Tissue Res.* 2003, 311: 47-51.
- [19] Mills, N.L., Amin, N., Robinson, S.D., Anand, A., Davies, J., Patel, D., De La Fuente, J.M., Cassee, F.R., Boon, N.A., Macnee, W., Millar, A.M., Donaldson, K., Newby, D.E. Do inhaled carbon nanoparticles translocate directly into the circulation in humans? *Am. J. Respir. Crit. Care Med.* 2006, 173: 426-431.
- [20] S. Gelperina, K. Kisich, M.D. Iseman, L. Heifets, The potential advantages of nanoparticle drug delivery systems in chemotherapy of tuberculosis, *Am. J. Respir. Crit. Care Med.* 2005, 172(12): 1487-1490.
- [21] World Health Organization, 2006. Global Tuberculosis Control: Surveillance, planning, financing WHO Report 2006. WHO/HTM/TB/2006.362 World Health Organization (WHO), Geneva. Available at [http://www.who.int/tb/publications/global\\_report/2006/en/](http://www.who.int/tb/publications/global_report/2006/en/).
- [22] Gupta UD, Katoch VM. Animal models of tuberculosis for vaccine development. *Indian J Med Res* 2009; 129: 11-19.
- [23] Du Toit LC *et al.* Tuberculosis chemotherapy: current drug delivery approaches. *Resp Res* 2006; 7: 1-18.
- [24] Gelperina S *et al.* The potential advantages of nanoparticles drug delivery systems in chemotherapy of tuberculosis. *Am J Resp Crit Care Med* 2005; 172: 1487-1490.

- [25] Kreuter J. Nanoparticles. In: Kreuter J, editor. Colloidal drug delivery systems, vol. 66. Marcel Dekker: New York; 1994, p 219-342.
- [26] Soppimath KS *et al.* Biodegradable polymeric nanoparticles as drug delivery devices. *J Contr Rel* 2001; 70: 1–20.
- [27] Shirzad Azarmi, Wilson H. Roa, Raimar Löbenberg. Targeted delivery of nanoparticles for the treatment of lung diseases. *Advanced Drug Delivery Reviews* 2008, 60: 863-875.
- [28] Zhang Q, Shen Z, Nagai T. Prolonged hypoglycemic effect of insulin-loaded polybutylcyanoacrylate nanoparticles after pulmonary administration to normal rats. *Int J Pharm* 2001, 218(1–2):75–80.
- [29] Brzoska M, Langer K, Coester C, Loitsch S, Wagner TO, Mallinckrodt C. Incorporation of biodegradable nanoparticles into human airway epithelium cells-in vitro study of the suitability as a vehicle for drug or gene delivery in pulmonary diseases. *Biochem Biophys Res Commun* 2004, 318(2):562–570.
- [30] Dailey LA, Jekel N, Fink L, Gessler T, Schmehl T, Wittmar M, Kissel T, Seeger W. Investigation of the proinflammatory potential of biodegradable nanoparticle drug delivery systems in the lung. *Toxicol Appl Pharmacol* 2006, 215(1):100-108.
- [31] Salama, R.O., Traini, D., Chan, H.K., Sung, A., Ammit, A.J., Young, P.M. Preparation and evaluation of controlled release microparticles for respiratory protein therapy. *Journal of Pharmaceutical Sciences* 2009, 98: 2709-2717.
- [32] Cal, K., Sollohub, K. Spray drying technique. I: hardware and process parameters. *Journal of Pharmaceutical Sciences* 2010, 99: 575-586.



- [33] Heng, D., Cutler, D.J., Chan, H.K., Yun, J., Raper, J.A. What is a suitable dissolution method for drug nanoparticles? *Pharmaceutical Research* 2008, 25: 1696-1701.
- [34] Xiang Li, Nicolas Anton, Cordin Arpagaus, Fabrice Belleteix, Thierry F. Vandamme. Nanoparticles by spray drying using innovative new technology: The Büchi Nano Spray Dryer B-90. *Journal of Controlled Release* 2010, 147: 304-310.
- [35] Wurster, D. E. J. Am. Pharm. Assoc. (Sci. Edi.) 49:82, 1960.
- [36] Kaori Jono, Hideki Ichikawa, Masahito Miyamoto, Yoshinobu Fukumori. A review of particulate design for pharmaceutical powders and their production by spouted bed coating. *Powder Technology* 2000, 113: 269–277.
- [37] Albericio F *et al.* New trends in peptide coupling reagents. *Org Prep Proc Int* 2001; 33: 203-303.
- [38] Sabatino G *et al.* Assessment of new 6-Cl-HOBt based coupling reagents for peptide synthesis. Part 1: coupling efficiency study *Lett Pep Sci* 2009; 9: 119-123.
- [39] Cassano R *et al.* A novel dextran hydrogel linking trans-ferulic acid for the stabilization and transdermal delivery of vitamin E. *Eur J Pharm Biopharm* 2009; 72: 232-238.
- [40] Siddiqi SH *et al.* Evaluation of arapid radiometric method for drug susceptibility testing of Mycobacterium tuberculosis. *J Clin Microbiol* 1981; 13: 908-912.
- [41] Li DX *et al.* Novel gelatin micro-capsule with bioavailability enhancement of ibuprofen using spray drying technique. *Int J Pharm* 2008; 355: 277-284.
- [42] Vasir JK *et al.* Nanosystems in drug targeting: opportunities and challenges. *Current Nanoscience* 2005; 1: 47-64.

Section 3 – PART A

- [43] Panickar JR, Hoskyns W. Treatment failure in tuberculosis. *Eur Respir J* 2007; 29: 561-564.
- [44] Iseman MD. Tuberculosis therapy: past, present and future. *Eur Respir J* 2002; 20: 87s-94s.

## **PART B**

### **COLLAGEN $\alpha$ -TOCOPHERULATE FOR TOPICAL APPLICATIONS: PREPARATION, CHARACTERIZATION AND ANTIOXIDANT ACTIVITY EVALUATION [1]**

#### **Abstract**

*Aims:* Synthesis of collagen  $\alpha$ -tocopherulate for topical treatments. Collagen is a natural polymer largely applied to enhance wound repairing.  $\alpha$ -Tocopherol is a known antioxidant used for the treatment of various skin diseases. The linking to collagen through covalent bonds could improve its transport and metabolic stability, reducing the rate of degradation and insuring a longer persistence than that of free antioxidant.

*Methods:* The new biopolymer was prepared by solid-phase synthesis employing a carboxypolystyrene resin. Its antioxidant activity in rat liver microsomal membranes was also evaluated.

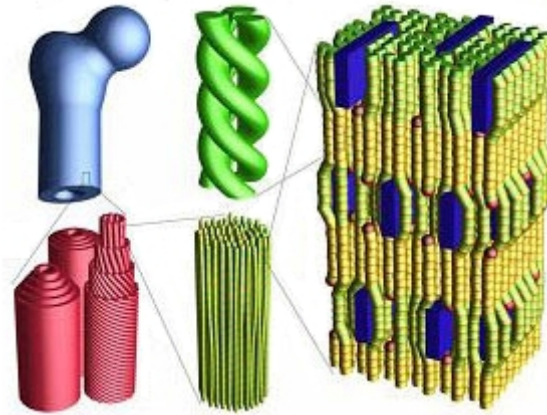
*Conclusions:* The developed collagen-based biomaterial is a new prodrug of alpha-tocopherol that could be used for various biomedical applications in wounds healing and tissues repair.

#### **1. Introduction**

Over the last decades, significant progresses have been made in the development of biodegradable polymeric materials for biomedical applications. They are, at present, the structures of choice for the development of therapeutic devices, such as temporary prostheses, porous three-dimensional structures, vehicles for the controlled and/or delayed release of drugs and materials for tissue engineering [2]. Actually, there are many biocompatible natural or synthetic materials that can undergo

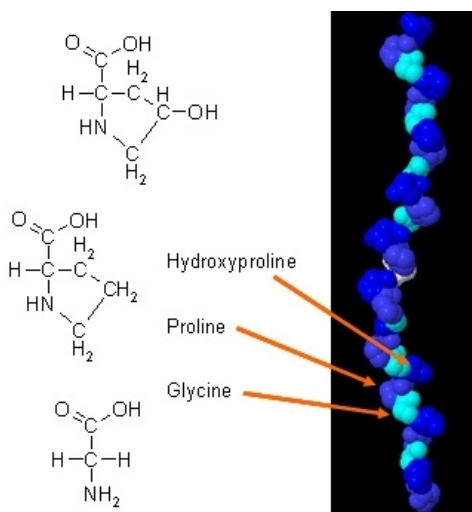
hydrolytic or enzymatic degradation for biomedical applications [3]. Among these, collagen is considered as one of the most useful biomaterials. Its excellent biocompatibility and its safety, mainly due to the biodegradability and weak antigenicity [4], make it one of the primary resources in biomedical applications. Collagen, a well-known protein, has been widely used in medical applications. Many natural polymers and their synthetic analogues are used as biomaterials, but the characteristics of collagen as a biomaterial are distinct from those of synthetic polymers mainly in its mode of interaction in the body. Collagen plays an important role in the formation of tissues and organs, and is involved in various functional expressions of cells. Collagen is a good surface-active agent and demonstrates its ability to penetrate a lipid-free interface. It exhibits biodegradability, weak antigenicity and superior biocompatibility compared with other natural polymers, such as albumin and gelatin. The primary reason for the usefulness of collagen in biomedical application is that collagen can form fibers with extra strength and stability through its self-aggregation and cross-linking. In most of drug delivery systems made of collagen, in vivo absorption of collagen is controlled by the use of crosslinking agents, such as glutaraldehyde, chromium tanning, formaldehyde, polyepoxy compounds, acyl azide, carbodiimides and hexamethylenediisocyanate. Physical treatment, such as ultra-violet/gamma-ray irradiation and dehydrothermal treatment, have been efficiently used for the introduction of crosslinks to collagen matrix. Collagen can be extracted into an aqueous solution and molded into various forms of delivery systems. The use of collagen as a drug delivery system is very comprehensive and diverse: the main applications of collagen as drug delivery systems are collagen shields in ophthalmology, sponges for burns/wounds, mini-pellets, nanoparticles and tablets for

protein delivery, and for transdermal delivery. In particular collagen sponges have been very useful in the treatment of severe burns and as a dressing for many types of wounds, such as pressure sores, donor sites, leg ulcers and decubitus ulcers as well as for in vitro test systems [5]. Collagen plays an important role in the formation of tissues and organs, and is involved in various functional expressions of cells. It is a primary structural constituent of vertebrates, as well as the most abundant protein in mammals, accounting for roughly 20-30% of the total protein in the body (Figure 1).



**Figure 1:** *Demonstration of mechanical strength of collagen*

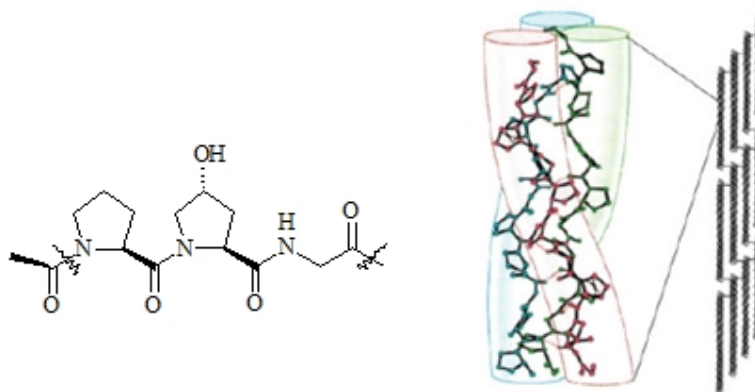
It is present in tissues such as skin, bones, tendons and ligaments, with a predominantly mechanical function, and preserves, in addition, the structural integrity of all our internal organs. The structural unit of collagen is represented by the tropocollagen, a protein with a molecular mass of approximately 285 kDa, composed of three polypeptide chains that are associated with left-handed pattern to form a right-handed triple helix (Figure 2).



**Figure 2:** *Structure of collagen*

The largest amounts of collagen, which is currently used for biomedical applications, are obtained from the skin of cattle or swine or from bovine Achilles tendon. One disadvantage of these collagen-based biomaterials and the limiting factor for their clinical applications is their mild immunogenicity, given by the composition of the terminal region of the chains. The immune response was found to be different depending on the species from which the collagen has been isolated, or on the implant site; the immunogenicity was reduced by pretreatment of the protein before application. Other limits to its use can also result from the high cost of pure collagen, from its poor chemical stability, from the risk of transmission of infectious diseases due to allogeneic or xenogeneic origin of the material. Several recombinant systems are currently being developed for the production of human collagen [6]. Collagen undergoes enzymatic degradation within the body by enzymes such as collagenase and metalloproteinase, releasing the corresponding aminoacids that compose itself. Collagen is synthesized by fibroblasts, which usually

originate from pluripotential adventitial cells or reticulum cells. The molecular structure of collagen has been firmly established on the evidence from earlier studies, such as amino acid composition analysis, X-ray diffraction analysis, electron microscopy and physicochemical examination of solutions. Collagen has a unique structure, size and amino acid sequence. The collagen molecule consists of three polypeptide chains twined around one another as in a three-stranded rope. Each chain has an individual twist in the opposite directions [7]. The principal feature that affects a helix formation is a high content of glycine and aminoacid residues. The strands are held together primarily by hydrogen bonds between adjacent -CO and -NH groups, but also by covalent bonds. The basic collagen molecule is rod-shaped with a length and a width of about 3000 and 15 Å, respectively, and has an approximate molecular weight of 300 kDa (Figure 3).



**Figure 3:** *Collagen as a rod-shaped molecule*

Table 1 summarizes the major characteristics of collagen, which are suitable for medical and pharmaceutical applications.

<p><i>Advantages</i></p> <ul style="list-style-type: none"><li>High available from living organisms;</li><li>Non-antigenic;</li><li>Biodegradable and bioreabsorbable;</li><li>Non-toxic and biocompatible;</li><li>Synergic with bioactive components;</li><li>High tensile strength and minimal expressibility;</li><li>Hemostatic;</li><li>Biodegradability can be regulated by cross-linking;</li><li>Easily modifiable by utilizing its functional groups;</li><li>Compatible with synthetic polymers.</li></ul>
<p><i>Disadvantages</i></p> <ul style="list-style-type: none"><li>High cost of pure type I collagen;</li><li>Variability of isolated collagen;</li><li>Hydrophilicity and more rapid release;</li><li>Variability in enzymatic degradation rate;</li><li>Side effects, such as bovine spongiform encephalopathy (BSF) and mineralization.</li></ul>

**Table 1:** *Advantages and disadvantages of collagen as a biomaterial*

Collagen can be solubilized into an aqueous solution, particularly in acidic aqueous media, and can be engineered to exhibit tailor-made properties. Collagen is relatively stable due to its function as the primary structural protein in the body, but it is still liable to collagenolytic degradation by enzymes, such as collagenase and telopeptide-cleaving enzymes.

### *1.1 Adverse reactions to Collagen*

Reports of adverse reactions to collagen have been restricted to localized redness and swelling following plastic surgery using collagen implants and wound breakdown with the use of catgut suture material. Clinical reactions to collagen were rare, but two cases of allergic (IgE-mediated) reactions to bovine collagen were reported [8]. Patients in both cases



developed conjunctive edema in response to the topical application of highly purified bovine collagen to eye during ophthalmic surgery. When irritant effects and cytotoxicity of various products developed from collagen were evaluated, cell response to exogenous collagen starts shortly after the material is kept in contact with tissues, evoking a local and fast inflammatory response, whose intensity depends on the pharmaceutical formulation in use. Even though, unknown reverse effects may be discovered in the future application of collagen for gene delivery or tissue engineering, since collagen can help to avoid side effects originated from incorporated drugs, therapeutic peptides and proteins, the need for the continuous effort in development and evaluation of collagen based systems is manifest.

### *1.2 Biodegradability and collagenases*

Biodegradability is a valuable aspect for most collagen-based biomaterials. Collagen biocompatibility and possible degradation by human collagenases are responsible for the widespread use of this material in many biomedical applications. On the other hand, the rate of the degradation process often needs to be regulated using diverse methods such as crosslinking techniques or a structural modification agent like epigallocatechin-3-gallate (EGCG). Therefore, biodegradation of collagen-based biomaterials for applications such as tissue engineering could potentially lead to the restoration of tissue structure and functionality [9]. Collagenases such as matrix metalloproteinase (MMP) are responsible for most collagen degradation *in vivo*. It is also important to know that all collagenases have a different rate of collagen hydrolysis. The collagenolytic activity of all these MMP rely on three principles: the

ability to bind collagen molecules, the ability to unwind the three  $\alpha$  chains and the ability to cleave each strand of the triple helix.

### *1.3 Immunogenicity and biocompatibility*

The use of biological materials for medical applications requires a distinction between immunogenicity and antigenicity. Immunogenicity is about triggering an immune response while antigenicity refers to the interaction between the antibodies and the antigenic determinants or epitopes. An immune response against collagen mainly targets epitopes in the telopeptide region at each end of the tropocollagen molecule. However, the conformation of the helical part and the amino acid sequence on the surface of the polymerized collagen fibril, also influence the immunologic profile of the collagen molecule. Thus, the difference of immunogenicity between polymerized collagen and their smaller counterpart lies on the accessibility of the antigenic determinants that decrease during the polymerisation process [10].

### *1.4 Collagen in wounds healing*

Since collagen is the main component of the extracellular matrix and acts as a natural substrate for cells connection, proliferation and differentiation, it is understandable the increasing interest in using it as an ideal material for the medical tissutal engineering. When tissues are injured due to trauma, collagen is needed to repair the defect and restore the structure and hence function. An excessive deposition of collagen can induce fibrosis, compromising the structure and the function of the damaged site. Conversely, if the quantity of deposited collagen is insufficient, the tissue hardly undergoes complete regeneration. A spongy matrix, containing collagen and oxidized cellulose, has been recently

introduced in the European market for the treatment of exuding wounds in patients with diabetic ulcers [11]. Of great importance also its use as a substitute for skin in the treatment of burn injury . Wound healing is a highly specified process. The healing process starts with the formation of granulation tissue and ends with scar formation. In most of the cases, the complication in wound healing is due to inflammation. Inflammation results in a continuous generation of reactive species, such as the superoxide radical or the non-radical hydrogen peroxide. Superoxide radical species, hydrogen peroxide and hydroxyl radical species are strongly implicated in the pathogenesis of chronic wounds [12]. Even though ROS play a fundamental role in killing invading microbial pathogens, excessive overproduction of ROS can be detrimental to the host tissues by inactivating enzymic antioxidants and significantly depleting non enzymic antioxidants levels. Evidence for the potential role of oxidants in the pathogenesis of many diseases suggests that antioxidants may be of therapeutic use in these conditions. Due to its excellent biocompatibility and safety, the use of collagen in biomedical application has been rapidly growing and widely expanding to bioengineering areas. However, some disadvantages of collagen-based systems arose from the difficulty of assuring adequate supplies, their poor mechanical strength, and ineffectiveness in the management of infected sites [13].

### *1.5 Collagen-based drug delivery systems*

The main applications of collagen as drug delivery systems are collagen shields in ophthalmology, sponges for burns/wounds, mini-pellets and tablets for protein delivery, gel formulation in combination with liposomes for sustained drug delivery as controlling material for

transdermal delivery and nanoparticles for gene delivery. In addition, its uses as surgical suture, hemostatic agents, and tissue engineering including basic matrices for cell culture systems and replacement/substitutes for artificial blood vessels and valves are already known in literature [14]. Collagen films/sheets/discs have been used for the treatment of tissue infection, such as infected corneal tissue or liver cancer. Soluble ophthalmic insert in the form of a wafer or a film was introduced as a drug delivery system for the treatment of infected corneal tissue using a high dose of antibiotic agents, such as gentamicin and tetracycline [15]. Microfibrous collagen sheets as a local delivery carrier for the treatment of cancer were evaluated [16]. A transdermal delivery device containing nifedipine, whose release rate was well controlled by an attached membrane made of chitosan, showed the highest therapeutic efficacy in the treatment of tissue infection [17, 18].

#### *1.6 Collagen sponges for wounds healing*

Collagen sponges have been very useful in the treatment of severe burns and as a dressing for many types of wounds, such as pressure sores, donor sites, leg ulcers and decubitus ulcers as well as for in vitro test systems. Human collagen membrane has been a major resource of collagen sponge used as a biological dressing since 1930s. Collagen sponges have the ability to easily absorb large quantities of tissue exudate, smooth adherence to the wet wound bed with preservation of low moist climate as well as its shielding against mechanical harm and secondary bacterial infection. Experiments using sponge implantation demonstrated a rapid recovery of skin from burn wounds by an intense infiltration of neutrophils into the sponge. Coating of a collagen sponge with growth factor further facilitates dermal and epidermal wound healing. Collagen

sponges were found suitable for short term delivery (3–7 days) of antibiotics, such as gentamicin [19].

### *1.7 Collagen as skin replacement*

Collagen based implants have been widely used as vehicles for transportation of cultured skin cells or drug carriers for skin replacement and burn wounds. Since sponge implant was originally developed for recovery of skin and was very efficient in that purpose, various types of artificial skin were developed as a form of sponge. Cultured skin substitutes developed on collagen lattice were also used for skin replacement and skin wounds [20].

### *1.8 Collagen as bone substitute*

Among the many tissues in the human body, bone has been considered as a powerful marker for regeneration and its formation serves as a prototype model for tissue engineering based on morphogenesis. Collagen has been used as implantable carriers for bone inducing proteins. Recently, collagen itself was used as bone substitutes due to its osteoinductive activity. Collagen in combination with other polymers or chemicals was also used for orthopaedic defects [21].

### *1.9 Collagen as bioengineered tissues*

Collagen gel as human skin substitutes has demonstrated its usefulness in tissue engineering and led to the development of bioengineered tissues, such as blood vessels, heart valves and ligaments. Collagen shows hemostatic properties that promote blood coagulation and play an important role in tissue repair processes. Collagen sponge or gel initiates adhesion and aggregation of platelets that lead to a thrombus formation.

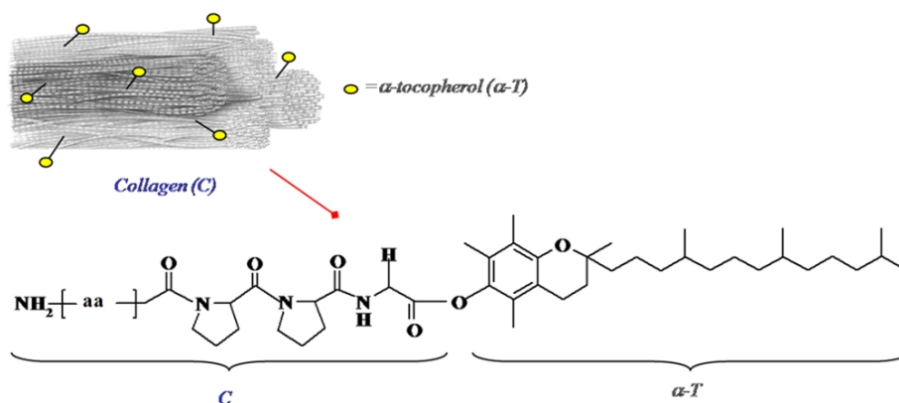
Monomeric collagen does not activate platelet aggregation, while polymeric collagen having a regular arrangement of the molecules with a length of around 1  $\mu\text{m}$  does activate it. Arginine side chains of collagen seemed to be responsible for its interaction with platelets. Three-dimensional collagen scaffolds, that are biodegradable in vivo and have a large surface area for cell attachment, can support vascularization processes and can be used as artificial blood vessels, heart valves or cell transplant devices [22].

*1.10 Recent Advances in Collagen-Based Biomaterials: Dermal filler, wound dressing and delivery systems*

FDA approved dermal filler commonly used in facial rejuvenation or reconstructive surgery. Collagen used for these purposes comes from three distinct sources: Bovine Zyderm<sup>®</sup>, porcine Evolence<sup>™</sup>, human CosmoDerm<sup>®</sup> and Cymetra<sup>®</sup> [23]. Although other collagen-based biomaterials are available for this purpose [24], these products can be useful for medical office-based interventions. The overgrowing popularity for these collagen-based dermal fillers is also due to the long-term side effect observed with nondegradable fillers like Bio-Alcamid<sup>™</sup>, which are susceptible to form granulomas [25]. Wound dressings that are also delivery systems represent an interesting application for collagen based applications. Recent studies have shown the feasibility and more importantly the benefits of implants delivering antibiotics [26]. The delivery properties of collagen-based biomaterials also display great potential for ulcer treatment and abdominal wall defect reconstruction.

### 1.11 Aim of the project

The aim of the present work was the obtaining of an antioxidant biomaterial useful as a carrier system through the functionalization of collagen with  $\alpha$ -tocopherol (vitamin E), an antioxidant molecule (Figure 4). The obtained biopolymer is an  $\alpha$ -tocopherol prodrug that could be used in the preparation of unconventional collagen-based drug delivery systems for wounds healing and tissues repairs. Particularly, synthesis was carried out in solid phase by using a carboxypolystyrene resin.



**Figure 4:** Schematic representation of collagen  $\alpha$ -tocopherol-linked.

## 2. Materials and Methods

### 2.1 Materials

All solvents of analytical grade, were purchased from Carlo Erba Reagents (Milan, Italy): dichloromethane, diethylether, N-methylpyrrolidone, thionyl chloride, collagen from bovine Achilles tendon (freeze-dried, insoluble),  $\alpha$ -tocopherol, dicyclohexylcarbodiimide (DCC) and trifluoroacetic acid, potassium chloride (KCl), ethylenediaminetetraacetic acid (EDTA), sucrose, 4-(2-hydroxyethyl)-1-piperazineethanesulfonic acid (HEPES), trichloroacetic acid (TCA), hydrochloric acid, butylated hydroxytoluene (BHT), tert-butyl

hydroperoxide (tert-BOOH), and 2-thiobarbituric acid (TBA) were purchased from Sigma-Aldrich (Sigma Chemical Co, St. Louis, MO, USA). Resin (carboxypolystyrene HL, 100-200 MESH, 1% DVB) was purchased from Merck AG.

## *2.2 Instruments*

Infrared spectra were recorded on KBr pellets using a FT-IR spectrometer Perkin-Elmer 1720. UV-VIS spectra were realized through a UV-530 JASCO spectrophotometer. The samples were lyophilized utilizing a "Freezing-drying" Micro moduly apparatus, Edwards. The calorimetric analyses (DSC) were performed using a Netzsch DSC200 PC.

## *2.3 Collagen derivatization*

The derivatization reaction was carried out in a vial Disa, suitably flamed, under stirring and nitrogenum atmosphere at room temperature for 3 hours. In order to activate the carboxylic function available on the resin, we generated the corresponding acyl chloride by adding thionyl chloride ( $\text{SOCl}_2$ , 0,022 ml, 0,3 mmol) in slight excess in a ratio of 1.5:1 compared to the resin (0.2 mmol; 0.2 g). As reaction solvent we used N-methylpyrrolidone, the only one that was able to solubilize the collagen under heat treatment (70 °C) and stirring for a minimum of 40 minutes. After the activation of carboxylic groups present on the resin with acryloyl chloride, collagen (0.008g) was added. In this way collagen was covalently linked to the resin; afterthat  $\alpha$ -tocopherol and a coupling agent such as dicioesilcarbodimmide (DCC) were added. We used a slight excess of antioxidant (0.3 mmol, 0.129 g) than the resin (0.2 mmol) and DCC (0.3 mmol, 0.062g) in equal amounts with  $\alpha$ -tocopherol. Reaction was conducted at room temperature for 72 hours. In order to obtain the



cleavage of the derivatized protein from the resin, 0.5 ml of trifluoroacetic acid (TFA) 5% in 10 ml of dichloromethane (DCM) were added. This reaction was conducted under nitrogen atmosphere and continuous magnetic stirring. We performed a filtration under reduced pressure on a porous filter. We got a clear and yellow filtrate. The resin, recovered by filtration, has been retained for reuse after washing. The obtained product was washed with several aliquots of diethyl ether and extracted with chloroform. The product was then dried at reduced pressure and characterized (Yield: 70%).

#### *2.4 Antioxidant activity evaluation trough rat liver microsomal membranes*

The antioxidant activity in inhibiting the lipid peroxidation, in rat-liver microsomal membranes, induced in vitro by a source of free radicals tert-butyl hydroperoxide (tert-BOOH), was evaluated. Liver microsomes were prepared from Wistar rats by tissue homogenization with 5 volumes of ice-cold 0.25 M sucrose containing 5 mM Hepes, 0.5 mM EDTA, pH 7.5 in a Potter–Elvehjem homogenizer [27]. Microsomal membranes were isolated by the removal of the nuclear fraction at 8000g for 10 min, and by the removal of the mitochondrial fraction at 18,000g for 10 min. The microsomal fraction was sedimented at 105,000g for 60 min, and the fraction was washed once in 0.15 M KCl, and was collected again at 105,000g for 30 min [28]. The membranes, suspended in 0.1 M potassium phosphate buffer, pH 7.5, were stored at -80 °C. Microsomal proteins were determined by the Bio-Rad method [29]. Aliquots of collagen derivative and of  $\alpha$ -tocopherol in the range of 0.5–6 mg/ml were added to the microsomes. The microsomes were gently suspended by a Dounce homogenizer, and then the suspensions were incubated at 37 °C in a

shaking bath under air in the dark. Malondialdehyde (MDA) was extracted and analyzed as indicated. Briefly, aliquots of 1 mL of microsomal suspension (0.5 mg proteins) were mixed with 3 mL of 0.5% TCA and 0.5 mL of TBA solution (two parts 0.4% TBA in 0.2 M HCl and one part distilled water), and 0.07 mL of 0.2% BHT in 95% ethanol. Samples were then incubated in a 90 °C bath for 45 min. After incubation, the TBA-MDA complex was extracted with 3 mL of isobutyl alcohol. The absorbances of the extracts were measured by the use of UV spectrophotometry at 535 nm, and the results were expressed as percent of MDA inhibition, using an extinction coefficient of  $1.56 \cdot 10^5 \text{ L mmol}^{-1} \text{ cm}^{-1}$ .

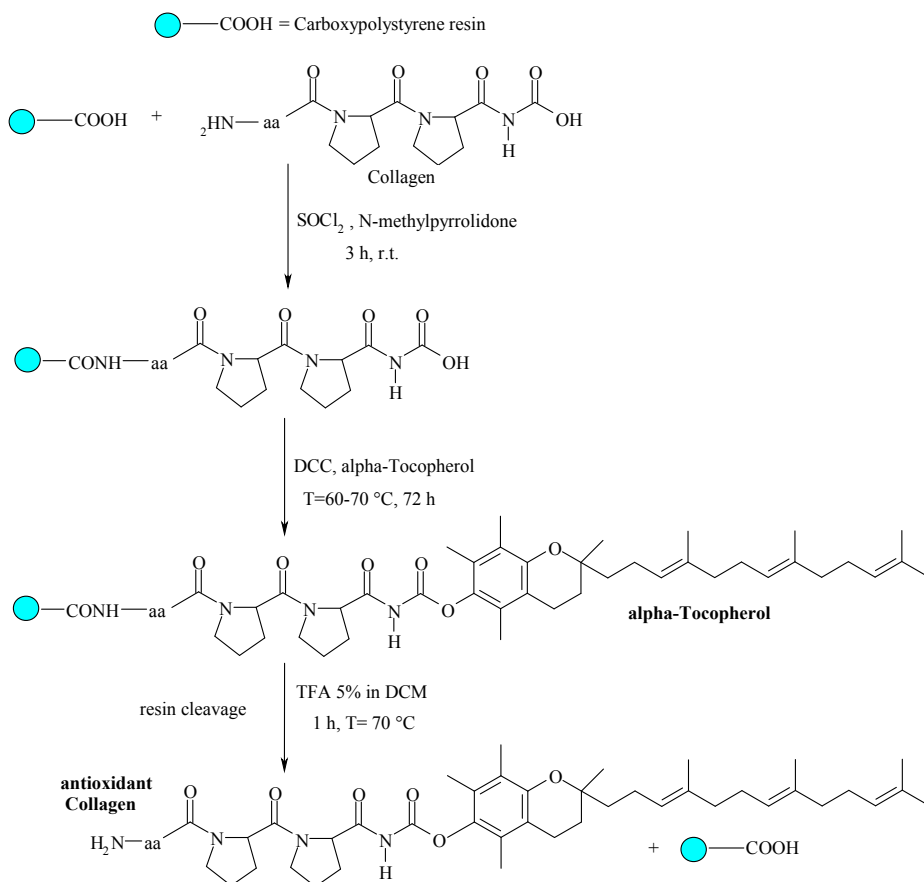
### **3. Results and discussion**

As evidenced by the abundance of data in the literature, a growing interest is now attributed to the design and implementation of biocompatible systems for pharmaceutical applications. For these purposes, recently more and more attention is directed to the use of natural polymers or compounds synthesized from materials of natural origin that best meet the needs of biocompatibility [30-32]. The purpose of this work was to synthesize a pro-drug collagen-based and therefore compatible with tissues to exploit its intrinsic properties in order to convey the active ingredient bound to collagen and to facilitate tissue repair.

#### *3.1 Solid phase synthesis of collagen derivative*

Since the collagen is a highly composite protein, consisting of a huge number of aminoacids, before to functionalize it with an antioxidant, we performed a preventive treatment in order to anchor the protein to a resin acting as a protecting group of collagen terminal amino-group. After the

collagen binding to the resin through its amino-terminal group, and activation of its C-terminal group with thionyl chloride, we proceeded to the functionalization of the protein with an antioxidant agent,  $\alpha$ -tocopherol, through the formation of an ester bond. After that we cleaved the functionalized collagen from the resin (Scheme 1).

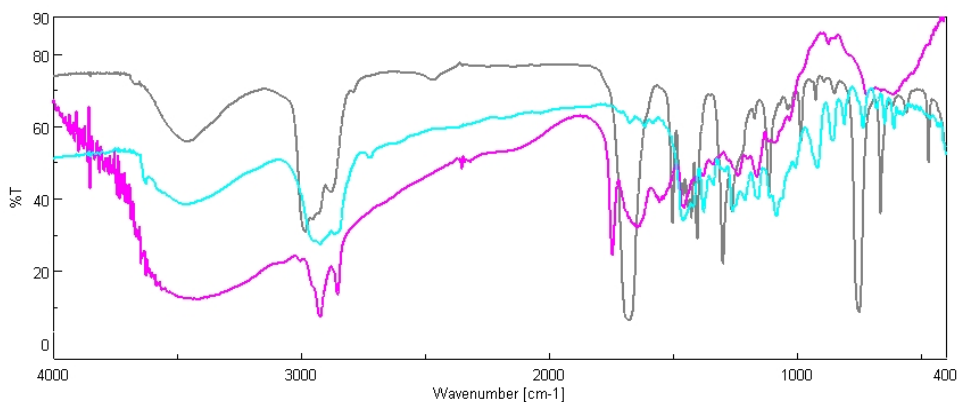


**Scheme 1:** Synthetic route.

In particular, we carried out a heterogeneous synthesis; in particular, the ester-linkages between resin and protein has been facilitated by a prior chlorination of-COOH groups of the resin. The formation of acylic chloride, with markedly electrophilic character and hence more reactive

than the corresponding carboxyl function was carried out by treatment of the resin, dissolved in N-methylpyrrolidone, with acryloyl chloride. The choice to anchor the collagen on the resin surface for its functionalization with  $\alpha$ -tocopherol has been considered mainly in order to avoid the difficulties in conducting the synthesis, which could result from the excessive size of the collagen itself. These problems inherent in this characteristic of the protein matrix would have been difficult to be managed in a more common synthesis in homogeneous phase. Moreover, we chose the heterogeneous synthesis to facilitate the management of several functional groups in the aminoacids side chain that constitute the collagen. Once the N-terminal function of the polypeptide was locked, our attention has been paid to the free functional groups on the other side of collagen itself. Carboxylic acid functions useful for the functionalization with the  $\alpha$ -tocopherol phenolic hydroxyl group are, not only those C-terminals, but also those exposed in the side chain of the amino acids constituting the protein. The bond between the resin acyl chloride and the  $\alpha$ -tocopherol hydroxyl group is a relationship of ester. It is generated by reaction between the nucleophilic group (-OH) present on the antioxidant phenolic ring, and the resin -COCl groups, with a strong electrophile character. The covalent bond of the antioxidant moiety on the collagen matrix has something very important from the point of view of the use of this product as a potential prodrug. The protein, in fact, possessing itself a therapeutic action, is enriched and strengthened of the antioxidant properties. The resin can be removed from the derivatized collagen by breaking the ester bond. For this purpose we used, a mild acid treatment which do not affect the ester bond between the protein and the antioxidant. The resin was removed by filtration. The filtrate was washed with diethyl ether to induce precipitation of the product and thus allowing

its separation and recovery. The spectrum of non-derivatized collagen shows a high amount of functional groups, relating to the numerous side chains of amino acids that make up the structure. However, comparing starting collagen and functionalized one, we noted the presence of typical bands of ester bonds (Figure 5).



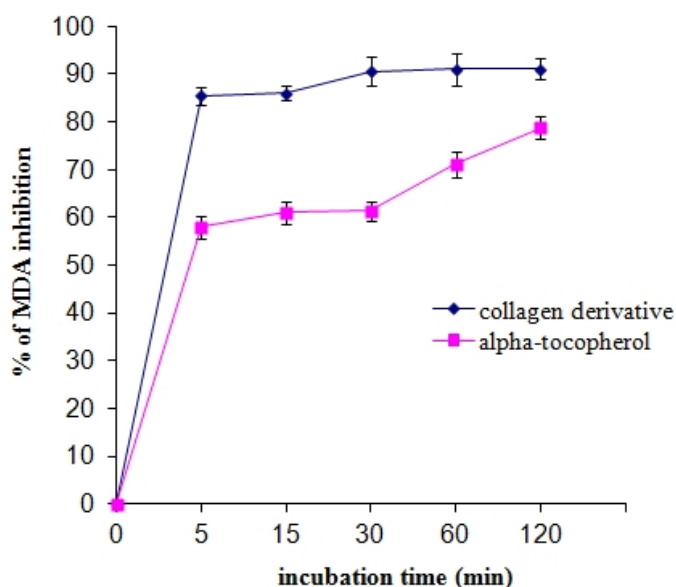
**Figure 5:** FT-IR analyses of (—) C- $\alpha$ T, (—)  $\alpha$ T, (—) C.

Calorimetric analysis for commercial collagen revealed the presence of a large endothermic at 207.1 °C. On the other hand, the DSC spectrum of derivatized collagen, shows the absence of the transition of commercial vitamin E (113°C) and the presence of a broad peak similar to that observed for the non-derivatized collagen.

### 3.2 Antioxidant activity evaluation

The collagen derivative was then tested for its antioxidant activity. Results showed that collagen esterified with  $\alpha$ -tocopherol possesses protective activity against peroxy-radicals. The ability of collagen derivative in inhibiting lipid peroxidation induced by a source of free radicals, such as *tert*-BOOH, was examined in rat liver microsomal membranes over 120 minutes of incubation. In order to draw comparisons

with the non-functionalized collagen, even this has been tested for its antioxidant capacity (data not shown). The ability of the synthesized material to inhibit lipid peroxidation is time-dependent, in addition the collagen derivative maintains the antioxidant activity and trend over time of the commercial  $\alpha$ -tocopherol (Figure 6).



**Figure 6:** Percentage of inhibition of *tert*-BOOH induced MDA formation in rat microsomal membranes. The microsomal membranes were incubated with  $0.25 \times 10^{-3}$  M *tert*-BOOH at 37 °C under air in the dark. The results represent the mean  $\pm$  standard error of the mean (SEM) of six separate experiments.

#### 4. Conclusions

A growing interest is reserved nowadays in the research and the development of natural or synthetic materials capable of combining the characteristics of biocompatibility with the site-specificity against target organ [33-35]. For these same reasons was realized a prodrug composed of collagen, a natural protein, and an antioxidant moiety,  $\alpha$ -tocopherol, in

order to obtain a biocompatible carrier with antioxidant properties. Evidence for the potential role of oxidants in the pathogenesis of many diseases suggests that antioxidants may be of therapeutic use in these conditions. To facilitate the peptide derivatization, it was decided to conduct the entire process in heterogeneous phase. On the collagen derivative we carried out some analysis such as FT-IR spectroscopy and DSC analysis. It was then tested its antioxidant activity on rat liver microsomal membranes, in order to evaluate the antioxidant activity of functionalized collagen. The data obtained by this procedure show that the derivatized product maintains the typical  $\alpha$ -tocopherol antioxidant activity which is able to improve significantly wound healing and protect tissues from oxidative damage.

## References

- [1] Sonia Trombino, Roberta Cassano, Teresa Ferrarelli, Benedetta Isacchi, Anna Rita Bilia and Nevio Picci. Collagen  $\alpha$ -tocopherulate for topical applications: preparation, characterization and antioxidant activity evaluation. *Macromolecular Research*. SUBMITTED.
- [2] G. Pitarresi, F. S. Palumbo, G. Cavallaro, S. Fare', G. Giammona, *J. Biomed. Mater. Res. Part A* **2008**, 87A, 770.
- [3] L. S. Nair, C. T. Laurencin, *Prog. Polym. Sci.* **2007**, 32: 762.
- [4] R. Timpl, in *Extracellular Matrix Biochemistry*, K. A. Piez, A. H. Reddi, Eds., Elsevier, New York, **1984**, p. 159-190.
- [5] C. H. Lee, A. Singla, Y. Lee, *Int. J. Pharm.* **2001**, 221: 1.
- [6] D. Olsen, C. Yang, M. Bodo, R. Chang, *Adv. Drug Deliv. Rev* **2003**, 55: 1547.
- [7] Rémi Parenteau-Bareil, Robert Gauvin, François Berthod. Collagen-Based Biomaterials for Tissue Engineering Applications. *Materials* **2010**, 3, 1863-1887.
- [8] Mullins, R.J., Richards, C., Walker, T. Allergic reactions to oral, surgical and topical bovine collagen. Anaphylactic risk for surgeons. *Austr. New Zealand J. Ophthalmol.* **1996**, 24(3): 257-260.
- [9] Goo, H.C.; Hwang, Y.S.; Choi, Y.R.; Cho, H.N.; Suh, H. Development of collagenase-resistant collagen and its interaction with adult human dermal fibroblasts. *Biomaterials* **2003**, 24, 5099-5113.
- [10] Prockop, D.J.; Kivirikko, K.I. Collagens: Molecular biology, diseases, and potentials for therapy. *Annu Rev Biochem* **1995**, 64, 403-434.
- [11] F. Thornton, R. J. Rohrich, *Plast. Reconstruct. Sur.* **2005**, 116: 677.
- [12] M. J. White, F. R. Heckler, *Clin. Plast. Surg.* **1990**, 17: 473.



- [13] Huynh, T., Abraham, G., Murray, J., Brockbank, K., Hagen, P.-O., Sullivan, S. Remodeling of an acellular collagen graft into a physiologically responsive neovessel. *Nat. Biotechnol.* **1999**, 17: 1083-1086.
- [14] Bloomfield, S.E., Miyata, T., Dunn, M.W., Bueser, N., Stenzel, K.H., Rubin, A.L. Soluble gentamycin ophthalmic inserts as a drug delivery system. *Arch. Ophthalmol.* **1978**, 96: 885-887.
- [15] Minabe, M., Takeuchi, K., Tamura, K., Hori, T., Umemoto, T. Subgingival administration of tetracycline on a collagen film. *J. Periodontol.* **1989**, 60: 552-556.
- [16] Sato, H., Kitazawa, H., Adachi, I., Horikoshi, I. Microdialysis assessment of microfibrillar collagen containing a p-glycoprotein-mediated transport inhibitor, cyclosporine A, for local delivery of etoposide. *Pharm. Res.* **1996**, 13: 1565-1569.
- [17] Thacharodi, D., Rao, K.P. Rate-controlling biopolymer membranes as transdermal delivery systems for nifedipine: development and in vitro evaluations. *Biomaterials* **1996**, 17: 1307-1311.
- [18] Murata, M., Maki, F., Sato, D., Shibata, T., Arisue, M. Bone augmentation by onlay implant using recombinant human BMP-2 and collagen on adult rat skull without periosteum. *Clin. Oral Implants Res.* **2000**, 11(4): 289-295.
- [19] Wachol-Drewiek, Z., Zpfeiffer, M., Scholl, E. Comparative investigation of drug delivery of collagen implants saturated in antibiotic solutions and a sponge containing gentamycin. *Biomaterials* **1996**, 17: 1733-1738.
- [20] Supp, A.P., Wickett, R.R., Swope, V.B., Harriger, M.D., Hoath, S.B., Boyce, S.T. Incubation of cultured skin substitutes in reduced

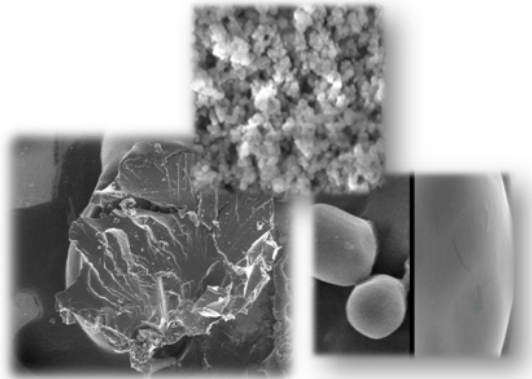
- humidity promotes cornification in vitro and stable engraftment in athymic mice. *Wound Repair Rege.* **1999**, 7: 226-237.
- [21] Shahram M Ghanaati, Benjamin WThimm, Ronald E Unger, Carina Orth, Thomas Kohler, Mike Barbeck, Ralph Muller and C James Kirkpatrick. Collagen-embedded hydroxylapatite-beta-tricalcium phosphate–silicon dioxide bone substitute granules assist rapid vascularization and promote cell growth. *Biomed. Mater.* **2010**, 5.
- [22] Chi H. Lee, Anuj Singla, Yugyung Lee. Biomedical applications of collagen. *International Journal of Pharmaceutics* **2001**, 221: 1-22.
- [23] Bentkover, S.H. The biology of facial fillers. *Facial Plast. Surg.* **2009**, 25: 73-85.
- [24] Gurney, T.A.; Kim, D.W. Applications of porcine dermal collagen (ENDURAGen) in facial plastic surgery. *Facial Plast. Surg. Clin. North Am.* **2007**, 15: 113-121.
- [25] Pons-Guiraud, A. Adverse reactions to injectable fillers. *Ann. Dermatol. Venereol.* **2008**, 135: 171-174.
- [26] Adhirajan, N.; Shanmugasundaram, N.; Shanmuganathan, S.; Babu, M. Collagen-based wound dressing for doxycycline delivery: in-vivo evaluation in an infected excisional wound model in rats. *J. Pharm. Pharmacol.* **2009**, 61:1617-1623.
- [27] V. L. Tatum, C. Changoit, C. K. Chow, *Lipids* **1990**, 25: 226.
- [28] S. Trombino, S. Serini, F. Di Nicuolo, L. Celleno, S. Andò, N. Picci, G. Calviello, P. Palozza, *J. Agric. Food Chem.* **2004**, 52: 2411.
- [29] M. M. Bradford, *Anal. Biochem.* **1976**, 72: 248.
- [30] R. Cassano, S. Trombino, T. Ferrarelli, R. Muzzalupo, L. Tavano, N. Picci, *Carbohy. Polym.* **2009**, 78: 639.
- [31] R. Cassano R, S. Trombino, R. Muzzalupo, L. Tavano, N. Picci, *Eur. J. Pharm. Biopharm.* **2009**, 72: 232.

- [32] R. Cassano, S. Trombino, T. Ferrarelli, E. Barone, V. Arena V, C. Mancuso, N. Picci, *Biomacromol.* **2010**, 11: 1139.
- [33] X. Duan, C. McLaughlin, M. Griffith, H. Sheardown, *Biomaterials*, **2007**, 28: 78.
- [34] M. Radhika, P. K. Sehgal, *J. Biomed. Mat. Res.* 1997, 35: 497.
- [35] M. Gruessner, P. V. Clemens, P. Pahlplatz, J. Sperling, P. Sperling, *Am. J. Surg.* **2001**, 182:502.



## SECTION 4

### HYDROGELS AND MICROSPHERES BASED ON ACTIVE MOLECULES



- **Part A:** Preparation, characterization and *in vitro* activities evaluation of curcumin based microspheres for azathioprine oral delivery;
- **Part B:** Respirable Rifampicin-Based Microspheres Containing Isoniazid for Tuberculosis Treatment;
- **Part C:** A new Hydrogel Ellagic acid and Glycine-based Containing Folic acid as Subcutaneous Implant For Breast Cancer Treatment.

## PART A

### PREPARATION, CHARACTERIZATION AND *IN VITRO* ACTIVITIES EVALUATION OF CURCUMIN BASED MICROSPHERES FOR AZATHIOPRINE ORAL DELIVERY [1]

#### **Abstract**

*Aim:* The main target of this study was the preparation, characterization and *in vitro* activities evaluation of microspheres curcumin-based able to incorporate azathioprine, useful for psoriasis treatment.

*Methods:* Curcumin was derivatized with acryloyl chloride in order to introduce polymerizable groups in its structure. The obtained polymerizable drug was characterized by Fourier transform infrared (FT-IR), to confirm ester linkages, and by <sup>1</sup>H-NMR, to establish the functionalization degree. The ability of the curcumin derivative to inhibit cell proliferation, in human breast cancer cells, gave an IC<sub>50</sub> value for viability of 20 μM.

*Results:* Acrylated curcumin showed also a strong antioxidant activity against lipid peroxidation induced in rat liver microsomal membranes. Then, spherical microparticles, based on a curcumin derivative, have been prepared by suspension radical copolymerization. The obtained microparticles have been characterized by FT-IR spectroscopy, dimensional and morphological analysis. Particle size investigation revealed a mean diameter of around 5.8 μm. Microspheres showed a very good swelling behaviour in simulating intestinal fluids. Their azathioprine loading efficiency, determined by spectrophotometric analysis was equal to 80%. Release profile of azathioprine showed an initial burst of around 60% and a further release for 24 hours.

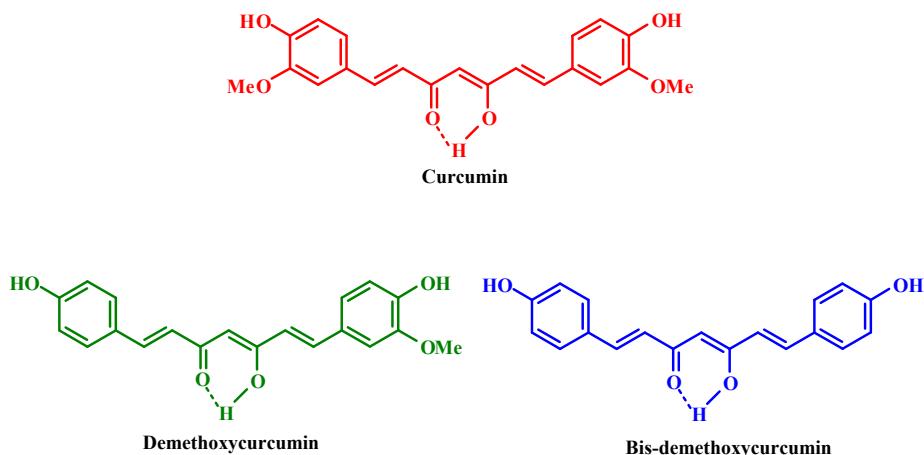
*Conclusions:* Obtained microspheres due to the displayed swelling behaviour and release profile are excellent candidates as oral carrier of azathioprine.

## **1. Introduction**

### *1.1 Curcumin and Azathioprine pharmacological activities*

Curcumin, is a yellow pigment derived from *Curcuma longa L.* characteristic representative of natural polyphenols, useful in medicinal and cosmetic preparations for its antiproliferative, anti-inflammatory and antioxidant properties [2]. Clinic studies demonstrate the curcumin positive effects against psoriasis promoting the skin regeneration, inhibition of cyclooxygenase activity and regulation of pro-inflammatory cytokines. Recently many clinical trials suggest the efficacy and safety of oral administered curcumin for psoriasis treatment [3,4]. Generally, moderate psoriasis is treated with corticosteroids, also used in combination with calcipotriene tazarotene and other retinoids derived from vitamin A [5,6]. On the other hand, all these drugs can cause serious side effects and, for these reasons, a great deal of researchers proposed both the associations of conventional drugs, to obtain synergistic effects, that of alternative molecules such as antioxidant polymers receiving ever-increasing attention. Although *in vitro* curcumin has been shown to block pathways necessary to develop psoriasis, it is possible that, after oral administration, it will not produce a desired clinical effect because low bioavailability [7] due to its conjugation in the intestinal tract [8]. It is possible that curcumin oral use at higher doses or combining it with agents that may enhance its absorption, may result in better efficacy. Several studies in recent years have shown that curcumin has antioxidant, anti-inflammatory, anti-microbial, anti-parasitic, anti-mutagen and

anticancer properties [9]. Recently, the effect of curcuminoids was examined on the proliferation of MCF-7 human breast tumour cells. It was reported that demethoxycurcumin showed the best inhibition of MCF-7 cells, followed by curcumin and bisdemethoxycurcumin [10]. Pure curcumin, bisdemethoxycurcumin and demethoxycurcumin are not available from commercial sources. Commercial curcumin contains 77% curcumin, 17% demethoxycurcumin and 3% bisdemethoxycurcumin [11]. Curcumin, demethoxycurcumin and bisdemethoxycurcumin exhibited various degrees of antioxidant capacity. The antioxidant capacities of curcuminoids were found to decrease in the order: curcumin>demethoxycurcumin>bisdemethoxycurcumin (Figure 1). Curcumin acts as a superoxide radical scavenger and as a singlet oxygen quencher. Of the naturally occurring curcuminoids, tetrahydrocurcumin, one of the main metabolites of curcumin, exhibits the most potent antioxidant activity [12].



**Figure 1:** Structure of Curcuminoids

The use of azathioprine has been limited due to its toxicity, thus, the vehiculation of this substance in our curcumin acrylated-based



microspheres, has the purpose, not only to obtain an azathioprine targeted delivery, but also the potential advantage of providing a local therapeutic effect reducing systemic azathioprine toxicity [13]. Azathioprine is among the oldest pharmacologic immunosuppressive agents in use today. Initially developed as a long-lived prodrug of 6-mercaptopurine (6-MP), it was quickly found to have a more favorable therapeutic index. It was soon found that 6-MP could produce remissions in childhood acute leukemia and later, that azathioprine could prolong renal allograft survival. Over the past 50 years, azathioprine has been used in the treatment of hematologic malignancies, rheumatologic diseases, solid organ transplantation, and inflammatory bowel disease. The drug is a purine analog, and the accepted mechanism of action is at the level of DNA [14]. Both in vitro and in vivo, azathioprine is metabolized to 6-MP through reduction by glutathione and other sulphhydryl-containing compounds and then enzymatically converted into 6-thiouric acid, 6-methyl-MP, and 6-thioguanine interfere (6-TG). Ultimately, azathioprine can then become incorporated into replicating DNA and can also block the de novo pathway of purine synthesis. It is this action that is thought to contribute to its relative specificity to lymphocytes due to their lack of a salvage pathway. However, the effects on the blockade of DNA replication have never fully explained all of the laboratory and clinical findings of azathioprine-induced immunosuppression [15].

### *1.2 Microspheres as drug delivery systems for oral administration of drugs*

Conventional oral drug administration does not usually provide rate-controlled release or target specificity. In many cases, conventional drug delivery provides sharp increases of drug concentration at potentially

toxic levels. Following a relatively short period at the therapeutic level, drug concentration eventually drops off until re-administration. Today new methods of drug delivery are possible: desired drug release can be provided by rate-controlling membranes or by implanted biodegradable polymers containing dispersed medication. Over the past 25 years much research has also been focused on degradable polymer microspheres for drug delivery. Administration of medication via such systems is advantageous because microspheres can be ingested or injected; they can be tailored for desired release profiles and in some cases can even provide organ-targeted release [16-18]. Spherical droplets are formed by oil-soluble organic monomers dispersed in aqueous media (oil in water, O/W) or by water-soluble monomers dissolved in water dispersed in an organic medium (water in oil, W/O) [19]. The polymerization of dispersed monomers is achievable by various methods including emulsion, suspension, and dispersion techniques [20]. Emulsions are typically used to form uniform spheres on nanometer or micrometer scales. The technique typically involves the dispersion of a hydrocarbon monomer in water with a water-soluble initiator. A surfactant is employed for the formation of uniform micelles; polymerization takes place inside micelles and not inside the dispersed organic monomer droplets since the initiator is not miscible there. The resulting polymer beads can be so uniform on the nano or micro-scale that they may diffract visible light [21]. Dispersion polymerization results in particle sizes in the range of 0.5–10  $\mu\text{m}$  and all of the reagents including monomer, initiator, and stabilizer (often an organic polymer consisting of hydrophobic and hydrophilic parts) are dissolved in an organic medium. Since the initiator is soluble inside the monomer, polymerization takes place inside the monomer droplets. The polymer beads, insoluble in the organic solvent,

precipitate, and the stabilizer prevents bead flocculation [22]. Suspension polymerizations are typically employed for micron-sized particles 50-500  $\mu\text{m}$ . In suspension polymerization the monomer is dispersed in a water phase with a stabilizer; the initiator is soluble in the monomer phase where polymerization occurs. The size and quantity of the particles is determined by the size and quantity of dispersed monomer droplets and by the speed of mechanical stirring (Table 1).

Method of preparation	Size range
Emulsion polymerization	0.01–1 $\mu\text{m}$
Dispersion polymerization	0.5–10 $\mu\text{m}$
Suspension polymerization	50–500 $\mu\text{m}$

**Table 1:** *Different methods of preparation of microparticles*

Increasing or controlling the encapsulation efficiency (EE) is desirable, it can prevent the loss of precious medication and it can help to extend the duration and dosage of treatment. The drug content of the encapsulated microspheres can be described by two quantities. The most common, also used in this paper, is the EE, where  $EE = \Delta D / DT$ ;  $DT$  is the total amount of drug employed and  $\Delta D$  is  $DT$  minus the amount of unloaded drug. On the other hand, the loading capacity (LC) is defined as  $LC = \Delta D / S_w$ , where  $S_w$  is the weight of the sphere [23].

Microspheres size can be affected by the polymer concentration in the emulsion, temperature, viscosity, the stirring rate and the amount of emulsifier employed. Considering the effect of polymer concentration, it has often been reported that increasing the concentration of polymer in the emulsion increases sphere size [24-26]. Porosity has an important

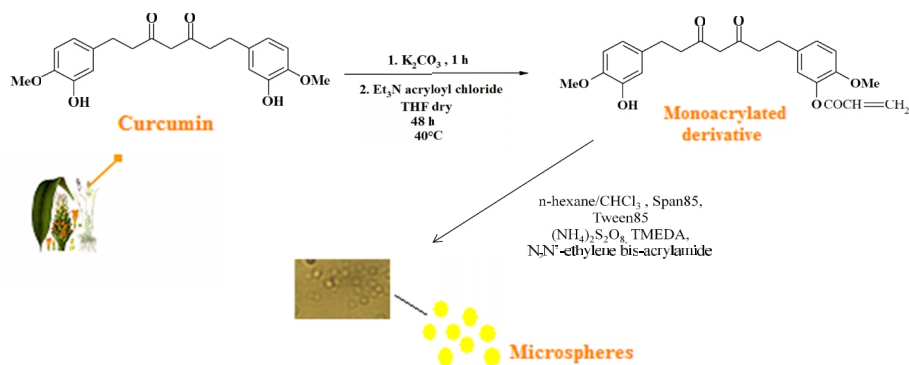
effect on drug release characteristics; a large number of pores may greatly increase the rate of drug expulsion [27, 28]. The most desirable release profile would show a constant release rate with time. However, in many cases release profiles are more complicated and often contain two main expulsion processes: the first being an initial burst of expelled medication from the sphere surface; the second, a usually more constant stage with release rates dependent on diffusion and degradation [29, 30]. How the drug is distributed in the medium can also vary its release profile [31]. Drug release begins at the sphere surface followed by release from the inner layers of the sphere; therefore the diffusional distance between the initial drug location inside the sphere affects the release profile. The release profiles are also dependent on the size of the microspheres; the rate of drug release was found to decrease with increasing sphere size [32]. Added control over drug delivery can be achieved by employing pH-triggered release. Therefore by the incorporation of pH-sensitive groups, microspheres can be targeted to various biological environments or to specific organs. Researchers also demonstrated that controlled release is possible for acrylamide-based microsphere systems which are both pH- and temperature-sensitive [33].

The use of microspheres for drug delivery is not limited to any specific illness, rather they can be widely applied to many situations where continuous and controlled drug administration is essential.

### *1.3 Aim of the project*

The present project concerns on: (i) the synthesis and characterisation of monoacrylated curcumin and of microspheres curcumin acrylated -based; (ii) the evaluation of their antiproliferative and antioxidant activities [34]; (iii) microspheres swelling degree, azathioprine loading efficiency and

release behaviour. Clearly a new drug delivery system was projected to enhance curcumin oral bioavailability. In particular, we linked acrylic moieties to curcumin by covalent bond (Scheme 1) to produce a polymeric carrier that can act both against oxidative stress, frequent in psoriasis, and entrap another antipsoriatic drug, like azathioprine, to obtain a synergic action with curcumin.



**Scheme 1:** Synthetic route to CA and microspheres preparation

## 2. Materials and Methods

### 2.1 Chemicals

All solvents were obtained from Carlo Erba Reagents (Milan, Italy). N,N'-ethylen bis-acrilammide (EBA) and acryloyl chloride, were supplied by Sigma (Sigma Chemical Co, St. Louis, MO) and distilled before using. Curcumin from *Curcuma longa*, azathioprine, potassium carbonate ( $K_2CO_3$ ), ammonium persulfate [ $(NH_4)_2S_2O_8$ ], sorbitan trioleate (Span 85), polyoxyethylene sorbitan monolaureate (Tween 85), N,N,N',N'-tetramethylethylenediamine (TMEDA), potassium chloride (KCl), ethylenediaminetetraacetic acid (EDTA), sucrose, 4-2-hydroxyethyl-1-piperazineethanesulfonic acid (HEPES), trichloroacetic acid (TCA), hydrochloric acid, butylated hydroxytoluene (BHT), *tert*-butyl

## Section 4 – PART A

hydroperoxide (*tert*-BOOH), and 2-thiobarbituric acid (TBA) were purchased from Aldrich Chemical Co. and used as received. DMEM/F-12, L-glutamine, Eagle's nonessential amino acids, penicillin, streptomycin, fetal calf serum, BSA, and PBS were purchased from Gibco (USA).

### *2.2 Measurements*

NMR spectra were acquired on Bruker VM-300 ACP. FT-IR spectra were measured on a Jasco 4200 using KBr disks. UV-VIS spectra were performed by V-530 JASCO spectrophotometer. The GC-MS spectra were obtained by Hewlett Packard 5972 instrument. The morphological studies were performed using optical microscopy. The light scattering was performed with a Brookhaven 90 plus particle size analyzer. The samples were lyophilized utilizing a "Freezing-drying" Micro moduly apparatus, Edwards. Scanning electron microscopy (SEM) photographs of the microspheres were obtained with a JEOL JSMT 300 A; the surface of the samples was made conductive by deposition of a gold layer on the samples in a vacuum chamber.

### *2.3 Synthesis of Monoacrylated Curcumin (CA)*

CA was prepared as follows. Curcumin (1 g, 2.71 mmol), dissolved in dry tetrahydrofuran, was treated with potassium carbonate ( $K_2CO_3$ ) in equimolar ratio (0.374 g) to avoid disubstitution and then with acryloyl chloride (2.71 mmol, 0.218 ml) using  $Et_3N$  as the base (0.379 ml, 2.71 mmol) [35,36]. The reaction was left under reflux at 40°C for 48 hours under magnetic stirring. The monosubstituted derivative was obtained from raw product by chromatographic column (silica gel 60-230 mesh,

eluent mixture CHCl<sub>3</sub>/CH<sub>3</sub>OH 1:1). Afterwards, the target molecule was investigated by GC/MS, FT-IR and <sup>1</sup>H-NMR spectroscopies [36].

#### *2.4 Antiproliferative Activity Evaluation of CA*

The antiproliferative effect of CA was evaluated in MCF-7 human breast cancer cells. These latter were a generous gift from Dr. B. Van der Burg (Utrecht, The Netherlands). Cells were maintained in DMEM/F-12 medium containing 5% fetal calf serum, 1% L-glutamine, 1% Eagle's nonessential amino acids, and 1 mg/ml penicillin/streptomycin in a 5% CO<sub>2</sub> humidified atmosphere. 48 h before each experiment, cells were maintained in phenol red-free DMEM/F-12, 0.5% BSA and 2 mM L-glutamine. Treatment was performed in phenol red-free DMEM/F12 containing 5% charcoal-treated fetal calf serum to reduce the endogenous steroid concentration [37]. For our purposes MCF-7 human breast cancer cells were assessed by the MTT assay [38]. The experiment was repeated in triplicate (n=3).

#### *2.5 Antioxidant Activity Evaluation of CA*

The ability of curcumin derivative to protect against lipid peroxidation induced by *tert*-BOOH, was examined in rat liver microsomal membranes during 120 minutes of incubation. Aliquots of curcumin and CA were added to the microsomal suspension. Then the suspensions were incubated at 37 °C in a shaking bath under air in the dark. After incubation, the thiobarbituric acid-malondialdehyde complex (TBA-MDA) formation was monitored by the use of UV-VIS spectrophotometry at 535 nm [39-41]. The experiment was repeated in triplicate (n=3).

### 2.6 Microspheres Preparation

Microspheres curcumin based were produced by radical copolymerization technique. Briefly, a cylindrical glass reactor of 100-150 ml equipped with mechanical stirrer and dripping funnel, screw cap with puncture-proof rubber septum was flamed in a nitrogen flow and after cooling was immersed in a bath thermostatically controlled at 40° C. Then, required amount of *n*-hexane (20 ml) and chloroform (18 ml) were introduced into the reactor. After 30 min of N<sub>2</sub> bubbling, this mixture was treated with distilled water containing CA, EBA and ammonium persulfate such as radical initiator. Under stirring at 1000 rpm, the mixture was treated with Span85 and Tween85, then after 10 min with TMEDA and stirring was continued for another 60 min [42].

The amounts of all reagents used in these experiments are reported in Table 2. The microspheres so obtained were filtered, washed with 50 ml portions of 2-propanol, ethanol, acetone and diethyl ether and dried overnight under vacuum at 40 °C. Their characterization was effected by light scattering, FT-IR spectrometry, optical microscopy and SEM.

Aqueous dispersed phase Reagents (mg)	Organic continuous phase CHCl <sub>3</sub> /esano (ml/ml)	Microspheres mg (conv. %)
CA(1.2·10 <sup>3</sup> mg) EBA (440 mg)	18/20	1·10 <sup>3</sup> mg(83%)

*For polymerisation, the amount of aqueous phase is 3 ml; initiator system is (NH<sub>4</sub>)<sub>2</sub>S<sub>2</sub>O<sub>8</sub>/TMEDA (150 mg/150 µl); surfactants are Span 85/Tween 85 (100 µl /50 µl).*

**Table 2:** Copolymerization of CA with EBA

### 2.7 Swelling Studies

The swelling behaviour was investigated in order to check the hydrophilic



affinity of spherical microparticles. Typically, aliquots (50 mg) of dried materials were placed in a tared 5-ml sintered glass filter ( $\text{\O}$  10 mm; porosity G3), weighed, and left to swell by immersing the filter in a beaker containing the swelling media (phosphate buffer pH 6.8, simulated intestinal fluid). At fixed times (1, 6, 12 and 24 h), the excess of water was removed by percolation and then the filter was centrifuged at 3500 rpm for 15 min and weighed. The filter tare was determined after centrifugation with only water. The weights recorded at different times were averaged and used to give the equilibrium swelling degree ( $W_t(\%)$ ) by the Eq. (1) where  $W_s$  and  $W_d$  are the weights of swollen and dried microspheres, respectively. Each experiment was carried out in triplicate and the results were in agreement within  $\pm 4\%$  standard error.

$$W_t(\%) = (W_s - W_d)/W_s \cdot 100 \quad (1)$$

### *2.8 Azathioprine Loading by Soaking Procedure*

Incorporation of drugs into microspheres was performed by soaking procedure as follows: 150 mg of preformed empty microspheres (prepared as described above) were wetted with 10 ml of distilled water in a concentrated azathioprine solution (0.03 g). The amount of drug solubilized was chosen in order to have a drug loading of 20% (w/w). After 3 days, under slow stirring at 37°C, the microspheres were filtered and dried at reduced pressure in presence of  $\text{P}_2\text{O}_5$  to constant weight. The loading efficiency percent (LE, %) of all samples were determined by spectrophotometric analysis ( $\lambda = 280 \text{ nm}$ ) of filtered solvent according to Eq. (2):

$$\text{LE}(\%) = (C_i - C_o)/C_i \cdot 100 \quad (2)$$

#### Section 4 – PART A

Here  $C_i$  was the concentration of drug in solution before the loading study,  $C_o$  the concentration of drug in solution after the loading study respectively.

#### *2.9 Drug Release Studies*

Dried microspheres (10 mg) were dispersed in 6 ml of swelling media (phosphate buffer pH 6.8, simulated intestinal fluid). The test tubes were maintained at 37°C in an horizontal-shaking bath and shaken at a rate of 100 rpm. At fixed intervals, the samples were centrifuged, 5 ml of supernatant were removed and the medium was replaced with fresh solutions to maintain the same total volume throughout the study. The concentration of azathioprine was determined by UV spectrophotometry at 280 nm. The experiment was repeated in triplicate (n=3). The release was calculated in terms of drug release percentage.

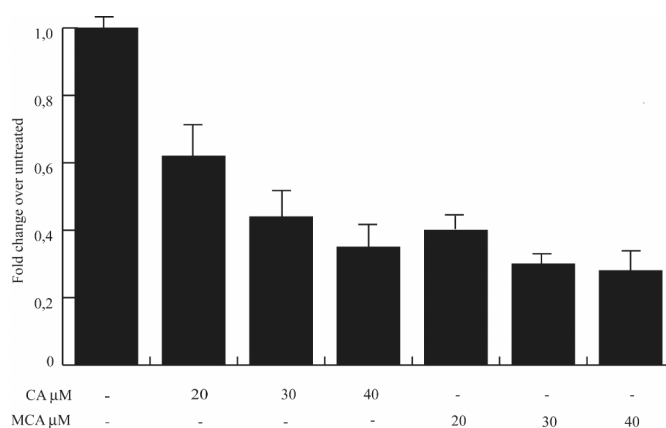
#### *2.10 Statistical Analysis*

Each datum point represents the mean  $\pm$  SD of three different experiments. Data were analyzed by Student's t test using the GraphPad Prism 4 software program.  $P < 0.05$  was considered as statistically significant.

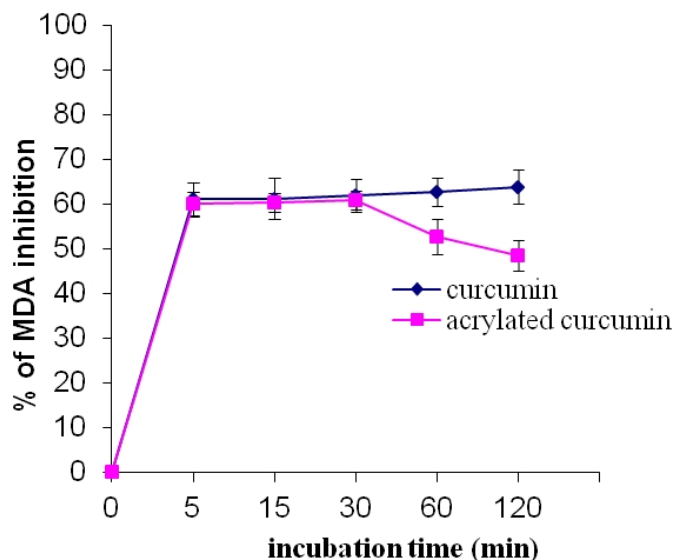
### **3. Results and Discussion**

Chemical groups susceptible of radical polymerization were introduced onto curcumin structure by esterification with acryloyl chloride in THF. Monoacrylated curcumin structure was confirmed by GC/MS, FT-IR and  $^1\text{H-NMR}$  analysis [36]. Initial cell proliferation assays were performed with different concentrations (from 20 to 40  $\mu\text{M}$ ) of curcumin and CA, in MCF-7 human breast cancer cell lines. Proliferating cells were exposed to

the compounds for 4 days and then analyzed in MTT growth assays. 20 $\mu$ M curcumin significantly inhibited basal cell proliferation (40%). With increasing doses (30 and 40  $\mu$ M), MCF-7 cell number was reduced by 56% to 77% respectively (IC<sub>50</sub> value for viability was 30  $\mu$ M). Moreover cell growth was also markedly reduced with CA treatment and it is worth of notice that the inhibitory activity on cell proliferation of CA (IC<sub>50</sub> value for viability was 20  $\mu$ M) was more effective than curcumin itself (Figure 2). The evaluation of its antioxidant activity revealed that its effect on the lipid peroxidation was time-dependent. Results are brought as percentage (%) of malondialdehyde (MDA) inhibition (Figure 2) and demonstrated that monoacrylated curcumin was also a strong antioxidant in protecting the membranes from *tert*-BOOH induced lipid peroxidation showing a higher efficiency than that of curcumin itself at 60 and 120 min of incubation, and the preservation of antioxidant activity up to 2 h (Figure 3). This behaviour was probably due to the major radical stabilization for the presence of acrylic group.

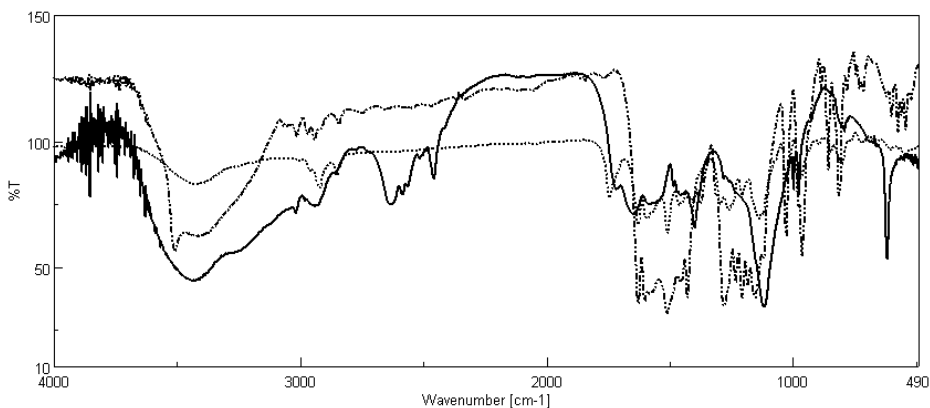


**Figure 2:** MTT assay. Cells, serum starved, were exposed to vehicle (-), or different concentrations of curcumin or CA in medium containing 1% dextran charcoal-stripped FBS for 4d (treatments were renewed every 2d). Results indicate mean of three independent experiments done in triplicate; bars SD



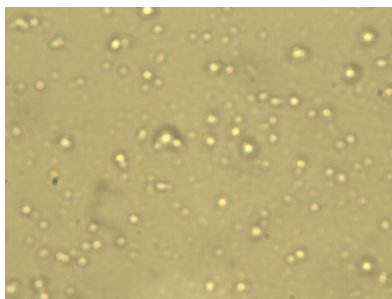
**Figure 3:** Antioxidant activity. Results indicate mean of three independent experiments done in triplicate; bars SD

Microspheres curcumin-based were prepared by reverse phase suspension copolymerization of CA with EBA. The reaction was started using TMEDA and ammonium persulfate as initiator system. The obtained materials were characterized by Fourier Transform IR spectrophotometry, particle size distribution analysis and morphological analysis. The FT-IR spectra of curcumin, CA and microparticles curcumin based are compared in Figure 4. In particular, as reported, the FT-IR spectra of monomer CA shows the characteristic peak due to C=O stretching vibration belonging to the carboxylic group of the ester at  $1746\text{ cm}^{-1}$ . Additionally, the microspheres spectrum shows the appearance of a band attributable to C=O stretching vibration of comonomer amidic group ( $1650\text{ cm}^{-1}$ ). In all spectra the peaks between  $3000$  and  $3100\text{ cm}^{-1}$  are assigned to C–H (aromatic) stretching vibration due to the phenyl group of curcumin itself.



**Figure 4:** --- *curcumin*; ... *monoacrylated curcumin*; — *microspheres*

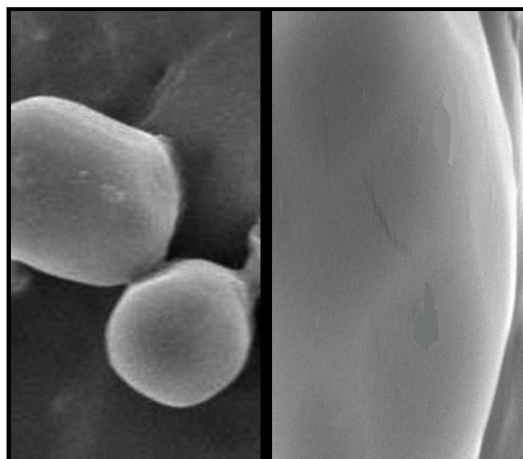
Using optical microscopy we were able to check that the microparticles had a spherical shape (Figure 5).



**Figure 5:** *Optical micrography showing spherical shape of microparticles*

In Fig. 5 the spherical shapes are evident. In our experiments a mean particle diameter of around 5.8  $\mu\text{m}$  was calculated by using dimensional light scattering.

Moreover we performed morfological analysis by using scanning electron microscopy (SEM) that confirmed the spherical shape and showed a homogeneous surface morphology (Figure 6).



**Figure 6:** *Scanning electron micrograph of microparticles*

Microspheres swelling studies were also conducted and showed a very good swelling behaviour in simulating intestinal fluids (Table 3).

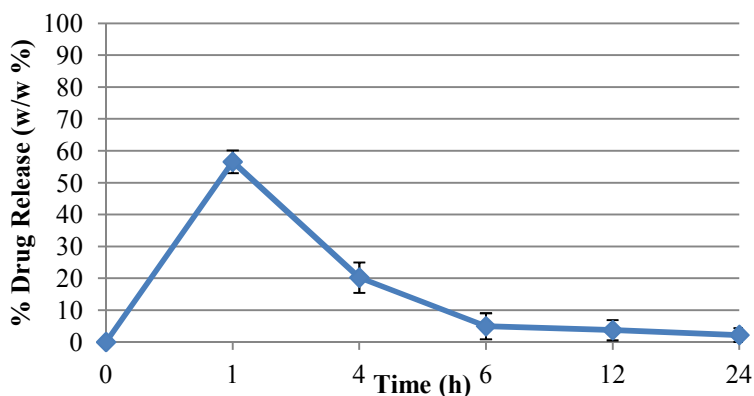
Time	Swelling ( $W_t$ %)		
	pH 1.2	pH 6.8	pH 7.4
1h	13	120	66
6h	21	135	83
12h	25	149	85
24h	27	151	86

**Table 3:** Microspheres swelling behaviour

Investigation of the applicability of curcumin based particles in controlled release was done by studying their swelling behaviour. The value of contained water percentage was determined in aqueous media which simulates some biological fluids, such as gastric (pH 1.2) and intestinal (pH 6.8) at 37 °C. Data reported in Table 1 illustrate the water uptake, in grams per grams of dry copolymer, for each pH studied. The prepared

materials showed different water affinity at pH 6.8 and acid pH 1.2 due to pendant ionizable groups in the polymeric chains. In particular, at pH 1.2 there is a considerable lowering of the water affinity due to pendant groups unionized at this pH value. When the pH is 6.8, the water content is greater than that found at pH 1.2. It is possible to explain this behaviour as a consequence of electrostatic repulsions between polymeric chains due to the increase of dissociated groups at pH 6.8. The pendant groups responsible of this behaviour are the acidic ones of comonomer (EBA) having pKa 6,1-7,1. In order to estimate the ability of prepared matrices to release encapsulated drug, the microspheres were loaded with azathioprine by soaking procedure and the loading efficiency (LE, %) was determined by spectrophotometric analysis such as reported in experimental section. The data showed that azathioprine was almost completely loaded on the polymeric beads (LE (%)=80). It is possible to explain this behaviour as consequence of strong interactions between polymeric matrix and drug molecules. Drug release profile was determined by spectrophotometric analysis. The drug release was expressed as the percent of drug delivered, related to the effectively entrapped total dose, as a function of time. These experiments were carried out the *in vitro* at 37°C. Considering the poor swelling degree at pH 1.2 the release study was effected mimicking the intestine pH value (6.8). Data showed a significative azathioprine release in these conditions (Figure 7): the total amount of azathioprine, released in 24 hours in the dissolution medium, was of 88%. It is possible to observe an initial burst release after 1 h due both to the desorption of drug trapped on the surface than to the release of loaded one through the matrix. After 4 h the percent of drug released remains considerable showing that our loaded microspheres could be a useful way to target azathioprine to the intestinal

environment thus reducing its systemic toxicity. Moreover, in the intestinal pH conditions, curcumin was not released from matrix (data not shown); for this reason it is possible to conclude that the polymerized substance could potentially act as a prodrug too.



**Figure 7:** *Graph of azathioprine release from microspheres. Results indicate mean of three independent experiments done in triplicate; bars SD*

#### **4. Conclusions**

Curcumin, a natural antioxidant and anti-inflammatory constituent, was successfully derivatized by reaction with acryloyl chloride in order to obtain a sample which contains chemical groups able to undergo radical polymerization. The antioxidant activity of new monomer was evaluated through rat-liver microsomal membranes and the results suggested that curcumin, linked to acrylic moieties, maintains its excellent antioxidant activity. The increased conjugation due to the curcumin-polymerizable group linkage explains its major lipid peroxidation inhibition after 30 min with respect to the unconjugated curcumin. Additionally, curcumin derivative inhibits cell proliferation more than commercial curcumin, as



examined in human breast cancer cells “in vitro”. Using the radical copolymerization technique, healing beads with spherical shape and an omogeneous diameter of 5.8  $\mu\text{m}$ , were obtained. Such materials could be used to transport other active substances such as azathioprine and act in a synergistic way. In fact, the release profile of azathioprine in a medium that mimics the intestinal tract showed that the drug was quasi-totally released (87.8%) during 24 hours.

## References

- [1] Roberta Cassano, Sonia Trombino, Teresa Ferrarelli, Anna Rita Bilia, Maria Camilla Bergonzi, Alessandra Russo, Francesca De Amicis and Nevio Picci. *European Polymer Journal*. SUBMITTED.
- [2] Bondi' ML, Craparo EF, Picone P, Di Carlo M, Di Gesu' R, Capuano G and Giammona G. Curcumin entrapped into lipid nanosystems inhibits neuroblastoma cancer cell growth and activates Hsp70 protein. *Current Nanosci* **2010**; 6: 439-445.
- [3] Kurd SK, Smith N, VanVoorhees A, Troxel AB, Badmaev V, Seykora JT and Gelfand JM. Oral curcumin in the treatment of moderate to severe psoriasis vulgaris: A prospective clinical trial. *J Am Acad Dermatol* **2008**; 58: 625-31.
- [4] Heng MC, Song MK, Harker J and Heng MK. Drug- induced suppression of phosphorylase kinase activity correlates with resolution of psoriasis as assessed by clinical, histological and immunohistochemical parameters. *Dermatol* **2000**; 143: 937-949.
- [5] Lebwohl M. Topical application of calcipotriene and corticosteroids: combination regimens. *J Am Acad Dermatol* **1997**; 37: 55-58.
- [6] Patel B, Siskin S, Krazmien R and Lebwohl M. Compatibility of calcipotriene with other topical medications. *J Am Acad Dermatol* **1998**; 38: 1010-1011.
- [7] Grant KL and Schneider CD. Turmeric. *Am J Health Syst Pharm* **2000**; 57: 1121-1122.
- [8] Ireson CR, Jones DJ, Orr S, Coughtrie MW, Boocock DJ and Williams ML. Metabolism of the cancer chemopreventive agent curcumin in human and rat intestine. *Cancer Epidemiol Biomarkers Prev* **2002**; 11: 105-111.
- [9] Khanna, N. Turmeric-nature's precious gift. *Current Science* **1999**, 76: 1351-1356.

- [10] Simon, A., Allais, D. P., Duroux, J. L, Basly, J. P., Durand-Fontanier, S., & Delage, C. Inhibitory effect of curcuminoids on MCF-7 cell proliferation and structure-activity relationships. *Cancer Lett.* **1998**, 129(1): 111-6.
- [11] Ahsan, H., Parveen, N., Khan, N. U., Hadi, S. M. Prooxidant, antioxidant and cleavage activities on DNA of curcumin and its derivatives demethoxycurcumin and bisdemethoxycurcumin. *Chemico-Biological Interactions* **1999**, 121, 161-175.
- [12] G.K. Jayaprakasha, L. Jaganmohan Rao, K.K. Sakariah. Antioxidant activities of curcumin, demethoxycurcumin and bisdemethoxycurcumin. *Food Chemistry* **2006**, 98: 720-724.
- [13] Van and Os EC. Azathioprine pharmacokinetics after intravenous, oral, delayed release oral and rectal foam administration. *Gut* **1996**, 39: 63-68.
- [14] Aarbakke, J., Janka-Schaub, G., and Elion, G.B. Thiopurine biology and pharmacology. *Trends Pharmacol. Sci.* **1997**, 18:3-7.
- [15] Jonathan S. Maltzman, Gary A. Koretzky. Azathioprine: old drug, new actions. *J. Clin. Invest.* **2003**, 111: 1122-1124.
- [16] Folkman, J., Long, D.M. The use of silicone rubber as a carrier for prolonged drug therapy. *J. Surg. Res.* **1964**: 4, 139-142.
- [17] Desai, S.J., Siminelli, A.P., Higuchi, W.I. Investigation of factors influencing release of solid drug dispersed in inert matrixes. *J. Pharm. Sci.* **1965**, 54: 1459-1464.
- [18] Kiminta, D.M.O., Braithwaite, G., Luckham, P.F., **1996**. Colloidal dispersions, nanogels. In: Salamone, J.C. (Ed.), *Polymer Materials Encyclopedia*. CRC Press, Boca Raton, pp. 1298-1309.
- [19] Candau, F., **1985**. Microemulsion polymerization. In: Mark, H.F., Bikales, N.M., Overberger, C.G., Menges, G., Kroschwitz, J.I. (Eds.),

*Encyclopedia of Polymer Science and Engineering*, 2<sup>nd</sup> ed. John Wiley and Sons, New York, pp. 719-723.

[20] Piirma, I., **1985**. Colloids. In: Mark, H.F., Bikales, N.M., Overberger, C.G., Menges, G., Kroschwitz, J.I. (Eds.), *Encyclopedia of Polymer Science and Engineering*, 2nd ed. John Wiley and Sons, New York, pp. 125-130.

[21] Weissman, J.M., Sunkara, H.B., Tee, A.S., Asher, S.A. Thermally switchable periodicities and diffraction from mesoscopically ordered materials. *Science* **1996**, 274: 959-965.

[22] Shi, M., Yang, Y.-Y., Chaw, C.-S., Goh, S.-H., Moochhala, S.M., Ng, S., Heller, J. Double walled POE/PLGA microspheres: encapsulation of water-soluble and waterinsoluble proteins and their release properties. *J. Control Release* **2003**, 89: 167-177.

[23] Gupta, K.C., Kumar, M.N.V.R. pH dependent hydrolysis and drug release behavior of chitosan/poly(ethylene glycol) polymer network microspheres. *J. Mater. Sci. Mater. Med.* **2001**, 12, 753-759.

[24] Lin, Y.-H.E., Vasavada, R.C. Studies on microencapsulation of 5-fluorouracil with poly(ortho ester) polymers. *J. Microencapsul.* **2000**, 17: 1-11.

[25] Yang, Y.-Y., Chung, T.-S., Bai, X.-L., Chan, W.-K. Effect of preparation conditions on morphology and release profiles of biodegradable polymeric microspheres containing protein fabricated by double-emulsion method. *Chem. Eng. Sci.* **2000**, 55: 2223-2236.

[26] Jalil, R., Nixon, J.R. Microencapsulation using poly(l-lactic acid) II: preparative variables affecting microcapsule properties. *J. Microencapsul.* **1990**, 7: 25-39.

[27] Yang, Y.-Y., Chung, T.-S., Bai, X.-L., Chan, W.-K. Effect of preparation conditions on morphology and release profiles of

biodegradable polymeric microspheres containing protein fabricated by double-emulsion method. *Chem. Eng. Sci.* **2000**, 55: 2223-2236.

[28] S. Freiberg, X.X. Zhu. Polymer microspheres for controlled drug release. *International Journal of Pharmaceutics* **2004**, 282: 1-18.

[29] Mogi, T., Ohtake, N., Yoshida, M., Chimura, R., Kamaga, Y., Ando, S., Tsukamoto, T., Nakajima, T., Uenodan, H., Otsuka, M., Matsuda, Y., Ohshima, K., Makino, K. Sustained release of estradiol from poly(lactide-co-glycolide) microspheres in vitro and in vivo. *Colloid Surface B.* **2000**, 17, 153-165.

[30] Park, T.G. Degradation of poly(D,L-lactic acid) microspheres: effect of molecular weight. *J. Control Release* **1994**, 30: 161-173.

[31] Kakish, H.F., Tashtoush, B., Ibrahim, H.G., Najib, N.M. A novel approach for the preparation of highly loaded polymeric controlled release dosage forms of diltiazem HCl and diclofenac sodium. *Eur. J. Pharm. Biopharm.* **2002**, 54: 75-81.

[32] Bezemer, J.M., Radersma, R., Grijpma, D.W., Dijkstra, P.J., Blitterswijk, C.A.V., Feijen, J. Microspheres for protein delivery prepared from amphiphilic multiblock copolymers 2. Modulation of release rate. *J. Control Release* **2000**, 67: 249-260.

[33] Fang, S.-J., Kawaguchi, H. A thermosensitive amphoteric microsphere and its potential application as a biological carrier. *Colloid Polym. Sci.* **2002**, 280: 984-989.

[34] Trombino S, Serini S, Di Nicuolo F, Celleno L, Andò S, Picci N, Calviello G and Palozza P. Antioxidant effect of ferulic acid in isolated membranes and intact cells: synergistic interactions with R-tocopherol,  $\alpha$ -Carotene, and ascorbic acid. *J Agric Food Chem* **2004**, 52: 2411-2420.

[35] Cassano R, Dabrowski R, Dziaduszek J, Picci N, Chidichimo G, De Filpo G, Muzzalupo R and Puoci F. The synthesis of new liquid-

crystalline mesogens containing bicyclohexane units. *Tetrah Lett* **2007**, 48: 1447-1450.

[36] Compound CA: orange powder, yield 17 g (43%).

GC/MS: 294 (1%), 210 (30%), 110 (100%).

FT-IR (KBr)  $\nu$  in  $\text{cm}^{-1}$ : 3076, 3031, 2941, 2851, 1699, 1275, 1020, 973, 942.

$^1\text{H-NMR}$  ( $\text{CDCl}_3$ )  $\delta$  (ppm): 1.1 (m, 10H), 1.41 (m, 8H), 1.59–1.72 (m, 16H), 2.1 (m, 2H), 3.42 (t, 4H), 3.93 (t, 4H), 4.8 (m, 2H), 4.44 (s, 4H), 6.82 (m, 4H), 7.23 (m, 10H), 7.9 (m, 4H).

[37] van der Burg B, Rutteman GR, Blankenstein MA, de Laat S W, and van Zoelen EJ. Mitogenic stimulation of human breast cancer cells in a growth factor-defined medium: synergistic action of insulin and estrogen. *J Cell Physiol* **1988**, 34:101-108.

[38] Hansen M, Nielsen S and Berg K. Re-examination and further development of a precise and rapid dye method for measuring cell growth/cell Kill. *J Immunol Methods* **1989**, 119: 203-210.

[39] Cassano R, Trombino S, Muzzalupo R, Tavano L and Picci N. A novel dextran hydrogel linking trans-ferulic acid for the stabilization and transdermal delivery of vitamin E. *Eur J Pharm Biopharm* **2009**, 72: 232-238.

[40] Trombino S, Cassano R, Bloise E, Muzzalupo R, Leta S, Puoci F and Picci N. Design and synthesis of cellulose derivatives with antioxidant activity. *Macromol Biosci* **2008**, 8: 86-95.

[41] Trombino S, Cassano R, Bloise E, Muzzalupo R, Tavano L and Picci N. Synthesis and antioxidant activity evaluation of a novel cellulose hydrogels containing trans-ferulic acid. *Carbohydr Polym* **2009**, 75: 184-188.

[42] Iemma F, Spizzirri UG, Puoci F, Muzzalupo R, Trombino S, Cassano R, Leta S and Picci N. pH-Sensitive hydrogels based on bovine serum albumin for oral drug delivery. *Int J Pharm* **2006**, 312: 151-157.

## PART B

### RESPIRABLE RIFAMPICIN-BASED MICROSPHERES CONTAINING ISONIAZID FOR TUBERCULOSIS TREATMENT [1]

#### **Abstract**

*Purpose:* Development of small microspheres for delivering antimycobacterial drugs to infected host macrophages.

*Methods:* Microparticles rifampicin based were prepared. The drug was covalently linked to acrylic moieties to obtain a polymerizable derivative for the preparation of materials useful as drug delivery systems that then were loaded with isoniazid acting in synergy with rifampicin. Their antitubercular activity was determined *in vitro*.

*Results:* Fourier transform infrared spectroscopy confirmed hydrogel structure. Morphological analysis showed microparticles with spherical shape and homogeneous surface. *In vitro* release studies were performed in media simulating physiologic pH (7.4) and endosomal of alveolar macrophages pH (5.2). A similar amount of isoniazid was delivered within the first 6 hours at both pH, while a smaller amount of the drug was delivered at pH 7.4 in the last phase of the study. *In vitro* antitubercular activity showed a behavior comparable to that of rifampicin and isoniazid free.

*Conclusions:* Bioactive swelling matrices, showing a high swelling degree into a medium miming intra alveolar environment, were obtained. They could be applied for their antitubercular activity.

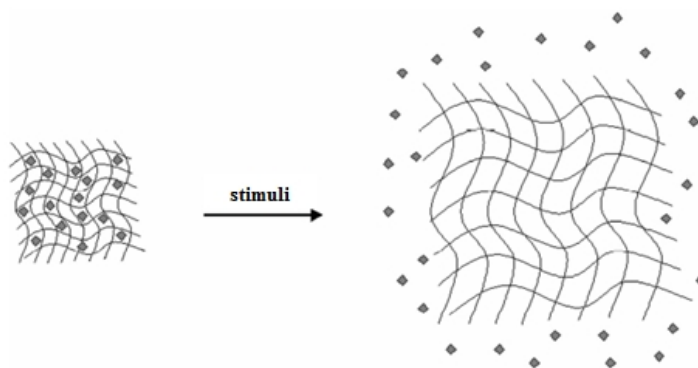


## **1. Introduction**

Controlled drug delivery systems, designed to release drugs at predetermined rates and for predefined periods of time, have been used to overcome the shortcomings of conventional drug formulations [2-4]. Hydrogels have emerged as a promising option in this regard [5-11]. They are crosslinked hydrophilic polymeric structures that can imbibe large amounts of water or biological fluids. Lately, stimuli-responsive hydrogels have been studied since they exhibit reversible swelling behaviour in response to external stimuli such as pH, temperature or magnetic and electric field [12-16]. In particular, pH-sensitive hydrogels are widely used because of variations in pH that are known to occur at several body sites such as the pulmonary and gastrointestinal tracts, vagina and blood vessels [17]. The design of a new biodegradable and biocompatible stimuli-sensitive polymeric systems represents an interesting incentive for several researchers [18-20]. It is possible to prepare these materials by using different polymerization techniques. Among these, reverse-phase suspension polymerization method allows to obtain spherical microparticles with a narrow size distribution [21,22]. Spherical shape should be advisable in order to avoid swelling anisotropic behaviour associated with other geometries [23]. The hydrophilicity of beads allowed to incorporate high concentrations of water-soluble drugs into the spheres after synthesis. Employing different model drugs, release profiles from microspheres were studied. In particular, the drug release features depended principally on crosslinking degree of polymers, ratio among functionalized drug and comonomer, and drug–matrix interactions.

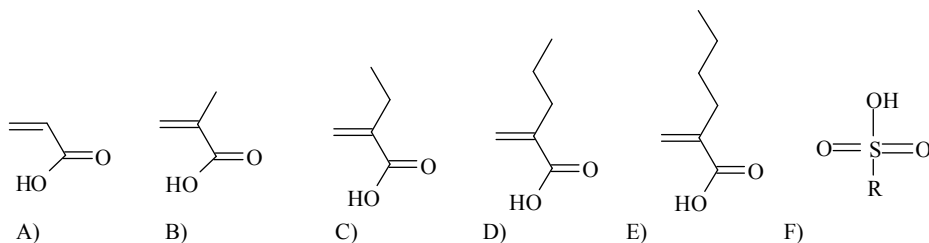
*1.1 Smart polymeric particles*

Natural and synthetic polymers have been used to fabricate different types of particles that vary in shape, size (micro- or nano-sized), degradability, and type of surface groups. These particles have been routinely used as vehicles for delivery of therapeutic agents due to their ability to protect the encapsulated drug coupled with their ease of fabrication, tunable degradation kinetics, and high surface to volume ratio, which allows the display of a large number of targeting agents and/or imaging probes. The first generation of polymeric particles released the encapsulated drug via degradation of the polymer matrix regardless of where these particles are located within the body. However, there is a significant interest in delivering therapeutic drug molecules selectively to diseased tissues by utilizing certain cues that are specific to the targeted tissue/cell to trigger the release of the encapsulated drug from the particulate carriers. This need catalyzed the development of “smart” particles (Figure 1), which are fabricated using stimuli-sensitive polymers that can sense and respond to small changes in environment conditions such as pH, temperature, light, and ionic strength [24].



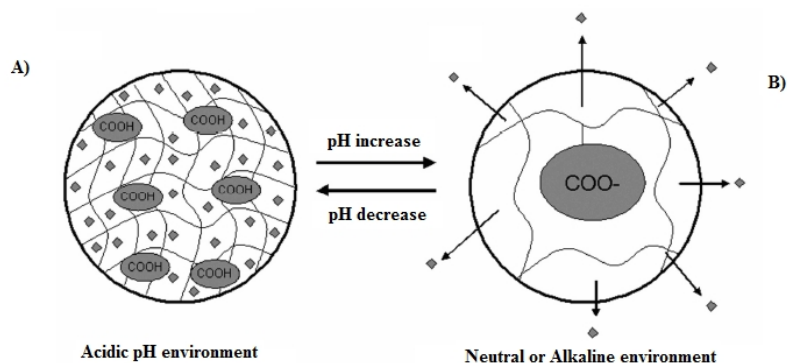
**Figure 1:** *A schematic drawing of “smart” sensitive*

Stimuli responsive particles sensible to the variations of pH can be based on different types of pH-sensitive polymers; one class of these polymers is constituted by polyelectrolytes or polyanions, which is characterized by a large number of ionizable acidic groups such as carboxylic or sulfonic acid groups (Figure 2).



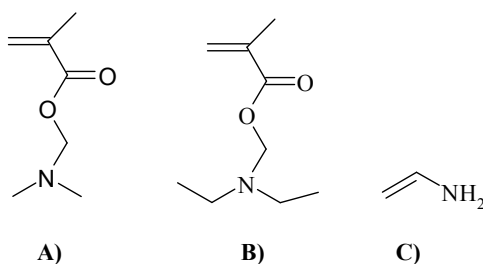
**Figure 2:** Chemical structures of: (A) acrylic acid, (B) methyl acrylic acid, (C) ethyl acrylic acid, (D) propyl acrylic acid, (E) butyl acrylic acid, and (F) sulfonic acid monomers used to synthesize “smart” pH-sensitive polymers.

This class of pH-sensitive polymers is represented by some common polyanions used in drug delivery such as poly(acrylic acid) and poly(sulfonic acid) based polymers. The pendant acidic groups of these polymers are typically ionized in neutral and alkaline solutions and their electrostatic repulsion affects the physical properties of the polymer. The pH at which the pendant acidic groups become ionized depends on the pKa (the log value of the acid dissociation constant) of the polymer, which in turn depends on the polymer’s composition and molecular weight [25]. Poly(acrylic acid) polymers have been formulated into drug-loaded particles for oral drug delivery where they retain their therapeutic cargo in the acidic environment of the stomach but release the encapsulated drug in the alkaline environment of the small intestine due to ionization of the carboxylic acid groups and swelling of the polymer matrix (Figure 3).



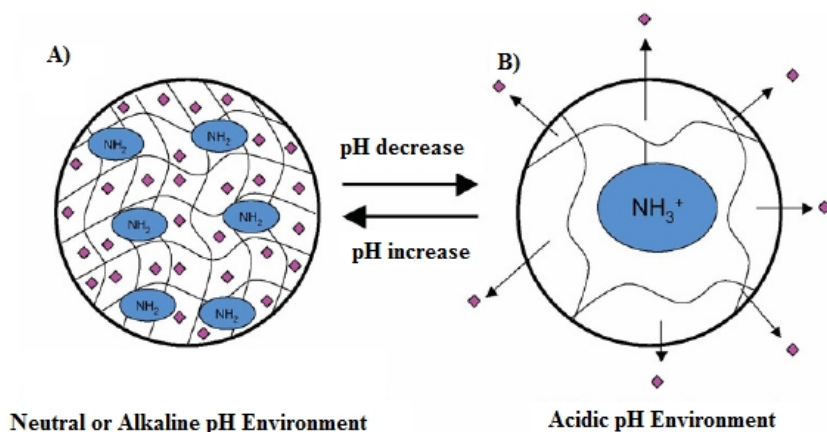
**Figure 3:** A schematic drawing of a drug-loaded particle formulated using poly(acrylic acid) polymers. (A) The pendant carboxylic acid groups are unionized in the acidic environment of the stomach and the particle retains the loaded drug. Whereas, in neutral and alkaline environments of the small intestine (B), the pendant carboxylic acid groups become ionized, the particle swells due to electrostatic repulsion of the ionized groups and release the loaded drug molecules into the surrounding medium.

There is another class of pH-sensitive polymers with basic functional groups such as primary, secondary, and tertiary amine groups that become ionized at low pH values (Figure 4).



**Figure 4:** The chemical structures of: (A) *N,N'*-dimethylaminoethyl methacrylate, (B) *N,N'*-diethylaminoethyl methacrylate, and (C) vinyl amine monomers, which are commonly used to prepare “smart” pH-sensitive cationic polymers.

Unlike anionic polymers, which exhibit pH-induced transitions in their physical conformation around pH 4-6, these cationic polymers display the change in their conformation at pH 8 or higher based on their pKa values (Figure 5).



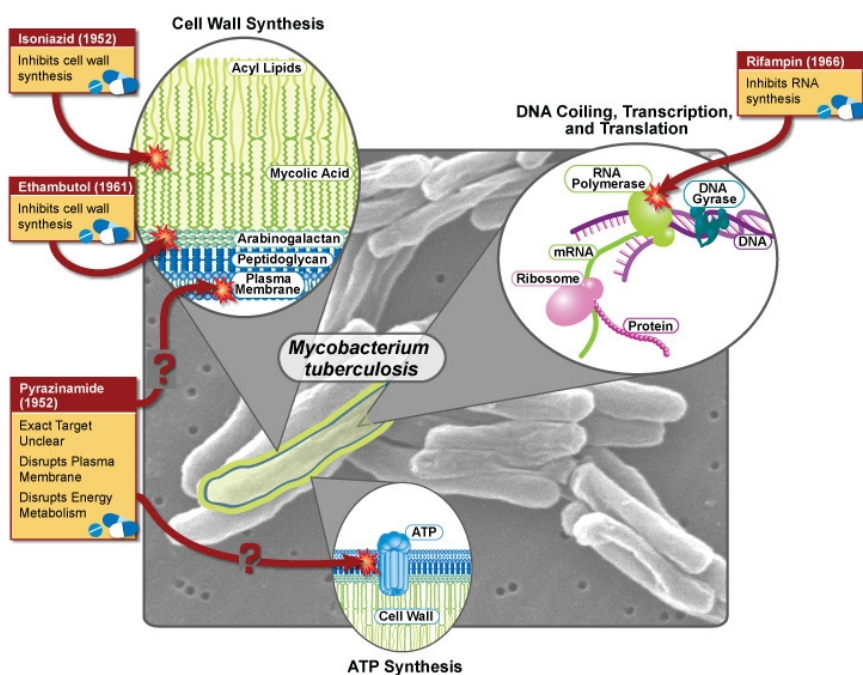
**Figure 5:** A schematic drawing of a drug-loaded particle formulated using poly(vinyl amine) polymers. (A) In a neutral or alkaline environment, the pendant amine groups remain unionized and the particle entraps the loaded drug. However, as the pH drops below the pKa value of these  $\text{NH}_2$  groups (B), they become protonated and the particle swells due to electrostatic repulsion between the positively charged groups and releases the loaded drug molecules into the surrounding medium.

Microsphere technology has been used to deliver several different types of drugs, including antigens, steroids, peptides, proteins, and antibiotics, by injection or oral administration [26,27].

### 1.2 Tuberculosis treatment

Pulmonary *Mycobacterium Tuberculosis* infection is characterized by alveolar macrophages containing large numbers of bacilli. Current treatment of pulmonary tuberculosis involves prolonged oral administration of large systemic doses of combined antibiotics, which are associated with unwanted side effects and poor patient compliance.

Targeting the drug to alveolar macrophages would be a rational addition to current therapy, potentially enhancing efficacy and reducing toxicity [28-31]. This could be done by using polymeric microparticles. Pulmonary infections, due to a variety of pathogens, are important causes of morbidity and mortality today especially in immuno-compromised individuals. TB is most often due to *Mycobacterium tuberculosis* (MTB), and the lungs are the primary site of infection for the systemic pathogen but MTB can also affect central nervous system (meningitis), lymphatic system, circulatory system (Miliary tuberculosis), genitourinary system, bones and joints (Figure 6).



**Figure 6:** *Mycobacterium tuberculosis*

*1.2.1 Particles for pulmonary targeted delivery*

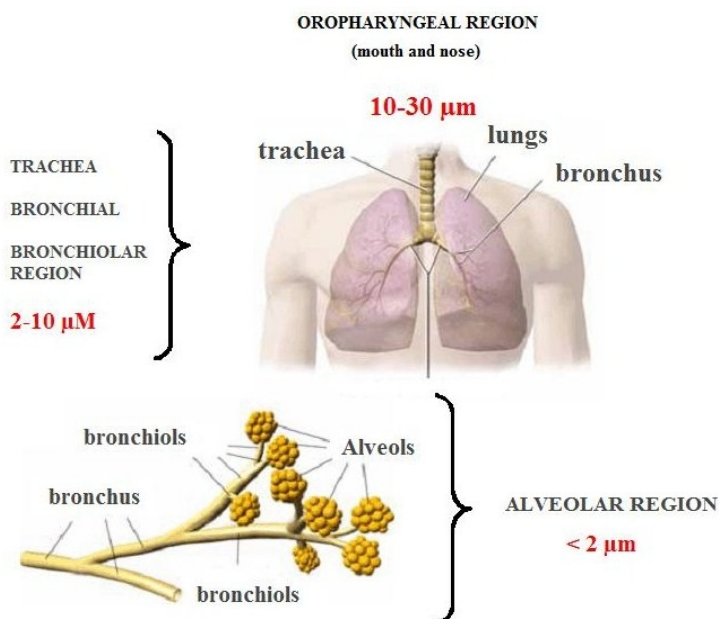
To understand the rationale behind therapeutic aerosol particle design, it is helpful to briefly review the concept of aerodynamic diameter and its relation to the pattern of particle deposition in the lungs. Aerodynamic diameter is the geometric diameter a particle appears to possess on the basis of its in-flight speed, were it assumed to be spherical and to possess a mass density of 1 g/cm<sup>3</sup>; stated differently, the geometric diameter of a spherical particle possessing unit mass density (1 g/cm<sup>3</sup>) is equivalent to its aerodynamic diameter. Because many naturally occurring particles possess a mass density near this value and because sphericity is a tendency of nature based on surface energetic considerations, such a “base-case” particle has proven useful for discussing the sites and extent of aerosol particle deposition in the lungs as a function of particle size. A more quantitative idea of aerodynamic diameter can be gathered by imagining a spherical particle falling under gravity through air; so long as the characteristic particle size is substantially larger than the mean free path of the surrounding air molecules, it can be shown that the particle will settle with a velocity ( $v$ )

$$v = \frac{mg}{3\pi\mu d}$$

where  $m$  is the particle mass,  $g$  is the gravitational constant,  $\mu$  is the viscosity of air, and  $d$  is the particle diameter. Because gravitational settling constitutes one of the principal mechanisms of aerosol particle deposition in the lungs, the concept of aerodynamic diameter becomes a useful intrinsic particle property with which to discuss a particle’s expected lung deposition performance following inhalation. Numerous experimental and theoretical studies have demonstrated that particles of

Section 4 – PART B

mean aerodynamic diameter of 1–3  $\mu\text{m}$  deposit minimally in the mouth and throat and maximally in the lung's parenchymal (i.e., alveolar or “deep-lung”) region (Figure 7). Due to their aerodynamic size, these particles will deposit in the periphery of the lung where they will be ingested by alveolar macrophages [32]. Tracheobronchial deposition, generally not desired for an inhalation therapy, is maximized for aerodynamic diameter between ,8 and 10  $\mu\text{m}$ . Particles possessing an aerodynamic diameter smaller than 1  $\mu\text{m}$  (although greater than several hundred nanometers) are mostly exhaled, and particles larger than ,10  $\mu\text{m}$  have little chance of making it beyond the mouth [33].



**Figure 7:** *Deposition of particles with different mean aerodynamic diameter in the respiratory tract*

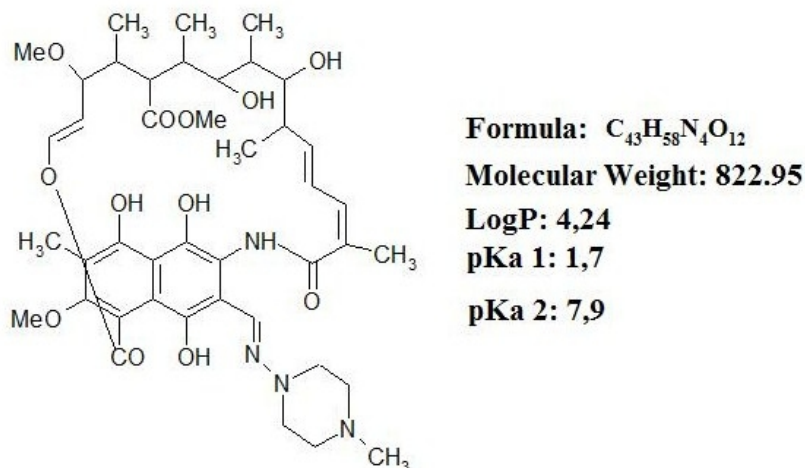
Recently, several particle technologies have emerged, which have enabled inhaled microspheres to seek to manipulate pulmonary biopharmaceuticals, and to improve therapeutic efficacy for both local



and systemic treatments. These microspheres may be designed to sustain drug release, to prolong lung retention, to achieve drug targeting and/or to enhance drug absorption and thereby, to seek the potentials of reducing dosing frequency and/or drug dose, while maintaining therapeutic efficacy and/or reducing adverse effects.

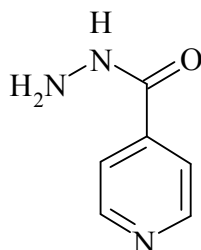
### *1.3 Antitubercular drugs*

In this work an antitubercular drug, rifampicin, was used to prepare a polymerizable monomer useful for the preparation of swellable microspheres carrying in their inner another drug, Isoniazid, acting in synergy. Rifampicin (RFP), 3-(4-methyl-1-piperazinyl-irrinomethyl) rifamycin is one of the most potent and broad spectrum antibiotics against bacterial pathogens and is a key component of anti-TB therapy. The introduction of RFP in 1968 greatly shortened the duration of TB chemotherapy. RFP diffuses freely into tissues, living cells, and bacteria, making it extremely effective against intracellular pathogens like *M. tuberculosis*. However, bacteria develop resistance to RFP with high frequency, which has led the medical community in the United States to commit to a voluntary restriction of its use for treatment of TB or emergencies. RFP is an amphiphilic compound. It is extensively recycled in the enterohepatic circulation, and metabolites formed by deacetylation in the liver are eventually excreted in the faeces (Figure 8).



**Figure 8:** Chemical structure of Rifampicin.

The bactericidal activity of RFP stems from its high affinity binding to, and inhibition of, the bacterial DNA-dependent RNA polymerase (RNAP) [34]. The loaded drug isoniazid (isonicotinyl hydrazide) is one of the most widely used chemotherapeutic agent for the treatment of tuberculosis. Isoniazid (INH) is chemically pyridine-4-carbohydrazide (Figure 9). It is a white, odourless, crystalline powder that is freely soluble in water and melts between 170 and 174 °C.



Molecular weight: 137.14 g/mol

**Figure 9:** Chemical structure of Isoniazid

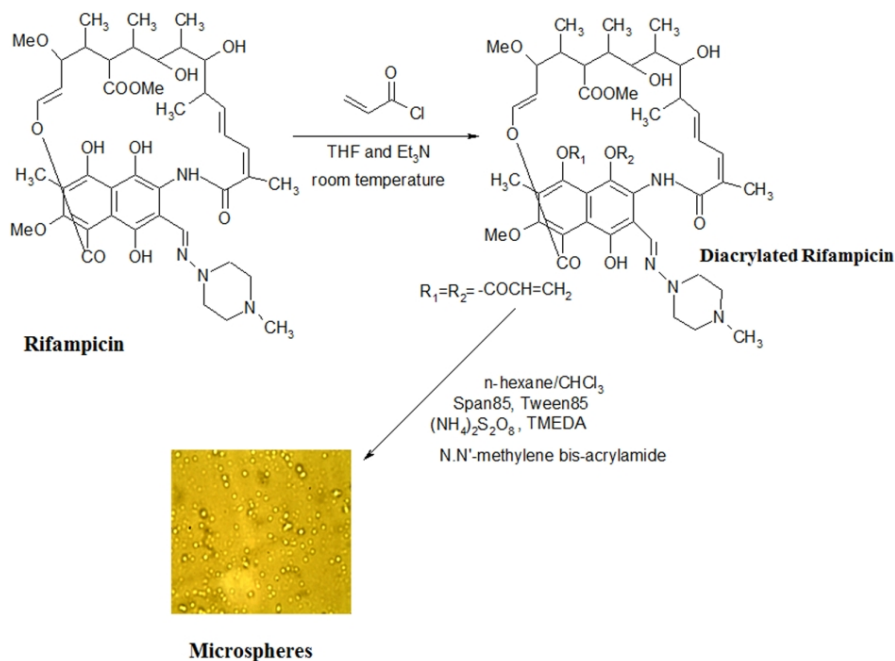
Although the mechanism of action of INH is not clearly known there is evidence that it inhibits the synthesis of mycolic acid, an essential components of the bacterial cell wall, and also combines with an enzyme that is uniquely found in INH-sensitive strains of mycobacteria. Resistance to INH can occur due to reduced intracellular penetration of the drug. According to Chambers and Jawetz [35] an INH–RIF combination administered for 9 months will cure 95–98% of cases of tuberculosis caused by susceptible strains. However, more effective strategies are now available for the treatment of intracellular bacterial infections. The concept of using micron and submicron carrier systems for the delivery of antibiotics [36] and tuberculostatic drugs has gained increasing interest in recent years.

#### *1.4 Aim of the project*

The purpose of this study was to develop small microspheres for delivery of antimycobacterial drugs to infected host macrophages. For these studies, rifampicin and isoniazid were chosen because they are two of the established first-line drugs used to treat tuberculosis.

In order to prepare pH-sensitive microspheres, suitable for aerosol drug administration, the present project describes the synthesis of materials by esterification of an antitubercular drug, like rifampicin, with a polymerizable group such as acrylic one for obtaining a bioactive monomer useful for the preparation of swellable hydrophilic microspheres through suspension radical polymerization (Figure 10).

## Section 4 – PART B



**Figure 10:** Synthetic route to obtain acrylated rifampicin and polymeric microspheres

The beads obtained were characterized by scanning electronic microscopy (SEM), Fourier Transform IR spectrophotometry, particle size distribution analysis, swelling and drug releasing behaviour. The polymeric network showed a pH-dependent behaviour. Finally, to obtain information about drug release profile, microparticles were soaked into a solution of isoniazid. In vitro release studies in simulated pulmonary fluids have shown the influence of the environmental pH on release profiles. The matrix of the beads was also subjected to spectrophotometric investigations concerning its hydrolysis at different pH and the results showed that the matrix releases small amounts of rifampicin and only after about six hours (data not shown). Moreover, microspheres antibacterial activity against *Mycobacterium Tuberculosis Complex* was evaluated.

## **2. Materials and Methods**

### *2.1 Apparatus*

The infrared spectra were obtained from KBr pellets using a FT-IR spectrometer Perkin-Elmer 1720, in the range 4000-400  $\text{cm}^{-1}$  (number of scans 16).  $^1\text{H-NMR}$  spectra were processed using a spectrometer Burker VM30; chemical shifts are expressed in  $\delta$  and referred to the solvent. The structures of the compounds synthesized were confirmed also by GC-MS Hewlett Packard 5972. UV-VIS spectra were realized through a UV-530 JASCO spectrophotometer. The light scattering was performed with a Brookhaven 90 plus particle size analyzer. The samples were lyophilized utilizing a "Freezing-drying" Micro moduly apparatus, Edwards. Scanning electron microscopy (SEM) photographs of the microspheres were obtained with a JEOL JSMT 300 A; the surface of the samples was made conductive by deposition of a gold layer on the samples in a vacuum chamber. Antitubercular activity was evaluated with the Becton Dickinson Detection Instrument (*Becton Dickinson, USA*).

### *2.2 Materials*

All solvents were obtained from Carlo Erba Reagents (Milan, Italy).  $\text{N,N}'$ -dimethylacrylamide (DMAA) and acryloyl chloride, were supplied by Sigma (Sigma Chemical Co, St. Louis, MO) and distilled before using. Rifampicin, potassium carbonate ( $\text{K}_2\text{CO}_3$ ), ammonium persulfate ( $(\text{NH}_4)_2\text{S}_2\text{O}_8$ ), sorbitan trioleate (Span 85), polyoxyethylene sorbitan monolaureate (Tween 85),  $\text{N,N,N}',\text{N}'$ -tetramethylethylenediamine (TMEDA) were purchased from Aldrich Chemical Co. and used as received. Middlebrook 7H9 medium was purchased from (Becton Dickinson, USA).

### *2.3 Rifampicin Derivatization*

The reaction was carried out according to the already known procedure [37]. In a three-neck flask fitted with a reflux condenser, dripping funnel, magnetic stirrer, carefully flamed and maintained in an inert atmosphere, a preset amount of rifampicin (0.5 g,  $6.07 \cdot 10^{-3}$  mol) was dissolved in 20 ml of tetrahydrofuran (THF) dry. Then we added 0.21 ml ( $1.48 \cdot 10^{-3}$  mol) of triethylamine and the reaction mixture was kept in continuous agitation at a temperature of 25° C. Afterwards, acryloyl chloride (0.12 ml,  $1.48 \cdot 10^{-3}$  mol) dissolved in 5 ml of tetrahydrofuran (THF) was added dropwise into the flask. The addition of the acrylate compound caused a change of solution color from dark red to orange. Then the reaction was allowed to reflux for about 12 hours and was constantly monitored by TLC on neutral alumina plates (using a mixture chloroform/methanol 9:1, v/v, as the eluent) until the existence of the link between rifampicin and the acrylic group was confirmed. The formation of the product was proved by FT-IR and  $^1\text{H-NMR}$ .

### *2.4 Microspheres preparation*

Rifampicin-based microspheres by radical copolymerization technique were produced. Briefly a mixture of *n*-hexane and chloroform was placed in a round-bottomed cylindrical glass reaction vessel fitted with an anchor-type stirrer and thermostated at 40 °C, then treated, after 30 min of  $\text{N}_2$  bubbling, with a solution of acrylated rifampicin (100 mg,  $1,14 \cdot 10^{-4}$  mol), comonomer DMAA ( $5,7 \cdot 10^{-5}$  mol) and ammonium persulfate (800 mg) in water such as radical initiator. The density of the organic phase was adjusted by the addition of  $\text{CHCl}_3$  or *n*-hexane so that the aqueous phase sank slowly when stirring stopped. Under stirring at 1000 rpm, the mixture was treated with Span85 and Tween85, then filtered, washed with

50 ml portions of 2-propanol, ethanol, acetone and diethyl ether and dried overnight under vacuum at 40 °C until constant weight. Before application, the microspheres were lyophilized to remove residual traces of all utilized solvents and of acrylic moieties.

### *2.5 Size distribution analysis*

The size of microparticles was determined by dynamic light scattering (DLS) using a 90 Plus Particle Size Analyzer (Brookhaven Instruments Corporation, New York, USA) at 25 °C by measuring the autocorrelation function at 90° scattering angle. Cuvettes were filled with 100 ml of sample solution and diluted to 4 ml with filtered (0.22 µm) water. The polydispersity index (PI), which indicates the measure of the distribution of nanoparticle populations, was also determined. Six separate measurements were made to derive the average. Data were fitted by the method of inverse “Laplace transformation” and Contin [38].

### *2.6 Swelling studies*

The swelling behaviour was investigated in order to check the hydrophilic affinity of spherical microparticles. Typically, aliquots (50 mg) of dried materials were placed in a tared 5-ml sintered glass filter (Ø 10 mm; porosity G3), weighed, and left to swell by immersing the filter in a beaker containing the swelling media. The pH values were selected to simulate physiologic pH (7.4) and endosomal pH of alveolar macrophages (5.2) [39]. Three replicates were used for each pH value. At predetermined times (1, 6, 12 and 24 h), the excess of water was removed by percolation and then the filter was centrifuged at 3500 rpm for 15 min and weighed. The filter tare was determined after centrifugation with only water. The weights recorded at different times were averaged and used to

give the equilibrium swelling degree [ Wt(%) ] by the Eq. (1) where  $W_s$  and  $W_d$  are the weights of swollen and dried microspheres, respectively. Each experiment was carried out in triplicate and the results were in agreement within  $\pm 4\%$  standard error.

$$Wt(\%) = (W_s - W_d) / W_s \times 100 \quad (1)$$

### *2.7 Drug Incorporation into preformed microspheres*

Incorporation of isoniazide into microspheres was performed as follows: 100 mg of preformed empty microspheres were soaked with 8 ml in a concentrated drug solution (2.5 mg/ml). The amount of drug dissolved was chosen so as to have a loading equal to 20% p/p. After 3 days, under slow stirring at 37 °C, the microspheres were filtered and dried at reduced pressure in presence of  $P_2O_5$  to constant weight. After that, the loading efficiency percentage (LE %) was determined by UV-VIS spectroscopy analysis of filtered solvent according to the following equation):

$$LE\% = \frac{M_i - M_0}{M_i} \times 100$$

Where  $M_i$  is the mass of drug in the solution prior to loading,  $M_0$  is the mass of drug in solution after loading, monitored by measuring absorbance at a wavelength of 202 nm.

### *2.8 In vitro drug release from microparticles*

Dried microspheres (10 mg) were dispersed in 6 ml of swelling media (7.4 physiologic pH and 5.2 endosomal of alveolar macrophages pH). The test tubes were maintained at 37°C in an horizontal-shaking bath and



shaked at a rate of 100 rpm. At predetermined intervals, the samples were centrifuged, 5 ml of supernatant was removed and the medium was replaced with fresh solution to maintain the same total volume throughout the study. The concentration of isoniazid was determined by UV spectrophotometry at fixed wavelengths ( $\lambda=202$  nm) employing different molar absorption coefficient depending on the release solutions ( $\epsilon=170$  L mol<sup>-1</sup> cm<sup>-1</sup> for solution with pH=5,2 and  $\epsilon=6820$  L mol<sup>-1</sup> cm<sup>-1</sup> for solution with pH=7,4). Each in vitro release study was performed in triplicate. Drug release was calculated in terms of percentage of drug released.

### *2.9 In vitro antitubercular activity evaluation*

The antitubercular activity of isoniazid loaded microspheres was tested in Mycobacteria Growth Indicator Tube (MGIT) [40]. The MGIT tube contains 7 ml of modified Middlebrook 7H9 broth and in the culture tubes is contained a fluorescent sensor embedded in silicone at the bottom which responds to the concentration of oxygen. Initial concentration of dissolved oxygen quenches the emission from the compound, and little fluorescence can be detected. Actively respiring micro organisms consume the oxygen which allows the compound to release fluorescence. In the isoniazid loaded microspheres the initial concentration of isoniazid was 2 µg/mL, the initial concentration of rifampicin was 20 µg/ml: in a MGIT tube was added in required amount to achieve a concentration of 0,1 µg/ml for isoniazid and a concentration of 1 µg/ml for rifampicin (according to chemosensitivity assays in vitro) and in the same tube was added 0.5 ml of broth culture positive for *Mycobacterium TB complex*; a second MGIT tube was added with not loaded microparticles to achieve a concentration of 1 µg/ml (according to chemosensitivity assays in vitro)

and 0.5 ml of broth culture positive for *Mycobacterium TB complex*, and a third MGIT tube (growth control) was added 0.5 ml of broth culture positive for *Mycobacterium TB complex* diluted 1:100 in distilled water before addition to the control tube (according to chemosensitivity assays in vitro). All MGIT tubes were supplemented with 0.8 ml of the provided enrichment (BACTEC MGIT 960 SIRE Supplement; Becton Dickinson). The tubes were placed in MGIT rack in a fixed sequence and the rack was incubated in the instrument MGIT 960 Becton Dickinson Detection Instrument (Becton Dickinson, USA) until the instrument has signaled the end of the test.

### *2.10 Statistical Analysis*

All data are presented as means  $\pm$  SD for three separate experiments. Data were analyzed by two way ANOVA test, followed by Bonferroni's post test, using the GraphPAD Prism4 software (GraphPad Software, USA). Differences were considered statistically significant at  $P < 0.05$ .

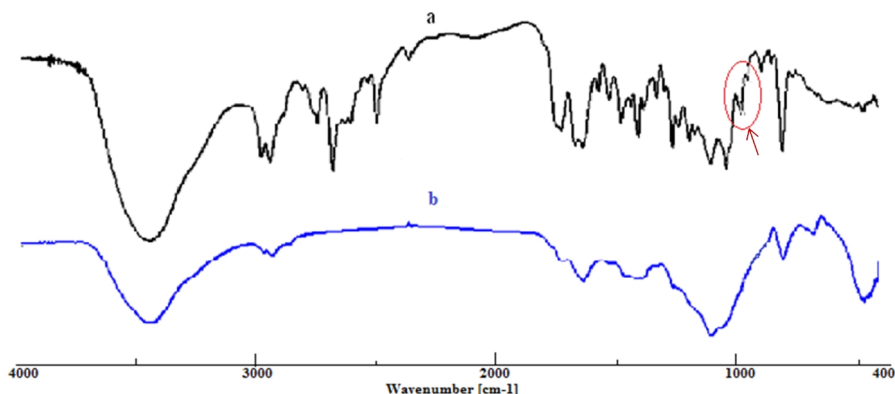
## **3. Results and Discussion**

Numerous literature data attest that the focus of current research is directed to the study of carrier molecules capable of promoting the site-specific drug release [41]. Rifampicin is a molecule that has many useful free hydroxyl groups to form ester bonds with acryloyl chloride. The rifampicin hydroxyl groups capable of reacting are those linked to benzene rings, because they have no steric encumbrance. After 24 hours, the reaction was monitored on TLC plates with aluminum oxide (using as eluent chloroform and methanol 9:1). The product was dried under vacuum and analyzed by FT-IR. The technique used for the preparation of acrylate rifampicin-based microspheres is the polymerization in

suspension. The aqueous solution of monomer (acrylate rifampicin) and comonomer (DMAA), which form the dispersed phase, was added to an excess of organic solvents (n-hexane and chloroform), immiscible with water, that form the dispersant phase. Under stirring, the dispersed phase forms small droplets that assume a spherical shape in order to reduce their interfacial free energy. The radical polymerization provides a chain mechanism for growth that begins with the generation of primary radicals following the cleavage of an appropriate initiator (ammonium persulphate). Then, these radicals react with the acrylic functions on the derivatized rifampicin determining its cross-linking. The reaction was started using TMEDA and ammonium persulfate as initiator system. In order to ensure a greater fragmentation of the phase containing the monomers, the density of the organic phase was adjusted by adding one of the two solvents to obtain an aqueous phase in equilibrium with the organic phase. To prevent the aggregation of spherical particles, the suspension was kept under constant agitation (1000 rpm). The spherical particles are more stable in the organic phase by adding a mixture of surfactants Span85 and Tween85. Optimization of the polymerization method required several attempts. It was observed that hydrophilic/lipophilic balance (HLB) of surfactants is very important. Many tests were carried out to determine the correct ratio for Span85 (HLB=1.8) and Tween85 (HLB=11). Finally, we observed that a system, with HLB=4.8, is able to stabilize the aqueous dispersed phase.

These additives stabilize the system, reducing the surface tension between the particles of monomer and the dispersant phase. The suspension polymerization allowed to obtain stable crosslinks, since covalent bonds formed between the derivatized rifampicin molecules. The obtained materials were characterized by Fourier Transform IR spectrophotometry,

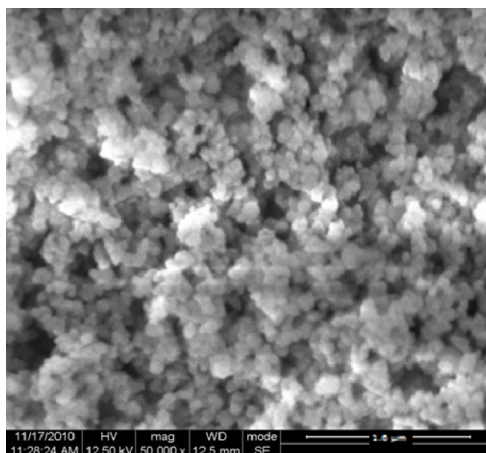
swelling behaviour, particle size distribution analysis, and morphological analysis. The spectrum of acrylate rifampicin (Figure 11) clearly shows two bands typical of the acrylic functions at  $949\text{ cm}^{-1}$  and  $976\text{ cm}^{-1}$  that confirm ester-linkages (black curve). These bands disappear in the spectra of cross-linked polymerized drug with DMAA (blue curve).



**Figure 11:** IR analysis of (a) diacrylated rifampicin, (b) hydrogel microspheres. Arrow indicates acrylic bands.

The  $^1\text{H-NMR}$  spectrum showed that the obtained derivative was diacrylated and allowed to locate the position of acrylic groups.  $^1\text{H-NMR}$  ( $\text{CDCl}_3$ ),  $\delta$  (ppm): 8.100 (1H), 7.295 (1H, d), 6.941 (1H, d), 6.921 (1H, dd), 6.899 (1H, dd), 6.453 (1H, dd), 6.401 (1H, dd), 6.399 (1H, dd), 6.294 (1H, dd), 6.084 (1H, dd), 6.082 (1H, dd), 5.725 (1H, dd), 4.209 (1H, dd), 3.974 (1H, dd), 3.779 (3H), 3.631 (3H), 3.530 (1H, dd), 3.364 (1H, ddd), 3.364 (1H, ddd), 3.200 (3H), 3.192 (1H, ddd), 3.192 (1H, ddd), 2.826 (1H, dqd), 2.813 (1H, ddd), 2.813 (1H, ddd), 2.636 (1H, ddd), 2.636 (1H, ddd), 2.579 (1H, qdd), 2.521 (1H, dd), 2.402 (3H), 2.214 (1H, dqd), 2.211 (3H), 2.121 (1H, dqd), 1.903 (3H), 1.259 (3H, d), 1.038 (3H, d), 1.027 (3H, d), 1.013 (3H, d).

The observation at the optical microscope of polymerized rifampicin shows the presence of spherical particles (Figure 10). The shape was confirmed using scanning electron microscopy (SEM) (Figure 12). In our experiments a mean particle diameter of around  $1.6 \mu\text{m} \pm 0.024$  was obtained.



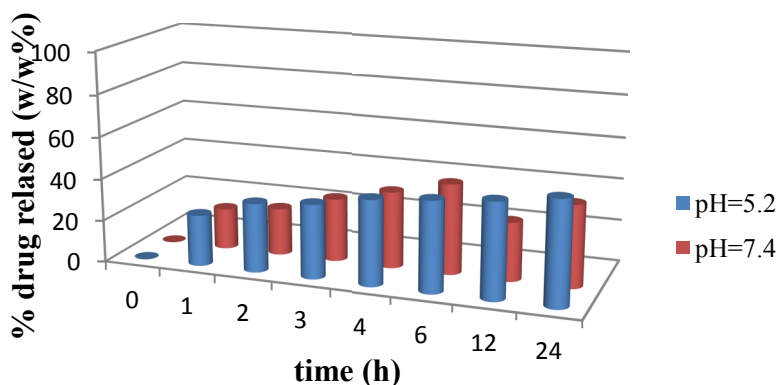
**Figure 12:** *SEM photomicrographs of microspheres.*

Investigation of the applicability of these hydrogels in controlled release was done by studying their swelling behavior in media simulating physiologic pH (7.4) and endosomal pH (5.2) of alveolar macrophages at 37 °C. Data reported in Table I illustrate the water uptake [42] at each studied pH.

In order to estimate the ability of the prepared matrices to release drug molecules, the beads were loaded with isoniazid by soaking procedure that allows the drug in contact with the outer surface of the microspheres to establish weak electrostatic interactions with the matrix (predominantly at the surface). However, the chemical nature of the drug and the matrix, as well as the loading time, make a proportion of active molecules to interact with the core of the microspheres. During the impregnation, the

Section 4 – PART B

synthesized biopolymer increases in volume but retains its three-dimensional structure without disintegrating because it is insoluble in water. Impregnation requires the interaction of a weighed amount of microspheres in a small volume of a solution at known drug concentration for 72 hours. The percentage of adsorbed drug (LE%) was evaluated through a spectrophotometer by measuring absorbance at a wavelength of 202 nm [43]; the obtained value showed that the polymer matrices is able to appreciably interact with the drug with loading percentages around 60%. We also carried out the in vitro drug release studies at 37 °C and both pH 5.2 and pH 7.4 for 24 h. The experimental data showed a constant increase of isoniazid release at pH 5.2 as a consequence of the polymer swelling behaviour at this pH, where it increased with time thus enhancing drug mobility and diffusion from the microspheres. As shown in Figure 13, at pH 7.4 lower amounts of isoniazid were released as a consequence of the lower water uptake and swelling in this environment.

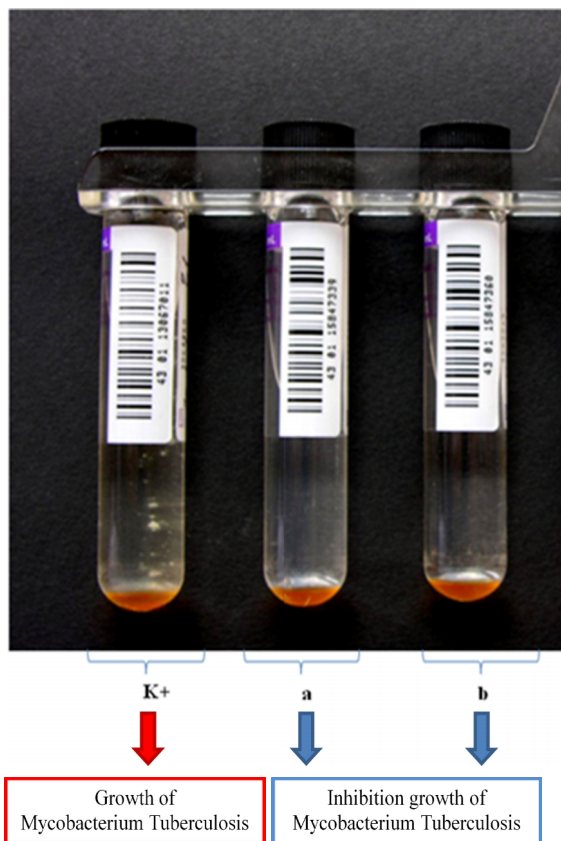


**Figure 13:** *Percentage of released isoniazid (%) from the hydrogel microspheres at pH 5.2 and 7.4. Results indicate mean of three independent experiments done in triplicate.*

This is due to the different water affinity, of prepared material, at pH 7.4 and pH 5.2. In particular, when the pH is 5.2, the water content was greater than that found at pH 7.4. It is possible to explain this behaviour as a consequence of rifampicin pKa (1.7 and 7.9). Based on these values, at pH 7.4, it is expected to witness a greater absorption of water. However, the results obtained, reported in Table 1, indicate the opposite. This is probably due to a partial hydrolysis of the polymer matrix as a result of the formation of phenate ions. This trend also justifies the minor release of isoniazid at pH 7.4 over time. Even at acid pH (1-3) the limited release is due to the formation of inner salts that inhibit the release process.

The antitubercular activity of isoniazid loaded microspheres was determined *in vitro* against *Mycobacterium Tuberculosis Complex* in Middlebrook 7H9 medium by the instrument MGIT 960 Becton Dickinson Detection Instrument (Becton Dickinson, USA) (43). Analysis of fluorescence in the microparticles-containing tubes compared to the fluorescence of the growth control tube is used by the instrument to determine susceptibility results.

As showed in the Figure 14b the isoniazid loaded particles showed antimicrobial activity. The MIC of isoniazid was  $\leq 0,1 \mu\text{g/ml}$  and for rifampicin  $\leq 1 \mu\text{g/ml}$ . Not loaded microparticles showed also an activity due to the presence of the rifampicin in their structure (MIC  $\leq 1 \mu\text{g/ml}$ ) (Figure 14a). In particular, Figure 14a (not loaded microparticles) shows a slight growth (not considered significant for the instrument, indeed *Mycobacterium Tuberculosis Complex* turned out sensitivity to rifampicin). On the contrary in the Figure 14b (isoniazid loaded microspheres) there was no growth: this highlights the drugs synergic action.



**Figure 14:** *In vitro* inhibition growth of *Mycobacterium Tuberculosis* Complex in the presence of a) not loaded microspheres and b) isoniazid loaded microspheres. The first tube represents the growth control.

#### 4. Conclusions

Rifampicin was successfully derivatized by reaction with acryloyl chloride in order to obtain an active substance which contains chemical groups able to undergo radical polymerization. The beads obtained by radical copolymerization with DMAA, showed spherical shape. The elevated water affinity and the high degree of swelling at pH 5.2, suggests that these materials can be used such as inhalable drug carriers for tuberculosis treatment. In order to test preformed microspheres as respirable drug carriers, isoniazid was chosen and drug entrapment percentual was determined. The drug release profiles, in media which



simulate physiologic as well as endosomal pH of the alveolar macrophages, depend on the hydrogel swelling degree. Concerning to microspheres antibacterial activity data showed a positive behavior of polymers in inhibition of bacteria proliferation. The results suggested that the microparticles possess an excellent antitubercular activity comparable to that of both free rifampicin and isoniazid in vitro [44].

## References

- [1] Roberta Cassano, Sonia Trombino, Teresa Ferrarelli, Maria Vittoria Mauro, Cristina Giraldi, Maria Manconi, Anna Maria Fadda and Nevio Picci. *Journal of Biomedical Materials Research: Part A*. IN PRESS. DOI: #3302.
- [2] Griffith, L.G. Polymeric biomaterials. *Acta Mater.* **2000**;48, 263-277.
- [3] Vasir JK, Tambwekar K, Garg S. Bioadhesive microspheres as a controlled drug delivery system. *Int J Pharm.* **2003**; 255:13-32.
- [4] Stubbe BG, De Smedt SC, Demeester J. Programmed Polymeric Devices for Pulsed Drug Delivery. *Pharm Res.* **2004**; 21:1732-1740.
- [5] Peppas NA, Bures P, Leobandung W, Ichikawa H. Hydrogels in pharmaceutical formulations. *Eur J Pharm Biopharm.* **2000**;50:27-46.
- [6] Byrne ME, Park K, Peppas NA. Molecular imprinting within hydrogels. *Adv Drug Deliv Rev.* **2002**;54:149-161.
- [7] Gupta P, Vermani K, Garg S. Hydrogels: from controlled release to pH-responsive drug delivery. *Drug Deliv Tod.* **2002**;7:569-579.
- [8] Hoffman AS. Hydrogels for biomedical applications. *Adv Drug Deliv Rev.* **2002**;43:3-12.
- [9] Freiberg S, Zhu XX. Polymer microspheres for controlled drug release. *Int J Pharm.* **2004**;282:1-18.
- [10] Kashyap N, Kumar N, Ravi Kumar EMNV. Hydrogel for pharmaceutical and biomedical applications. *Crit Rev Ther Carrier Syst.* **2005**; 22:107-149.
- [11] Omidian H, Rocca JG, Park K. Advances in superporous hydrogels. *J Contr Rel.* **2005**;102:3-12.
- [12] Kost J, Langer R. Responsive polymeric delivery systems. *Adv Drug Deliv Rev.* **2001**;46: 125-148.

- [13] Qiu Y, Park K. Environment-sensitive hydrogels for drug delivery. *Adv Drug Deliv Rev.* **2001**;53:321-339.
- [14] Miyata T, Uragami T, Nakamae K. Biomolecule-sensitive hydrogels. *Adv Drug Deliv Rev.* **2002**; 54:79-98.
- [15] Morishita M, Goto T, Peppas NA, Joseph JI, Torjman MC, Munsick C, Nakamura K, Yamagata T, Takayama K, Lowman AM. Mucosal insulin delivery systems based on complexation polymer hydrogels: effect of particle size on insulin enteral absorption. *J Contr Rel.* **2004**;97:115-124.
- [16] Murdan S. Electro-responsive drug delivery from hydrogels. *J Contr Rel.* **2003**; 92:1-17.
- [17] Guyton AC, Hall JE. Secretory functions of the alimentary tract. In: Guyton AC, Hall JE, editors. *Textbook of Medical Physiology*. W.B. Saunders Co; **1998**, 815-832.
- [18] Gil ES, Hudson SM. Stimuli-responsive polymers and their bioconjugates. *Prog Polym Sci.* **2004**; 29:1173-1222.
- [19] Leonard M, Rastello De Boisseson M, Hubert P, Dalençon F, Dellacherie E. Hydrophobically modified alginate hydrogels as protein carriers with specific controlled release properties. *J Contr Rel* **2004**; 98:395-405.
- [20] Sinha VR, Singla AK, Wadhawan S, Kaushik R, Kumria R, Bansal K, Dhawan S. Chitosan microspheres as a potential carrier for drugs. *Int J Pharm.* **2004**; 274:1-33.
- [21] Muzzalupo R, Iemma F, Picci N, Pitarresi G, Cavallaro G, Giammona G. Novel water-swallowable beads based on an acryloylated polyaspartamide. *Colloid Polym Sci.* **2001**; 279:688-695.

- [22] Pitarresi G, Pierro P, Giammona G, Iemma F, Muzzalupo R, Picci N. Drug release from  $\alpha,\beta$ -poly(N-2-hydroxyethyl)-dl-aspartamide-based microparticles. *Biomaterials*. **2004**; 25:4333-4343.
- [23] Park K. Enzyme-digestible swelling hydrogels as platforms for long-term oral drug delivery: synthesis and characterization. *Biomaterials*. **1988**;9:435-442.
- [24] MEH El-Sayed, AS Hoffman, PS Stayton, Smart polymeric carriers for enhanced intracellular delivery of therapeutic macromolecules. *Expert Opinion on Biological Therapy* **2005**, 5(1): 23-32.
- [25] AS Hoffman, PS Stayton, O Press, N Murthy, et al., Design of "Smart" Polymers that can direct intracellular drug delivery. *Polymers for Advanced Technologies* **2002**, 13: 992-999.
- [26] Cowsar DR, Tice TR, Gilley RM, English JP. Poly(lactide-co-glycolide) microcapsules for controlled release of steroids. *Methods Enzymol*. **1985**;112:101-116.
- [27] Jacob E, Setterstrom JA, Bach DE, Heath JR, McNiesh LM, Cierny IG. Evaluation of biodegradable ampicillin anhydrate microcapsules for local treatment of experimental staphylococcal osteomyelitis. *Clin Orthop Relat Res*. **1991**;267:237-244.
- [28] Manca ML, Mourtas S, Drakopoulos V, Fadda AM, Antimisiaris S. PLGA, chitosan or chitosan-coated PLGA microparticles for alveolar delivery? A comparative study of particle stability during nebulization. *Coll Surf B: Biointerf*. **2008**; 62: 220-131.
- [29] Zaru M, Sinico C, De Logu A, Caddeo C, Lai F, Manca ML, Fadda AM. Rifampicin-loaded liposomes for the passive targeting to alveolar macrophages: In vitro and in vivo evaluation. *J Lip Res*. **2009**;19(1):68-76.

- [30] Appleyard G.D., Clark E.G. Histologic and genotypic characterization of a novel Mycobacterium species found in three cats. *Journal of Clinical Microbiology* **2002**, 40: 2425-2430.
- [31] Brain JD. Mechanisms, measurement, and significance of lung macrophage function. *Environ Health Perspect.* **1992**, 97: 5-10.
- [32] Garcia-Contreras L, Sethuraman V, Kazantseva M, Godfrey V, Hickey AJ. Evaluation of dosing regimen of respirable rifampicin biodegradable microspheres in the treatment of tuberculosis in the guinea pig. *J Antimicrob Chemother* **2006**, 58:980-986.
- [33] Weers JG, Bell J, Chan HK, Cipolla D, Dunbar C, Hickey AJ, Smith IJ. Pulmonary formulations: what remains to be done? *J Aerosol Med Pulm Drug Deliv.* **2010**, 23: 5-23.
- [34] Hartmann G., Honikel K.O., Knusel F., Nuesch J. The specific inhibition of the DNA-directed RNA synthesis by rifamycin. *Biochim. Biophys. Acta.* **1967**, 145: 843-844.
- [35] Chambers, H.F., Jawetz, E., **1998**. Antimycobacterial drugs. In: Katzung, B.G. (Ed.), *Basic and Clinical Pharmacology*. Appleton and Lange, Connecticut, 770-779.
- [36] Gürsoy, A.,. Liposome-encapsulated antibiotics: physicochemical and antibacterial properties, a review. *S.T.P. Pharm. Sci.* **2000**, 10: 285-291.
- [37] Cassano R, Dabrowski R, Dziaduszek J, Picci N, Chidichimo G, De Filipo G, Muzzalupo R, Puoci F. The synthesis of new liquid-crystalline mesogens containing bicyclohexane units. *Tetrahedron Lett*, **2007**, 48:1447-1450.
- [38] Provencher SW. A constrained regularisation method for inverting data represented by linear algebraic or integral equations. *Comput Phys Commun.* **1982**, 27:213-227.

- [39] Khan MZI, Prebeg Z, Kurjakovic N. A pH dependent colon targeted oral drug delivery system using methacrylic acid copolymers: I. Manipulation of drug release using Eudragit® L100-55 and Eudragit® S100 combinations. *J Contr Rel.* **1999**, 58: 215-222.
- [40] Provencher SW. A constrained regularisation method for inverting data represented by linear algebraic or integral equations. *Comput Phys Commun.* **1982**, 27: 213-227.
- [41] Vedha Hari BN, Chitra KP, Bhimavarapu R, Karunakaran P, Muthukrishnan N, Samyuktha Rani B. Novel technologies: A weapon against tuberculosis, *Indian J Pharmacol.* **2010**, 42: 338-344.
- [42] Zhang J, Zhaoli D, Xu S, Zhang S. Synthesis and Characterization of Karaya Gum/Chitosan Composite Microspheres. *Iran Polym J* **2009**, 18:307-313.
- [43] Gupta KC, Ravi Kumar MN. Drug release behavior of beads and microgranules of chitosan. *Biomaterials* **2000**, 21:1115-1119.
- [44] Cardoso SH, de Assis JV, de Almeida MV. Synthesis and antitubercular activity of isoniazid condensed with carbohydrate derivatives. *Quim. Nova* **2009**, 32:1557-1560.

## PART C

### A NEW HYDROGEL ELLAGIC ACID AND GLYCINE-BASED CONTAINING FOLIC ACID AS SUBCUTANEOUS IMPLANT FOR BREAST CANCER TREATMENT: PREPARATION, CHARACTERIZATION AND ANTIOXIDANT ACTIVITY EVALUATION

#### **Abstract**

*Aims:* Creation of a hydrogel, ellagic acid and glycine based, for the treatment of breast cancer as a subcutaneous implant for the transport of folic acid. The function of folic acid is to selectively and actively target the attachment of the implant only towards tumor cells that, as well known, overexpress folic acid receptors on their surface.

*Methods:* A pro-drug L-glycine and ellagic acid based, was functionalized with a polymerizable group and properly loaded with folic acid to make it more natural, non-toxic, compatible and specific for the site of action. The obtained compounds were characterized by FT-IR and <sup>1</sup>H-NMR spectrometries.

*Results:* Release studies of folic acid were conducted on aliquots of preformed hydrogel at two different pH (6.2 and 7.4) and at different time-points (1h, 6h, 12h and 24h) by using a shaking water bath at 37 °C (body temperature). Results show that folic acid is characterized by a slow kinetic release especially at pH 6.2. This result suggests a possible use as subcutaneous implant for the treatment of breast cancer.

*Conclusions:* Implants based on polymers made of natural substances may find use in the treatment of tumors whose conventional therapy provides the medication causing the onset of serious side effects.

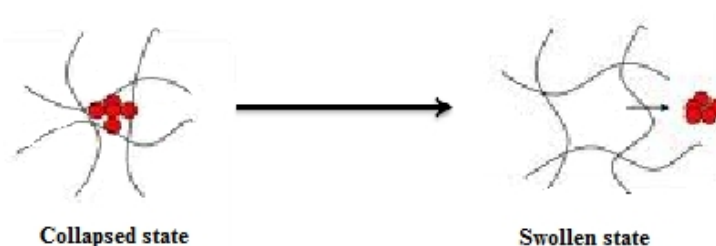
## **1. Introduction**

### *1.1 Hydrogels as drug delivery systems*

Hydrogels are three-dimensional, cross-linked networks of water-soluble polymers. They can be made from virtually any water-soluble polymer, encompassing a wide range of chemical compositions and bulk physical properties. Furthermore, hydrogels can be formulated in a variety of physical forms, including slabs, microparticles, nanoparticles, coatings, and films. As a result, hydrogels are commonly used in clinical practice and experimental medicine for a wide range of applications, including tissue engineering and regenerative medicine [1], diagnostics [2], cellular immobilization, separation of biomolecules or cells and barrier materials to regulate biological adhesions [3]. The unique physical properties of hydrogels have sparked particular interest in their use in drug delivery applications. Their highly porous structure can easily be tuned by controlling the density of cross-links in the gel matrix and the affinity of hydrogels for the aqueous environment in which they are swollen. Their porosity also permits loading of drugs into the gel matrix and subsequent drug release at a rate dependent on the diffusion coefficient of the small molecule or macromolecule through the gel network. Hydrogels are also generally highly biocompatible, as reflected in their successful use in the peritoneum [4] and other sites *in vivo*. Biocompatibility is promoted by the high water content of hydrogels and the physiochemical similarity of hydrogels to the native extracellular matrix, both compositionally (particularly in the case of carbohydrate-based hydrogels) and



mechanically. Biodegradability or dissolution may be designed into hydrogels via enzymatic, hydrolytic, or environmental (e.g. pH, temperature, or electric field) pathways; however, degradation is not always desirable depending on the time scale and location of the drug delivery device. Hydrogels are also relatively deformable and can conform to the shape of the surface to which they are applied. The high water content and large pore sizes of most hydrogels often result in relatively rapid drug release, over a few hours to a few days (Figure 1).

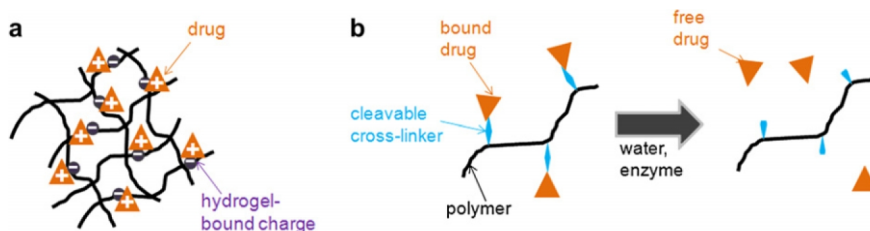


**Figure 1:** Drug release from a hydrogel

Hydrogels used in drug delivery are usually formed outside of the body and impregnated with drugs before placement of the hydrogel-drug complex in the body. A wide range of cross-linking strategies can be used, including UV photopolymerization and various chemical cross-linking techniques. Such cross-linking methods are useful only if toxic reagents can be completely removed prior to hydrogel implantation, which may be difficult to achieve without also leaching loaded drug out of the hydrogel. The main disadvantage of such approaches is that the preformed material must be implanted, since bulk hydrogels have a defined dimensionality and often high elasticity which generally excludes their extrusion through a needle. In some applications, the hydrogels can also be formed *in situ* (i.e. *in vivo*), although one then has to consider the

potential risks of exposure to UV irradiation (and the need for additional equipment) or to cross-linking chemicals. there has been considerable interest in formulations which exhibit the properties of linear polymer solutions outside of the body (allowing easy injection) but gel *in situ* within the body, providing prolonged drug release profiles. Both physical and chemical cross-linking strategies have been pursued to achieve *in situ* gelation. Physical cross-linking of polymer chains can be achieved using a variety of environmental triggers (pH, temperature, ionic strength) and a variety of physicochemical interactions (hydrophobic interactions, charge condensation, hydrogen bonding, stereocomplexation, or supramolecular chemistry).

Both physical and chemical strategies can be employed to enhance the binding between a loaded drug and the hydrogel matrix to extend the duration of drug release, as illustrated schematically in Figure 2.

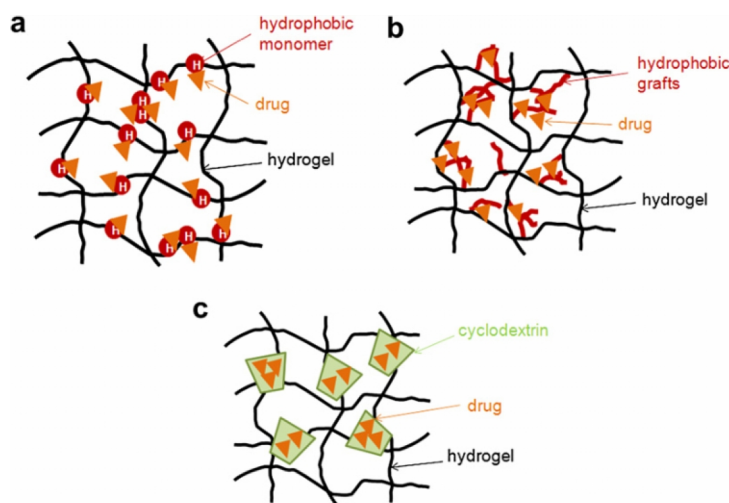


**Figure 2:** Physical (a) and chemical (b) strategies for enhancing the interaction between a loaded drug and a polymeric gel to slow drug release.

Charge interactions between ionic polymers and charged drugs have frequently been employed to increase the strength of the interactions between the gel and a target drug to delay drug release. Phosphate-functionalized polymers are effective because of their multivalent anionic charge. Phosphate-containing soft contact lenses can bind the cationic drug naphazoline in quantities directly proportional to the phosphate

content [5-7]. Drugs can also be covalently conjugated to the hydrogel matrix such that their release is primarily controlled by the rate of chemical or enzymatic cleavage of the polymer-drug bond [8]. Alternately, drug release may be regulated via the hydrolysis of the polymer backbone, possibly inducing the release of a partially modified drug analogue [9]. The cross-linker can also be engineered to give specific durations of release [10]. Classically, hydrogels have been used to deliver hydrophilic, small-molecule drugs which have high solubilities in both the hydrophilic hydrogel matrix and the aqueous solvent swelling the hydrogel. In this case, it is relatively simple to load a high quantity of drug into a swollen hydrogel by simple partitioning from a concentrated aqueous drug solution and subsequently release the hydrophilic drug payload into an aqueous environment. However, this process is relatively inefficient in the case of large macromolecular drugs (e.g. proteins, nucleic acids, etc.) which have diffusive limitations to their partitioning into a hydrogel phase or hydrophobic drugs which are sparingly soluble in both the aqueous and the hydrogel phases. A variety of strategies have been used to improve hydrophobic drug loading into hydrogels. One simple approach is to form a solid molecular dispersion of a poorly soluble drug, exploiting the enhanced solubility of many hydrophobic compounds in the amorphous state rather than the crystalline state. By this strategy, drugs are loaded into hydrogels in an appropriate solvent and bind strongly to the polymer chains in the hydrogel via hydrogen bonding interactions, preventing drug re-crystallization when the hydrogels are exposed to water and enhancing release of the hydrophobic drug. However, drug re-crystallization typically occurs over time, limiting the commercial use of solid molecular dispersions. However, such systems can be complex to fabricate and deliver. Instead, a variety of

strategies for introducing hydrophobic domains directly into otherwise hydrophilic hydrogel networks have permitted significant improvements in the loading of hydrophobic drugs (Figure 3).



**Figure 3:** Strategies for hydrophobic drug delivery via hydrogels (a) random copolymerization of a hydrophobic monomer; (b) grafting of hydrophobic side-chains; (c) incorporation of cyclodextrin.

The most common approach for generating hydrophobic domains within hydrogels is the copolymerization with hydrophobic comonomers, introducing statistically distributed hydrophobic sites within the networks. Alternately, hydrogel networks can be modified to generate hydrophobic domains with more localized and controllable distributions. Hydrophobic side chains can be grafted onto the polymer precursors which can self-assemble to form hydrophobic domains within the bulk hydrogel network and bind hydrophobic drugs [11]. Moreover, cyclodextrin-containing hydrogels can be prepared in many ways. Most simply, preformed cyclodextrine-drug complexes can be loaded into the hydrogel after or during gel cross-linking [12].

This project reports the synthesis of a hydrogel ellagic acid based for the delivery of folic acid. Ellagic acid can be defined as a depside (hydrolysable tannin whose molecule derived from the condensation of more elementary units of gallic acid). It is present in dried fruits and berries, including raspberries, strawberries, blackberries, cranberries, pomegranates and walnuts. Ellagic acid has different healing properties, among which include: antioxidant, antibacterial, anti-cancer and antiviral properties, preventive action against the onset of atherosclerosis. Numerous studies have shown that ellagic acid has anticancer activity on the tumor cells of breast, esophagus, pancreas, skin and prostate. The mechanism of action of ellagic acid on tumor cells consists in the inhibition and in the blocking of the replication of these cells and in their apoptosis [13]. The principal modes of cancer management are surgery, radiotherapy and chemotherapy. Recently, hormonal therapy and immunotherapy are increasingly being used as well, but their applications are limited for a few cancer types such as breast neoplasia [14]. Chemotherapy, the use of cytotoxic drugs to kill cancerous cells, remains the most common approach for cancer treatment. Generally, cytotoxic drugs are highly toxic but poorly specific, and do not differentiate between normal and cancer cells. Therefore, conventional chemotherapy administration or systemic administration has been shown to produce side effects [15]. Due to the short period of actions, repeated injections are often required, which can lead to exacerbation of side effects and inconvenience. In systemic administration, cytotoxic drugs are extensively transported to the whole body, therefore, only a small fraction of the drugs reach the tumor site and other healthy organs or tissues can be affected or damaged by the nonspecific action of the cytotoxic agents. Due to these obstacles, controlled and targeting or localized release

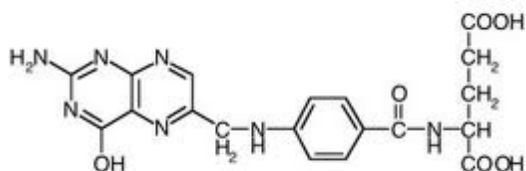
technology has been replacing the systemic administration and has shown lots of potential for cancer treatment.

Hydrogel implants have unique characteristics and can be engineered to release therapeutic agents at selected rates for periods of months to years. [16]. Thus, it is possible to achieve an intelligent response of environmentally responsive hydrogels that allows for a release controlled by the conditions of the environment [17, 18].

### *1.2 Folates in tumors targeting*

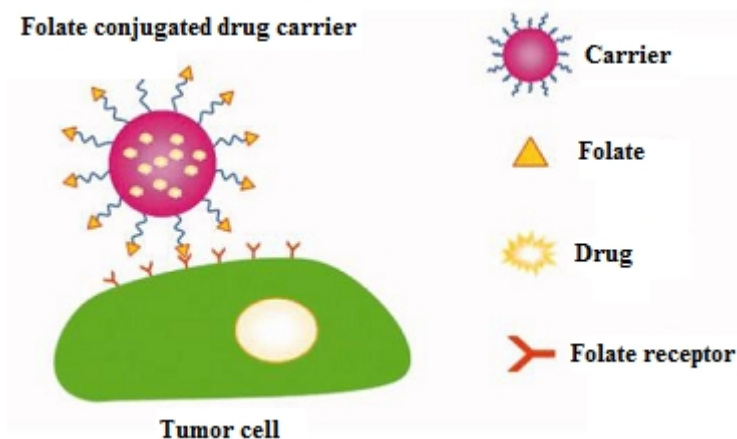
Folates are a class of pteridine compounds that are essential for normal growth and maturation. Folate is internalized by high-affinity receptors on the cell surface by a process that is similar to the receptor-mediated endocytosis of macromolecules. The receptor-mediated endocytosis uptake pathway for the vitamin folate was investigated as a target for tumor-selective pharmaceutical delivery. The molecular target for this delivery mechanism is a membrane-associated folate binding protein (FBP) that is overexpressed by a variety of malignant cell lines. Receptor-mediated endocytosis is an attractive mechanism for cell-selective drug targeting, since this process exhibits high transport capacity, as well as ligand-dependent cell specificity. In cultured cells it is well established that receptor mediated endocytosis of folate-conjugates can be employed to achieve tumor cell-selective uptake of a wide variety of exogenous molecules that are normally excluded from the cell. Folic acid is an essential dietary vitamin used by all eucaryotic cells for DNA synthesis and one-carbon metabolism. Some cells also possess a membrane-associated folate-receptor, folate binding protein (FBP), that additionally allows folate uptake via endocytosis. When folate is covalently conjugated to macromolecules via its gamma-carboxylate (Figure 4), the

folate moiety is no longer recognized by the facilitated transport system, but can still be recognized by the folate binding protein.



**Figure 4:** *Chemical structure of folic acid*

Thus, such folate-conjugates are selectively concentrated by cells that express the membrane folate receptor. A number of tumor cell types (e.g., breast, ovarian, cervical, colorectal, renal and nasopharyngeal) are known to overexpress FBP [19] (Figure 5).



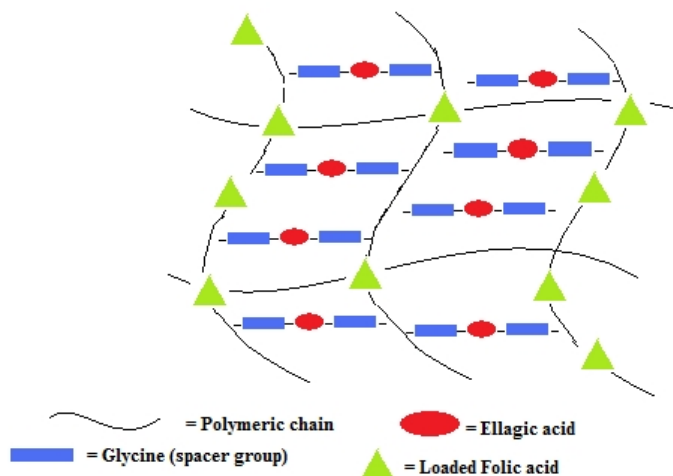
**Figure 5:** *Targeting of folate-conjugates*

Such expedient would appear to be a good method for tumor-selective pharmaceutical targeting via folate receptor-mediated endocytosis. Folate binding protein is so dramatically overexpressed in many tumors that this receptor has already been exploited in vitro as a marker to localize and visualize tumor cells [20].

### *1.3 Aims of the project*

In this context is placed the present project, whose aim was to create a hydrogel, ellagic acid and glycine based, for the treatment of breast cancer as a subcutaneous implant for the transport of folic acid. The function of folic acid is to selectively and actively target the attachment of the implant only towards tumor cells that, as well known, overexpress folic acid receptors on their surface. To achieve this goal, more precisely a pro-drug L-glycine and ellagic acid based, was functionalized with a polymerizable group and properly loaded with folic acid to make it more natural, non-toxic, compatible and specific for the site of action. The obtained compounds were characterized by FT-IR and <sup>1</sup>H-NMR spectrometries (Figure 6).





**Figure 6:** *Aim of the project*

Results confirmed the possibility that implants based on polymers made of natural substances may find use in the treatment of tumors whose conventional therapy provides the medication causing the onset of serious side effects.

## 2. Materials and Methods

### 2.1 Reagents

All solvents of analytical grade were purchased from Carlo Erba Reagents (Milan, Italy): acetone, chloroform, dichloromethane, ethanol, ethyl ether, methanol, n-hexane, acetonitrile and triethylamine. L-glycine (MW=75.07), 4,4'-dimetossitritil chloride (DMTrCl), trimethyl chlorosilanes ( $\text{Me}_3\text{SiCl}$ ), ellagic acid (MW=302.19), dicyclohexyl carbodiimide (DCC), dimethylaminopyridine (DMAP), acryloyl chloride, ammonium persulfate ( $(\text{NH}_4)_2\text{S}_2\text{O}_8$ ), N,N-dimetilacrilamide (DMAA), folic acid, tert-butyl hydroperoxide (t-BOOH) trichloroacetic acid (TCA) acid, 2-thiobarbituric (TBA), butylated hydroxytoluene (BHT) were

purchased from Sigma-Aldrich (Sigma Chemical Co, St. Louis, MO, USA).

## 2.2 Instruments

The infrared spectra were performed on KBr pellets using a FT-IR spectrometer Perkin-Elmer 1720, in the range 4000-400  $\text{cm}^{-1}$  (16 scans). The  $^1\text{H}$ -MNR were performed by a spectrometer Burker VM30; the chemical shifts are expressed in  $\delta$  and are related to the solvent. The structures of synthesized compounds was confirmed by GC-MS Hewlett Packard 5972. The UV-VIS spectra were carried out using JASCO-530 UV spectrophotometer. Samples were freeze-dried using a freeze-drying "Micro Modulyo Edwards apparatus".

## 2.3 Synthesis of *N*-trytil glycine (**1**)

Reaction was conducted according to the procedure reported in literature [21]. In a three-neck flask fitted with a reflux condenser, funnel dripper, magnetic stirring, thoroughly flamed and maintained under nitrogen bubbling, L-glycine (0.27 g, 13 mmoles) was dissolved in 1.22 mL mixture of chloroform (0.98 ml) and acetonitrile (0.24 mL). Reaction mixture was maintained at 30 °C under magnetic stirring. After dissolution, 0,42 mL (3.3 mmol) of trimethyl chlorosylane were added. Reaction was conducted for 2 hours at 30 °C. Consequently, we added 0,97 mL (6.9 mmol) of dry triethylamine and dropwise 4,4'-dimethoxytrytil chloride (1,20 g, 13 mmol) dissolved in chloroform (15,77 mL). Addition of 4,4'-dimethoxytrytil chloride causes a chromatic change from white to red. This mixture was maintained for 1 hour under magnetic stirring; afterthat 0,71 mL of methanol were added causing chromatic change from red to grey-green. Mixture was left under stirring

for 2 hours. Finally the colour was pale yellow. Reaction was monitored through TLC on aluminum oxide (eluent mixture: chloroform). Solvents were evaporated through evaporation under reduced pressure and the obtained solid was washed with diethyl ether and then with an aqueous solution of citric acid 5% w/v. Organic phase was treated with a solution of NaOH 1 N (7,18 mL) and water (3,59 mL). The obtained water phase was treated with cold diethyl ether (17,18 mL) and neutralized with glacial acetic acid. The obtained precipitate was washed with diethyl ether while the organic phase was washed with distilled water and dried for 2 hours with magnesium sulphate. Solution was filtered and dried under reduced pressure. The obtained product orange in colour was characterized through FT-IR.

#### *2.4 Esterification of N-tryptylglycine with Ellagic acid (2)*

Reaction was conducted in agreement with the procedure reported in literature [22]. In a two-neck flask fitted with a reflux condenser, magnetic stirring, thoroughly flamed and maintained under nitrogen bubbling, 0,50 g (1,32 mmol) of **(1)** and 0,39 g (1,32 mmol) of ellagic acid dissolved in 2,64 mL of dichloromethane. After dissolution, we added DCC (0,35 g, 1,7 mmol) and DMAP (0,08 g, 0,65 mmol). Reaction mixture was maintained at room temperature under magnetic stirring for 12 hours. Reaction was monitored through TLC on silica gel (eluent mixture chloroform/n-hexane 5:5). Finally, the product was filtered to be purified from dicyclohexyl urea formed during the reaction. After that it was purified through a chromatographic column on silica gel (eluent mixture dichloromethane/petroleum ether 4:6). The obtained product was characterized through FT-IR.

*2.5 Detritylation reaction (Removal of trityl group) (3)*

Reaction was conducted in agreement with the procedure reported in literature [23]. In a three-neck flask fitted with a reflux condenser, magnetic stirring, thoroughly flamed and maintained under nitrogen bubbling, 0,15 g of **(1)** (0,22 mmol) were added in a solution of trifluoroacetic acid in dichloromethane 60% giving a red coloured solution. Afterthat, 0,45 mL of methanol (0.59 mmol) were added and the mixture was stirred for 1 hour at room temperature until the observation of a chromatic shift from red to yellow-orange. The solvent was evaporated at reduced pressure and the obtained salt was dried. This latter was subsequently washed with 2,26 mL of a 1 N HCl solution in MeOH. Solvents were evaporated and the product was dried and washed with diethyl ether in order to eliminate the trityl moieties. The obtained product was dried under reduced pressure and characterized through FT-IR and <sup>1</sup>H-NMR. Yield: 98%.

*2.6 Acrylation of (3)*

In a three-neck flask fitted with a reflux condenser, magnetic stirring, thoroughly flamed and maintained under nitrogen bubbling, product **3** (0,30 g, 0,83 mmol) was dissolved in 6 mL of dichloromethane. Afterthat, we added 0,08 mL (0.99 mmol) of acryloyl chloride and 0,14 mL (0.1 mmol) of triethylamine. Solution appears yellow coloured. The reaction was maintained for 12 hours at room temperature and was monitored through TLC on silica gel (eluent mixture chloroform/methanol 9:1). Finally, the solvent was evaporated under reduced pressure and characterized through the FT-IR and <sup>1</sup>H-NMR.

### *2.7 Hydrogel preparation*

In a two-neck flask fitted with a reflux condenser, magnetic stirring, thoroughly flamed and maintained under nitrogen bubbling, product **4** (0,65 g, 1,57 mmol) was solubilized in an aqueous solution of NH<sub>3</sub>/urea. Subsequently, we added DMAA (0.16 mL, 0.1 mmol) and ammonium persulphate (80,35 g, 0.35 mol). finally, the reaction was carried out at 60 °C until the formation of the hydrogel. The obtained hydrogel was washed with diethyl ether in a porous filter, dried under vacuum and characterized trough FT-IR [24].

### *2.8 Antioxidant activity evaluation*

The ability of the obtained hydrogel to protect against lipid peroxidation induced by *tert*-BOOH, was examined in rat liver microsomal membranes during 120 minutes of incubation. Aliquots of both ellagic acid and hydrogel were added to the microsomal suspension. Then the suspensions were incubated at 37 °C in a shaking bath under air in the dark. After incubation, the thiobarbituric acid-malondialdehyde complex (TBA-MDA) formation was monitored by the use of UV-VIS spectrophotometry at 535 nm [25]. The experiment was repeated in triplicate (n=3).

### *2.9 Swelling studies*

The swelling characteristics of the hydrogel were determined in order to check its hydrophilic affinity. Typically aliquots (40–50 mg) of dried to constant weight hydrogel were placed in a tared 5-ml sintered glass filter (Ø10 mm; porosity, G3), weighted, and left to swell by immersing the filter plus support in a beaker containing the swelling media, i.e. phosphate buffers at pH 6.2, to mimic the conditions typical of tumor pathology, and pH 7.4, to simulate the physiological environment. At a

predetermined time, the excess water was removed by percolation at atmospheric pressure. Then, the filter was placed in a properly sized centrifuge test tube by fixing it with the help of a bored silicone stopper, then centrifuged at 3500 rpm for 15 min and weighted. This operation was repeated at the different times (1, 6, 12 and 24 h). The filter tare was determined after centrifugation with only water. The weights recorded at the different times were averaged and used to give the water content percent (WR, %) by the following equation:

$$\alpha\% = \frac{(W_s - W_d)}{W_d} \cdot 100$$

Where  $W_s$  and  $W_d$  are weights of swollen and dried hydrogels, respectively.

#### *2.10 Incorporation of folic acid into preformed hydrogel*

Incorporation of drugs into microspheres was performed as follows: 500 mg of preformed empty hydrogel (prepared as described above) were wetted with 6 ml in a concentrated drug solution (15 mg/ml). After 3 days, under slow stirring at 37 °C, the microspheres were filtered and dried at reduced pressure in presence of  $P_2O_5$  to constant weight. The loading efficiency percent (LE, %) of all samples are determined by UV-Vis spectrophotometry analysis of filtered solvent according to the following equation:

$$LE(\%) = C_i - C_0 / C_i \times 100$$

Here  $C_i$  was the concentration of drug in solution before the loading study,  $C_0$  the concentration of drug in solution after the loading study.

Loading efficiency was measured spectrophotometrically ( $\lambda = 365\text{nm}$ ,  $\epsilon = 7595 \text{ mol}^{-1}\text{dm}^3\text{cm}^{-1}$ ).

### *2.11 Drug release studies*

Dried hydrogel (10 mg) was dispersed in 6 ml of swelling media (phosphate buffers at pH 6.2, to mimic the conditions typical of tumor pathology, and pH 7.4, to simulate the physiological environment). The test tubes were maintained at 37°C in an horizontal-shaking bath and shaken at a rate of 100 rpm. At predetermined intervals, the samples were centrifuged, 5 ml of supernatant were removed and the medium was replaced with fresh solutions to maintain the same total volume throughout the study. The concentration of azathioprine was determined spectrophotometrically at 365 nm. The experiment was repeated in triplicate (n=3). The release was calculated in terms of drug release percentage.

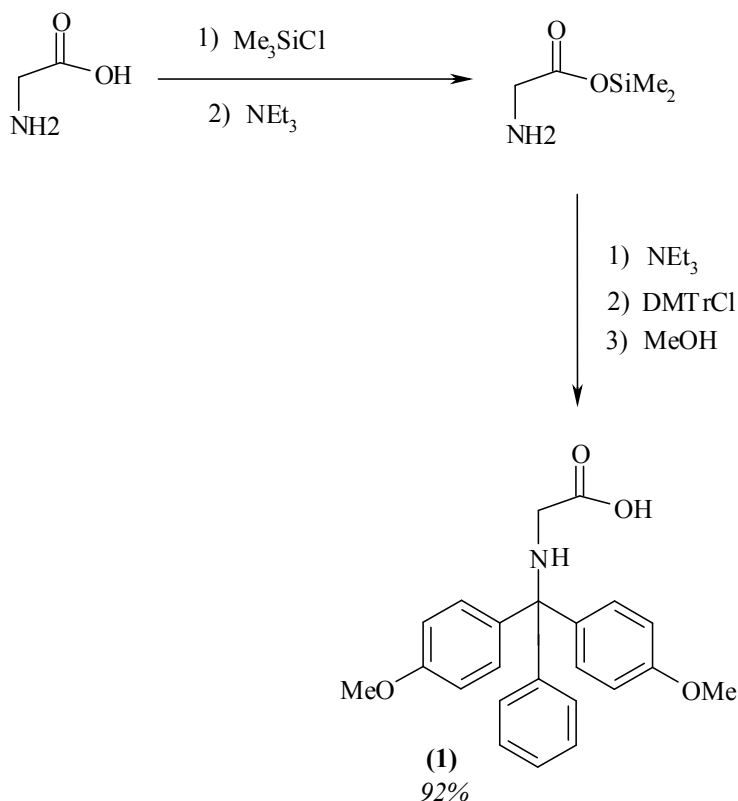
## **3. Results and Discussion**

The extensive research on the study of carrier molecules for the preparation of prodrugs useful as implants for the controlled release of active molecules, shows an increasing interest towards higher biocompatible and site-specific materials. The aim of this project has been the preparation of a hydrogel useful as subcutaneous implant, made of ellagic acid and L-glycine, an aminoacid presenting two sites of functionalization. In particular, in this case glycine acts as a spacer group linked to an active substance, such as ellagic acid, and a polymerizable group; thanks to the presence of an acrylic moiety, it is possible to perform a copolymerization reaction for the obtainment of a hydrogel potentially employable in the treatment of breast cancer.

### 3.1 Synthesis of *N*-trytil glycine (I)

The first step of the whole process was the protection of the aminic group of glycine conducted in the presence of trimethyl chlorosilane, a temporary protecting group for the carboxylic function. For this purpose, reaction was carried out using triethylamine and methanol to enhance the binding of trimethyl chlorosilane and its elimination after protection of the aminic group. 4,4'-dimethoxytrityl chloride was chosen as protecting group of the aminic moiety since it is a very hindered and easily removable one. Both the protections, the temporary one for -COOH and the stable one for -NH<sub>2</sub>, were used in a stoichiometric amount. The most likely mechanism of action involves the binding of the carboxyl group of glycine with Me<sub>3</sub>SiCl releasing a mole of hydrochloric acid. After that DMTrCl was added and it was attacked on its electrophilic carbon by the nucleophilic -NH<sub>2</sub> releasing another mole of hydrochloric acid. The addition of methanol resulted in the liberation of Me<sub>3</sub>SiCl from the carboxyl group of glycine (Scheme 1). The product of this first step was characterized the most common spectroscopic techniques. FT-IR (KBr)  $\nu$  (cm<sup>-1</sup>): 3066 e 3035 (aromatics -CH), 1725 (-COOH), 1654 (-CONH). M/Z: 320 (63 %), 77 (38 %). <sup>1</sup>H-NMR (CDCl<sub>3</sub>)  $\delta$  (ppm): 9.80 (s, 1H), 6.90-7.94 (m, 13H), 4.04 (s, 2H), 3.85 (s, 6H) 3.61 (sb, 1H). Yield: 92%.





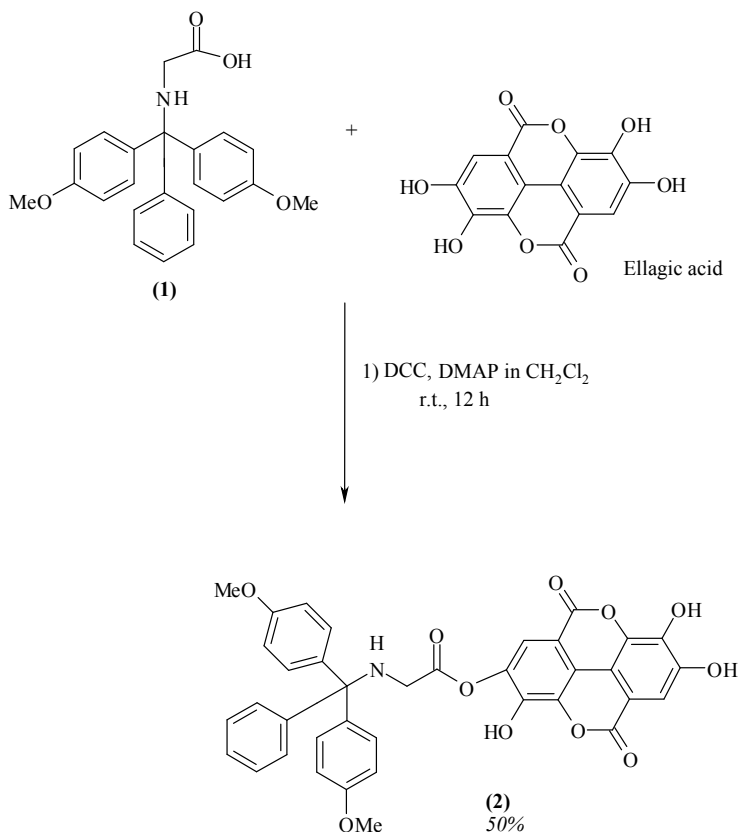
**Scheme 1:** Synthetic route to *N*-trytil glycine

### 3.2 Esterification of *N*-trytilglycine with Ellagic acid (2)

The second step of the whole synthesis was the esterification of the carboxyl group of glycine with one of the hydroxyl groups of ellagic acid. For this condensation a coupling agent such as dicyclohexyl carbodiimide (DCC) that binding the -OH group of -COOH makes it to become more electrophilic towards the nucleophilic attack of hydroxyl groups of ellagic acid. A base, dimethyl aminopyridine (DMAP), was used as buffer system and nucleophilic catalyst to promote the deprotonation of the hydroxyl groups of ellagic acid that become more nucleophilic. The esterification involves the formation of dicyclohexyl urea (DCU) as leaving group that can be removed by filtration (Scheme 2). The obtained

## Section 4 – PART C

product was dried under vacuum, purified through a chromatographic column and characterized through FT-IR and  $^1\text{H-NMR}$ . FT-IR (KBr)  $\nu$  ( $\text{cm}^{-1}$ ): 3068 e 3034 (aromatics -CH), 1769 (-C=O ester), 1718 (-C=O ester), 1653 (-CONH).  $^1\text{H-NMR}$  ( $\text{CDCl}_3$ )  $\delta$  (ppm): 6.80-7.88 (m, 15H), 3.91 (s, 2H), 3.82 (s, 6H). Yield: 50%.

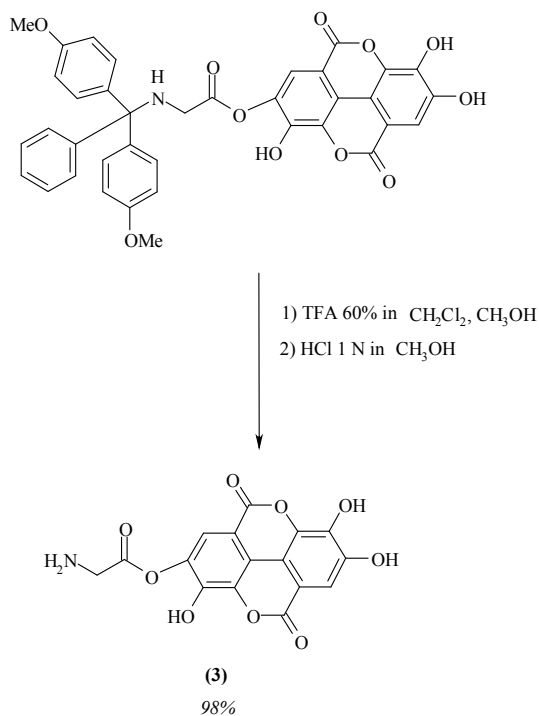


**Scheme 2:** Esterification reaction

### 3.4 Detritylation reaction (Removal of trityl group) (3)

The third step involves the removal of trityl group linked to the amino group of glycine in order to make it free for the next step of acrylation. This protecting group was removed by using a solution of trifluoroacetic

acid 60% v/v in dichloromethane. This reaction gives the corresponding chloridrate amine ( $-\text{NH}_2 \cdot \text{HCl}$ ); to obtain the free aminic group it was necessary to add a solution of hydrochloric acid 1 N in methanol to the dry salt. In order to remove all the free protecting group the product was washed with diethyl ether and the dried under vacuum and characterized through FT-IR and  $^1\text{H-NMR}$  (Scheme 3). FT-IR shows the disappearance of the amidic band at  $1653\text{ cm}^{-1}$  and the preservation of characteristic stretching of ester bonds.  $^1\text{H-NMR}$  ( $\text{C}_2\text{D}_6\text{SO}$ )  $\delta$  (ppm): 7.25 (s, 1H), 7.10 (s, 1H), 4.04 (s, 2H). Yield: 98%.



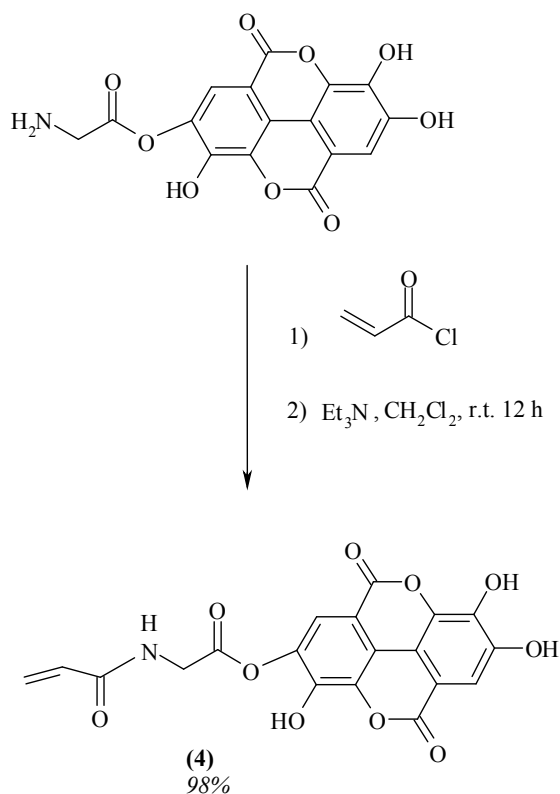
**Scheme 3:** *Deprotection*

### 3.5 Acrylation of (3)

The hydroxyl groups of ellagic acid linked to glycine were esterified using acryloyl chloride. The mechanism of this reaction consists in the

Section 4 – PART C

nucleophilic attack of the amino group of L-glycine towards the electrophilic carbonyl of acryloyl chloride by liberation of HCl (Scheme 4). The insertion of an acrylic moiety is important for the following (next) step of copolymerization. The obtained product was characterized through FT-IR and  $^1\text{H-NMR}$ . FT-IR (KBr)  $\nu$  ( $\text{cm}^{-1}$ ): 3067, 3034 (aromatics -CH), 1767 (-C=O ester), 1722 (-C=O ester), 1661 (-CONH), 995, 914 (vinyl group).  $^1\text{H-NMR}$  ( $\text{C}_2\text{D}_6\text{SO}$ )  $\delta$  (ppm): 7.30 (s, 1H), 7.05 (s, 1H), 6.43 (dd, 1H), 6.11 (dd, 1H), 5.80 (dd, 1H), 4.10 (s, 2H). Yield: 98%.



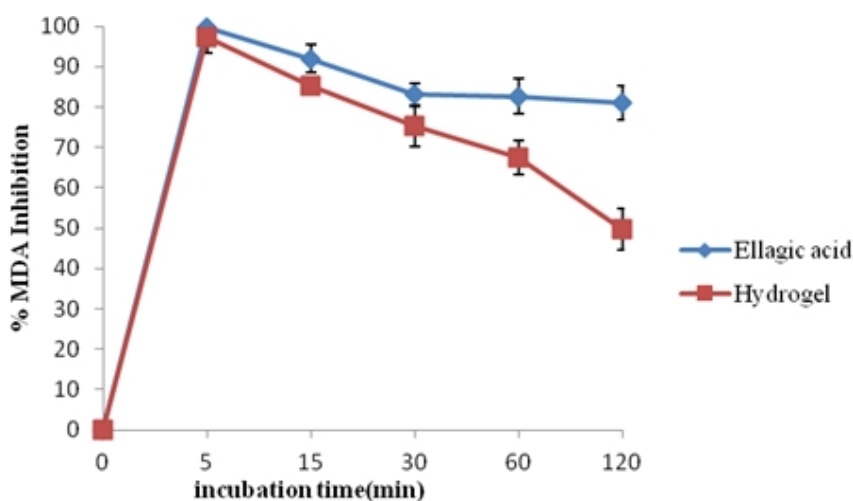
**Scheme 4: Acrylation**

### 3.6 Hydrogel preparation

Product (4) was dissolved in a  $\text{NH}_3$ /urea aqueous solution; after that ammonium persulfate and dimethyl acrylamide, a monofunctional comonomer, were added at a temperature of  $60^\circ\text{C}$ . Reaction was carried out until the formation of the hydrogel occurred and in the end the obtained product was washed several times with distilled water, dried under vacuum and characterized through FT-IR. This latter shows the disappearance of the bands attributable to the acrylic double bond.

### 3.7 Antioxidant activity evaluation

The ability of the obtained hydrogel to inhibit lipid peroxidation in rat liver microsomal membranes during 120 minutes of incubation was examined and compared to the antioxidant activity of free ellagic acid. Results revealed (Figure 1) that the ability of the obtained material to inhibit lipid peroxidation was time-dependent and follows the same trends of ellagic acid.



**Figure 7:** Antioxidant activity evaluation

### *3.8 Swelling studies*

The swelling behaviour at two different pH values was examined during 24 hours and at different time-points (1h, 6h, 12h e 24h). Each experiment was carried out in triplicate and the results were in agreement within  $\pm 4\%$  standard error. The  $\alpha$  (%) for the prepared material are reported in Table 1.

<b>Time</b>	<b>Swelling (<math>\alpha</math>%)</b>	
	<b>pH=6.2</b>	<b>pH=7.4</b>
<b>1h</b>	125	482
<b>6h</b>	224	712
<b>12h</b>	252	752
<b>24h</b>	277	771

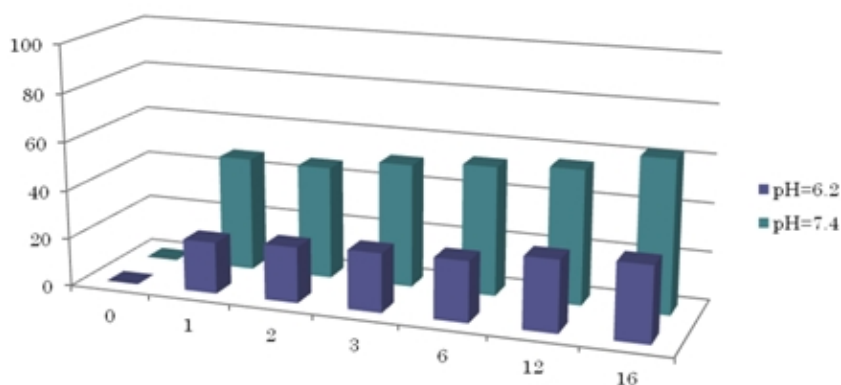
**Table 1:** *Swelling behaviour of hydrogels*

### *3.9 Folic acid loading by soaking procedure*

The drug was entrapped into the preformed hydrogel by a soaking procedure consisting in the dissolution of folic acid in a solution that allows the swelling of polymeric matrix. Loading efficiency was calculated by UV-Vis spectrophotometric analysis of the filtered solution ( $\lambda = 365\text{nm}$ ,  $\epsilon = 7595 \text{ mol}^{-1}\text{dm}^3\text{cm}^{-1}$ ). Experiment was repeated in triplicate and results showed that the drug is almost completely loaded into the matrix or on its surface. The entrapment efficiency was  $75\% \pm 1,8$ .

### 3.10 *In vitro* release studies

Release studies of folic acid were conducted on aliquots of preformed hydrogel at two different pH (6.2 and 7.4) and at different time-points (1h, 6h, 12h and 24h) by using a shaking water bath at 37 °C (body temperature). Results show that folic acid is characterized by a slow kinetic release especially at pH 6.2 (Figure 8). This result suggests a possible use as subcutaneous implant for the treatment of breast cancer.



**Figure 8:** *In vitro* release studies

## 4. Conclusions

The aim of the present project was the realization of a biocompatible hydrogel, based on ellagic acid and glycine carrying folic acid, a model molecule, useful as subcutaneous implant in breast cancer treatment. Results confirm the possibility that polymeric systems based on natural substances may find use in the treatment of cancers whose conventional therapy provides the onset of serious side effects. The swelling degree of the hydrogel not containing folic acid has been studied by conducting them at two different pH values and at fixed time intervals. In particular, we used phosphate buffers at pH 6.2, to mimic the conditions typical of

tumor pathology, and pH 7.4, to simulate the physiological environment. The obtained results show that this hydrogel swells more at pH 7.4. This could be attributed to the numerous phenolic groups of ellagic acid, that being predominantly in their ionic form, increase the hydrophilicity of the hydrogel. This latter, loaded with folic acid, was also subjected to preliminary release studies conducted in pH conditions described above. These studies have shown that folic acid is released similarly from the matrix irrespective of pH. More precisely, the drug release occurs slowly during the first 6 hours and then increases gradually probably thanks to the greater swelling of the hydrogel. In particular, folic acid is released over time in relatively small quantities. Therefore, it can be concluded that more amount of drug could be released after 24 hours. Finally, studies aimed at assessing antioxidant activity of the hydrogel not containing folic acid have shown the preservation of ellagic acid behaviour. These studies were performed by monitoring the levels of malondialdehyde (MDA) in rat liver microsomal membranes. These data show that ellagic acid based hydrogels could be used as a subcutaneous implant for controlled and site-specific release of drugs useful in the treatment of breast cancer. There are ongoing *in vitro* studies aimed at evaluating the pharmacological activity of this new material.



## References

- [1] Lee KY, Mooney DJ. *Chemical Reviews* **2001**, 101(7):1869-80.
- [2] van der Linden HJ, Herber S, Olthuis W, Bergveld P. *Analyst* **2003**, 128: 325-31.
- [3] Bennett SL, Melanson DA, Torchiana DF, Wiseman DM, Sawhney AS. *Journal of Cardiac Surgery* **2003**, 18(6):494-9.
- [4] Sutton C. *The Obstetrician and Gynaecologist* **2005**, 7:168-76.
- [5] Sato T, Uchida R, Tanigawa H, Uno K, Murakami A. *Journal of Applied Polymer Science* **2005**, 98(2):731-5.
- [6] Andrade-Vivero P, Fernandez-Gabriel E, Alvarez-Lorenzo C, Concheiro A. *Journal of Pharmaceutical Sciences* **2007**, 96(4): 802-13.
- [7] Zumbuehl A, Ferreira L, Kuhn D, Astashkina A, Long L, Yeo Y, et al. *Proceedings of the National Academy of Sciences of the United States of America* **2007**,104(32):12994-8.
- [8] Nuttelman CR, Tripodi MC, Anseth KS. *Journal of Biomedical Materials Research Part A* **2006**, 76(1):183-95.
- [9] Feeney M, Giannuzzo M, Paolicelli P, Casadei MA. *Drug Delivery* **2007**, 14(2):87-93.
- [10] Schoenmakers RG, van de Wetering P, Elbert DL, Hubbell JA. *Journal of Controlled Release* **2004**, 95(2):291-300.
- [11] Todd R. Hoare, Daniel S. Kohane. Hydrogels in drug delivery: Progress and challenges. *Polymer* **2008**, 49:1993-2007.
- [12] Kanjickal D, Lopina S, Evancho-Chapman MM, Schmidt S, Donovan D. *Journal of Biomedical Materials Research Part A* **2005**, 74(3): 454-60.

- [13] Dong Hoon Han, Min Jeon Lee, Jeong Hee Kim. Antioxidant And Apoptosis-Inducing Activities Of Ellagic Acid. *Anticancer Research* **2006**, 26: 3601-3606.
- [14] H. Wong, R. endayan, A.M. Rauth, Y. Li, X.Y. Wu, Chemotherapy with anticancer drugs encapsulated in solid lipid nanoparticles *Adv. Drug Deliv. Rev.* **2007**, 59: 491-504.
- [15] M.N.V.R. Kumar, A review of chitin and chitosan applications, *React. Funct. Polym.* **2000**, 46: 1-27.
- [16] Kuzma P, Moo-Young A, Moro D, *et al*: Subcutaneous hydrogel reservoir system for controlled drug delivery. *Macromolecular Symp* **1996**, 109:15-26.
- [17] Ulijn RV, Enzyme-responsive materials: a new class of smart biomaterials, *J Mater Chem* **2006**, 16, 2217-2225.
- [18] Angius R, Murgia S, Berti D, Baglioni P, Monduzzi M, Molecular recognition and controlled release in drug delivery systems based on nanostructured lipid surfactants. *J Phys Condens Matter* **2006**, 18: 2203-2220.
- [19] Lu, Y., Low, P.S., Folate-mediated delivery of macromolecular anticancer therapeutic agents. *Adv. Drug Del. Rev.* **2002**, 54: 675-693.
- [20] Mathias CJ, Wang S, Lee RJ, Waters DJ, Low PS, Green MA. Tumor-selective radiopharmaceutical targeting via receptor-mediated endocytosis of gallium-67-deferoxamine-folate. *J Nucl Med.* **1996**, 37(6):1003-8.
- [21] K. Barlos, D. Papaioannou, D. Theodoropoulos. “Efficient “One-Pot” Synthesis of N-Trytil Amino Acids”. *J. Org. Chem.* **1982**, 47: 1324-1326.

- [22] B. Vanhaecht, M.N. Teerenstra, D.R. Suwier, C.E. Koning. “Dicyclohexylcarbodiimide assisted synthesis of aliphatic polyesters at room temperature”. University Brussels. 15 May 2000.
- [23] V.Theodorou, V. Ragoussis, A. Strongilos, E. Zelepos, A. Eleftheriou, M. Dinitriou. “ A convenient method for the preparation of primary amines using tritylamine”. 2004
- [24] Cassano R, Trombino S, Muzzalupo R, Tavano L and Picci N. A novel dextran hydrogel linking trans-ferulic acid for the stabilization and transdermal delivery of vitamin E. *Eur J Pharm Biopharm* **2009**, 72: 232-238.
- [25] Trombino S, Cassano R, Bloise E, Muzzalupo R, Leta S, Puoci F and Picci N. Design and synthesis of cellulose derivatives with antioxidant activity, *Macromol Biosci* **2008**, 8: 86-95.

## **Acknowledgements**

I would like to thank and express my deepest gratitude to my supervisor, guide and mentor, Dr. Sonia Trombino, for her excellent conduct and supervision and for giving me such an opportunity to work in her research group on such a promising field of research. I want like to thank Dr. Roberta Cassano, who has guided me, given me valuable advices and helped me to continue in the right track. This project would not have been possible without her expertise advice and patient approach. I owe a special thanks and acknowledgement to Professor Nevio Picci, who allowed me to work in his lab. I would like to thank all the people I met during this wonderful experience in the lab of “Macromolecular Chemistry and Pharmaceutical Technology” and my colleagues in lab 326 at the School of Pharmacy: Sahar Awwad and Francesca Citossi, who really helped me and spent many nights and days working hardly to achieve excellent results. I also give a special thanks to Professor Ijeoma Uchegbu and Dr. Andreas Schatzlein who accepted me in their lab at the School of Pharmacy giving me the opportunity of working in such a fascinating field of research.

No project can go smoothly without the help and support of your own family so a big thank you to all my relatives who were always there as my backbone and who encouraged me throughout never leaving me alone.